A Self-consistent Treatment of the Parity Non-conserving Interaction in Atoms

A thesis submitted for the degree of

Doctor of Philosophy

by

Edmund Plummer

Jesus College & Theoretical Chemistry

Oxford

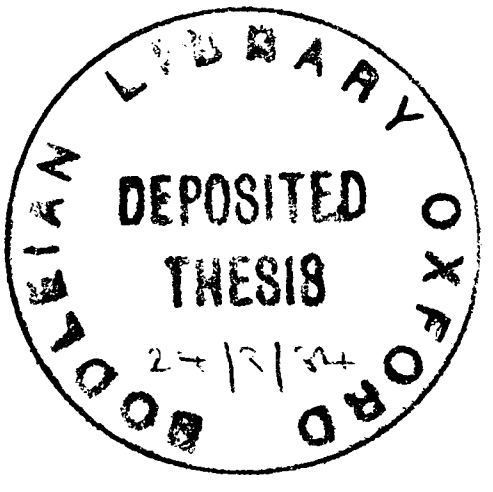

Hilary Term

1984

Abstract

And I gave my heart to seek and search out by wisdom concerning all things that are done under heaven.

Solomon (-950)

ABSTRACT

A self-consistent treatment of the parity non-conserving interaction in atoms

E.P. Plummer
Jesus College

D.Phil.
Hilary Term 1984

The Weinberg-Salam model of the weak interaction predicts that any wavefunction contains a small admixture of functions of the opposite parity. As a result, radiative transitions which would have pure magnetic dipole (M1) character in the absence of weak parity mixing interactions acquire a small component of electric dipole (E1) character, implying that atoms will show weak optical activity in proportion to the ratio of the matrix elements R = E1/M1.

This work describes a generalization of the MCDF procedure to include the weak interaction. This allows us to treat correlation, exchange, orthogonality and shielding in a consistent and rigorous manner.

A pilot calculation on bismuth using a model potential highlighted numerical problems associated with the use of a uniform nuclear density distribution. Therefore we have used a Fermi distribution in the main calculations to avoid these difficulties.

We give results for bismuth, thallium, lead and cesium; correlation (for the first three of these) and shielding (for all of these atoms) have been included by means of configuration interaction. We give the ratio R in both Coulomb (velocity) and Babushkin (length) gauges, and for bismuth, thallium and cesium a reasonable level of gauge invariance in the unshielded calculations was obtained, in contrast to other calculations.

The final results are as follows:

bismuth	λ=876nm	$R = -10.9 \times 10^{-8}$
bismuth	λ=648nm	$R = -9.1 \times 10^{-8}$
lead	λ=462nm	$R = -11.1 \times 10^{-8}$
thallium	$6p_{\frac{1}{2}} \rightarrow 7p_{\frac{1}{2}}$	$E1 = 1.61 \times 10^{-13}$ a.u. (corresponding to a matrix element of r of 1.86×10^{-10} a.u.)
cesium	$6s \rightarrow 7s$	$E1 = -1.10 \times 10^{-14}$ a.u. (corresponding to a matrix element of r of 7.1×10^{-12} a.u.)

Acknowledgements

Let us now praise famous men,
and our fathers that begat us.
Such as did bear rule in their kingdoms,
men renowned for their power,
giving counsel by their understanding,
and declaring prophecies:
Leaders of the people by their counsels,
and by their knowledge of learning meet for the people,
wise and eloquent in their instructions.

Joshua ben Sira (-180)

ACKNOWLEDGEMENTS

First and foremost I wish to thank Dr. Ian Grant for supervising me over the last five years. He not only rescued me from the Mathematical Institute, but taught me most of the atomic physics I know; and he was always ready to explain what I did not understand, and to give practical advice when I encountered problems that I could not see how to tackle. Without his friendly and cheerful help I could not have completed this work.

Financing a research degree is always a problem; this was accentuated by my dubious nationality: coming from Guernsey meant that I was not eligible for a SRC grant. Jesus College most generously responded to my need with the award of a King Charles I Scholarship and a Research and Advanced Study Fund Bursary, the latter of which they extended for an extra term to allow me to finish my research. To the Governing Body of Jesus College, and especially to the Senior Tutor, Mr. Donald Hay, who drew my attention to the bursary, I am most sincerely grateful.

All the computational results in this thesis were calculated using SRC computers, mainly those at the Rutherford Appleton Laboratory. The generous allocations of time and the excellent service provided have made my work much easier.

In the research life, no man is an island unto himself; and I wish to record my thanks to all those who have helped me. In particular, Drs. Bruce McKenzie and Patrick Norrington helped me to learn how to run the MCDF program; Dr. Ken Dyall

gave me invaluable advice on correlation; and I have had illuminating discussions on the PNC problem with Professor Sandars and Dr. Martensson. I have also made considerable use of the D.Phil. theses of D.H. Shun and C.E. Loving for the isotope shift and PNC problems respectively.

I must also thank Professor March for acting as my supervisor for Trinity Term 1981, when Dr. Grant was on sabbatical leave.

Finally, I am most grateful to Dr. Connerade and Dr. Clayton who arranged and permitted access to the Rutherford Laboratory from Imperial College. This saved me a large number of trips up to Oxford.

And last, but not least, this thesis was typed by Jackie Drew, who not only survived living in the office underneath me for three years, but heaped burning coals on my head by converting a manuscript that was usually unintelligible and at times illegible into the excellent typescript that is now presented.

Edmund Plummer
The Feast of St. Blasius, 1984

Contents

I've got a little list.....

Gilbert (1885)

CONTENTS

Abstract ii

Acknowledgements iv

Chapter 1. Introduction 1

§ 1.1 Motivation for this work 2
§ 1.2 Plan of the thesis 2
§ 1.3 Units 5
§ 1.4 Notation 5

Chapter 2. Basic multiconfigurational Dirac-Hartree-Fock theory 8

§ 2.1 The Dirac equation for hydrogen and its solution 9
§ 2.2 Many-electron atoms 12
§ 2.3 The Breit interaction 18
§ 2.4 Oscillator strengths 20
§ 2.5 The computer program 30
§ 2.6 Conclusion 31

Chapter 3. Isotope shift 33

§ 3.1 Introduction 34
§ 3.2 The use of the MCDF equations to calculate the field effect in isotope shift 34
§ 3.3 The breakdown of the Broch formula 37
§ 3.4 Results 38
§ 3.5 Conclusion 43

Chapter 4. The background to parity non-conservation in atoms 45

§ 4.1 Introduction 46
§ 4.2 Parity non-conservation 49
§ 4.3 The PNC Hamiltonian 51
§ 4.4 Perturbation theory 55
§ 4.5 The quantity of experimental interest 59

§ 4.6 Other calculations 61

§ 4.7 Connection with isotope shift 68

§ 4.8 Experimental results 72

Chapter 5. The single-particle theory of parity non-conservation in atoms 76

§ 5.1 Introduction 77

§ 5.2 The derivation of the single-particle PNC equations 77

§ 5.3 The numerical solution of the PNC equations 82

§ 5.4 Oscillator strengths 84

§ 5.5 Results 87

§ 5.6 Numerical dependence of results on computational parameters 90

§ 5.7 Numerical instability 95

§ 5.8 Conclusions 102

Chapter 6. The many-particle theory of parity non-conservation in atoms 105

§ 6.1 Introduction 106

§ 6.2 The energy functional 106

§ 6.3 The MCDF-PNC equations 113

§ 6.4 The solution of the MCDF-PNC equations 121

§ 6.5 Investigation into the problems involved in the solution of the MCDF-PNC equations 124

§ 6.6 Stabilization of solutions of the MCDF-PNC equations 126

§ 6.7 Shielding 129

§ 6.8 PNC mixing with CSF's of the opposite parity 132

§ 6.9 PNC transition matrix elements 138

§ 6.10 Basis set expansion schemes 141

Chapter 7 The parity conserving calculation for atoms of interest 143

§ 7.1 Introduction 144

§ 7.2 Bismuth 144

§ 7.3 Thallium 161

§ 7.4 Lead 169

§ 7.5 Cesium 174

Chapter 8. Results of the PNC MCDF calculations 178

§8.1 Introduction 179

§8.2 General considerations 179

§8.3 Bismuth 182

§8.4 Thallium 192

§8.5 Cesium 196

§8.6 Lead 197

Chapter 9. Conclusions 203

§9.1 Novel features of these calculations 204

§9.2 Comparison of results with other calculations and experiment 205

§9.3 Deficiencies of the present calculations 213

§9.4 Suggestions for further work 214

§9.5 Numerical accuracy of the calculations 218

§9.6 Final remarks 227

Appendix 1. Detailed derivation of the parity mixed energy functional 228

Appendix 2. Basis set expansion schemes 241

Appendix 3. Formulae for the PNC Lagrange multipliers 258

Appendix 4. Description of the computer programs 262

Appendix 5. Listing of the computer programs 275

Appendix 6. Numerical parameters used in the solution of the PNC MCDF equations 295

References 306

Chapter 1

I may say with truth that whenever I consider in my thoughts the beautiful order, how one thing issues out of and is derived from another, then it is as though I had read a divine text, written into the world itself, not with letters but rather with essential objects, saying: Man, stretch thy reason hither, so that thou mayest comprehend these things.

Kepler (1604)

Introduction

CHAPTER 1

INTRODUCTION

§1.1 Motivation for this work

The theory of parity non-conservation in atoms is an important area of current research, since it throws light on fundamental inter-particle interactions at energies inaccessible to conventional high energy physics experiments. This is particularly so in view of the present interest in unified theories, especially that of Weinberg (1967) and Salam (1968).

At the time that this work was started no results had been published for a calculation of the MCDF type, although simpler calculations had been made, mostly based on a model potential. Since MCDF theory is well known (e.g. Grant (1979)) and a program (Grant et al. (1980)) is available to apply it, it seemed natural to extend both the theory and the program to this problem.

§1.2 Plan of the thesis

We shall conclude this chapter with a description of units and notation which, although standard in publications on relativistic atomic structure, may be unfamiliar to the non-specialist. These will then be used without explanation in the rest of the thesis.

Chapter two contains a description of the standard MCDF theory. This is a generalization of the relativistic self-consistent field method, and is the starting point from which

all further theory is developed. It is worth mentioning that all results in this thesis rely, directly or indirectly, on the use of the MCDF computer program.

In chapter three we report our first application of the MCDF program, to the problem of isotope shift. Although this lies outside the scope indicated by the thesis title, it has been included; for not only is it interesting in its own right, but there are similarities between it and the PNC problem, which are described in chapter four.

Chapter four sets the scene for the rest of the work; the introduction to the PNC problem has been delayed until this late stage so as to draw on our earlier experiences with isotope shift to give additional motivation for performing so complex a calculation.

Chapter five describes a pilot calculation, carried out with a model potential, which was undertaken to gain experience of the PNC problem and to develop routines which would be useful in the main calculations. These uncovered a number of numerical difficulties, which were traced to the use of a uniform nuclear density distribution.

Chapter six contains what is in effect a combination of the theory of chapters two and five, the derivation of the PNC MCDF equations. To do this we must first set up the parity mixed energy functional; since this is a rather long and involved process it has been placed in appendix one and only the briefest outline is given in the main text. We then discuss some of the problems involved in the practical solution of the PNC MCDF equations, and describe the methods used to overcome them. Finally, the question of shielding in a MCDF framework is discussed.

Chapter seven may seem like a diversion from the main subject of this thesis; however, the theory of chapter six shows that, before we can do a PNC calculation, we need energies, eigenvalues, Lagrange multipliers, mixing coefficients, wavefunctions and transition matrix elements from a parity conserving calculation. This chapter reports our attempts to obtain these by means of simple MCDF calculations, then by more complex ones in which correlation has been taken into account by means of configuration interaction (CI). The atoms considered are bismuth, cesium, thallium and lead, these being of experimental interest in PNC.

Equipped with the results of these parity conserving calculations, we attack the PNC problem. The results of this are given in chapter eight, where we display results with and without CI and with and without orthogonality constraints. Results for the PNC-induced E1 matrix element are given in both Coulomb (velocity form) and Babushkin (length form) gauges; the latter show greater stability and are the results we prefer. For cesium, thallium and bismuth we are able to obtain reasonable gauge invariance in the unshielded results, in contrast to the results of previous work by other investigators.

Finally, in chapter nine we compare our results with other calculations and with experiment, and draw our conclusions. A section suggesting further work is also included.

The appendices contain material that, although important, is not essential to the main text. The first has already been referred to, and contains a detailed derivation of the parity mixed energy functional. Appendix two contains a

description of some basis set expansion schemes that were used at one stage but not for any of the results quoted in this thesis. Appendix three gives analytic formulae for the PNC Lagrange multipliers, and appendix four describes the computer program which is listed in appendix five. Finally, in appendix six we give various parameters that would be useful to anyone wishing to reproduce these results.

§1.3 Units

In general standard atomic units (a.u.) have been used in this thesis. These are chosen such that $\hbar$, the electronic charge e, and the electronic mass m_e are unity. Then the unit of length is a_o, the radius of the first Bohr orbit in hydrogen, and the unit of time is the time taken for an electron in the first Bohr orbit in hydrogen to go through one radian. In these units the speed of light is $1/\alpha \simeq 137$, where α is the fine structure constant.

At times it is convenient to give energies in units of cm^{-1}, which is also referred to as the Kaiser (k); this is particularly so when we wish to make comparison between theoretical and experimental results. In this thesis, 1 a.u. has been taken to be equal to 219474.62 cm^{-1}, corresponding to $1/\alpha = 137.0373$; however, the effects of replacing this with a more recent value of $1/\alpha = 137.035968 \pm .000023$ (Tsui et al. (1982)) are negligible.

§1.4 Notation

In general, notation that is not completely standard will be introduced as it appears. However, the labelling of orbitals within a relativistic framework may not be familiar and so is described below.

As usual, we label an orbital by an integer followed by a letter, the integer representing the principal quantum number n (equivalent to the energy level in the simplest Schrödinger picture for hydrogen) and the letter the orbital angular momentum ℓ. However, in a relativistic formulation the total angular momentum j is also important; so if $j=\ell-\frac{1}{2}$ we will denote the orbital by $n\bar{\ell}$, whilst if $j=\ell+\frac{1}{2}$ we will denote it by $n\ell$. We will also write $n\ell-$ for $n\bar{\ell}$ at times. The κ-value of an orbital may be defined to contain information on both j and ℓ:

$$\kappa = -2(j-\ell)(j+\tfrac{1}{2}) \qquad (1.4.1)$$

The values of j, ℓ, κ and the parity of the orbitals referred to in this thesis are given in table 1.1.

A useful concept is that of a manifold. A manifold may be regarded as a collection of configurations which would all be the same if we neglected coupling and the total angular momenta of individual electrons. The total angular momentum of the configurations may or may not be specified.

Thus the manifold $6p^3$ contains the five configurations $(6\bar{p}^2 6p)_{3/2}$, $((6p^2)_0 6\bar{p})_{1/2}$, $((6p^2)_2 6\bar{p})_{3/2}$, $((6p^2)_2 6\bar{p})_{5/2}$ and $(6p^3)_{3/2}$, whilst the manifold $(6p^2)_2$ contains the configurations $(6\bar{p}6p)_2$ and $(6p^2)_2$.

TABLE 1.1

Angular quantum numbers

Orbital (NR)	$s_{1/2}$	$p_{1/2}$	$p_{3/2}$	$d_{3/2}$	$d_{5/2}$	$f_{5/2}$	$f_{7/2}$	$g_{7/2}$	$g_{9/2}$
(Rel.)	s	$\bar{p}$	p	$\bar{d}$	d	$\bar{f}$	f	$\bar{g}$	g
ℓ	0	1	1	2	2	3	3	4	4
j	1/2	1/2	3/2	3/2	5/2	5/2	7/2	7/2	9/2
κ	-1	+1	-2	+2	-3	+3	-4	+4	-5
parity	even	odd	odd	even	even	odd	odd	even	even

Chapter 2

The Revelations of Devout and Learn'd

Who rose before us, and as Prophets burn'd.....

Khayyám (1100b)

Basic Multiconfigurational Dirac-Hartree-Fock Theory

CHAPTER 2

BASIC MULTICONFIGURATIONAL DIRAC-HARTREE-FOCK THEORY

§2.1 The Dirac equation for hydrogen and its solution

We consider first the Dirac equation for hydrogen. There are a number of reasons for doing so; hydrogen is the simplest atom, and so the equations governing hydrogen are the simplest, and therefore show most clearly the principles which apply in all atoms and ions; and hydrogen is the only atom for which the solutions of the Dirac equation can be expressed in terms of mathematically well-known functions. Therefore we will set up and solve the Dirac equation for hydrogen before considering the general n-electron atom or ion.

The Dirac equation for a single-electron (i.e. hydrogenic) atom is

$$[c\underset{\sim}{\alpha}\cdot\underset{\sim}{p} + \beta c^2 + V(\underset{\sim}{r})]\ \psi(\underset{\sim}{r}) = E\psi(\underset{\sim}{r}) \qquad (2.1.1)$$

which is an eigenvalue problem, and which must be solved to give the eigenvalues E and eigenfunctions $\psi(\underset{\sim}{r})$. The quantities $\underset{\sim}{\alpha}$ and β are not uniquely defined, but are usually taken to be

$$\underset{\sim}{\alpha} = \begin{pmatrix} 0 & \underset{\sim}{\sigma} \\ \underset{\sim}{\sigma} & 0 \end{pmatrix} \quad \text{and} \quad \beta = \begin{pmatrix} I & 0 \\ 0 & -I \end{pmatrix} \qquad (2.1.2)$$

where $\underset{\sim}{\sigma}$ is a 3-vector whose components are the Pauli spin matrices and I is the unit 2×2 matrix; $\underset{\sim}{p}$ is the normal

momentum operator $\underset{\sim}{p} = -i\underset{\sim}{\nabla}$, c is the velocity of light and $V(\underset{\sim}{r})$ is the potential at $\underset{\sim}{r}$ due to the nucleus, i.e.

$$V(\underset{\sim}{r}) = -Z/|\underset{\sim}{r}-\underset{\sim}{r}_N| \qquad (2.1.3)$$

where $\underset{\sim}{r}_N$ is the position of the nucleus, if we assume that the nucleus is a point charge of magnitude Z and neglect the weak and Breit interactions.

To solve the Dirac equation (2.1.1), we assume for simplicity that the nucleus is fixed at the origin. This corresponds to an assumption that the nucleus is infinitely heavy. Then (2.1.1) becomes

$$[c\underset{\sim}{\alpha}\cdot\underset{\sim}{p} + \beta c^2 - Z/r]\ \psi(\underset{\sim}{r}) = E\psi(\underset{\sim}{r}) \qquad (2.1.4)$$

This has as solutions (Messiah (1965) p927)

$$\psi_{n\kappa m} = \begin{pmatrix} \frac{1}{r}\,\chi_{\kappa,m}(\theta,\phi) & P_{n\kappa}(r) \\ i\frac{1}{r}\,\chi_{-\kappa,m}(\theta,\phi) & Q_{n\kappa}(r) \end{pmatrix} \qquad (2.1.5)$$

$$n = 1,2,3,\ldots$$

$$\kappa = -n,\ -n+1,\ldots,-1,1,2,\ldots,n-1$$

where

$$\chi_{\kappa,m}(\theta,\phi) = \sum_{s=\pm\frac{1}{2}} C(\ell\tfrac{1}{2},j;m-s,s)\ Y_\ell^{m-s}(\theta,\phi)\Phi_{\frac{1}{2}}^{s} \qquad (2.1.6)$$

$$Y_\ell^{m-s}(\theta,\phi) = \frac{1}{\sqrt{\pi}}\ P_\ell^{m-s}(\theta)e^{i(m-s)\phi} \qquad (2.1.7)$$

is a spherical harmonic function, $P_\ell^{m-s}(\theta)$ is a Legendre polynomial normalized on the interval $[0,2\pi]$, $C(\ell,\frac{1}{2},j;m-s,s)$ is a Clebsch-Gordan coefficient,

$$\Phi^{\frac{1}{2}}_{\frac{1}{2}} = \begin{pmatrix}1\\0\end{pmatrix} \text{ and } \Phi^{-\frac{1}{2}}_{\frac{1}{2}} = \begin{pmatrix}0\\1\end{pmatrix} \tag{2.1.8}$$

$$j = |\kappa| - \tfrac{1}{2} \tag{2.1.9}$$

$$\begin{aligned} \ell &= \kappa \qquad \text{if } \kappa > 0 \\ \ell &= -\kappa - 1 \qquad \text{if } \kappa < 0 \end{aligned} \tag{2.1.10}$$

and, since (Grant (1970))

$$\underset{\sim}{j}^2 \chi_{\kappa,m} = j(j+1)\, \chi_{\kappa,m} \tag{2.1.11}$$

$$\underset{\sim}{\ell}^2 \chi_{\kappa,m} = \ell(\ell+1)\, \chi_{\kappa,m} \tag{2.1.12}$$

$$j_z \chi_{\kappa,m} = m \chi_{\kappa,m} \tag{2.1.13}$$

and

$$K\chi_{\kappa,m} = -\beta\kappa\chi_{\kappa,m} \tag{2.1.14}$$

where

$$\underset{\sim}{j} = \underset{\sim}{r} \times \underset{\sim}{p} + \tfrac{1}{2}\, \underset{\sim}{\sigma} \tag{2.1.15}$$

$$\underset{\sim}{\ell} = \underset{\sim}{r} \times \underset{\sim}{p} \tag{2.1.16}$$

and

$$K = \beta(1 + \underset{\sim}{\sigma} \cdot \underset{\sim}{\ell}) \tag{2.1.17}$$

the functions $P_{n\kappa}$ and $Q_{n\kappa}$ must satisfy

$$\begin{aligned} &\frac{dP_{n\kappa}(r)}{dr} + \frac{\kappa}{r} P_{n\kappa}(r) - \left(c + \frac{Z}{cr} - \frac{E}{c} \right) Q_{n\kappa}(r) = 0 \\ &\frac{dQ_{n\kappa}(r)}{dr} - \frac{\kappa}{r} Q_{n\kappa}(r) + \left(c + \frac{Z}{cr} - \frac{E}{c} \right) P_{n\kappa}(r) = 0 \end{aligned} \tag{2.1.18}$$

In general these equations have no normalizable solution; but for the eigenvalues $E_{n\kappa}$ of E there exist eigensolutions which are products of a polynomial of degree $n - |\kappa|$ and an exponential function. The corresponding eigenvalues may be shown to be degenerate in m:

$$E_{n\kappa} = E_{n\kappa m} = c^2 \left\{ 1 + \frac{(Z/c)^2}{\left[\sqrt{|\kappa|^2-(Z/c)^2} + (n - |\kappa|)\right]^2} \right\}^{-\frac{1}{2}} \tag{2.1.19}$$

A fuller treatment of this problem is given in many of the standard texts on Quantum Mechanics, e.g. Merzbacher (1970).

§2.2 Many-electron atoms

In this section we again assume an atom with an infinitely heavy nucleus located at the origin, and neglect the weak and Breit interactions. Under these conditions we may write the Dirac equation for an N-electron atom, as before, in the form

$$H\Psi = E\Psi \tag{2.2.1}$$

where

$$H = \sum_{k=1}^{N} \left[c\underset{\sim}{\alpha}_k \cdot \underset{\sim}{p}_k + (\beta_k - 1)c^2 + V(\underset{\sim}{r}_k) \right] - \sum_{1 \leq j < k \leq N} \frac{1}{|\underset{\sim}{r}_j - \underset{\sim}{r}_k|} \tag{2.2.2}$$

In general this equation is not soluble in terms of known mathematical functions, and so some approximate method must be used. The method outlined below is the "Multiconfigurational Dirac-Hartree-Fock" (MCDF) method.

Consider the functional

$$\mathcal{E}[\Psi] = \frac{\langle \Psi | \boldsymbol{H} | \Psi \rangle}{\langle \Psi | \Psi \rangle} \qquad (2.2.3)$$

Then it is well known (see, for example, Fischer (1977)) that the functions which give stationary values of $\mathcal{E}$ are the eigenfunction solutions of (2.2.1), and the eigenvalues of (2.2.1) are the corresponding values of $\mathcal{E}$.

Suppose we restrict the domain of the functional $\mathcal{E}$. Then any function which gives a stationary value of the restriction of $\mathcal{E}$ to that domain will approximate to an eigenfunction solution of (2.2.1), and the corresponding value of $\mathcal{E}$ to the corresponding eigenvalue. By a suitable choice of the domain we hope to obtain a function close to the eigenfunction solution of (2.2.1) in a computationally simple way.

We define our domain by requiring that the function Ψ may be expressed as

$$\Psi_a = \sum_{r=1}^{N_c} c_{ar} \Phi_r(\underset{\sim}{r}_1, \ldots, \underset{\sim}{r}_n) \qquad (2.2.4)$$

where each $\Phi_r(\underset{\sim}{r}_1, \ldots, \underset{\sim}{r}_n)$ is a sum of Slater determinants of single-particle functions $\psi_\alpha(\underset{\sim}{r})$ corresponding to one of the N_c jj-coupled configurations, and the functions $\psi_\alpha(\underset{\sim}{r})$ are required to conform to the restrictions

$$\langle \psi_\alpha | \psi_\beta \rangle = \delta_{\alpha\beta} \qquad (2.2.5)$$

$$\psi_\alpha(\underset{\sim}{r}) = \frac{1}{r} \begin{pmatrix} P_{n_\alpha, \kappa_\alpha}(r)\, \chi_{\kappa_\alpha, m_\alpha}(\theta, \phi) \\ iQ_{n_\alpha, \kappa_\alpha}(r)\, \chi_{-\kappa_\alpha, m_\alpha}(\theta, \phi) \end{pmatrix} \qquad (2.2.6)$$

and we also require that

$$\sum_{r=1}^{N_c} |c_{ar}|^2 = 1 \qquad (2.2.7)$$

Under these conditions $\langle\Psi|\Psi\rangle = 1$ and so we may write

$$E[\Psi_a] = \sum_{r,s} c_{ar} c_{as} H_{rs} \qquad (2.2.8)$$

where

$$H_{rs} = \langle\Phi_r|\mathcal{H}|\Phi_s\rangle \qquad (2.2.9)$$

$$= \sum_a q_a(r) I(aa) + \sum_{k;b\geq a} f_r^k(ab) F^k(ab)$$

$$+ \sum_{b>a} g_r^k(ab) G^k(ab) \qquad (r=s) \quad (2.2.10)$$

$$= \sum_{\substack{abcd \\ k}} V_{rs}^k(abcd) R^k(abcd) + \sum_{ab} T_{rs}(ab) I(ab) \qquad (r\neq s) \quad (2.2.11)$$

Here $q_a(r)$ is the occupation of orbital a in configuration r; $f_r^k(ab), g_r^k(ab), V_{rs}^k(abcd)$ and $T_{rs}(ab)$ are angular coefficients which may be expressed as functions of occupation numbers, recoupling coefficients, coefficients of fractional parantage, etc.; explicitly, if $q_a(r) = 2j_a+1$ or $q_b(r) = 2j_b+1$

$$\begin{aligned}
f_r^o(aa) &= \tfrac{1}{2} q_a(r)[q_a(r)-1] \\
f_r^k(aa) &= -\tfrac{1}{2} q_a(r)^2 \begin{pmatrix} j_a & k & j_a \\ \tfrac{1}{2} & 0 & -\tfrac{1}{2} \end{pmatrix}^2 \qquad k\neq 0 \\
f_r^o(ab) &= q_a(r) q_b(r) \qquad a\neq b \\
f_r^k(ab) &= 0 \qquad k\neq 0 \quad a\neq b
\end{aligned} \qquad (2.2.12)$$

and

$$g_r^k(ab) = -q_a(r)q_b(r) \begin{pmatrix} j_a & k & j_b \\ \frac{1}{2} & 0 & -\frac{1}{2} \end{pmatrix}^2 \qquad (2.2.13)$$

and if $q_a(r) < 2j_a+1$ and $q_b(r) < 2j_b+1$

$$f_r^k(ab) = V_{rr}^k(abab) \qquad (2.2.14)$$

$$g_r^k(ab) = V_{rr}^k(abba) \qquad (2.2.15)$$

where $V_{rs}^k(abcd)$ is an 'MCP coefficient'; also

$$I(ab) = \int_o^\infty dr\Big\{c(Q_aP_b'-P_aQ_b')-2c^2Q_aQ_b+\frac{c\kappa_b}{r}(P_aQ_b+Q_aP_b)$$

$$+V(r)(P_aP_b+Q_aQ_b)\Big\}\,\delta_{\kappa_a\kappa_b} \qquad (2.2.16)$$

$$F^k(ab) = R^k(abab) \qquad (2.2.17)$$

$$G^k(ab) = R^k(abba) \qquad (2.2.18)$$

$$R^k(abcd) = \int_o^\infty (P_aP_c+Q_aQ_c)\frac{1}{r}\,Y_k(bd;r)dr \qquad (2.2.19)$$

$$Y_k(bd;r) = r\int_o^\infty \frac{r_<^k}{r_>^{k+1}}\Big\{P_b(r')P_d(r')+Q_b(r')Q_d(r')\Big\}dr' \qquad (2.2.20)$$

The condition that $\boldsymbol{E}$ be stationary with respect to variations in the c_{ar} subject to (2.2.7) leads to the equation

$$\underline{\underline{H}}\,\underset{\sim}{c}_a = E_a\underset{\sim}{c}_a \qquad (2.2.21)$$

where $\underset{\sim}{c}_a$ is the column vector with the c_{ar} as its elements, from which we see that the $\underset{\sim}{c}_a$'s and E_a's are the eigenvectors and eigenvalues of the Hamiltonian matrix $\underline{\underline{H}}$. The condition that $\boldsymbol{E}$ be stationary with respect to variations in the P_a and

Q_a subject to the constraint (2.2.5) leads (Grant (1961)) to the Multiconfigurational Dirac-Hartree-Fock equations

$$\frac{dP_a}{dr} + \kappa_a \frac{P_a}{r} - \left(2c - \frac{\varepsilon_a}{c} + \frac{Y_a}{cr}\right) Q_a = - \frac{\chi_a^{(P)}}{r}$$

$$\frac{dQ_a}{dr} - \kappa_a \frac{Q_a}{r} + \left(-\frac{\varepsilon_a}{c} + \frac{Y_a}{cr}\right) P_a = - \frac{\chi_a^{(Q)}}{r} \qquad (2.2.22)$$

where

$$\chi_a^{(P)} = X_a^{(P)} + \frac{r}{c\bar{q}_a} \sum_{b\neq a} \varepsilon_{ab} Q_b$$

$$\chi_a^{(Q)} = X_a^{(Q)} - \frac{r}{c\bar{q}_a} \sum_{b\neq a} \varepsilon_{ab} P_b \qquad (2.2.23)$$

$$Y_a(r) = - rV(r) - \sum_{b,k} y^k(ab)\, Y_k(bb;r) \qquad (2.2.24)$$

$$y^k(ab) = \frac{1+\delta_{ab}}{\bar{q}_a} \sum_r d_r^2 f_r^k(ab) \qquad (2.2.25)$$

$$\bar{q}_a = \sum_r d_r^2 q_a(r) \qquad (2.2.26)$$

$$X_a^{(P)} = \frac{1}{c} \left\{ \sum_{\substack{bk \\ b\neq a}} x^k(ab) Y_k(ab;r) Q_b + \sum_{\substack{bcd \\ k}} x^k(abcd) Y_k(bd;r) Q_c \right\}$$

$$X_a^{(Q)} = \frac{-1}{c} \left\{ \sum_{\substack{bk \\ b\neq a}} x^k(ab) Y_k(ab;r) P_b + \sum_{\substack{bcd \\ k}} x^k(abcd) Y_k(bd;r) P_c \right\} \qquad (2.2.27)$$

$$x^k(ab) = \frac{1}{\bar{q}_a} \sum_r d_r^2 g_r^k(ab) \qquad (2.2.28)$$

$$x^k(abcd) = \frac{1}{\bar{q}_a} \sum_{rs} d_{rs} V_{rs}^k(abcd) \qquad (2.2.29)$$

$$d_r = c_{ar} \qquad (2.2.30)$$

and

$$d_{rs} = c_{ar}c_{as} \qquad (2.2.31)$$

The quantities ε_a and ε_{ab} are Lagrange multipliers corresponding to the condition (2.2.5) for a=b and a≠b respectively.

Thus, to solve the equation (2.2.21) for ζ_a we must know the functions P_a and Q_a; and to solve the equations (2.2.22) we must know the mixing coefficients ζ_a. In practice, we have to make initial estimates for both and then solve (2.2.21) and (2.2.22) in turn until the solutions to both have converged. We call this the "optimal level" (OL) method. It is very time-consuming and frequently there are instabilities which prevent the sequence of iterates from converging. Also, the calculation has to be repeated for each atomic state.

We therefore look for a simpler method. Suppose we find the functions P_a, Q_a by requiring them to give stationary values, not of the functional $\mathcal{E}[\Psi]$ of (2.2.8), but of

$$\mathcal{E}[\Psi] = \sum_r d_r{}^2 H_{rr} \qquad (2.2.32)$$

where the d_r are predetermined weights given at the outset; determine the $c_{\zeta a}$ from equation (2.2.21); and then stop. This will be less accurate; but it will be much faster; also, one calculation can yield information about a number of levels; and in practice it is found to be much more stable. We call this the "extended average level" (EAL) method. In practice the differences between results from this and the OL method are usually very small. All results reported in this thesis were calculated by this method. Relations between the OL and EAL methods in particular examples have been discussed by Hata and Grant (1983c,1983d) and Pyper (1983). See also §6.2 for a more detailed discussion of this point.

§2.3 The Breit Interaction

For many purposes, it is sufficient to write the total potential energy of an atom as

$$V_o = \sum_{i=1}^{N} \frac{-Z}{r_i} + \sum_{1\leq i<j\leq N} \frac{1}{r_{ij}} \qquad (2.3.1)$$

where $r_{ij} = |r_i - r_j|$. This corresponds to taking into account only the instantaneous Coulomb interaction between the electrons and between the electrons and the nucleus. For precise calculations, however, this is inadequate and a more accurate expression for the potential energy is necessary.

This more accurate form may be derived from the theory of quantum electrodynamics. There are a number of approaches (Breit (1929, 1930, 1932), Bethe and Salpeter (1957), Mann and Johnson (1971), Mittleman (1971, 1972), Grant and Pyper (1976)), but in all cases the result is the same. A further term must be added to the potential which has the form, to order $\alpha^2 = \frac{1}{c^2}$,

$$V_B = \tfrac{1}{2} \sum_{pqrs} N(a_p^\dagger a_q^\dagger a_r a_s) \langle p_1 q_2 | \tfrac{1}{2} \{B(\nu_{ps}, r_{12}) + B(\nu_{qr}, r_{12})\} | s_1 r_2 \rangle \qquad (2.3.2)$$

where the notation of second quantization has been used; i.e. $N(...)$ denotes normal ordering as usual, $a_p^\dagger$ is a creation operator for orbital p, and a_r is an annihilation operator for orbital r. Also

$$\nu_{ps} = \frac{\varepsilon_p - \varepsilon_s}{c} \qquad (2.3.3)$$

and

$$B(\nu,r) = -\left(\alpha_1\cdot\alpha_2\ \frac{\cos \nu r}{r} - (\alpha_1\cdot\nabla)(\alpha_2\cdot\nabla)\ \frac{1-\cos \nu r}{\nu^2 r}\right) \qquad (2.3.4)$$

Alternative forms of (2.3.4) in which the limit $\nu \to 0$ is taken, the gradient operators are replaced by ∇_1 and ∇_2, or the final term is neglected, may be found in the literature.

Thus, if we take the potential to be

$$V' = V_o + V_B \qquad (2.3.5)$$

this will be correct to $o(1/c^2)$. We could, in theory, include this potential in the MCDF equations; however, it is computationally much more convenient to treat V_B as a perturbation as far as calculating the wavefunctions is concerned, but to include it when diagonalizing the Hamiltonian. This leads to results which can be thought of as solutions of the corresponding problem in standard perturbation theory which are correct to all orders within the subspace defined by the chosen set of CSF coupled by the interaction V' (Hata and Grant 1983[e]). Accordingly we proceed as follows.

We already know the matrix elements

$$H^{(o)}_{rs} = \langle\Phi_r| \sum_{i=1}^{N} h_i + V_o |\Phi_s\rangle \qquad (2.3.6)$$

(c.f.(2.2.9)); so we calculate the matrix elements

$$\tilde{H}_{rs} = \langle\Phi_r| \sum_{i=1}^{N} h_i + V_o + V_B |\Phi_s\rangle \qquad (2.3.7)$$

$$= H^{(o)}_{rs} + \langle\Phi_r| V_B |\Phi_s\rangle \qquad (2.3.8)$$

and then recalculate the eigenvalues and eigenvectors of the matrix $\tilde{H}_{rs}$ to give the new atomic energy levels and mixing coefficients.

It may be shown (McKenzie and Grant (1980)) that the matrix element

$$\langle\Phi_r|\ V_B\ |\Phi_s\rangle = \sum_{\substack{abcd \\ \mu\nu}} \tau_{rs}^{\mu\nu}(abcd) R_\mu^{\ \nu}(abcd) \qquad (2.3.9)$$

where the quantities $\tau_{rs}^{\mu\nu}(abcd)$ depend only on the occupations and angular quantum numbers of the orbitals a,b,c,d, the angular nature of the configurations r and s, and the parameters μ and ν, and the quantities $R_\mu^{\nu}(abcd)$ are double integrals involving only the radial wavefunctions and various mathematically well-known functions (Bessel functions and powers of r). Their exact form need not concern us.

At the same time as the Breit corrections are included certain other quantum electrodynamic effects (explicitly, the Lamb shift and vacuum polarization) are allowed for. These normally give small effects compared to the Breit interaction.

In some of the calculations reported in this thesis the Breit interaction has been included; in others not. It will be made clear which is the case at the relevant point.

§2.4 Oscillator strengths

It is frequently of interest to know matrix elements of multipole transition operators, for instance in order to calculate transition probabilities from one atomic state to another, to calculate lifetimes of states, or, more recently, to calculate the weak-interaction-induced optical rotation in atomic systems. This particular topic is reported in greater detail since the author of this thesis helped in the development of the theory and programming of it.

The theory is basically as developed by Grant (1974),

but is here extended to the many-electron case. However, it should be noted that there are a number of sign errors in that paper which are corrected below.

§§2.4.1 The electromagnetic 4-potential

The electromagnetic 4-potential must satisfy the wave equation

$$\Box A^{\mu} = 0 \qquad 0 \leq \mu \leq 3 \tag{2.4.1}$$

and the Lorentz gauge condition

$$\partial_{\mu} A^{\mu} = 0 \tag{2.4.2}$$

Then the general scalar potential solution of (2.4.1) and (2.4.2) having the time-dependence factor $\exp(-i\omega t)$ may be written as a linear combination of terms of the form

$$\Phi_{LM} = i^{L}(2L+1) j_{L}\left(\frac{\omega r}{c}\right) C_{M}^{L}(\theta,\phi)\, e^{-i\omega t} = cA^{o}_{LM} \tag{2.4.3}$$

where $j_L(\omega r/c)$ is a spherical Bessel function and $C_M^L(\theta,\phi)$ is a component of the usual spherical tensor,

$$C_{M}^{L}(\theta,\phi) = \sqrt{\frac{4\pi}{2L+1}}\, Y_{L}^{M}(\theta,\phi) \tag{2.4.4}$$

and the vector potential solution may be written as a linear combination of terms of the form

$$\underset{\sim}{A}^{e}_{LM} = \frac{1}{\omega\sqrt{L(L+1)}}\, \underset{\sim}{\nabla}\times\underset{\sim}{L}\, \Phi_{LM}$$

$$\underset{\sim}{A}^{\ell}_{LM} = \frac{1}{i\omega}\, \underset{\sim}{\nabla}\, \Phi_{LM} \tag{2.4.5}$$

and

$$\underset{\sim}{A}^{m}_{LM} = \frac{1}{c\sqrt{L(L+1)}}\, \underset{\sim}{L}\, \Phi_{LM}$$

These are all elements of tensors of rank L.

After a considerable amount of algebra we obtain

$$\underset{\sim}{A}^{e}_{LM} = \frac{-i^{L+1}}{c}\left\{\sqrt{L(2L+3)}\left[\underset{\sim}{e}\,\underset{\sim}{C}^{L+1}\right]^{L}_{M} j_{L+1}\left(\frac{\omega r}{c}\right) - \sqrt{(L+1)(2L-1)}\left[\underset{\sim}{e}\,\underset{\sim}{C}^{L-1}\right]^{L}_{M} j_{L-1}\left(\frac{\omega r}{c}\right)\right\}$$

$$\underset{\sim}{A}^{\ell}_{LM} = \frac{-i^{L+1}}{c}\left\{\sqrt{(L+1)(2L+3)}\left[\underset{\sim}{e}\,\underset{\sim}{C}^{L+1}\right]^{L}_{M} j_{L+1}\left(\frac{\omega r}{c}\right) + \sqrt{L(2L-1)}\left[\underset{\sim}{e}\,\underset{\sim}{C}^{L-1}\right]^{L}_{M} j_{L-1}\left(\frac{\omega r}{c}\right)\right\} \qquad (2.4.6)$$

$$\underset{\sim}{A}^{m}_{LM} = -\frac{i^{L}}{c}(2L+1)\left[\underset{\sim}{e}\,\underset{\sim}{C}^{L}\right]^{L}_{M} j_{L}\left(\frac{\omega r}{c}\right)$$

where $\underset{\sim}{e}$ is a unit vector perpendicular to the direction of propagation of the wave.

Since $\underset{\sim}{A}^{e}_{LM}$ and $\underset{\sim}{A}^{\ell}_{LM}$ have the same parity we combine them and write the potential as

$$A^{\mu}(x) = \sum_{\substack{LM\\ \omega}} c_{LM}(\omega)\left\{\sqrt{\frac{\omega}{\pi c}}\left[A^{e}_{LM}(\underset{\sim}{r}) + G_{L}A^{\ell}_{LM}(\underset{\sim}{r})\right]^{\mu} e^{-i\omega t}\right\} \quad \text{(electric type)}$$

$$A^{\mu}(x) = \sum_{\substack{LM\\ \omega}} c_{LM}(\omega)\left\{\sqrt{\frac{\omega}{\pi c}}\left[A^{m}_{LM}(\underset{\sim}{r})\right]^{\mu} e^{-i\omega t}\right\} \quad \text{(magnetic type)} \qquad (2.4.7)$$

The factor $\sqrt{\frac{\omega}{\pi c}}$ has been included so that the functions in curly brackets are delta-normalized. The $c_{LM}(\omega)$ and G_{L} are arbitrary expansion coefficients.

§§2.4.2 Reduction of general matrix elements to single-particle matrix elements

The quantity that we wish to calculate is the matrix element

$$\langle f|T(\omega)|i\rangle$$

where $|i\rangle$ and $|f\rangle$ are the initial and final atomic state wavefunctions and T is the interaction Hamiltonian corresponding to the transition from i to f. T will be expressed as a linear combination of the terms Φ_{LM}, A^{e}_{LM}, A^{ℓ}_{LM} and A^{m}_{LM}, and so we may write $T(\omega) = \sum_{LM} T^{L}_{M}(\omega)$ where T^{L}_{M} is an element of a tensor of rank L.

Then, applying the Wigner-Eckart Theorem

$$\langle f|T(\omega)|i\rangle = \sum_{LM} \langle f|T^{L}_{M}(\omega)|i\rangle$$

$$= \sum_{LM} (-1)^{j_f - m_f} \begin{pmatrix} j_f & L & j_i \\ -m_f & M & m_i \end{pmatrix} \langle f\|T^{L}(\omega)\|i\rangle \qquad (2.4.8)$$

The matrix element $\langle f\|T^{L}(\omega)\|i\rangle$ is then expressed in terms of the configuration state functions:

$$\langle f\|T^{L}(\omega)\|i\rangle = \sum_{r,s} c_{fr} c_{is} \langle r\|T^{L}(\omega)\|s\rangle \qquad (2.4.9)$$

These are then expressed in terms of single particle matrix elements

$$\langle r\|T^{L}(\omega)\|s\rangle = \sum_{ab} d^{L}_{ab}(rs) \langle a\|t^{L}(\omega)\|b\rangle \qquad (2.4.10)$$

The coefficients $d^{L}_{ab}(rs)$ are dependent only on the angular

characteristics of the configurations r and s and the orbitals a and b and are calculated by the modified MCT section of the MCDF program (Grant et al. (1980)). It is important that the indices a and b are not interchanged, as in the original version of MCT (Pyper et al. (1975)), since we have no simple relation between $\langle a\|t^L(\omega)\|b\rangle$ and $\langle b\|t^L(\omega)\|a\rangle$, although

$$\langle a\|t^L(\omega)\|b\rangle = \langle b\|t^L(-\omega)\|a\rangle(-1)^{j_a-j_b}\sqrt{\frac{2j_b+1}{2j_a+1}} \qquad (2.4.11)$$

Here $t^L(\omega)$ is the single-particle operator corresponding to the operator $T^L(\omega)$.

§§2.4.3 The interaction Hamiltonian

We are therefore interested in calculating the matrix elements of the interaction Hamiltonian

$$H_{int} = \int j^\mu(x)a_\mu(x)d^3x \qquad (2.4.12)$$

where

$$j^\mu(x) = \sum_{\alpha\beta} q_\alpha^\dagger \bar{\psi}_\alpha(x)\gamma^\mu\psi_\beta(x)q_\beta \qquad (2.4.13)$$

and

$$a^\mu(x) = cA^\mu(x) + c^\dagger[A^\mu(x)]^\dagger \qquad (2.4.14)$$

Here the c and $c^\dagger$ are photon annihilation and creation operators and the q_α and $q_\alpha^\dagger$ annihilation and creation operators for an electron in state α.

Then, writing

$$H_{int} = H^{em} + H^{abs} \tag{2.4.15}$$

with

$$H^{em} = \sum_{\alpha\beta} q_\alpha{}^\dagger q_\beta c^\dagger M^\dagger_{\alpha\beta}(t) \tag{2.4.16}$$

and

$$H^{abs} = \sum_{\alpha\beta} q_\alpha{}^\dagger q_\beta c M_{\alpha\beta}(t) \tag{2.4.17}$$

being the operators which give rise to emission and absorption of radiation, we obtain

$$M_{\alpha\beta}(t) = \sqrt{\frac{\omega}{\pi c}} \int \bar{\psi}_\alpha(x) c\gamma^\mu A_\mu(x) \psi_\beta(x) d^3x \tag{2.4.18}$$

The time factors may be removed easily

$$M_{\alpha\beta}(t) = M_{\alpha\beta} \exp[i(E_\alpha - E_\beta - \omega)t] \tag{2.4.19}$$

and, in more conventional notation,

$$M_{\alpha\beta} = \sqrt{\frac{\omega}{\pi c}} \int \psi_\alpha^*(\underset{\sim}{r}) \left[\Phi(\underset{\sim}{r}) - c\underset{\sim}{\alpha}\cdot\underset{\sim}{A}(\underset{\sim}{r})\right] \psi_\beta(\underset{\sim}{r}) d^3\underset{\sim}{r} \tag{2.4.20}$$

$$= \sqrt{\frac{\omega}{\pi c}} \langle\alpha|\Phi(\underset{\sim}{r}) - c\underset{\sim}{\alpha}\cdot\underset{\sim}{A}(\underset{\sim}{r})|\beta\rangle \tag{2.4.21}$$

§§2.4.4 Reduction to radial integrals

Comparison of equations (2.4.21), (2.4.10), (2.4.9), (2.4.8), and (2.4.6) shows that we must calculate matrix elements of the form

$$\langle a\| j_L\left(\frac{\omega r}{c}\right) C^L \|b\rangle \quad \text{and} \quad \langle a\| j_k\left(\frac{\omega r}{c}\right) [\underset{\sim}{\alpha}\, \underset{\sim}{C}^k]^L \|b\rangle$$

$$(k=L,\ L\pm1)$$

After considerable algebra we obtain

$$\langle a\| i^L(2L+1)j_L\left(\frac{\omega r}{c}\right)C^L\| b\rangle = (-1)^{j_a+\frac{1}{2}}\sqrt{(2j_a+1)(2j_b+1)}(2L+1)i^L \times \begin{pmatrix} j_a & L & j_b \\ \frac{1}{2} & 0 & -\frac{1}{2} \end{pmatrix} J^{(L)}(\omega) \qquad (2.4.22)$$

and

$$\langle a\| j_k\left(\frac{\omega r}{c}\right)[\alpha\, C^k]^L\| b\rangle = (-1)^{j_a+\frac{1}{2}}\sqrt{(2j_a+1)(2j_b+1)}\begin{pmatrix} j_a & L & j_b \\ \frac{1}{2} & 0 & -\frac{1}{2} \end{pmatrix} \times iK_{ab}^{(k,L)}(\omega) \qquad (2.4.23)$$

where

$$K_{ab}^{(L+1,L)}(\omega) = \frac{(\kappa_a-\kappa_b)I_{L+1}^{+}(\omega)+(L+1)I_{L+1}^{-}(\omega)}{\sqrt{(L+1)(2L+3)}}$$

$$K_{ab}^{(L,L)}(\omega) = \frac{-(\kappa_a+\kappa_b)I_L^{+}(\omega)}{\sqrt{L(L+1)}} \qquad (2.4.24)$$

$$K_{ab}^{(L-1,L)}(\omega) = \frac{(\kappa_a-\kappa_b)I_{L-1}^{+}(\omega)-LI_{L-1}^{-}(\omega)}{\sqrt{L(2L-1)}}$$

and

$$I_L^{\pm}(\omega) = \int_o^\infty (P_aQ_b \pm Q_aP_b)j_L\left(\frac{\omega r}{c}\right)dr \qquad (2.4.25)$$

$$J^{(L)}(\omega) = \int_o^\infty (P_aP_b+Q_aQ_b)j_L\left(\frac{\omega r}{c}\right)dr \qquad (2.4.26)$$

Then, from equations (2.4.26), (2.4.25), (2.4.24), (2.4.23) (2.4.22), (2.4.21) and (2.4.6)

$$M_{ab} = \sqrt{\frac{\omega}{\pi c}}\,(-1)^{j_a - m_a} \begin{pmatrix} j_a & L & j_b \\ -m_a & M & m_b \end{pmatrix} (-1)^{j_a - \frac{1}{2}} \sqrt{(2j_a+1)(2j_b+1)}$$

$$\times \begin{pmatrix} j_a & L & j_b \\ \frac{1}{2} & 0 & -\frac{1}{2} \end{pmatrix} \quad \bar{M}_{ab} \qquad (2.4.27)$$

where $\bar{M}_{ab}$ depends on the form of A taken; for magnetic multipoles

$$\bar{M}^{m}_{ab} = i^{L-1}\,\frac{2L+1}{\sqrt{L(L+1)}}\,(\kappa_a+\kappa_b)\,I^{+}_{L}(\omega) \qquad (2.4.28)$$

while for electric multipoles

$$\bar{M}^{e}_{ab}(G) = \bar{M}^{e}_{ab}(0) + G_L \bar{M}^{\ell}_{ab} \qquad (2.4.29)$$

where

$$\bar{M}^{e}_{ab}(0) = i^{L}\left\{\sqrt{\frac{L}{L+1}}\;[(\kappa_a-\kappa_b)\,I^{+}_{L+1} + (L+1)\,I^{-}_{L+1}]\right.$$

$$\left. -\sqrt{\frac{L+1}{L}}\;[(\kappa_a-\kappa_b)\,I^{+}_{L-1} - LI^{-}_{L-1}]\right\} \qquad (2.4.30)$$

$$\bar{M}^{\ell}_{ab} = i^{L}\left\{-(2L+1)J^{(L)} + (\kappa_a-\kappa_b)(I^{+}_{L+1} + I^{+}_{L-1})\right.$$

$$\left. - LI^{-}_{L-1} + (L+1)\,I^{-}_{L+1}\right\} \qquad (2.4.31)$$

§2.4.5 Application

Combining (2.4.27), (2.4.19), (2.4.15), (2.4.16), (2.4.17), (2.4.10), and (2.4.9) we obtain the final result for the transition matrix element:

$$\langle f\|T^L(\omega)\|i\rangle = \sum_{\substack{rs\\ab}} c_{fr}c_{is}d^L_{rs}(ab)(-1)^{j_a-\frac{1}{2}}\sqrt{(2j_a+1)(2j_b+1)} \times \begin{pmatrix} j_a & L & j_b \\ \frac{1}{2} & 0 & -\frac{1}{2}\end{pmatrix} \bar{M}_{ab} \tag{2.4.32}$$

where $\bar{M}_{ab}$ is as defined in (2.4.28)-(2.4.31).

The question as to whether we should take the magnetic or the electric form for the matrix element $\bar{M}_{ab}$ is decided by the value of L and the parity of the initial and final states (π_i and π_f); if

$$\pi_f\pi_i(-1)^L > 0 \qquad \text{the transition is electric}$$

and if (2.4.33)

$$\pi_f\pi_i(-1)^L < 0 \qquad \text{the transition is magnetic}$$

By the conservation of energy

$$\omega = E_f - E_i \tag{2.4.34}$$

Finally, it will be noted that the results for electric matrix elements depend on the value of G_L. It may be shown that, it the wavefunctions are such that the equation for conservation of charge

$$\text{div } \underset{\sim}{j} + \frac{\partial \rho}{\partial t} = 0, \tag{2.4.35}$$

where $\underset{\sim}{j}$ and ρ are defined in the usual way, is satisfied, then the terms dependent on G_L will vanish. Thus gauge invariance follows automatically if matrix elements are calculated using energies and wavefunctions calculated in any local potential

(for instance, a hydrogenic or semi-empirical model potential) or in developments of these using perturbation theory, and also in the random phase approximation (Johnson et al. (1980)) or time dependent Hartree-Fock; but does not follow automatically, and in general is not obtained, if the orbitals are defined in a non-local potential, as is the case in the MCDF (or, for that matter, the simpler Hartree-Fock) models. However, observable quantities should be gauge invariant; thus any failure to produce gauge invariant results is a major defect of the theoretical model used. However, even in the Hartree-Fock case, gauge invariance does not imply that the results are necessarily correct; Hibbert ( ) gives examples where good gauge invariance was obtained in a MCHF calculation but the matrix elements were not correct. Therefore, since some models, known to be inaccurate, give gauge invariant results, we can only say that gauge invariance is a necessary consequence of, but not a sufficient condition for, accurate transition matrix elements.

This matter is discussed further in the context of the present calculations in §9.5.4.

In practice we normally quote the results for $G_L = 0$ (Coulomb gauge) and $G_L = \sqrt{\frac{L+1}{L}}$ (Babushkin gauge), which for electric dipole transitions, in the nonrelativistic limit, become the velocity and length forms of the dipole operator respectively, multiplied by a few simple factors (Grant (1974)).

§2.5 The computer program

A computer program has been written which performs all the calculations referred to in this chapter. It has been more fully described elsewhere (Grant et al. (1980), McKenzie, Grant and Norrington (1980)).

In a full calculation there will be six distinct stages.

Firstly, the coefficients $V^k_{rs}(abcd)$ first introduced in equation (2.2.11) must be calculated (MCP stage). All the coefficients required are calculated and written to a file on disk.

Secondly, the equations (2.2.22), using the substitutions (2.2.23) to (2.2.31), must be solved, using the coefficients calculated in the MCP stage. Then the Hamiltonian matrix must be set up and diagonalized to give the mixing coefficients $\underset{\sim}{c}_a$ (c.f. (2.2.21)). The resulting wavefunctions and mixing coefficients are then written to another file on disk. This we call the MCDF stage.

In this part of the program, and later, we need to know the value of a number of functions, including the wavefunctions P_a and Q_a and the potentials Y_a, $\chi_a^{(P)}$, and $\chi_a^{(Q)}$. These are

calculated at points equally spaced on a grid logarithmic in r, i.e. at points

$$r_i = r_o e^{h(i-1)} \qquad i = 1,2,\ldots,N \qquad (2.5.1)$$

This choice was made because the wavefunctions vary more rapidly near the origin than further out. Normally we take $r_o = 10^{-5}$ a.u. and h = 0.05, but these can be altered if desired.

Thirdly, the coefficients $\tau^{\mu\nu}_{rs}(abcd)$ of equation (2.3.9) must be calculated (MCBP stage). These are written to a third file on disk.

Fourthly, the matrix of the Dirac Hamiltonian (including, this time, the Breit interaction) is set up and diagonalized (BENA stage). The resultant eigenvalues and eigenvectors are appended to the MCDF disk file.

Fifthly, the coefficients $d^{L}_{ab}(rs)$ of equation (2.4.10) are calculated and written to a fourth disk file (MCT stage).

Finally, the matrix elements of the multipole transition operators and the corresponding oscillator strengths are calculated (OSCL stage). The energies and mixing coefficients used may either be those from the MCDF or the BENA calculations.

§2.6 Conclusion

The foregoing theory has been developed over a number of years, as has the computer program which applies them. All the stages mentioned in §2.5 are integrated into a single package which will perform any combination of them. The time taken for the program to run varies widely depending on the

complexity of the problem, and on which stages are run; run-times can be as short as a fraction of a second for a simple oscillator strengths calculation to more than an hour for a MCP calculation on a complex atom with configuration interaction.

Providing correlation is adequately allowed for (by configuration interaction) agreement between experimental and computational results is almost perfect.

Chapter 3

And he said unto me,
'Observe, Enoch, these heavenly tablets,
And read what is written thereon,
And mark every individual fact'.

"Enoch" (-110)

Isotope Shift

CHAPTER 3

ISOTOPE SHIFT

§3.1 Introduction

The purpose of this investigation was to continue the work done by Shun (1977) on the use of Hartree-Fock calculations to determine isotope shifts.

Shun used a single configuration Hartree-Fock model to investigate a variety of atoms. His main investigation was on the effect of varying the nuclear size (nuclear field effect) on the orbital eigenvalues, but he also calculated the shift in some single electron transitions of interest in samarium and tin.

This chapter describes the generalization of his work to the MCDF approximation. The advantages of this are:

(i) Many atomic states cannot be adequately described by a single jj-configuration. However, given enough configurations, an atomic state may be described to any required accuracy.

(ii) Many transitions are not 'single electron' transitions, but consist of electronic rearrangements. In Shun's model, where the shift in a transition energy is equated to the difference in shifts of the two corresponding orbital eigenvalues, this is zero.

§3.2 The use of the MCDF equations to calculate the field effect in isotope shift

Different isotopes of an element have nuclei with the

same number of protons but with differing numbers of neutrons. Thus different isotopes have different masses and different nuclear sizes. The present discussion is only concerned with the effects of differing nuclear size, which is the dominant effect for heavy atoms.

The simplest model of a nucleus is one in which the charge density within the nucleus is uniform and the nucleon density is independent of the nuclear mass, A, i.e.

$$\rho(r) = \rho_o \qquad r \leq r_N$$

$$\rho(r) = 0 \qquad r > r_N \tag{3.2.1}$$

where

$$\rho_o = \frac{3Z}{4\pi\, r_N^{\,3}} \tag{3.2.2}$$

and the nuclear radius

$$r_N = a\, A^{1/3} \tag{3.2.3}$$

for some constant a. Experimentally it is found that on average $a = 2.2677 \times 10^{-5}$ a.u. is a good fit for stable nuclei, although individual variations from (3.2.3) cannot be ignored in practice.

A more realistic distribution is the Fermi distribution

$$\rho(r) = \frac{\rho_o}{1+e^{(r-R_h)/b}} \tag{3.2.4}$$

where b and R_h are called the skin thickness and half-radius respectively.

Experimentally, $R_h \tilde{=} 2.2677 \times 10^{-5} A^{1/3}$ a.u. and $b \tilde{=} 1.0353 \times 10^{-5}$ a.u., and ρ_o may be determined from the requirement that $\int_o^\infty 4\pi r^2 \rho(r) dr = Z$. It may be seen that the uniform distribution corresponds to the limit $b \to 0$, when $R_h = r_N$.

The nuclear potential, V(r) can then be calculated from the density:

$$V(r) = 4\pi \left[\frac{1}{r} \int_o^r \rho(r') r'^2 dr' + \int_r^\infty \rho(r') r' dr' \right] \qquad (3.2.5)$$

For the uniform distribution this integrates easily to give

$$\begin{aligned} V(r) &= -\frac{Z}{2} \frac{1}{r_N} \left[3 - (r/r_N)^2\right] && r \leq r_N \\ &= -Z/r && r > r_N \end{aligned} \qquad (3.2.6)$$

The potential due to a Fermi distribution is not easy to integrate analytically and so is determined numerically.

To calculate isotope shifts in transitions, we perform a number of MCDF calculations, each one using the nuclear potential corresponding to the nuclear size of the isotope of interest, but otherwise identical. Each calculation gives a transition energy; and these are subtracted to give the calculated isotope shift. This may seem unwise, since isotope shifts are of the order of 0.1k and energies are often accurate to only 1000k or so; and a variation of several k can be observed when the gridsize h or the inner integration point r_o are changed. However, Shun has established that, providing that all calculations use the same h and r_o, and the wavefunctions are sufficiently converged, then the differences in orbital eigenvalues are stable under variations in h and r_o

(for a treatment of the numerical analysis of this see Grant (1980)).

The present investigation verified that this stability also holds for differences in transition energies. In the multiconfigurational case the additional proviso must be made that the basis of configurations must be the same in each of the calculations.

§3.3 The breakdown of the Broch formula

Broch (1945) has shown that, providing we assume that the change in nuclear size has no effect on the potentials outside the nuclear region - an assumption that seems to be not unreasonable in view of equation (3.2.6) - then the change in an eigenvalue is given by the approximate formula

$$\delta\varepsilon = \varepsilon - \bar{\varepsilon} = - c \left[P\bar{Q} - \bar{P}Q\right]_{r = r_o} \qquad (3.3.1)$$

where r_o is larger than the nuclear radius but small compared to the size of the atom, and the barred terms refer to one isotope and the unbarred to another.

Shun has shown that, for the single configuration case, this approximation breaks down seriously for all except s electrons. He has also shown that the correct form, in the absence of off-diagonal Lagrange multipliers, is

$$\delta\varepsilon = \frac{\left\{-c\left[P\bar{Q}-Q\bar{P}\right]_{r_o} + \int_{r_o}^{\infty} (P\bar{P}+Q\bar{Q})\,\frac{Y-\bar{Y}}{r}\,dr \right.}{\left. -c\int_{r_o}^{\infty} (\bar{Q}\chi^{(P)} - \bar{P}\chi^{(Q)} - Q\bar{\chi}^{(P)} + P\bar{\chi}^{(Q)})\,\frac{1}{r}\,dr \right\}}{\int_{r_o}^{\infty} (P\bar{P}+Q\bar{Q})\,dr} \qquad (3.3.2)$$

In this equation we can identify the first term in the numerator as the Broch term. Since, for small r_o, we have $\int_{r_o}^{\infty} (P\bar{P}+Q\bar{Q}) \simeq 1$, if we assume that $Y=\bar{Y}$, $\chi^{(P)}=\bar{\chi}^{(P)}$, $\chi^{(Q)}=\bar{\chi}^{(Q)}$, $P=\bar{P}$, and $Q=\bar{Q}$ in the region $r > r_o$, this reduces to the Broch formula. The second term is a result of the fact that varying the orbitals varies the direct potential, and the third term is a consequence of the exchange potentials. These latter two terms are indirect effects - the eigenvalue is influenced by the wavefunctions via the potentials rather than directly as in the first term.

There is no reason to suppose that this equation fails to hold in the multiconfigurational case, or when off-diagonal Lagrange multipliers are included.

§3.4 Results

We have tested the validity of the equation (3.3.2) for the case of bismuth. The configurations used were all those derived from the $6p^3$ manifold, which yields five configurations - $6\bar{p}^2\ 6p$, $6\bar{p}(6p^2)_0$, $(6\bar{p}(6p^2)_2)_{3/2}$, $(6\bar{p}(6p^2)_2)_{5/2}$ and $6p^3$. The three J = 3/2 configurations interact strongly to give states which are a mixture of all three.

The results are shown in table 3.1. They show that the equation (3.3.2) is satisfied to about 1%, which we consider to be very satisfactory. As observed by Shun, the Broch formula breaks down seriously for all except s-electrons, and in many cases gives the wrong sign. In contrast to Shun, we note that in this case the terms derived from the exchange potentials make a non-negligable contribution to the total eigenvalue shift - 20% in the case of the 6p orbital.

TABLE 3.1

Verification of equation (3.3.2) for a 5 CSF calculation on the $6p^3$ manifold in bismuth

Orbital	Eigenvalue Difference	Calculated Difference	Broch Term	Direct Potential Term	Exchange Potential Term
1s	-1.287×10^{-2}	-1.286×10^{-2}	-1.317×10^{-2}	3.049×10^{-4}	3.060×10^{-6}
2s	-1.987×10^{-3}	-1.986×10^{-3}	-2.046×10^{-3}	7.779×10^{-5}	-1.719×10^{-5}
2p-	-7.101×10^{-5}	-7.095×10^{-5}	-1.681×10^{-4}	9.703×10^{-5}	1.352×10^{-7}
2p	7.508×10^{-5}	7.506×10^{-5}	-3.455×10^{-9}	7.514×10^{-5}	-7.260×10^{-8}
3s	-4.588×10^{-4}	-4.598×10^{-4}	-4.748×10^{-4}	2.284×10^{-5}	-7.832×10^{-6}
3p-	-1.608×10^{-5}	-1.733×10^{-5}	-4.385×10^{-5}	2.728×10^{-5}	-7.682×10^{-7}
3p	2.314×10^{-5}	2.194×10^{-5}	-9.650×10^{-10}	2.212×10^{-5}	-1.827×10^{-7}
3d-	2.181×10^{-5}	2.054×10^{-5}	-8.429×10^{-12}	2.025×10^{-5}	2.857×10^{-7}
3d	2.064×10^{-5}	1.934×10^{-5}	-1.998×10^{-16}	1.905×10^{-5}	2.909×10^{-7}
4s	-1.178×10^{-4}	-1.179×10^{-4}	-1.216×10^{-4}	6.877×10^{-6}	-3.180×10^{-6}
4p-	-3.022×10^{-6}	-3.133×10^{-6}	-1.112×10^{-5}	8.345×10^{-6}	-3.552×10^{-7}
4p	7.062×10^{-6}	7.067×10^{-6}	-2.472×10^{-10}	7.092×10^{-6}	-2.435×10^{-8}
4d-	6.212×10^{-6}	6.211×10^{-6}	-2.371×10^{-12}	6.065×10^{-6}	1.458×10^{-7}
4d	6.483×10^{-6}	5.917×10^{-6}	-5.620×10^{-17}	5.782×10^{-6}	1.351×10^{-7}
4f-	4.585×10^{-6}	4.451×10^{-6}	-5.642×10^{-20}	4.379×10^{-6}	7.216×10^{-8}
4f	4.394×10^{-6}	4.365×10^{-6}	0.0	4.279×10^{-6}	6.750×10^{-8}
5s	-2.424×10^{-5}	-2.423×10^{-5}	-2.511×10^{-5}	1.912×10^{-6}	-1.033×10^{-6}
5p-	3.610×10^{-7}	3.641×10^{-7}	-2.080×10^{-6}	2.486×10^{-6}	-4.187×10^{-7}
5p	2.370×10^{-6}	2.370×10^{-6}	-4.463×10^{-11}	2.183×10^{-6}	1.870×10^{-7}
5d-	1.718×10^{-6}	1.725×10^{-6}	-3.075×10^{-13}	1.663×10^{-6}	6.201×10^{-8}
5d	1.632×10^{-6}	1.632×10^{-6}	-7.063×10^{-18}	1.593×10^{-6}	3.973×10^{-8}
6s	-3.218×10^{-6}	-3.216×10^{-6}	-3.117×10^{-6}	2.268×10^{-7}	-3.253×10^{-7}
6p-	3.017×10^{-7}	2.901×10^{-7}	-1.754×10^{-7}	4.810×10^{-7}	-1.553×10^{-8}
6p	4.654×10^{-7}	4.627×10^{-7}	-3.222×10^{-12}	3.533×10^{-7}	1.094×10^{-7}

In all cases the normalization integral is 1.000
Atomic units are used.
Fermi nucleus, $R_h = 1.34145 \times 10^{-4}$ and 1.34567×10^{-4} a.u. (corresponding to A = 207 and 209 respectively); $r_o = 2 \times 10^{-4}$ a.u.

Although bismuth is of great interest in this thesis, its isotope shift has been of little experimental interest, and no experimental results exist for shifts within the $6p^3$ manifold. However, isotope shifts do play an important role in the analysis of the spectra of lanthanides and actinides (Rajnak (1976)). An element of especial interest both experimentally (Blaise and Radziemski (1976)) and theoretically (Pyper and Grant (1979)) is uranium. The spectrum of uranium is very complicated due to the vast number of configurations present; the ground state is assigned to the manifold $5f^36d7s^2$ $J = 6$, which contains 44 configurations, and this interacts strongly with the manifold $5f^36d^27s$ $J = 6$ which contains 396 configurations. Thus a calculation on these two manifolds alone is impracticably complex, and to get reliable results we would also have to consider configuration interaction with several other manifolds, such as $5f^46s7p$, $5f^26d^27s7p$ and $5f^46d7p$.

We therefore selected 62 configurations with $J = 6$, this being the largest calculation we considered to be practical, comprising the 44 configurations of $5f^36d7s^2$ and the configurations derivable from $\overline{f}^3_{9/2}\,\overline{d}^2_{2}s$, $\overline{f}^2_{4}f\overline{d}^2_{2}s$ and $\overline{f}^3_{9/2}\overline{d}ds$. We thought that these would provide the main contributions to the low-lying states in which we are most interested; they include all the 30 configurations used by Pyper and Grant (1979). The results of this calculation are shown in table 3.2 and are disappointing. The correlation between the calculated and experimental results is nearly non-existent, and we cannot say for certain which calculated level corresponds to which experimental level, so any attempt to compare experimental and theoretical isotope shifts is doomed to failure.

TABLE 3.2

Calculated and experimental low-lying levels in uranium $f^3ds^2 + f^3d^2s$ $J = 6$

Calculated	Experimental
0	0
4389	4276
5316	6249
9467	7005
13380	10289
14418	10988
15469	11457
16235	12911
17375	13362
17968	13403
18917	14174
20103	14544
	15435
	15804
	15906
	16376

The experimental results are taken from Blaise and Radziemski (1976).

It might be thought that these results are useless. In fact this is not the case; we can obtain one useful result.

It is usual to assume (Rajnak and Fred (1977)) that the isotope shift of a line T is proportional to the electron density at the origin:

$$\Delta E_T = A_T |\psi(0)|^2 \qquad (3.4.1)$$

although this has been challenged recently (Bauche (1981)).

In a MCDF calculation, the shift in the energy of a transition from state i to f is calculated to be

$$IS_T = \Delta(E_i - E_f) \qquad (3.4.2)$$

where we know that

$$E_i = \sum_r c_{ri}^2 H_{rr} + \sum_{r\neq s} c_{ri} c_{si} H_{rs} \qquad (3.4.3)$$

where H_{rs} is defined in equation (2.2.9), and a similar equation holds for E_f. Thus

$$IS_T = \sum_r (c_{ri}^2 - c_{rf}^2)\Delta H_{rr} + \Big\{2 \sum_r (c_{ri}\Delta c_{ri} - c_{rf}\Delta c_{rf})H_{rr}$$

$$+ \Delta\Big(\sum_{r\neq s} c_{ri} c_{si} H_{rs} - c_{rf} c_{sf} H_{rs}\Big)\Big\} \qquad (3.4.4)$$

If the off-diagonal terms are unimportant and the mixing coefficients do not change much, and if the shift of a configurational energy is approximately dependent only on the manifold it is in, then the equation (3.4.1) will be approximately satisfied.

Empirically, it is found that the main contribution to the isotope shift in equation (3.4.4) is from the first term, and so the above assumptions are not unreasonable.

In figure 3.1 we have plotted the calculated f^3ds^2 content of each level against the calculated isotope shift, and we can see that, to a reasonable degree of accuracy, the equation (3.4.1) does hold. A best fit line gives a difference in shifts between the two configurations of 680 mk, which is in good agreement with Rajnak and Fred's semi-empirical value of 630 mK.

§3.5 Conclusion

These results indicate that, if correlation could be accounted for satisfactorily by configuration interaction, that we should be able to calculate reliable isotope shifts, even in the open shell case. This would then be a useful tool in the identification of experimental lines and levels, since we would be able to compare not only experimental and theoretical energies but also isotope shifts.

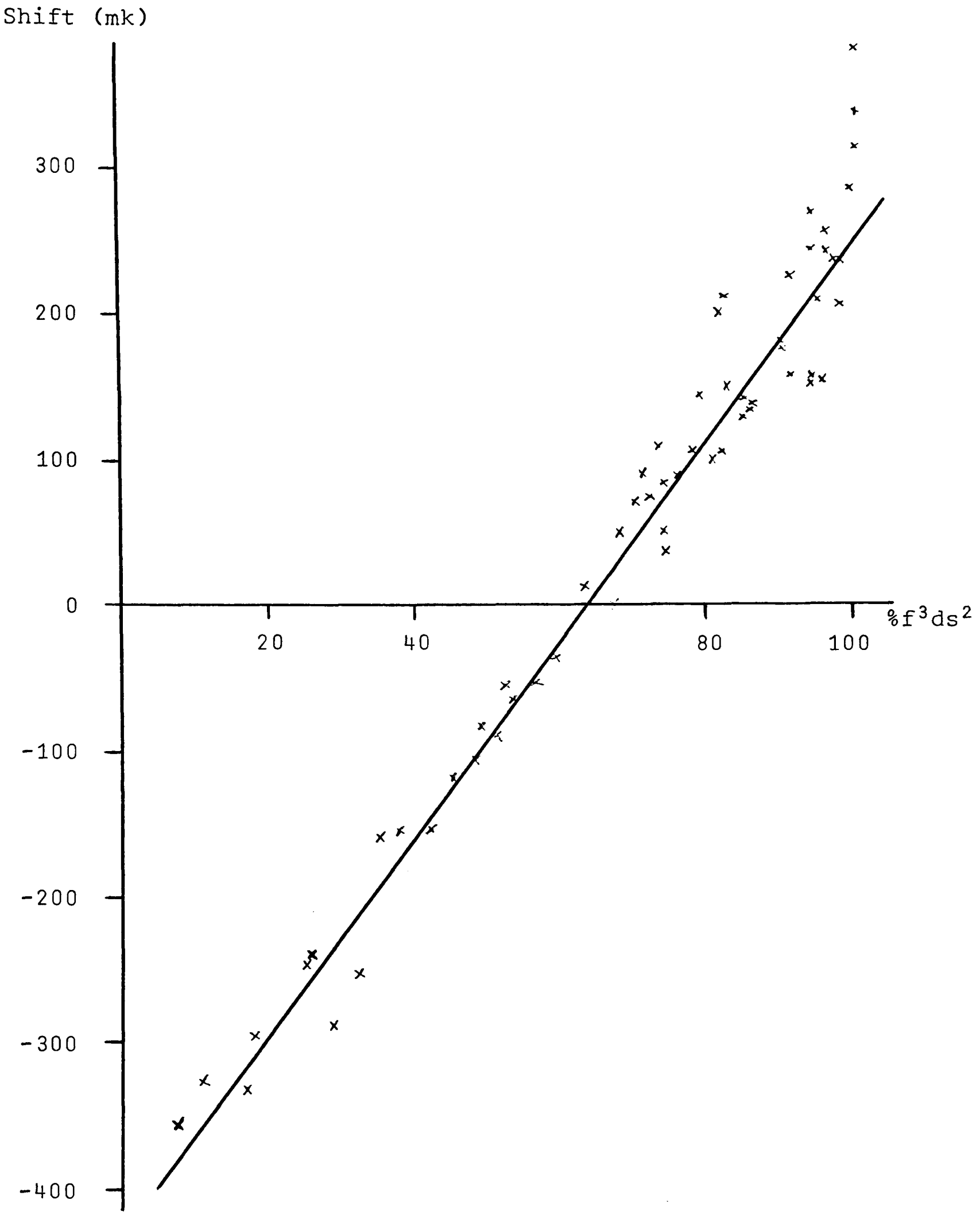

Figure 3.1. Plot of calculated isotope shift versus calculated f^3ds^2 component for the levels of the 62 CSF calculation on uranium.

Chapter 4

And he (Uriel, the holy angel) showed me all their laws exactly as they are, and how it is with regard to all the years of the world and until eternity, till the new creation is accomplished which dureth till eternity.

"Enoch" (-110)

The Background to Parity Non-conservation in Atoms

CHAPTER 4

THE BACKGROUND TO PARITY NON-CONSERVATION IN ATOMS

§4.1 Introduction

It is generally believed that all physical phenomena can be explained in terms of four fundamental interactions: the electromagnetic, the gravitational, the strong, and the weak. In the remainder of this thesis we will be concerned with the interplay between the first and the last of these.

The weak interaction is best known as the controlling force behind beta-decay. It is also observed in many of the reactions in high energy physics.

Early theories of the weak interaction failed to produce results in agreement with experiment, and produced some nonsensical results. The theory of Weinberg (1967) and Salam (1968) was the first to explain the observed phenomena in a satisfactory way. This was done in a framework similar to that of quantum electrodynamics, and was able to unite both QED and the weak interaction within a single theory.

This theory also predicted a "weak neutral current", this being the effect of the interchange of heavy neutral bosons (Z^{o}). Observations consistent with this have been made subsequently in high energy physics (Hasart et al. (1973), Benvenuti et al. (1973), Barish et al. (1974)). It is with some of the consequences of these currents that we concern ourselves in this thesis.

The reason for the interest in results for atoms may be seen at once when we realise that all the early (i.e. pre-1978)

high energy physics experiments which detected neutral currents involved neutrinos; more recently this has changed with the observation of neutral current effects in the inelastic scattering of polarized electrons off deuterium and hydrogen at SLAC (Prescott et al. (1978), (1979)) and the production of both charged and neutral heavy bosons from proton-antiproton collisions at CERN (Arnison et al. (1983a,b), Banner et al. (1983)) They also - obviously - take place at high energies; the CERN experiments involve 10^{12} times the energy of the atomic transitions described in this thesis, the SLAC experiments 10^{10} times, and even the "low energy" neutrino experiments of Pasierb et al. (1979) are in the MeV range, 10^{6} times the energy of interest in atomic physics experiments. Also, they are concerned with quantities like transition probabilities which involve only the square of the relevant transition matrix elements. The consequences for atomic physics, on the other hand, do not involve neutrinos; they take place at low energies; they depend - as will be shown later - on the sign of the transition matrix elements; and, unlike the SLAC and CERN experiments, do not involve reactions on the elementary particle level. Thus we are exploring areas that are untested by conventional high energy experiments.

There are now many field theories which are able successfully to unify electromagnetism and the weak interaction; the advantage of that of Weinberg and Salam is that it involves only one empirical factor - the Weinberg angle θ_W. The other theories have a greater number. Therefore, accurate calculations of the consequences of such theories and good experimental results are necessary to establish which theories may be

accepted and which rejected.

In the rest of this chapter we first digress into a discussion of the meaning of the term "parity non-conservation" (PNC); we then introduce the PNC Hamiltonian and describe briefly some of its main properties in terms of perturbation theory; next we outline the other calculations to date giving details for comparison with the present work; then we shall discuss the connections between this work and the results on isotope shift described in the previous chapter; and finally we shall give, for reference, the experimental results to date.

§4.2 Parity non-conservation

It is not easy to imagine the consequences of a parity non-conserving interaction, since the interactions with which we are familiar - the gravitational and the electromagnetic - do conserve parity.

Mathematically, the question reduces to the enquiry into the behaviour of the wavefunction under the transformation $\underset{\sim}{r} \to -\underset{\sim}{r}$. In the parity conserving case, $\psi(\underset{\sim}{r}) = \pm\psi(-\underset{\sim}{r})$, corresponding to even and odd parity respectively; in the parity non-conserving case neither of these relations will hold.

Since an inversion is equivalent to a reflection followed by a rotation of 180° about an axis perpendicular to the plane of reflection, the physical interpretation of this is: if we watched an experiment in a mirror, would we be able to tell that we were looking in a mirror, rather than directly at the experiment? If not, then the experiment features only parity conserving interactions; otherwise, parity is not conserved.

Consider the case of a hydrogen atom (with a Coulomb potential); we may represent it schematically as in figure 4.1a. If we reflect it through a plane we will obtain figure 4.1b which is again a perfectly reasonable physical situation. Thus we say that the electromagnetic interaction conserves parity. The diagram could just as well be of a planet revolving around a star, and so the gravitational interaction also conserves parity.

However, if we turn to the weak interaction, the situation is different. We take as an example hyperon decay, as described

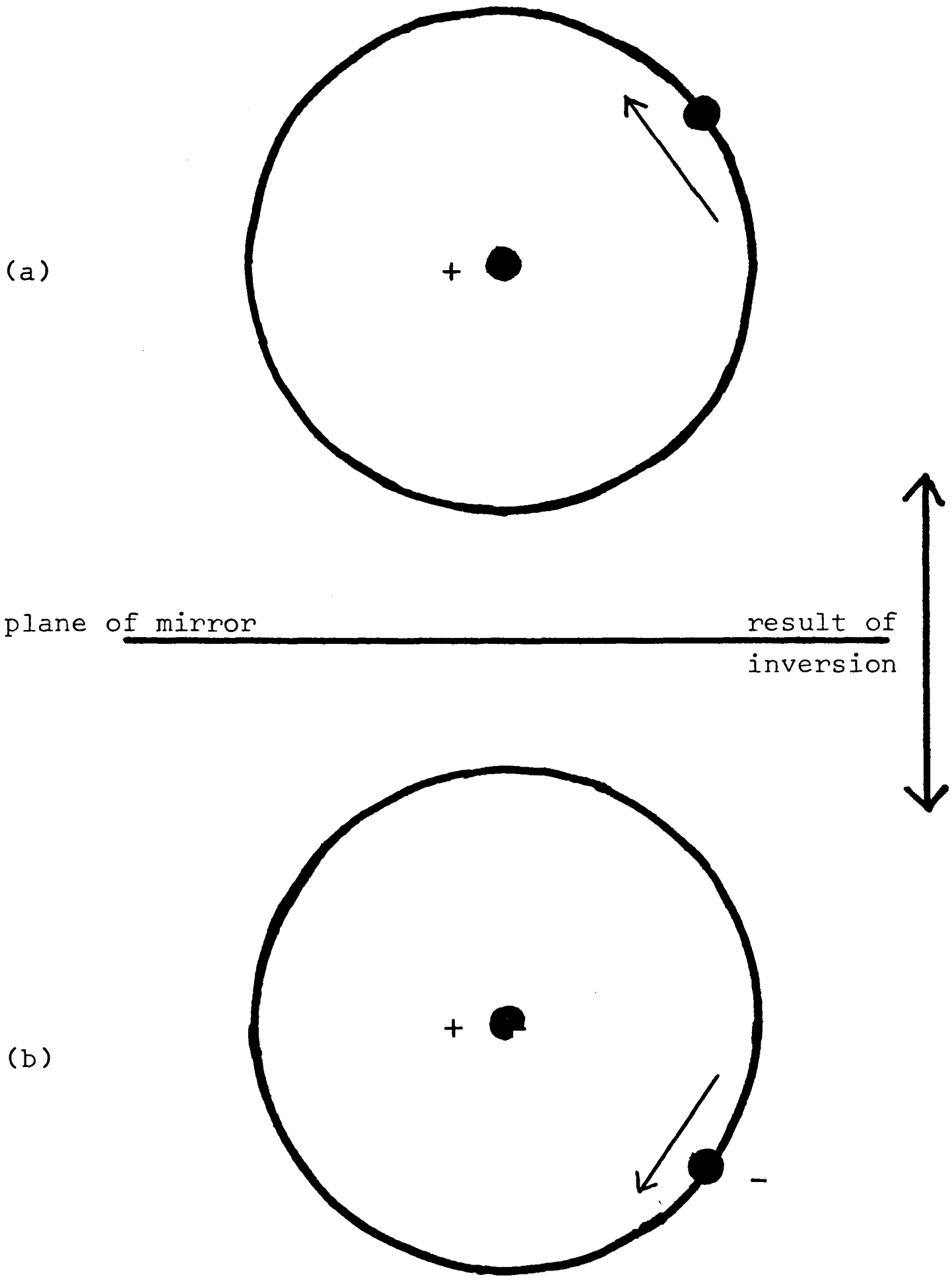

Figure 4.1 The electromagnetic interaction: parity conserving

by Sakurai (1964). This is much clearer than the usual examples, since it involves only particles, and not coils, magnets or currents.

A pion may interact strongly with a proton:

$$\pi^- + p \rightarrow \Lambda^o + K^o$$

The Λ^o then decays to form a nucleon and a pion via the weak interaction:

$$\Lambda^o \rightarrow \begin{cases} p + \pi^- \\ n + \pi^o \end{cases}$$

The pion produced in this way is found (with a probability of about 60%) to move "upwards", as in figure 4.2a. The mirror image of this is shown in figure 4.2b, which occurs with a probability of only 40%. Thus, if we watched this process occurring, we would soon be able to tell if we were watching in a mirror, or if we were watching directly.

Thus we say that the weak interaction does not conserve parity.

§4.3 The PNC Hamiltonian

The PNC Hamiltonian has been derived by Bouchiat (1977). He gives the result

$$H_{PNC} = \frac{G_F}{\sqrt{2}} \int (\overline{\Psi_E}\gamma^\mu \Psi_E)(C_{Ap}\overline{\Psi_p}\gamma_\mu\gamma_5\Psi_p + C_{An}\overline{\Psi_n}\gamma_\mu\gamma_5\Psi_n)\, d^3x$$
$$+ \frac{G_F}{\sqrt{2}} \int \overline{\Psi_E}\gamma^\mu\gamma_5\Psi_E\,(C_{vp}\overline{\Psi_p}\gamma_\mu\Psi_p + C_{vn}\overline{\Psi_n}\gamma_\mu\Psi_n)\, d^3x \qquad (4.3.1)$$

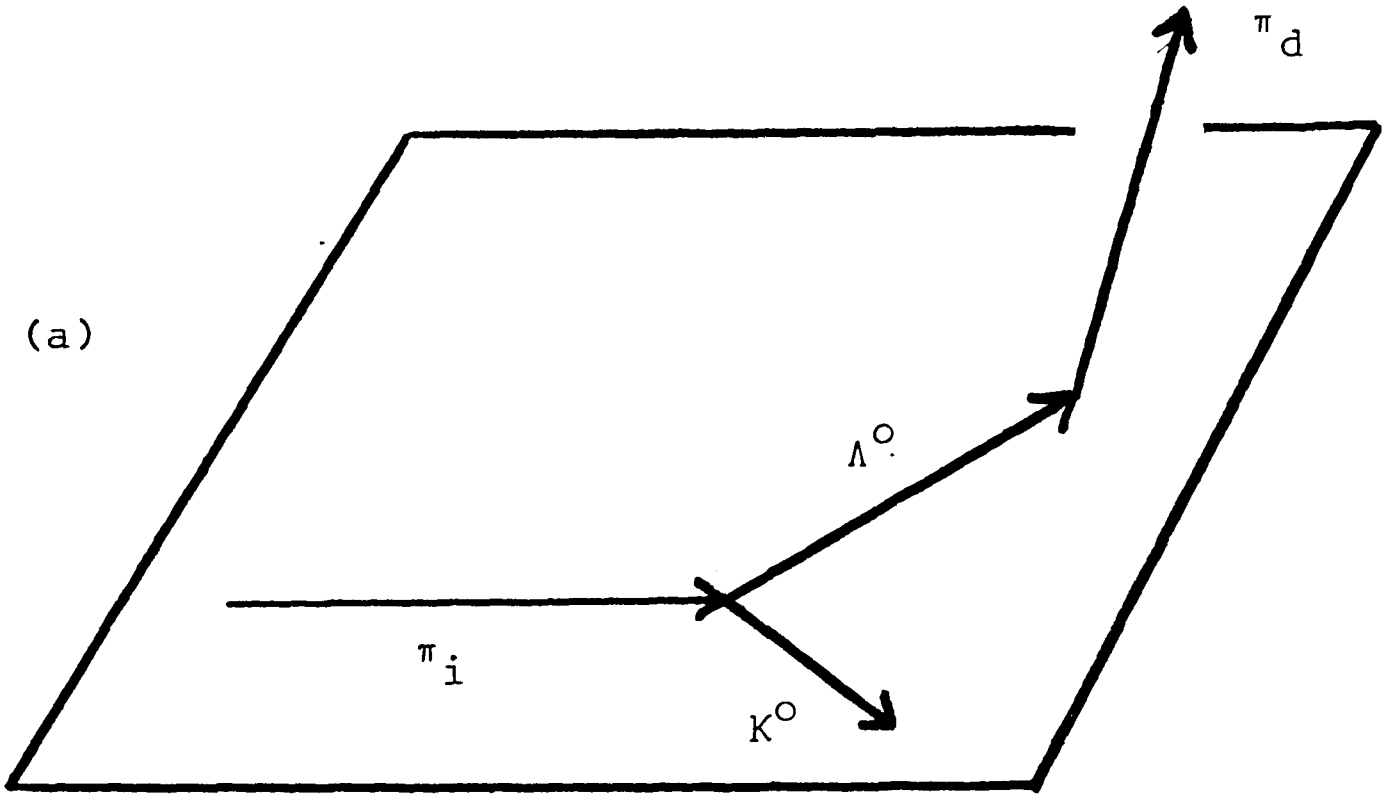

$$\alpha = (\underset{\sim}{p}_{\pi_i} \times \underset{\sim}{p}_{\Lambda^o}) \cdot \underset{\sim}{p}_{\pi_d} > 0$$

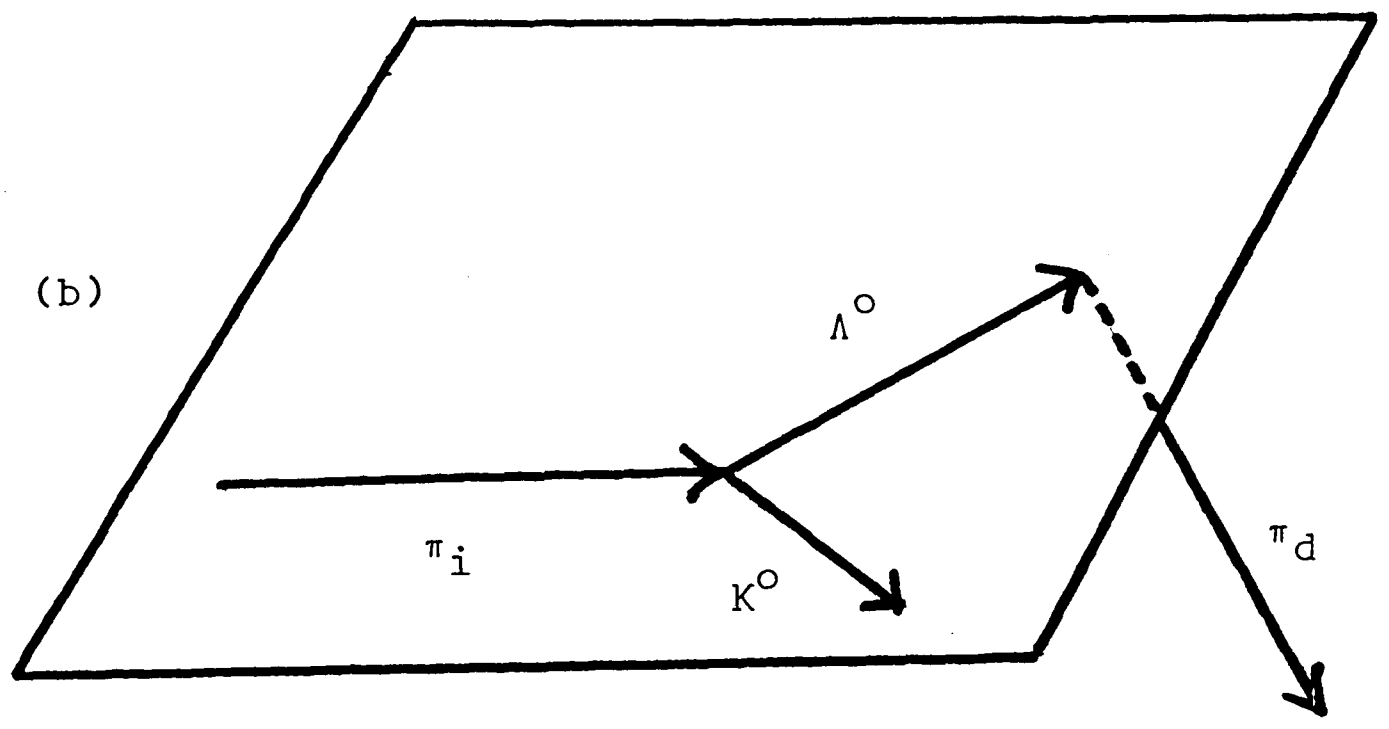

$$\alpha = (\underset{\sim}{p}_{\pi_i} \times \underset{\sim}{p}_{\Lambda^o}) \cdot \underset{\sim}{p}_{\pi_d} < 0$$

Figure 4.2 The weak interaction: parity non-conserving

where Ψ_E, Ψ_n and Ψ_p are the Dirac fields associated with the electron, neutron and proton respectively, and $\bar{\Psi}$ represents the Dirac adjoint of Ψ, $\bar{\Psi} = \Psi^* \gamma^0$

$$\gamma_5 = \begin{pmatrix} \underline{\underline{0}} & \underline{\underline{I}} \\ \underline{\underline{I}} & \underline{\underline{0}} \end{pmatrix} \qquad (4.3.2)$$

where $\underline{\underline{I}} = \begin{pmatrix} 1 & 0 \\ 0 & 1 \end{pmatrix}$ and $\underline{\underline{0}} = \begin{pmatrix} 0 & 0 \\ 0 & 0 \end{pmatrix}$, and, according to the Weinberg-Salam model,

$$\begin{aligned} C_{vp} &= -2 \sin^2\theta_W + \tfrac{1}{2} \\ C_{Ap} &= -\lambda(2 \sin^2\theta_W - \tfrac{1}{2}) \\ C_{An} &= \lambda(2 \sin^2\theta_W - \tfrac{1}{2}) \\ C_{vn} &= -\tfrac{1}{2} \end{aligned} \qquad (4.3.3)$$

As mentioned above, θ_W is the Weinberg angle, $\sin^2\theta_W = 0.23 \pm 0.01$ (Abbot and Barnett (1979)), λ is the ratio between the vector and axial coupling and neutron β decay, $\lambda \tilde{=} 1.25$, and G_F is the Fermi weak interaction constant $G_F = 2.22 \times 10^{-14}$.

This may be written more conveniently in the form (Fortson and Wilets (1980))

$$H'_{PNC} = \frac{G_F}{\sqrt{2}} \sum_{eN} \left[C_{vN} \int \psi_N^* \psi_N \psi_e^* \gamma_5 \psi_e \, d\underset{\sim}{r} + C_{AN} \int \psi_N^* (\underset{\sim}{\gamma}\gamma_5)_N \psi_N \cdot \psi_e^* \underset{\sim}{\alpha} \psi_e \, d\underset{\sim}{r} \right] \qquad (4.3.4)$$

where

$$\underset{\sim}{\chi} = \gamma^0 \underset{\sim}{\alpha} \qquad (4.3.5)$$

and the subscript N takes the values n or p.

It may be shown that the summands in the first term add coherently, but the summands in the second term, being proportional to the nucleon spin, add destructively to give a term proportional to the total nuclear spin. Therefore, for heavy atoms the first term will dominate, and we need consider only the interaction due to

$$H_{PNC} = \frac{G_F}{\sqrt{2}} \frac{Q}{2} \int \rho_N \sum_e \psi_e^* \gamma_5 \psi_e \, d\underset{\sim}{r} \tag{4.3.6}$$

where ρ_N is a nucleon density normalized to 1, i.e.

$$\int \rho_N \, d\underset{\sim}{r} = 1 \tag{4.3.7}$$

and

$$Q = 2 \, (ZC_{vp} + NC_{vn}), \tag{4.3.8}$$

Z and N being the number of protons and neutrons in the nucleus.

From (4.3.6) we can see clearly that we must consider the effects of the Hamiltonian operator

$$H_{PNC} = \sum_i h_{PNC}(i) \tag{4.3.9}$$

where

$$h_{PNC}(i) = \frac{G_F Q}{2\sqrt{2}} \rho_N \gamma_5 \tag{4.3.10}$$

and the summation in (4.3.9) runs over all the electrons. For convenience we absorb all the numerical factors into a single parameter:

$$h_{PNC}(i) = G\rho_N \gamma_5 \tag{4.3.11}$$

where

$$G = \frac{G_F Q}{2\sqrt{2}} \tag{4.3.12}$$

§4.4 Perturbation theory

It is shown in standard texts on quantum mechanics (e.g. Merzbacher (1970)) that, if the eigenvalues and eigenvectors of the equation

$$H\Psi = E\Psi \tag{4.4.1}$$

where

$$H = H_{PC} + \lambda H_{PNC} \tag{4.4.2}$$

are expanded in the form

$$\Psi = \Psi_0 + \lambda\Psi_1 + \lambda^2\Psi_2 + \ldots \tag{4.4.3}$$

$$E = E_0 + \lambda E_1 + \lambda^2 E_2 + \ldots \tag{4.4.4}$$

then

$$H_{PC}\Psi_0 = E_0\Psi_0 \tag{4.4.5}$$

which is the unperturbed equation whose practical solution has been described in chapter 2, and

$$E_1 = \langle\Psi_0|H_{PNC}|\Psi_0\rangle. \tag{4.4.6}$$

If we have a complete set of eigenfunctions of (4.4.5) $\{\Phi_i\}$ with corresponding eigenvalues E^i_0, then

$$\Psi_1 = \sum_i \frac{\langle \Phi_i | H_{PNC} | \Psi_0 \rangle}{E_0 - E^i{}_0} \Phi_i \qquad (4.4.7)$$

where the sum is over all states i, including those in the continuum, except the one for which $E^i{}_0 = E_0$. The case of degenerate states is more complex, but need not detain us here.

The matrix element $\langle \Phi_i | H_{PNC} | \Psi_0 \rangle$ may be broken down into single particle matrix elements by virtue of the form of H_{PNC} given in equation (4.3.9).

$$\langle \Phi_i | H_{PNC} | \Psi_0 \rangle = \sum_{\substack{ab \\ rs}} d_{rs}(ab) \langle a | h_{PNC} | b \rangle \; c_{ir} c_{0s} \qquad (4.4.8)$$

where the $d_{rs}(ab)$ are coefficients similar to those introduced in equation (2.4.10).

Since

$$h_{PNC} = G\rho_N \gamma_5 \qquad (4.4.9)$$

and

$$|\alpha\rangle = \begin{pmatrix} P_{n_\alpha \kappa_\alpha}(r) & \chi_{\kappa_\alpha m_\alpha}(\theta,\phi) \\ iQ_{n_\alpha \kappa_\alpha}(r) & \chi_{-\kappa_\alpha m_\alpha}(\theta,\phi) \end{pmatrix} \qquad (4.4.10)$$

we may write

$$\langle a | h_{PNC} | b \rangle =$$

$$\int \begin{bmatrix} P_{n_a \kappa_a}(r) \; \chi_{\kappa_a m_a}(\theta,\phi) \\ iQ_{n_a \kappa_a}(r) \; \chi_{-\kappa_a m_a}(\theta,\phi) \end{bmatrix}^* G\rho_N \begin{pmatrix} \underline{\underline{0}} & \underline{\underline{I}} \\ \underline{\underline{I}} & \underline{\underline{0}} \end{pmatrix} \begin{bmatrix} P_{n_b \kappa_b}(r) \; \chi_{\kappa_b m_b}(\theta,\phi) \\ iQ_{n_b \kappa_b}(r) \; \chi_{-\kappa_b m_b}(\theta,\phi) \end{bmatrix} d^3 r$$

$$= \int \Big\{ P_{n_a \kappa_a}(r)\ \chi^*_{\kappa_a m_a}(\theta,\phi) . iQ_{n_b \kappa_b}(r)\ \chi_{-\kappa_b m_b}(\theta,\phi)$$

$$-iQ_{n_a \kappa_a}(r)\ \chi^*_{-\kappa_a m_a}(\theta,\phi)\ P_{n_b \kappa_b}(r)\ \chi_{\kappa_b m_b}(\theta,\phi) \Big\}\ G\rho_N d^3r$$

$$= \delta_{\kappa_a,-\kappa_b}\ \delta_{m_a m_b}\ iG \int_o^\infty \rho_N(r) \Big\{ P_a(r)Q_b(r) - Q_a(r)P_b(r) \Big\} dr \qquad (4.4.11)$$

where we have used the orthogonality relation

$$\int \chi^*_{\kappa m}(\theta,\phi)\ \chi_{\kappa' m'}(\theta,\phi)\ d\Omega$$

$$= \delta_{\kappa\kappa'}\ \delta_{mm'} \qquad (4.4.12)$$

to obtain the last line. Thus we may conclude that the PNC Hamiltonian has non-zero matrix elements only between orbitals of the same m-value (as usual) and the κ-value of opposite sign. This means that a and b have the same j-value and opposite ℓ-value - which, since the parity of an orbital is $(-1)^\ell$, gives a further illustration of the term "parity non-conserving" discussed in §4.2. By virtue of the nature of the coefficients $d_{rs}(ab)$ introduced in equation (4.4.8) we will also have the result that

$$\langle T|H_{PNC}|T'\rangle = 0 \qquad (4.4.13)$$

unless the states $|T\rangle$ and $|T'\rangle$ have the opposite parity. Therefore we can see that the sum in equation (4.4.7) extends over only states Φ_i with the opposite parity to Ψ_0, so that the function Ψ_1 is of the opposite parity to Ψ_0. This is the basis of statements like "H_{PNC} mixes states of the opposite parity into the unperturbed state".

A simple application of equation (4.4.13) is as follows. If we consider the first order change in the energy of an atom due to the PNC interaction, then, by first order perturbation theory, this equals

$$E_1 = \langle \Psi_0 | H_{PNC} | \Psi_0 \rangle . \qquad (4.4.14)$$

Since the unperturbed states are of pure parity, equation (4.4.13) immediately yields

$$E_1 = 0 \qquad (4.4.15)$$

In practice, as described in the next section, we are interested in matrix elements $\langle \Psi' | D | \Psi \rangle$ where D is the electric dipole operator, and

$$\langle \Psi'_0 | D | \Psi_0 \rangle = 0.$$

To first order in G this reduces to

$$G\{\langle \Psi_1' | D | \Psi_0 \rangle + \langle \Psi_0' | D | \Psi_1 \rangle\}$$

where, using equation (4.4.7), we may write

$$\langle\Psi_0'|D|\Psi_1\rangle = \sum_i \frac{\langle\Psi_0'|D|\Phi_i\rangle\langle\Phi_i|H_{PNC}|\Psi_0\rangle}{E_0 - E_0^i} \qquad (4.4.16)$$

with a similar equation for $\langle\Psi_1'|D|\Psi_0\rangle$.

The sum in equation (4.4.16) is an infinite one which must extend over all bound and continuum states, and so cannot be explicitly calculated in practice. It can be avoided either by including only terms which give a large contribution, or by summing over all the states analytically by the Sternheimer technique (Sternheimer (1951), Dalgarno and Lewis (1955)) which involves solving an inhomogeneous differential equation for either $|\Psi_1\rangle$ or for

$$\langle\Psi_D| = \sum_i \frac{\langle\Psi_0'|D|\Phi_i\rangle\langle\Phi_i|}{E_0 - E_0^i} \qquad (4.4.17)$$

§4.5 The quantity of experimental interest

The main experimental consequence of PNC, as far as atomic physics is concerned, is that atoms become optically active. As a result, a polarized beam of light passing through an atomic vapour will emerge with its plane of polarization rotated.

It may be shown rigorously (Fortson and Wilets (1980)) that for light at the resonant frequency, and a zero line width, the angle of rotation, taking account only of E1 and M1 radiation, is given by

$$\phi_{PNC} = -\frac{4\pi\ell(n-1)}{\lambda}R \qquad (4.5.1)$$

where λ is the wavelength of the light, ℓ is the pathlength, n is the reference index of the vapour, and

$$R = \frac{Im(E1\ M1)}{|E1|^2+|M1|^2} \qquad (4.5.2)$$

Since $|E1| << |M1|$ for all transitions considered in this thesis, we may approximate (following the convention that M1 should be real)

$$R \tilde{=} \frac{Im(E1)}{M1} \qquad (4.5.3)$$

For a resonance of non-zero width τ and radiation of frequency ω close to the resonant frequency ω_0, the angle of rotation is given (Henley and Wilets (1976)) by

$$\phi_{PNC} = \alpha \ell \frac{\omega-\omega_0}{\tau/2} R \qquad (4.5.4)$$

where ℓ is the pathlength and α is the aborption coefficient

$$\alpha = 2N\ |\langle f|M1|i\rangle|^2 \frac{\tau/2}{(\omega-\omega_0)^2+(\tau/2)^2} \qquad (4.5.5)$$

Here N is the number density of the atoms.

This is the formula actually used in the interpretation of experimental results. Since all the terms in (4.5.4) except R are known, it is this quantity that we wish to calculate.

If the transition is one in which the radiation corresponding to some other multipoles is of comparable intensity to the M1 radiation - and it is frequently the case that the M1 and E2 intensities are about the same - then the equations

(4.5.2) and (4.5.3) no longer hold (Blin-Stoyle (1960)) and we must replace (4.5.2) by

$$R = \frac{\mathrm{Im}[E1\ M1 + E2\ M2 + \ldots\ldots\ ]}{|E1|^2 + |M1|^2 + |E2|^2 + |M2|^2 + \ldots} \qquad (4.5.6)$$

In the cases of interest to us we will need to consider only E1, M1 and E2 radiation, and, since we will still have $|E1| << |M1|$ and $|E1| << |E2|$,

$$R \simeq \frac{\mathrm{Im}\ \ (E1)}{M1\ \left(1 + \left(\frac{E2}{M1}\right)^2\right)} \qquad (4.5.7)$$

Alternatively, following Sandars (1977b), we may retain the definition (4.5.3) of R but multiply the term on the right-hand side of equations (4.5.1) and (4.5.4) by a correction factor θ which takes into account the contribution of the non zero E2 matrix element to the overall refractive index.

However, the way that the E2 matrix element enters is further complicated by the hyperfine interaction (due to the nuclear spin). For these reasons and for comparison with other results, we will give the values of $\mathrm{Im}(E1)/_{M1}$ and E2 separately.

§4.6 Other calculations

In this section we will trace the development of calculations that have been made by other workers in the field of PNC in atoms. The work can be broken down into that

done by various groups, and we will therefore consider it group by group. We will present the results at the end.

The present investigation was limited to parity violation in atoms. It is therefore beyond the scope of this thesis to discuss the work done on parity violation in molecular systems, notably thallium fluoride (see, for instance, Coveney and Sandars (1983)and the references contained therein); various calculations have been carried out, and some experiments performed, which together lead to upper limits on the electric dipole moment of the proton and electron. In these systems, the effects of interactions (if any) which violate both parity and time reversal symmetry is investigated, as opposed to the effects of parity (only) non-conservation which is our present concern.

The hydrogenic problem will not be considered either, since it is quite simple from a theoretical point of view; the computer programs used to generate the numbers presented in this thesis were used in an attempt to solve the problem, but difficulties associated with the near-degeneracy of ns and $n\bar{p}$ (see §6.5 for further details) and a lack of time precluded the calculation of any usable numbers; and the experiments in progress to try to measure R in hydrogen have not yet reached anywhere near the necessary accuracy due to problems with background radiation (Commins (1979), Levy et al. (1982)).

§4.6.1 Bouchiat and Bouchiat

The first calculations on the magnitude of PNC in atoms (Zeldovich (1959), Michel (1965)), showed that they were too

small to be measured, and interest waned until Bouchiat and Bouchiat (1974) showed, in a brilliant piece of mathematical analysis, that the PNC-induced rotation was given by the approximate formula

$$|R| \sim 10^{-14} Z^3 K_r \qquad (4.6.1)$$

where K_r is a relativistic correction factor and Z is the nuclear charge of the atom under consideration. Their work used a Fermi-Segré-type approximation, was basically non-relativistic (hence the correction factor K_r) and assumed a point nucleus; nevertheless it did provide an estimate for R which, for an element of $Z \sim 80$, in which case $K_r \sim 9$, was definitely within reach of experimental measurement:

$$R \sim 10^{-7} \qquad (4.6.2)$$

They suggested that useful transitions to examine for PNC effects were the $6s \rightarrow 7s$ transition in cesium ($R \sim 10^{-4}$) and $6\bar{p} \rightarrow 7\bar{p}$ transition in Tℓ ($R \sim 3\times10^{-4}$) and the $6p^2\,{}^3P_o \rightarrow 6p^2\,{}^1S_o$ transition in Pb ($R \sim 3\times10^{-4}$), all of which were increased due to the very small value of the M1 transition matrix element. In a later paper they suggested an experimental method for the cesium transition (Bouchiat and Bouchiat (1975)).

These calculations made no pretence to be particularly accurate, being based, as they were, on very approximate methods. However, they did show that there might be observable PNC effects in atoms, and as such paved the way for subsequent more accurate calculations and experiments.

More recently they have performed some more detailed calculations on the $6s \rightarrow 7s$ cesium transition using various

model potentials, and allowing for the effects of shielding (Bouchiat (1980), Bouchiat et al. (1983)).

§§4.6.2 Sandars and co-workers - the Oxford group

The calculations of the Oxford group have been mainly concerned with bismuth, this being in support of their experiments on that atom. In their calculations (Loving and Sandars (1975), Brimicombe, Loving and Sandars (1976), Sandars (1977a), Loving (1978), Harris, Loving and Sandars (1978), Sandars (1980)) they have used an independent particle model, with the electrons moving in a parameterized model potential. A uniform nuclear charge distribution is assumed. Results have been calculated for the $6s \rightarrow 7s$ (λ = 540 nm) transition in cesium and the $6\bar{p}^2 6p \rightarrow (6\bar{p}(6p^2)_2)_{3/2}$ (λ = 876 nm) and $6\bar{p}^2 6p \rightarrow (6\bar{p}(6p^2)_2)_{5/2}$ (λ = 648 nm) transitions in bismuth, the latter in both jj and L-S coupling. These are of experimental interest due to the ready availability of suitable laser sources of monochromatic light.

The calculations have been extended for bismuth. The deficiencies of the model potential have been overcome by treating the deviations from it by means of perturbation theory. Shielding - due to the tendency of the electrons to move under the influence of electromagnetic radiation to reduce its effects - for the n = 6 electrons has also been allowed for by means of time-dependent-Hartree-Fock theory.

In all calculations the E1 matrix element has been expressed in terms of the matrix element of r (length form).

§§4.6.3 The Seattle group

The Seattle group have made several calculations for bismuth (Henley and Wilets (1976), Henley et al. (1977), Martensson et al. (1981)) and one for thallium (Henley and Wilets (1976)). The 1976 calculations used a "quasi-relativistic' Hartree-Fock formulation, i.e. wavefunctions were solutions of the Schrödinger equation with relativistic corrections, using the code of Cowan (1967), which were then matched with Dirac functions at the nuclear boundary. The perturbation expansion (equation (4.4.16)) was used, being summed by a Sternheimer technique for thallium but not for bismuth, where the expanded form was used. No configuration interaction was included and only the electric dipole length matrix element was used.

The 1977 paper examined the effects of configuration interaction in bismuth and concluded that they were negligible, using a relativistic parametric potential to solve the Dirac equations.

The 1981 calculations were for bismuth, and were similar to those in this thesis. We consider them to be the best so far. Calculations were made for the solution of the Dirac equation in an optimized Hartree-Fock-Slater potential and also a Hartree-Fock potential. Exchange terms were included by perturbation theory, or incorporated into the PNC differential equations for some orbitals. Shielding terms were included, but found to give a smaller than expected contribution due to large cancellation effects. Effects of parity conserving correlation were neglected, and only the

length form was used for electric dipole matrix elements.

§§4.6.4 The Novosibirsk Group

The calculations of the Novosibirsk group have been on thallium, lead and bismuth, with the emphasis on bismuth, in which the group is also interested experimentally. Calculations have been based on the analytical form of Bouchiat and Bouchiat (q.v.) (Khriplovich (1975), Moskalev (1976)) or on a parametric potential model (Novikov et al. (1976), Sushkov et al. (1976), Barkov et al. (1979)), the parameters being derived from the requirement that transition energies and various other atomic properties (e.g. hyperfine structure) calculated should be in good agreement with experiment. The Novikov (1976) calculation also allowed for the effects of shielding to some extent. The distinctive feature of these calculations is the inclusion of as much empirical data as possible.

§§4.6.5 Other calculations

Rose (1979) has calculated the optical rotation for bismuth using equation (4.4.16), with the sum restricted to the manifolds $6s^2 6p 7s$ and $6s6p^4$, using the MCDF package described in Chapter 3. He calculated results in the Coulomb and Babushkin gauges.

The calculations on bismuth of Carter and Kelly (1979) are interesting because they are the only ones to date which compare the results of determining the electric dipole matrix element using length and velocity forms other than the results of Rose. They used the MCDF code of Desclaux (1975) to cal-

culate the wavefunctions for $6p^3$, $6p^2ns$ and $[ns]6p^4$, which they then substituted in the perturbation expansion (4.4.16). They used experimental energies in the calculation of matrix elements, and found reasonable agreement between their length form results and other results, but these differed by a large factor from the velocity form results; this was put down to correlation effects, and they concluded that the length form was to be preferred.

Neuffer and Commins (1971) have calculated the optical rotation in thallium, using the experimental value of the M1 matrix element, and calculating the E1 matrix element by solving the Dirac equation in a modified Tietz potential chosen to give the correct energy for the 6s electron and using the perturbation expansion (4.4.16). These results have been modified by Bardsley and Norcross (1980) who recalculated the electric dipole matrix elements using wavefunctions calculated in a scaled Thomas-Fermi-Dirac potential with extra terms added to allow for core polarization effects.

Finally, Das et al. (1981,1982) have recently published some results for thallium and cesium. They have used relativistic many-body perturbation theory to calculate E1 matrix elements for these atoms, taking into account indirect, consistency and correlation effects. To obtain R they have used the experimental value of M1.

§§4.6.6 Results

The results of the above calculations for the transitions of greatest interest are presented in table 4.1. We prefer the

TABLE 4.1

The PNC Ratio : Theoretical Results

All normalized to $\sin^2\theta_W = 0.25$

Transition	R		Reference
Bismuth λ = 648 nm $6\bar{p}^2 6p \rightarrow (6\bar{p}(6p^2)_2)_{5/2}$	-32×10^{-8}		Brimicombe et al.(1976)
	$\sim -10 \times 10^{-8}$		Moskalev (1976)
	-24×10^{-8}	(U)	Novikov et al. (1976)
	-18×10^{-8}	(S)	
	-12×10^{-8}		Harris et al.(1978)
	-15×10^{-8}		Loving (1978)
	-23×10^{-8}	(L)	Carter and Kelly (1979)
	-3×10^{-8}	(V)	
	-38×10^{-8}	(U)(B)	Rose (1979)
	-160×10^{-8}	(U)(C)	
	-27×10^{-8}	(G)(U)(B)	
	-13×10^{-8}	(G)(S)(B)	
	-11×10^{-8}		Martensson et al.(1981)
Bismuth λ = 876 nm $6\bar{p}^2 6p \rightarrow (6\bar{p}(6p^2)_2)_{3/2}$	-24×10^{-8}		Brimicombe et al.(1976)
	-28×10^{-8}		Henley & Wilets (1976)
	$\sim -10 \times 10^{-8}$		Moskalev (1976)
	-18×10^{-8}	(U)	Novikov et al. (1976)
	-14×10^{-8}	(S)	
	-9×10^{-8}		Harris et al.(1978)
	-13×10^{-8}		Loving (1978)
	-17×10^{-8}	(L)	Carter and Kelly (1979)
	-14×10^{-8}	(V)	
	-15×10^{-8}	(U)(B)	Rose (1979)
	-77×10^{-8}	(U)(C)	
	-13×10^{-8}	(G)(U)(B)	
	-6×10^{-8}	(G)(S)(B)	
	-8×10^{-8}		Martensson et al.(1981)

TABLE 4.1 (Continuation)

Transition	R	Reference
Thallium λ = 293 nm $6P_{\frac{1}{2}} \rightarrow 7P_{\frac{1}{2}}$	1.0×10^{-3} (A)	Bouchiat & Bouchiat (1975)
	1.2×10^{-3}	Sushkov et al. (1976)
	1.5×10^{-3}	Chu et al. (1977)
	1.1×10^{-3}	Neuffer & Commins (1977a)
	1.11×10^{-3} (L)(A)	Bardsley & Norcross (1980)
	1.00×10^{-3} (M)(E)	
	1.06×10^{-3} (M)(T)	
	1.46×10^{-3} (L)(F)	
	1.5×10^{-3}	Kelly & Carter (1980)
	0.89×10^{-3}	Das (1981), Das et al. (1982)
Thallium $6P_{\frac{1}{2}} \rightarrow 6P_{3/2}$ λ = 1283 nm	-1.7×10^{-7}	Novikov et al. (1976)
	1.8×10^{-7}	Neuffer & Commins (1977a)
Cesium 6S → 7S λ = 540 nm	$\sim 10^{-4}$	Bouchiat & Bouchiat (1974)
	-2.0×10^{-14}/M1	Bouchiat & Bouchiat (1974)
	$\sim 10^{-4}$	Khriplovich (1975)
	-2.44×10^{-14}/M1 (X)	Loving & Sandars (1975)
	$\sim 10^{-4}$	Moskalev (1976)
	-6.5×10^{-5}	Neuffer & Commins (1977b)
	-1.72×10^{-14}/M1 (P)(U)(X)	Bouchiat (1980), Bouchiat et al. (1983)
	-1.58×10^{-14}/M1 (P)(S)(X)	
	-1.58×10^{-14}/M1 (N)(U)(X)	
	-1.47×10^{-14}/M1 (N)(S)(X)	
	-1.60×10^{-14}/M1 (X)	Das (1981)
Lead all transitions	$\sim 4 \times 10^{-8}$	Bouchiat & Bouchiat (1974)
	$\sim 10^{-7}$	Moskalev (1976)
Lead $6p^2\,{}^3P_o \rightarrow 6p^2\,{}^3P_1$ λ = 1279 nm	-1.4×10^{-7}	Novikov et al. (1976)
Lead $6p^2\,{}^3P_o \rightarrow 6p^2\,{}^1S_o$ λ = 339 nm	$\sim 3 \times 10^{-4}$	Moskalev (1976)
	2.7×10^{-5}	Shushkov et al. (1976)

NOTES ON TABLE 4.1

(A) Assuming M1 = -2.11×10^{-5} μ_B (standard definition of M1) (experimental value).

(B) Babushkin gauge for E1

(C) Coulomb gauge for E1

(E) Using experimental energy

(F) Using calculated value of M1

(G) Values derived from mixing coefficients chosen to give correct G-factors

(L) Length form for E1

(M) Using matrix elements of $\underset{\sim}{\alpha}$ for E1

(N) Norcross potential

(P) Stone potential

(S) Screened values

(T) Using theoretical energy

(U) Unscreened values

(V) Velocity form for E1

(X) The M1 matrix element must be given as a reduced matrix element of the operator used in chapter 2

N.B. Some calculations on thallium and bismuth involving other transitions have been carried out, but will not be discussed since they appear to be of no experimental interest at present.

results of Martensson et al. since these take account of the various effects most fully:

§4.7 Connection with isotope shift

At first glance it might appear that there is little connection with isotope shift - after all, in PNC we are concerned with calculating matrix elements, and we know that the effect of the weak interaction on energies and eigenvalues is zero to the first order, whilst in isotope shift studies we are only concerned with shifts in eigenvalues.

However, both calculated eigenvalues and matrix elements are dependent on the wavefunctions for their values, directly or indirectly. Also, the potential change which causes isotope shift is non-zero only in the region of the nucleus, as is the weak interaction potential. It is therefore not impossible that the results from the previous chapter may shed some light on the processes involved in the PNC problem. In the bismuth PNC calculation, the $\underline{E1}^{PNC}$ matrix element depends mainly on the matrix elements $\langle 6\bar{p}||E1||6p\rangle$ and $\langle 6\bar{p}||E1||\overline{6p}\rangle$. Here $|\overline{n\kappa}\rangle$ is a PNC wavefunction, which will be precisely defined in the next chapter; the point is that we are very interested in the 6p- and 6p PNC wavefunctions.

Consider now the results in table 3.1. As we remarked in chapter 3, the indirect terms in the shift $\Delta\varepsilon_{6p-}$ are of the same magnitude as the direct term, and are in fact larger; whilst the indirect terms in $\Delta\varepsilon_{6p}$ are five orders of magnitude larger than the direct term, with the effect that

$\Delta\varepsilon_{6p}$ is actually larger than $\Delta\varepsilon_{6p-}$.

Suppose we extend the analogy between isotope shift and PNC further by noting that the Broch formula is obtained by simple perturbation theory or by using a single-particle model. This may well correspond to the majority of PNC calculations up to this date - those which rely on a model potential or on simple perturbation theory. If this is so we can expect that the $\langle 6\bar{p}||E1||6p\rangle$ matrix element may be wrong by a considerable amount, and the usual result - namely that $\langle \overline{6p}||E1||6\bar{p}\rangle$ is negligible (see, for instance, the next chapter) may be totally false - in fact it may be larger than the former matrix element. Certainly we may well discover that such results are seriously in error.

These arguments make no pretence to be rigorous, but they do suggest that a full calculation of the MCDF type is necessary.

§4.8 Experimental results

A number of experiments have been performed on bismuth, thallium and cesium to look for PNC-induced optical activity.

The experiments on bismuth are, conceptually at least, the simplest. In them, light from a tunable laser at near the resonant frequency is passed in turn through a polarizer, an oven containing bismuth vapour, and another polarizer at right angles to the first. Any light passing through the second polarizer will be an indication of a rotation of the plane of polarization of the light between the two polarizers, i.e. a consequence of the optical activity of the bismuth

vapour. In practice, the amount of light passing through the second polarizer due to the optical activity of the bismuth vapour would be too small to be measurable, since it is proportional to the square of the angle of rotation of the plane of polarization of the light; thus it is arranged that some light always passes through either intentionally de-orthogonalizing the polarizers by $\sim 10^{-3}$ rad. (Barkov and Zolotorev), or (in other experiments) by inserting a Faraday cell in series with the bismuth oven between the two polarizers, which will cause a rotation of the plane of polarization of the light (of $\sim 10^{-3}$ rad) by virtue of the magnetic field it produces. Scanning the frequency of the laser through the resonant frequency allows the PNC - induced component of the rotation of the plane of polarization of the light to be extracted by virtue of its unusual anti-symmetric behaviour near the resonance - see equation (4.5.4), which contrasts with the more symmetric Faraday rotation or constant contribution due to non-orthogonality of the polarizers.

The experiments on cesium are complicated by the small value of the M1 matrix element. Although this has the advantage of increasing the E1/M1 ratio, it does mean that the M1 transition is so weak as not to be directly observable. Instead the cesium vapour is placed in an electric field, and the $E1^{PNC}$ - $E1^{Stark}$ interference is analysed. The M1 matrix element can also be obtained, this coming from M1 - $E1^{Stark}$ interference. In order to analyse the $E1^{PNC}$ - $E1^{Stark}$ interference, the circular polarization of fluorescence from the vapour is determined at a frequency of 7357.27 cm^{-1},

corresponding to the $7S_{\frac{1}{2}} \rightarrow 6P_{\frac{1}{2}}$ transition. This is proportional to the electronic polarization of the atoms in the $7S_{\frac{1}{2}}$ state, which is itself proportional to the quantity R which enters as the difference between the tendency of the unexcited cesium atom to absorb left or right polarized photons.

For thallium, the situation is further complicated by that fact that the frequency of the $7P_{\frac{1}{2}} \rightarrow 7S_{\frac{1}{2}}$ transition (corresponding to $7S_{\frac{1}{2}} \rightarrow 6P_{\frac{1}{2}}$ in cesium) is such that the transition cannot be observed conveniently. Instead, $7P_{\frac{1}{2}}$ atoms are excited to $8S_{\frac{1}{2}}$ and the polarization of the 323 nm radiation from the $8S_{\frac{1}{2}} \rightarrow 6P_{\frac{3}{2}}$ transition is measured; otherwise, however, the same principles apply as in cesium.

The results of these experiments are shown in table 4.2.

Since the author of this thesis is not an experimentalist, he feels that he is not competent to comment on the relative merits of the results. However, it is clear that there are some major discrepancies, which must lead us to regard them with some caution.

TABLE 4.2

PNC. in atoms : experimental results

Transition	R	Reference
	Radians × 10^{-8}	
	~ 5 ± 5	Baird et al. (1976)
	+2.7 ± 4.7	Baird et al. (1977)
Bismuth	-20 ± 5	Barkov and Zolotorev (1978a), Barkov et al (1979)
λ = 648 nm		
J = 3/2 → 5/2	-25 ± 5	Barkov and Zolotorev (1978b)
	-10.7 ± 1.5	Baird (1980)
	-0.22 ± 1.0	Bogdanov et al. (1980a)
	+0.4 ± 2	Bogdanov et al. (1980b)
	Radians × 10^{-8}	
Bismuth	-0.7 ± 3.2	Lewis et al. (1977)
λ = 876 nm	+0.2 ± 1.5	Fortson (1978)
J=3/2 → 3/2	-10.4 ± 1.7	Hollister et al. (1981)
Thallium	Radians × 10^{-3}	
6p → 7p	2.6 ± 1.2	Conti et al. (1979)
λ=292nm	1.4 ± 0.5	Bucksbaum et al (1981)
Cesium	Radians × 10^{-4}	
λ=540nm	5.6 ± 18	Bouchiat & Pottier (1977)
6s → 7s	$(-1.07 \pm .26) \times 10^{-14}$/M1	Bouchiat et al. (1982)

Chapter 5

For in much wisdom is much grief:

and he that increaseth knowledge

increaseth sorrow.

Solomon (-950)

The Single-particle Theory of Parity Non-conservation in Atoms

CHAPTER 5

THE SINGLE-PARTICLE THEORY OF PARITY NON-CONSERVATION IN ATOMS

§5.1 Introduction

The study of the single-particle theory of parity non-conservation in atoms was undertaken here for a variety of reasons. Firstly, there were other calculations (Loving (1978)) with which the present investigations could be directly compared. Secondly, the theory is reasonably simple to develop and the resulting equations are quite simple. Thirdly, the theory was relatively easy to program, and the techniques used to solve the single-particle theory were deliberately chosen so as to be easily generalizable to a many-particle theory. Finally, the experience gained here was very useful for developing a many-particle theory, and the good agreement between the present results and those of other workers gives confidence that the many-particle results will be reliable.

§5.2 The derivation of the single particle PNC equations

We will derive the single-particle PNC equations by setting up an energy functional which we will require to be given a stationary value, in a manner exactly analagous to the method used to obtain the usual M C D F equations in chapter 2.

The functional we consider is

$$\mathcal{E}[\psi] = \langle \psi | \mathcal{H} | \psi \rangle \qquad (5.2.1)$$

where $\mathcal{H}$ is the parity violating Hamiltonian

$$\mathcal{H} = h + G\bar{h} \tag{5.2.2}$$

and

$$h = c\underset{\sim}{\alpha}\cdot\underset{\sim}{p} + (\beta-1)\,c^2 - \frac{Z}{r} \tag{5.2.3}$$

is the usual Dirac Hamiltonian,

$$\bar{h} = \gamma_5\rho_N(r) \tag{5.2.4}$$

$$\gamma_5 = \begin{pmatrix} 0 & 0 & 1 & 0 \\ 0 & 0 & 0 & 1 \\ 1 & 0 & 0 & 0 \\ 0 & 1 & 0 & 0 \end{pmatrix} \tag{5.2.5}$$

$$G = \frac{G_F Q}{2\sqrt{2}} = 4\pi G_N \tag{5.2.6}$$

and

$$\Psi = \psi + iG\bar{\psi} \tag{5.2.7}$$

Here $\rho_N(r)$ is the nucleon density normalized to unity

$$\int \rho_N(r)\, d^3\underset{\sim}{r} = 1, \tag{5.2.8}$$

ψ is the usual parity conserving wavefunction

$$\psi(\underset{\sim}{r}) = \frac{1}{r}\begin{pmatrix} P(r)\,\chi_{\kappa,m}(\theta,\phi) \\ iQ(r)\,\chi_{-\kappa,m}(\theta,\phi) \end{pmatrix} \tag{5.2.9}$$

and $\bar{\psi}$ is a wavefunction corresponding to the same j- and m-values but opposite ℓ-value:

$$\bar{\psi}(\mathbf{r}) = \frac{1}{r}\begin{pmatrix} \bar{P}(r)\ \chi_{-\kappa,m}(\theta,\phi) \\ i\bar{Q}(r)\ \chi_{\kappa,m}(\theta,\phi) \end{pmatrix} \tag{5.2.10}$$

As usual we place a normalization condition on Ψ; the one which we use is

$$\langle\Psi|\Psi\rangle = 1 \tag{5.2.11}$$

Then the condition that we have a stationary value of $\mathcal{H}$ subject to the constraint (5.2.11) may be written as

$$\delta J[\Psi,\varepsilon] = 0 \tag{5.2.12}$$

where

$$J[\Psi,\varepsilon] = \mathcal{E}[\Psi] + \varepsilon\langle\Psi|\Psi\rangle \tag{5.2.13}$$

and ε is, as usual, a Lagrange multiplier. To solve (5.2.12) we note that

$$\begin{aligned} J[\Psi,\varepsilon] &= \langle\Psi|\mathcal{H}|\Psi\rangle + \varepsilon\langle\Psi|\Psi\rangle \\ &= \langle\psi|h|\psi\rangle + G^2\langle\bar{\psi}|h|\bar{\psi}\rangle \\ &\quad -iG^2\{\langle\bar{\psi}|\bar{h}|\psi\rangle - \langle\psi|\bar{h}|\bar{\psi}\rangle\} \\ &\quad + \varepsilon\{\langle\psi|\psi\rangle + G^2\langle\bar{\psi}|\bar{\psi}\rangle\} \end{aligned} \tag{5.2.14}$$

where, as usual (c.f. (2.2.16)),

$$\begin{aligned} \langle\psi|h|\psi\rangle = \int_0^\infty dr\ \Big\{ & cQ\left(\frac{d}{dr} + \frac{\kappa}{r}\right) P - cP\left(\frac{d}{dr} - \frac{\kappa}{r}\right)Q \\ & - 2c^2Q^2 - \frac{Z}{r}(P^2 + Q^2)\Big\} \end{aligned} \tag{5.2.15}$$

and

$$\langle\bar{\psi}|h|\bar{\psi}\rangle = \int_o^\infty dr \left\{c\bar{Q}\left(\frac{d}{dr} - \frac{\kappa}{r}\right)\bar{P} - c\bar{P}\left(\frac{d}{dr} + \frac{\kappa}{r}\right)\bar{Q}\right.$$

$$\left. - 2c^2\bar{Q}^2 - \frac{Z}{r}(\bar{P}^2 + \bar{Q}^2)\right\} \qquad (5.2.16)$$

After a little algebra we obtain

$$\langle\psi|\bar{h}|\bar{\psi}\rangle = -\langle\bar{\psi}|\bar{h}|\psi\rangle$$

$$= i\int_o^\infty (P\bar{Q} - Q\bar{P})\,\rho_N dr \qquad (5.2.17)$$

and, as always,

$$\langle\psi|\psi\rangle = \int_o^\infty (P^2 + Q^2)dr \qquad (5.2.18)$$

$$\langle\bar{\psi}|\bar{\psi}\rangle = \int_o^\infty (\bar{P}^2 + \bar{Q}^2)dr \qquad (5.2.19)$$

Using these equations, the equation (5.2.12) takes the form

$$2\int_o^\infty dr \left\{\delta Q\left[c\left(\frac{d}{dr} + \frac{\kappa}{r}\right)P - \left(2c^2 + \frac{Z}{r}\right)Q\right]\right.$$

$$\left. - \delta P\left[c\left(\frac{d}{dr} - \frac{\kappa}{r}\right)Q + \frac{Z}{r}P\right]\right\}$$

$$+2G^2\int_o^\infty dr \left\{\delta\bar{Q}\left[c\left(\frac{d}{dr} - \frac{\kappa}{r}\right)\bar{P} - \left(2c^2 + \frac{Z}{r}\right)\bar{Q}\right]\right.$$

$$\left. - \delta\bar{P}\left[c\left(\frac{d}{dr} + \frac{\kappa}{r}\right)\bar{Q} + \frac{Z}{r}\bar{P}\right]\right\}$$

$$+2G^2\int_o^\infty dr\,(Q\delta P + P\delta Q - P\delta Q - Q\delta P)\,\rho_N(r)$$

$$+ 2\varepsilon\int_o^\infty dr\,(\delta P.P + \delta Q.Q)$$

$$+ 2\varepsilon G^2\int_o^\infty dr\,(\delta\bar{P}.\bar{P} + \delta\bar{Q}.\bar{Q}) = 0 \qquad (5.2.20)$$

where terms of the form $P\frac{d}{dr}(\delta Q)$ have been removed by partial integration:

$$\int_o^\infty P\frac{d}{dr}(\delta Q) = -\int_o^\infty \delta Q.\frac{dP}{dr} \qquad (5.2.21)$$

since $P(0) = 0$ and $P(\infty) = 0$.

Since (5.2.20) must hold for all variations δP, δQ, $\delta\overline{P}$ and $\delta\overline{Q}$ it immediately yields the equations

$$c(\frac{d}{dr} + \frac{\kappa}{r})P - (2c^2 + \frac{Z}{r} - \varepsilon)Q + G^2\rho_N\overline{P} = 0 \qquad (5.2.22)$$

$$-c(\frac{d}{dr} - \frac{\kappa}{r})Q - (\frac{Z}{r} - \varepsilon)P - G^2\rho_N\overline{Q} = 0 \qquad (5.2.23)$$

$$c(\frac{d}{dr} - \frac{\kappa}{r})\overline{P} - (2c^2 + \frac{Z}{r} - \varepsilon)\overline{Q} - \rho_N P = 0 \qquad (5.2.24)$$

$$-c(\frac{d}{dr} + \frac{\kappa}{r})\overline{Q} - (\frac{Z}{r} - \varepsilon)\overline{P} + \rho_N Q = 0 \qquad (5.2.25)$$

These equations are true for any value of G. In fact $G \sim 10^{-12}$ so in (5.2.22) and (5.2.23) we neglect the terms in G^2 to obtain the usual radial Dirac equations

$$c(\frac{d}{dr} + \frac{\kappa}{r})P - (2c^2 + \frac{Z}{r} - \varepsilon)Q = 0 \qquad (5.2.26)$$

$$-c(\frac{d}{dr} - \frac{\kappa}{r})Q - (\frac{Z}{r} - \varepsilon)P = 0 \qquad (5.2.27)$$

It might seem that this last step cannot lead to any appreciable errors. In fact this is so, but it is not obvious, because $\rho_N \sim 10^{11} \sim 1/G$ and the functions $\overline{P}$ and $\overline{Q}$ are not normalized so that, if they were very large, and since ρ_N is so large, the terms

$$G^2\rho_N\bar{P} \text{ and } G^2\rho_N\bar{Q}$$

might be non-negligible. We will return to this point later.

§5.3 The numerical solution of the PNC equations

The standard MCDF package of routines (Grant et al.(1980)) can be used to solve the equations (5.2.26) and (5.2.27) where $Z = Z(r)$ is a model effective charge. The values of ε and the functions P, Q are then used in the equations (5.2.24) and (5.2.25). These are solved by similar numerical methods to those used for the equations (5.2.26) and (5.2.27) (Desclaux et al.(1971)), the differences being that the ε-value is now fixed and the wavefunctions are no longer normalized. We make an initial estimate for the initial slope of the $\bar{P}$-wavefunction, P_o; we then integrate outwards by a step-by-step method until such a method becomes unstable; we then integrate inwards, setting the wavefunctions to zero at infinity, and matching the values of the $\bar{P}$-wavefunction at the join point. We then use the discrepancy in the values of the $\bar{Q}$-wavefunction, as calculated by the inward and outward integrations, at the join point, to predict a new P_o-value as follows.

If we have chosen our estimate P_o incorrectly, the correct value for this will be

$$P_o + \delta P_o$$

Then we would have

$$\left(\bar{Q} + \frac{\partial\bar{Q}}{\partial P_o} \cdot \delta P_o\right)_{out} = \left(\bar{Q} + \frac{\partial\bar{Q}}{\partial P_o} \cdot \delta P_o\right)_{in} \qquad (5.3.1)$$

to first order in δP_o.

Thus

$$\delta P_o = - \frac{\bar{Q}_{out} - \bar{Q}_{in}}{\frac{\partial \bar{Q}_{out}}{\partial P_o} - \frac{\partial \bar{Q}_{in}}{\partial P_o}} \qquad (5.3.2)$$

The functions $\frac{\partial \bar{Q}}{\partial P_o}$ can be calculated easily by observing that, differentiating (5.2.25) partially with respect to P_o

$$-c\left(\frac{d}{dr} + \frac{\kappa}{r}\right) \frac{\partial \bar{Q}}{\partial P_o} - \left(\frac{Z}{r} - \varepsilon\right) \frac{\partial \bar{Q}}{\partial P_o} = 0 \qquad (5.3.3)$$

which may be solved by the same routines as (5.2.24) and (5.2.25). The new value for P_o is then used as a new estimate and the process continues until

$$\left| \frac{\bar{Q}_{out} - \bar{Q}_{in}}{\bar{Q}} \right| < 10^{-10} \qquad (5.3.4)$$

and

$$|\delta P_o| < 10^{-10} \qquad (5.3.5)$$

The algorithm is found to be very stable, and able to cope with initial P_o estimates which are incorrect by several orders of magnitude.

Trouble with convergence was experienced with some orbitals. This was found to be due to the fact that a small change in P_o may have a comparatively large effect on the quantity

$$\left. \frac{\bar{Q}_{out} - \bar{Q}_{in}}{\bar{Q}} \right|_{\text{join point}}$$

particularly if $\bar{Q}$ is small or the join point a long way out.

This is overcome by letting the iteration process continue for a maximum of twenty cycles; if convergence has not occurred by this time the join point is slowly moved inwards until convergence occurs. This is quite acceptable numerically since the inward integration routine is stable at all points.

§5.4 Oscillator strengths

The quantity that is measured experimentally, and that we wish to calculate, has been defined in chapter 4, equation (4.5.3), as

$$R = \frac{\mathrm{Im}(E1^{PNC})}{M1} \qquad (5.4.1)$$

The oscillator strengths part of the MCDF program described in chapter 2 was modified to calculate the $E1^{PNC}$ matrix elements.

For bismuth, the atom for which all these calculations were performed, in the one-particle approximation the transitions of interest reduce to

$$6\bar{p} \rightarrow 6p$$

and so the calculation of $E1^{PNC}$ is reduced to the calculation of the reduced matrix element

$$\langle 6p^{PM} || E1 || 6\bar{p}^{PM} \rangle$$

$$= iG\langle 6p || E1 || \overline{6\bar{p}} \rangle - iG\langle \overline{6p} || E1 || 6\bar{p} \rangle \qquad (5.4.2)$$

However, the $|\overline{6p}\rangle$ wavefunction is several orders of magnitude

smaller than the $|\overline{6\bar{p}}>$, and so the second term can be neglected.

To check for consistency the matrix element $<\alpha||E1||\beta>$ is calculated in three different ways. Using the notation of §2.4 we write

$$<\alpha||E1||\beta> = \kappa_{\alpha\beta}\ \bar{M}_{\alpha\beta} \tag{5.4.3}$$

where $\kappa_{\alpha\beta}$ is an angular factor whose form need not concern us at the present. Then, following Grant (1974), we may write

$$\bar{M}_{\alpha\beta} = \bar{M}^{e}_{\alpha\beta}(0) = i\{\frac{1}{\sqrt{2}}\ [(\kappa_\alpha-\kappa_\beta)\ I_2^{+} + 2I_2^{-}]$$

$$- \sqrt{2}[(\kappa_\alpha-\kappa_\beta)\ I_0^{+} - I_0^{-}]\} \tag{5.4.4}$$

$$\bar{M}_{\alpha\beta} = \bar{M}^{e}_{\alpha\beta}(\sqrt{2}) = i.\frac{3}{\sqrt{2}}\ \{-2J^{(1)} + [(\kappa_\alpha-\kappa_\beta)\ I_2^{+} + 2I_2^{-}]\} \tag{5.4.5}$$

$$\bar{M}_{\alpha\beta} \simeq \bar{M}^{NR}_{\alpha\beta} = \frac{-i\sqrt{2}\omega}{c}\int_0^\infty (P_\alpha P_\beta + Q_\alpha Q_\beta).r\ dr \tag{5.4.6}$$

where

$$\omega = E_\alpha - E_\beta \tag{5.4.7}$$

is the transition energy from state α to state β,

$$I_L^{\pm}(\omega) = \int_0^\infty (P_\alpha Q_\beta \pm Q_\alpha P_\beta)\ j_L(\frac{\omega r}{c})\ dr \tag{5.4.8}$$

and

$$J^{(L)}(\omega) = \int_0^\infty (P_\alpha P_\beta + Q_\alpha Q_\beta)\ j_L(\frac{\omega r}{c})\ dr \tag{5.4.9}$$

$\bar{M}^{e}_{\alpha\beta}(0)$ is the result obtained using the Coulomb gauge and reduces in the nonrelativistic limit to the usual velocity form for the corresponding matrix element. $\bar{M}^{e}_{\alpha\beta}(\sqrt{2})$ is the

result obtained using the Babushkin gauge and reduces in the nonrelativistic limit to $\bar{M}^{NR}_{\alpha\beta}$, the usual length form for the corresponding matrix element.

It should be noted at this point that equation (5.4.6) is a nonrelativistic approximation to equation (5.4.5) and so would not be expected to yield identical answers. Also the equality of the equations (5.4.4) and (5.4.5) only holds analytically when applied to matrix elements of the form

$$<\alpha^{PM}\|E1\|\beta^{PM}>$$

and not to the individual components

$$<\alpha||E1||\bar{\beta}> \quad \text{and} \quad <\bar{\alpha}\|E1\|\beta>.$$

In the problem under consideration we have, as already remarked,

$$|<\bar{6p}||E1||6\bar{p}>| << |<6p||E1||\bar{6\bar{p}}>|$$

and so we would expect equations (5.4.4) and (5.4.5) to give approximately equal results for the calculation of $<6p\| E1||\bar{6\bar{p}}>$ but not necessarily for $<\bar{6p}||E1||6\bar{p}>$, a result found to be true in practice.

For M1 matrix elements the situation is slightly different since the M1 transition is allowed, even when parity mixing is not taken into account, which means that the PNC part of the wavefunction may be neglected. To check for consistency we again calculate $<\alpha||M1||\beta>$ in three ways, viz.

$$<\alpha||M1||\beta> = \kappa_{\alpha\beta} M^{m}_{\alpha\beta} \qquad (5.4.10)$$

where

$$M^{m}_{\alpha\beta} = \frac{3}{\sqrt{2}} (\kappa_\alpha + \kappa_\beta) I_1^{+}(\omega) \qquad (5.4.11)$$

This has the nonrelativistic approximation

$$M^{m}_{\alpha\beta} = \frac{(\kappa_\alpha + \kappa_\beta)(\kappa_\alpha + \kappa_\beta - 1)}{2\sqrt{2}c^2} \int_0^\infty R_\alpha R_\beta \, dr \qquad (5.4.12)$$

where

$$R_\alpha = 1 + \frac{1}{4c^2}\left(-\tfrac{1}{2}\frac{d^2}{dr^2} + \frac{\ell_\alpha[\ell_\alpha+1]}{2r^2}\right) P_\alpha \qquad (5.4.13)$$

which can also be written

$$M^{m}_{\alpha\beta} = \frac{(\kappa_\alpha + \kappa_\beta)(\kappa_\alpha + \kappa_\beta - 1)}{2\sqrt{2}c^2} \int_0^\infty (P_\alpha P_\beta + Q_\alpha Q_\beta) dr \qquad (5.4.14)$$

§5.5 Results

In order to solve the equations (5.2.22) to (5.2.25) we must define the model potential Z(r) introduced at the beginning of section 5.3. A suitable function for bismuth (corresponding to a uniform nuclear change distribution) is

$$Z(r) = \left[1 + \frac{Z - 1}{H\{\exp(r/d) - 1\} + 1}\right] \qquad r \leq r_N \qquad (5.5.1)$$

(Green et al. (1969)) and

$$Z(r) = \frac{Z}{2r_N}\left[3 - (r/r_N)^2\right] \qquad r > r_N \qquad (5.5.2)$$

where we take

$$d = 0.7503 \text{ a.u.} \tag{5.5.3}$$

and

$$H = 4.6653 \tag{5.5.4}$$

with

$$Z = 83; \tag{5.5.5}$$

the first two values are selected so as to give reasonable values for the fine structure splitting of the 6p shell and the energy of the 7s state (Loving (1978)). As usual, r_N is nuclear radius. Thus the following results and those of Loving for the $\langle 6p||E1||6\bar{p}\rangle$ matrix elements are directly comparable.

TABLE 5.1

Calculated values of $\langle 6p||E1||6\bar{p}\rangle$

	EPP	CEL
eq. (5.4.4)	.4302817	
eq. (5.4.5)	.4302813	
eq. (5.4.6)	.4302821	.4180

A further check on the consistency of the results suggested by Loving was a comparison of the matrix elements

$\langle \overline{6s} | 6\overline{p} \rangle$ and $\langle \overline{6\overline{p}} | 6s \rangle$

If orthogonality is to be ensured between the $|6s^{PM}\rangle$ and $|6\overline{p}^{PM}\rangle$ wavefunctions - it may be shown to occur analytically in this model - these should be equal. The results are shown in Table 5.2.

TABLE 5.2

	Calculated overlap integrals	
	EPP	CEL
$\langle \overline{6s} \| 6\overline{p} \rangle$	241.1473	234.40341
$\langle \overline{6\overline{p}} \| 6s \rangle$	241.1680	234.39681
Difference	-.0207	0.00660

The value of the $\langle \overline{6p} \| E1 \| 6\overline{p} \rangle$ matrix element is, as predicted, less certain and much smaller:

eq.(5.4.4)	$.14300439 \times 10^{-6}$
eq.(5.4.5)	$.20365994 \times 10^{-6}$
eq.(5.4.6)	$.20366004 \times 10^{-6}$

A similar investigation into the $\langle 6p \| M1 \| 6\overline{p} \rangle$ matrix element shows good agreement between values calculated by each of the three equations (5.4.11), (5.4.12) and (5.4.14). These are also in broad agreement with the results of Loving.

We may now return to the problem raised in §5.2, namely, whether the terms in G^2, neglected in equations (5.2.22) and (5.2.23), really are negligible. Eq. (5.2.22) may be rewritten

$$c \frac{dP}{dr} = (2c^2 + \frac{Z}{r} - \varepsilon)Q - \frac{\kappa c}{r} P - G^2 \rho_N \overline{P} \qquad (5.5.6)$$

So we will say that the $G^2\rho P$ term is negligible if

$$|G^2\rho_N\bar{P}| \ll |(2c + \frac{Z}{r} - \varepsilon)\,Q - \frac{\kappa c}{r}P| \qquad \text{for all } r \qquad (5.5.7)$$

If $r > r_N$ this is obviously true (for $\rho_N = 0$ then). In the region $r < r_N$ we test this for the $6\bar{p}$ orbital

$r\times10^5$(a.u.)	1	1.568	3.320	7.029	9.974	14.154($\tilde{=}r_N$)
$G^2\rho_N\bar{P}\times10^{14}$	3.73	9.21	40.7	173.6	329.7	614.3
$(2c^2 + \frac{Z}{r} - \varepsilon)Q$						
$-\frac{\kappa c}{r}P$	-104	-161	-333	-623	-757	-732

and we see that in this case the ratio of the two terms is always in excess of 10^{14}. This gives us complete confidence that the term $G^2\rho_N\bar{P}$ really is negligible. Similar observations apply to the $G^2\rho_N\bar{Q}$ term in equation (5.2.23).

§5.6 Numerical dependence of results on computational parameters

There are three numerical parameters that can be changed easily: the gridsize, h; the inner point of integration, r_o; and the accuracy of convergence of the parity conserving calculation, ACCY. (For the first two, see eq. (2.5.1)). The results of changing these are shown in tables 5.3 to 5.5.

The effect of the variation of ACCY in the range 10^{-6} to 10^{-10} is minimal. Even an increase to 10^{-4} affects only the difference $\langle\overline{6s}|6\bar{p}\rangle - \langle\overline{6\bar{p}}|6s\rangle$, and that to only a few percent.

Changing h or r_o, however, causes more considerable

TABLE 5.3

Variation of the matrix element $1000\ \langle 6p \| E1 \| 6\bar{p} \rangle$ with numerical parameters

		h = .05	h = .055	h = .06	h = .07	h = .09
$r_o = 10^{-7}$	R			442.1094		
	C			442.1095		
	B			442.1085		
$r_o = 2 \times 10^{-7}$	R			409.7852		
	C			409.7852		
	B			409.7844		
$r_o = 10^{-6}$	R		430.0503	397.7089		
	C		430.0501	397.7090		
	B		430.0495	397.7082		
$r_o = 10^{-5}$	R	430.2821	421.1280	423.9651	372.8746	404.7924
	C	430.2817	421.1278	423.9652	372.8753	404.7956
	B	430.2813	421.1272	423.9643	372.8738	404.7916
$r_o = 3 \times 10^{-5}$	R		419.4597			
	C		419.4595			
	B		419.4589			
$r_o = 10^{-5}$ no difference corrections	R	440.6927				
	C	445.0449				
	B	440.6919				

		PC ACCY 10^{-4}	PC ACCY 10^{-6}	PC ACCY 10^{-8}	PC ACCY 10^{-10}
PNC ACCY 10^{-10}	R	430.2801	430.2820	430.2821	430.2820
	C	430.2782	430.2815	430.2817	430.2817
	B	430.2792	430.2811	430.2813	430.2812

C: Matrix element calculated in a fully relativistic formulation using the Coulomb gauge.

B: Matrix element calculated in a fully relativistic formulation using the Babushkin gauge.

R: Use the approximate formula

$$\langle a||E1||b\rangle = \frac{\sqrt{2}\omega}{c} \int^{\infty} r\,(P_a P_b + Q_a Q_b)\,dr.\ \kappa_{ab}$$

where κ_{ab} is an angular factor ($1/\sqrt{3}$ in this case) (c.f. Grant (1974))

Compare this with Loving (R) 418.0 ($h = 0.017$ ACCY $= 10^{-4}$ $r_o = 1.7 \times 10^{-7}$)

Table 5.4

Numerical values of the overlap integral $\langle 6\bar{p}|\overline{6s}\rangle$

(i) PC ACCY = 10^{-8} PNC ACCY = 10^{-10}

	h=.05	h=0.55	h=.06	h=.07	h=.09
$r_o = 10^{-7}$			247.80		
$r_o = 2\times10^{-7}$			229.68		
$r_o = 10^{-6}$	239.39	241.03	222.91		
$r_o = 10^{-5}$	241.15	236.03	237.63	209.02	227.05
$r_o = 3\times10^{-5}$		235.09			

(ii) h = .05
$r_o = 10^{-5}$

	PC ACCY 10^{-4}	PC ACCY 10^{-6}	PC ACCY 10^{-8}	PC ACCY 10^{-10}
PNC ACCY 10^{-10}	241.1483337	241.1473319	241.1473018	241.1473010

Table 5.5

Difference in overlap integrals $\langle 6s|\overline{6\bar{p}}\rangle - \langle 6\bar{p}|\overline{6s}\rangle$

(i) PNC ACCY = 10^{-10} PC ACCY = 10^{-8}

	h=.05	h=.055	h=.06	h=.07	h=.09
$r_o = 10^{-7}$			0.04366		
$r_o = 10^{-6}$	0.02057	0.03016	0.03928		
$r_o = 10^{-5}$	0.02072	0.02954	0.04187	.06732	.19276
$r_o = 3\times10^{-5}$			0.02944		

(ii) h = .05 $r_o = 10^{-5}$

	PC ACCY 10^{-4}	PC ACCY 10^{-6}	PC ACCY 10^{-8}	PC ACCY 10^{-10}
PNC ACCY 10^{-10}	0.0195233	0.0206829	0.0207208	0.0207217

variations. In general these appear to be random, except for the difference $\langle\overline{6s}|6\bar{p}\rangle - \langle\overline{6\bar{p}}|6s\rangle$ which is approximately proportional to h^4. Since the numerical methods we use are of accuracy h^4 (e.g. Simpson's rule) it is very probable that the difference here is due to these numerical errors (truncation error) and not to any fundamental nonorthogonality of the parity mixed wavefunctions.

A closer investigation of the variation of the results reveals that they do, in fact, depend on h and r_o in a regular way; the apparent randomness of the results noted above is only a result of changing h and r_o too much. When very small changes are made to h and r_o a regular 'sawtooth' pattern can be seen; see fig. 5.1 to 5.6. The reason for this becomes apparent when we note that the discontinuities in the graphs always occur when $\frac{\log_e(r_N/r_o)}{h}$ is an integer (r_N is the nuclear radius); and since the nuclear distribution is uniform, the effective nuclear radius is the distance from the origin of the last point that is inside the nucleus. As r_o or h gradually increases this increases until the point crosses the nuclear boundary when the effective nuclear radius changes discontinuously to the distance from the origin of the next point, and then increases again smoothly.

The M1 matrix elements show no appreciable variation with h and r_o.

§5.7 Numerical instability

Mention should be made of the "spike" in the PNC wavefunctions at the nuclear boundary. Because of the assumption that the nucleus has a uniform density, the last term in each

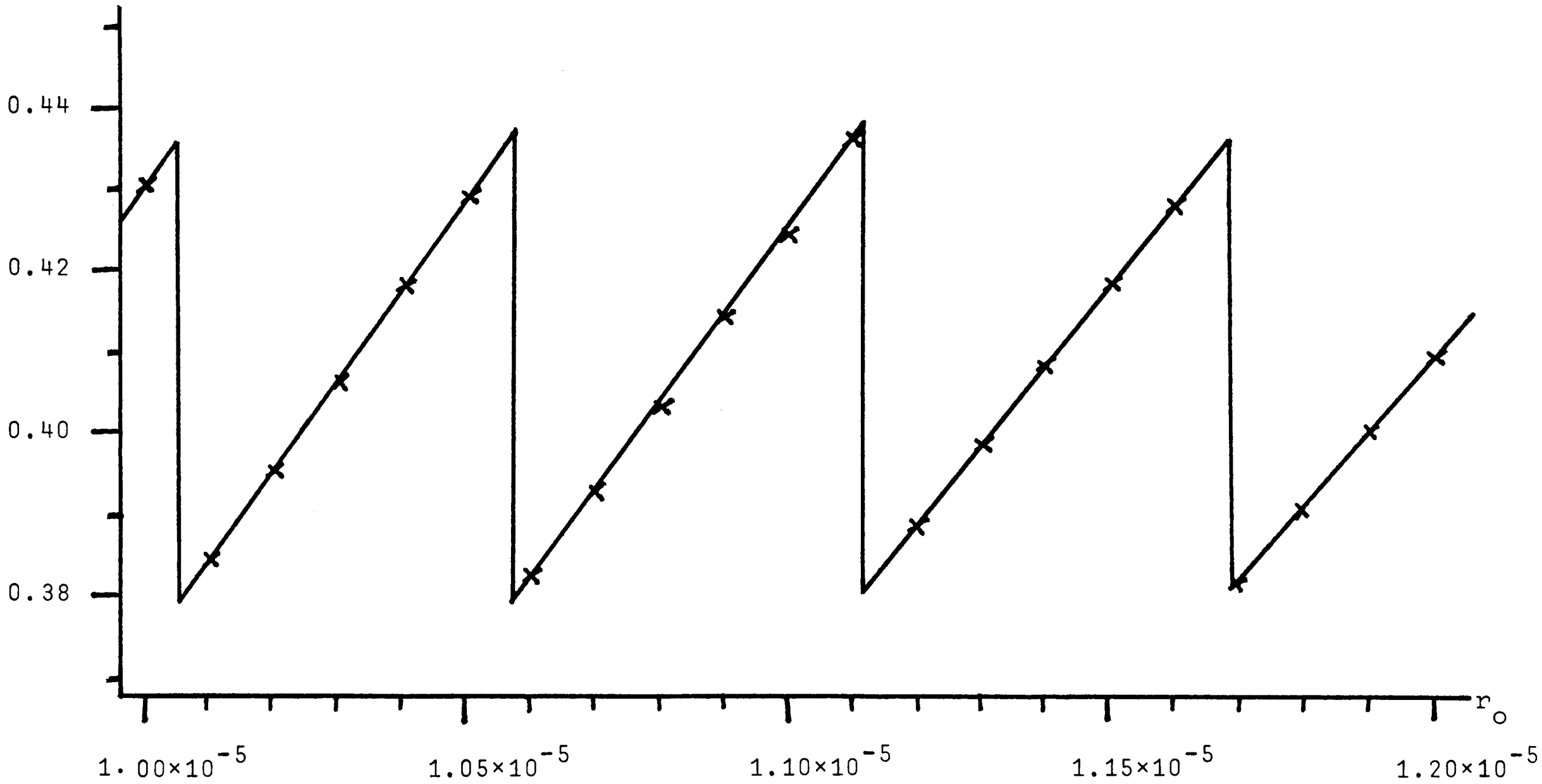

Figure 5.1. Dependence of E1 matrix element on inner integration point

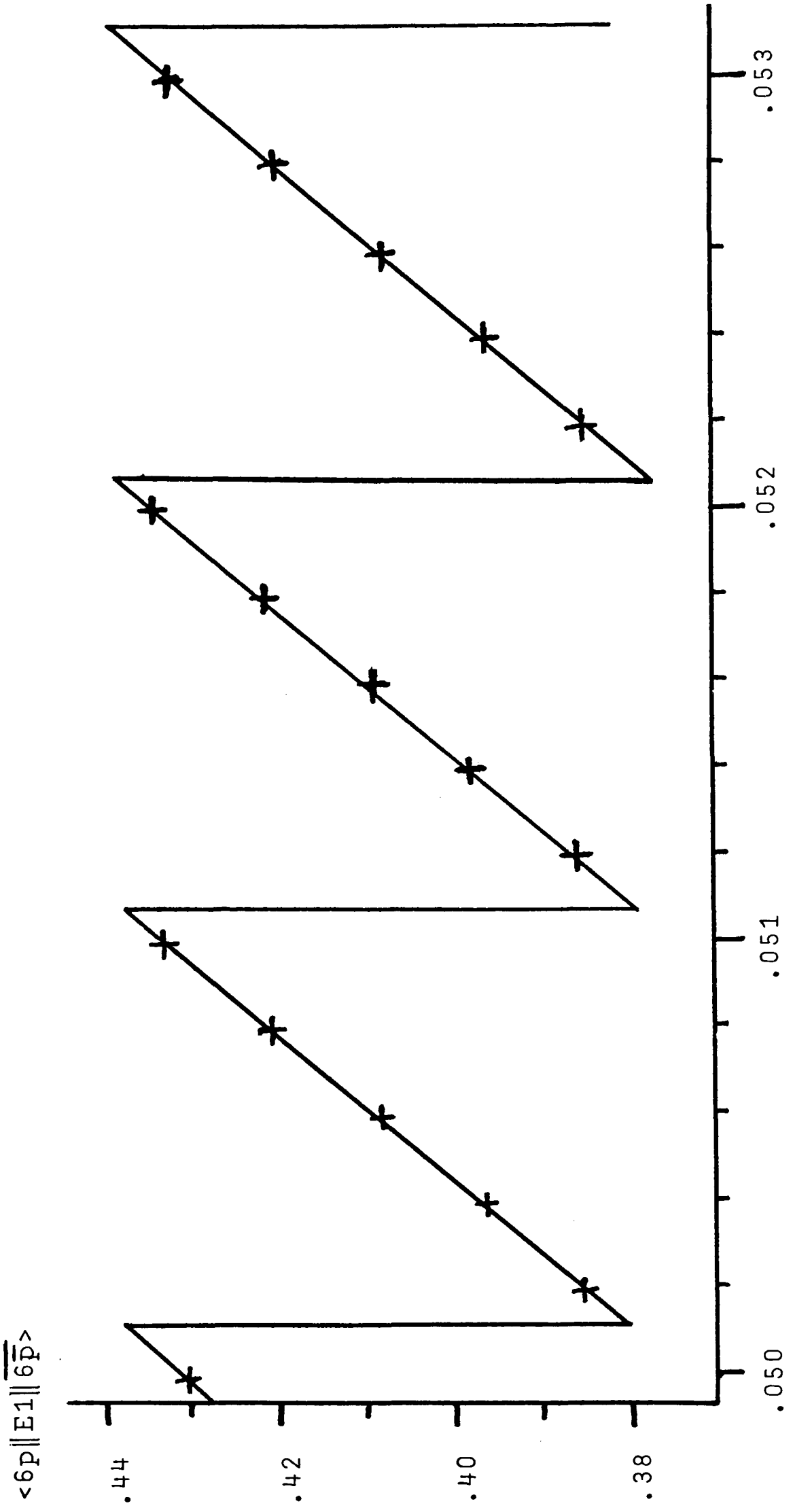

Figure 5.2. Dependence of E1 matrix ele

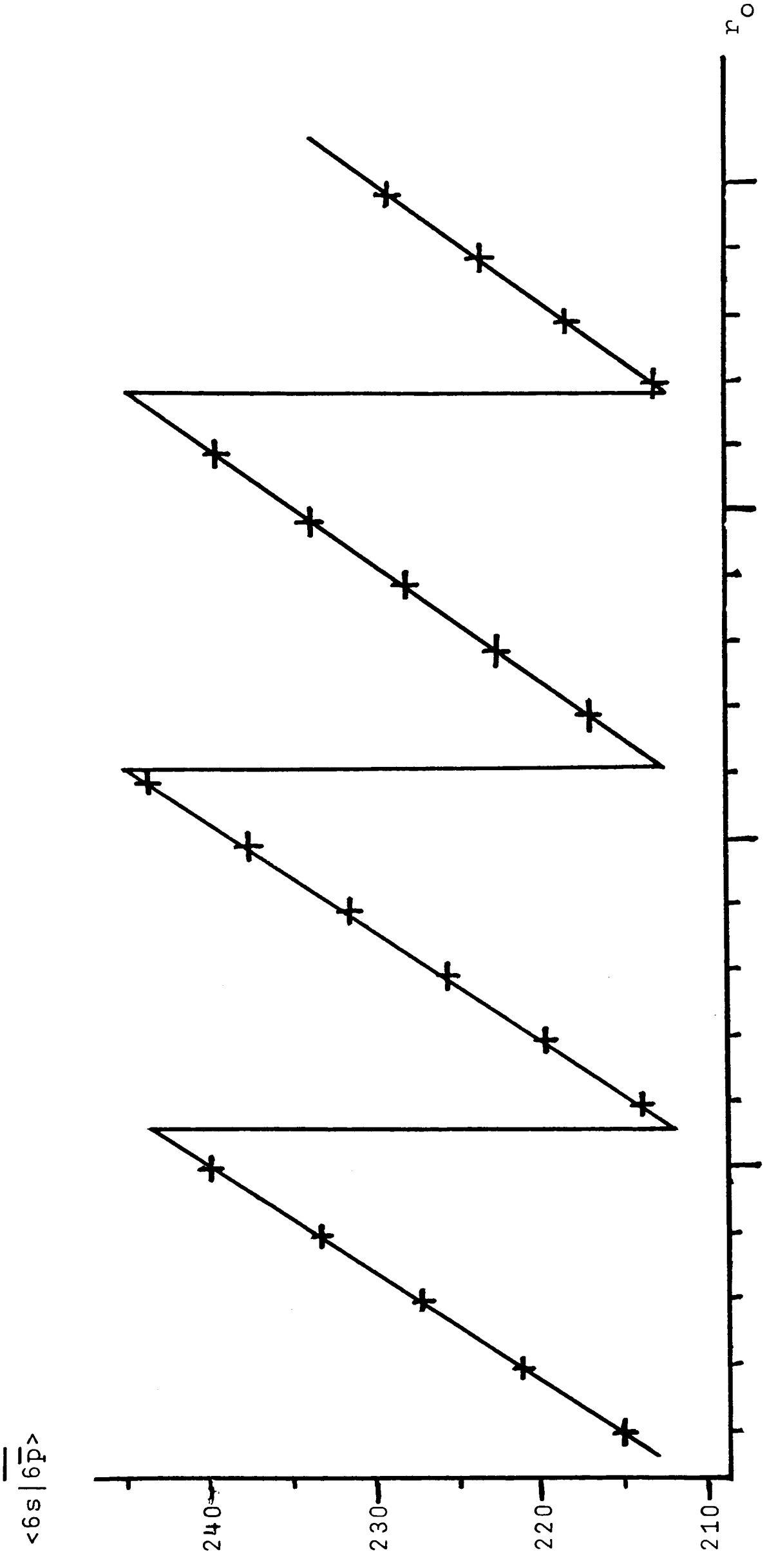

Figure 5.3. Dependence of overlap integral on inner point of integration.

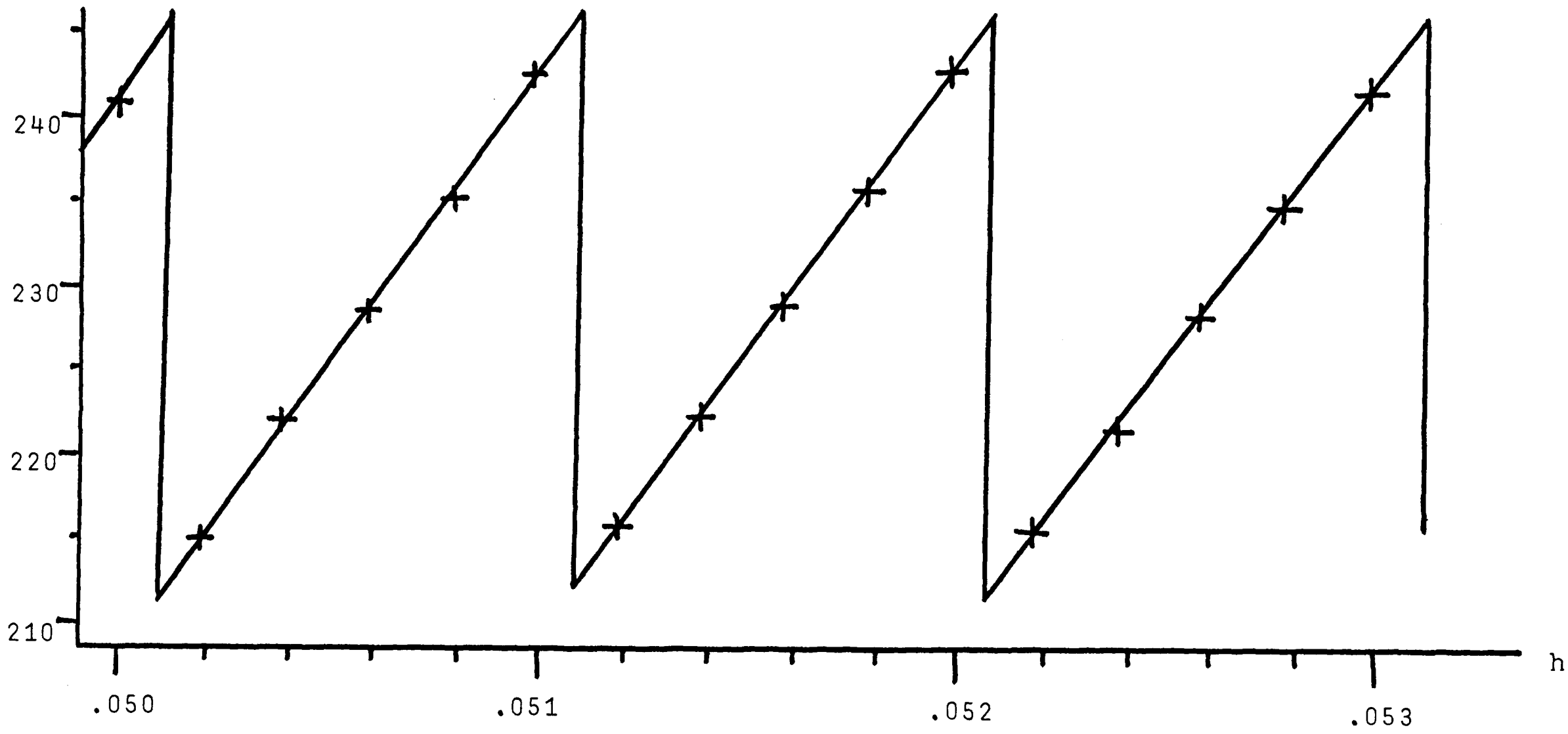

Figure 5.4. Dependence of overlap integral on gridsize

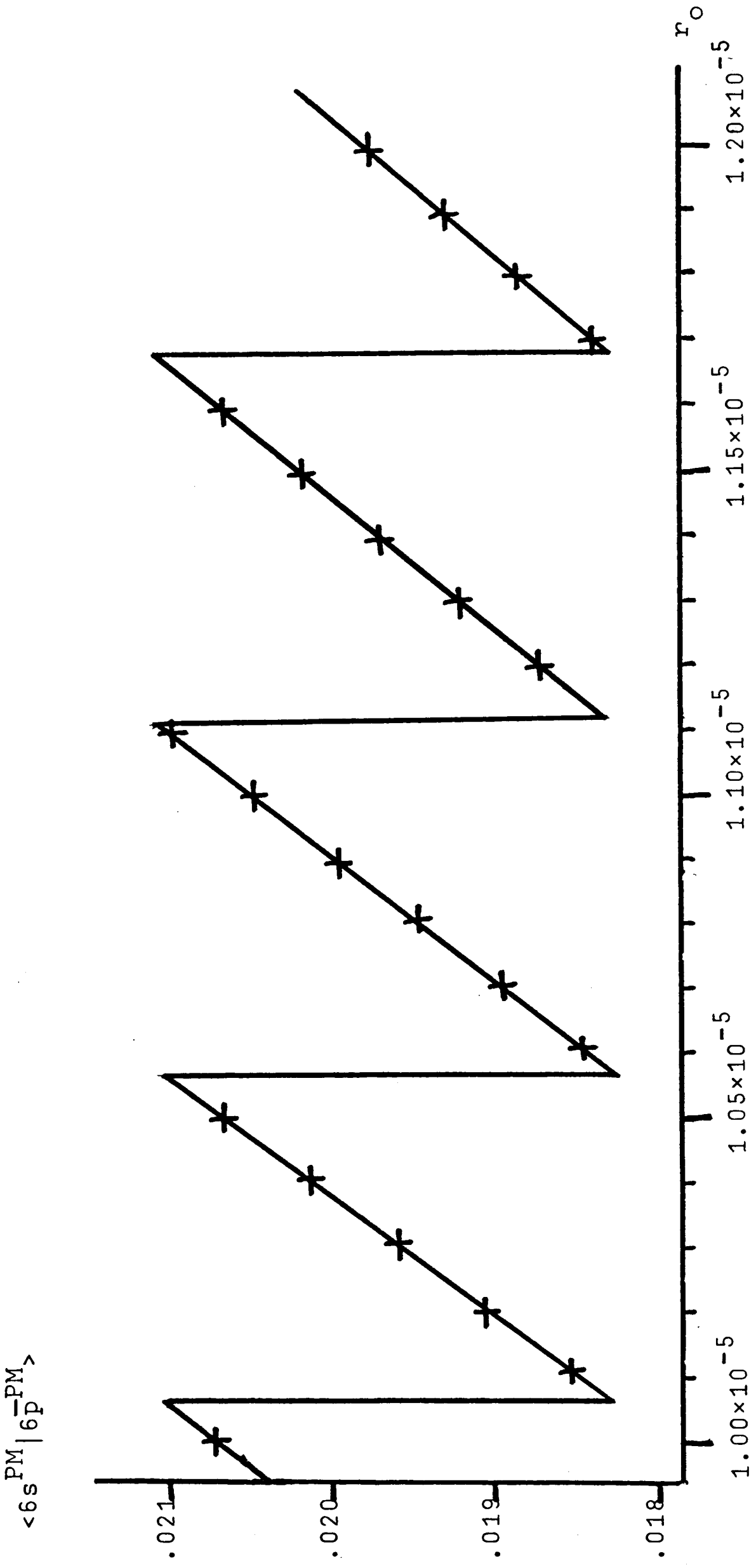

Figure 5.5. Dependence of orthogonality on inner point of integration

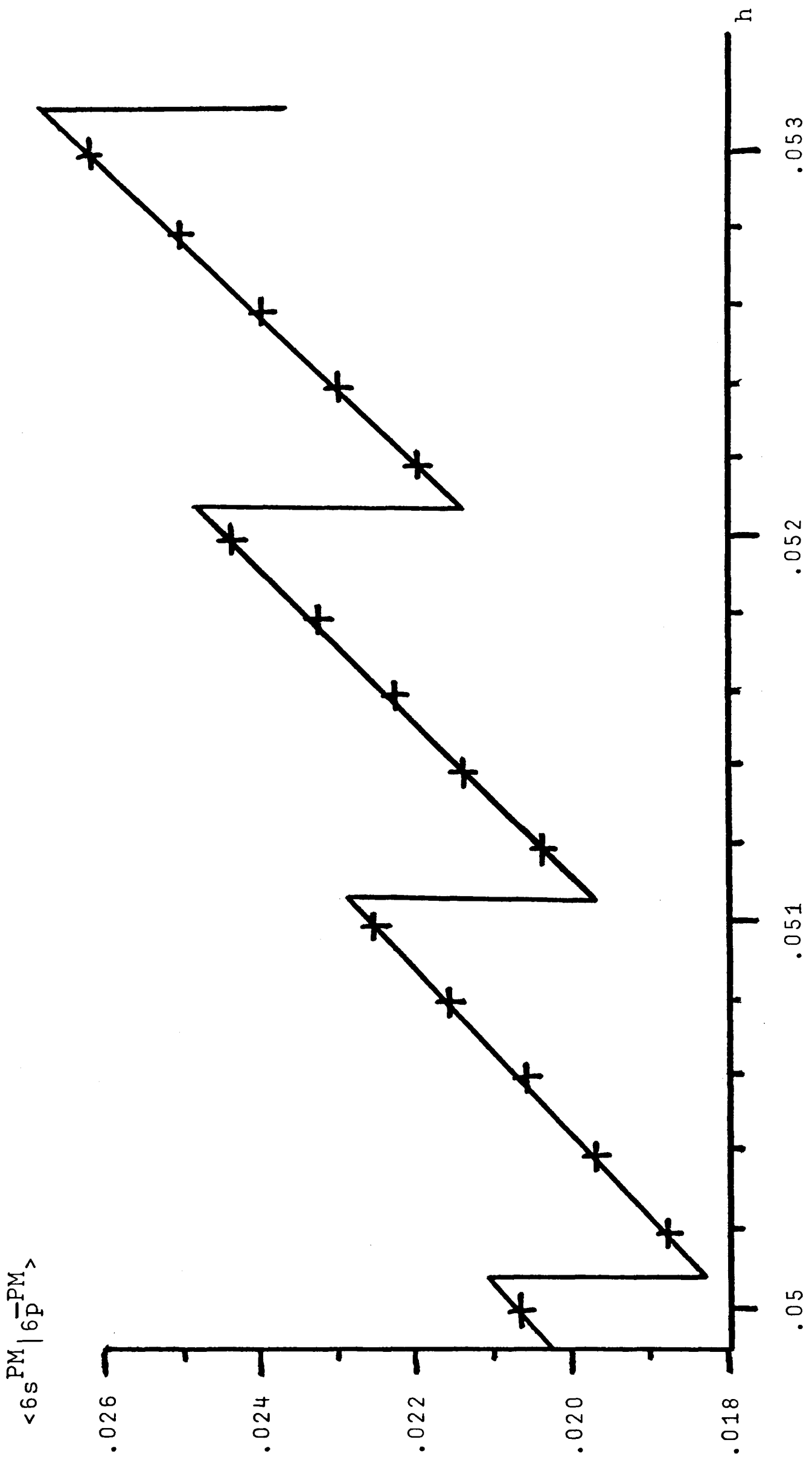

Figure 5.6. Dependence of orthogonality on gridsize

of equations (5.2.24) and (5.2.25) will be discontinuous at the nuclear boundary, since at this point ρ_N drops from $\sim 10^{12}$ to 0. This will cause the derivatives $\frac{d\bar{P}}{dr}$ and $\frac{d\bar{Q}}{dr}$ to be discontinuous, as can be seen from the graphs of $\bar{P}$ and $\bar{Q}$ (figure 5.7).

It is clear that such a state of affairs is most unsatisfactory, since we use the wavefunctions to form integrands in the calculation of matrix elements - see equations (5.4.6) (5.4.7) and (5.4.8). Such integrations must be carried out numerically by a procedure such as Simpson's rule. However, it is shown in standard texts on numerical analysis (e.g. Phillips and Taylor (1973) p. 133) that Simpson's rule for the calculation of $\int_A^B f(x)\,dx$ is stable only if all the derivatives $f'(a)$, $f''(x)$, $f'''(x)$ and $f^{iv}(x)$ exist and are bounded on the interval (A,B); and if f(x) contains terms like $\bar{P}$ or $\bar{Q}$ then $f'(x)$ will not be defined at the nuclear boundary, much less $f''(x)$, $f'''(x)$ or $f^{iv}(x)$. Similar results hold for all numerical methods for integration.

§5.8 Conclusions

These calculations, and the results reported here, are not intended to be exhaustive, they are only intended to be a stage in the development of a program to solve the problem of many-particle PNC theory. The data presented show that the results are reliable, being in good agreement with those calculated by a different program. They also show that the results obtained using the usual values of h, r_o and ACCY (.05, 10^{-5} and 10^{-8} respectively) are approximately independen

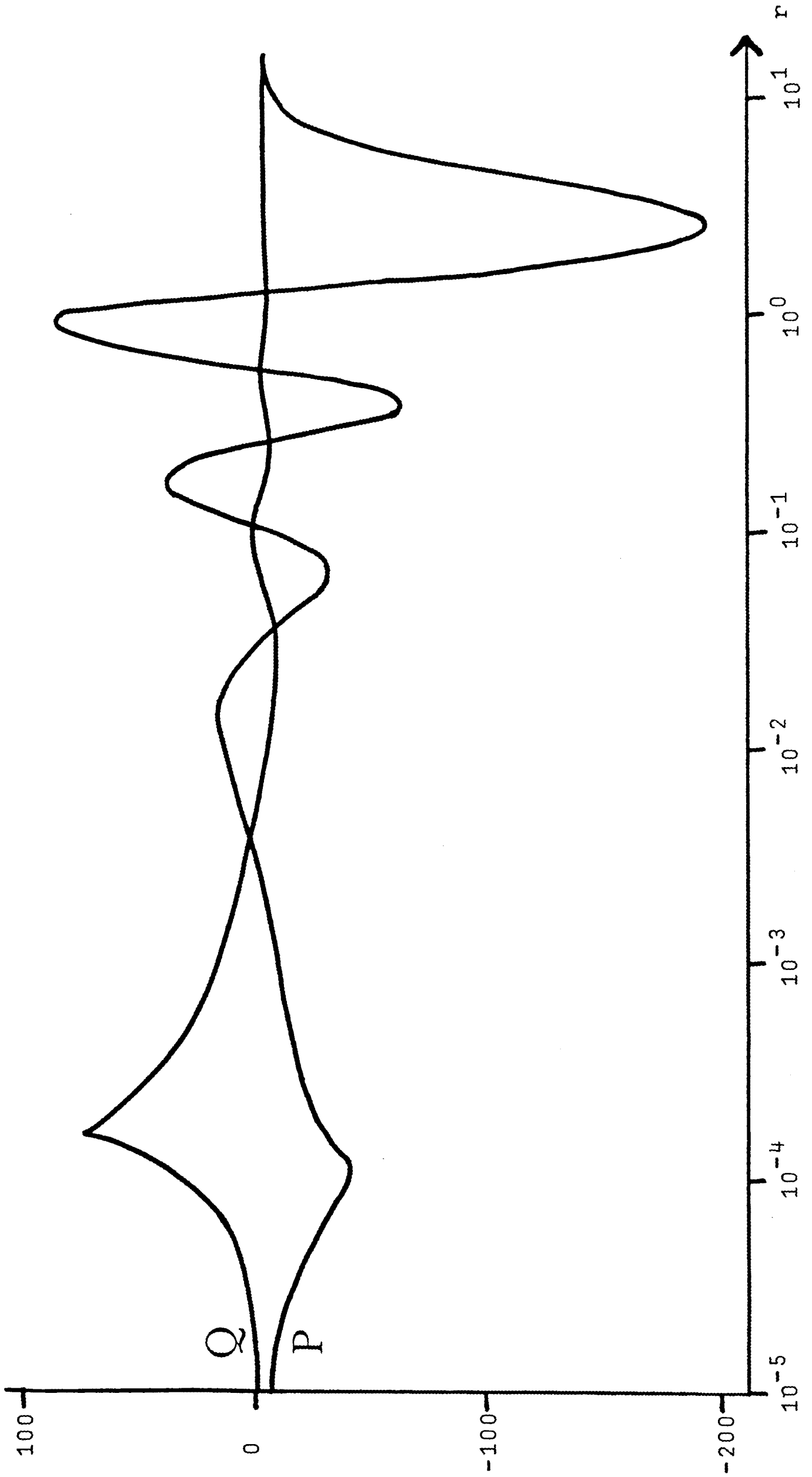

Figure 5.7 Graph of the PNC wavefunction

of any variations in these parameters, to an accuracy of about 10%, with the exception of orthogonality integrals which show a marked h^4 dependence.

The problems involving the discontinuity of the inhomogeneous term in the PNC equations and the consequent numerical problems may be overcome by using a more physical nuclear distribution - say a Fermi two-parameter distribution. However, the present calculations indicated that we could expect that a many-particle theory could be developed and solved using a modification of these techniques, and because of the author's enthusiasm for that problem the single-electron problem was not taken any further.

Chapter 6

O come with old Khayyám, and leave the wise
To talk....

Khayyam (1100b)

The Many-particle Theory of Parity Non-conservation in Atoms

CHAPTER 6

THE MANY-PARTICLE THEORY OF PARITY NON-CONSERVATION IN ATOMS

§6.1 Introduction

The earlier investigations into the field effect of isotope shift have revealed that indirect effects are often of the same magnitude as direct effects. The purpose of this investigation was to determine whether this was true for parity non-conserving matrix elements.

In this chapter the parity non-conserving equivalents of the MCDF equations are derived, and some theoretical aspects of their solution are discussed. The results of the calculations will be given in chapter 8.

§6.2 The energy functional

At this stage we combine the approach used in chapter 2 to obtain the MCDF equations for the EAL problem and that used in chapter 5 to obtain the single-particle PNC equations. The theory then proceeds in much the same way as before.

There are a number of reasons for selecting the EAL method rather than the OL or EOL method, which we discuss before deriving the energy functional.

For consistency, we should choose the same method for both the parity conserving and parity violating calculations. This will become apparent as this chapter is read, since it will be shown that both the parity conserving and the PNC MCDF

equations are derived from a single energy functional. If we are unable to perform an OL or an EOL calculation for the parity conserving problem, then we should perform only an EAL calculation for the PNC problem. In practice, it was found that there were severe convergence problems with the "correlation orbitals" (this term will be defined in Chapter 7) when OL or EOL calculations were attempted on bismuth and that these could not be overcome. These arise because, for correlation orbitals, the occupation numbers $\bar{q}_a$ which appear in the MCDF equations (2.2.22) to (2.2.31) are small, and, since they occur in the denominator of the MCDF equations, give rise to great instabilities.

The question, in the parity conserving case, of the relative merits of the EAL and OL methods has been discussed in detail (Grant, Mayers and Pyper (1976), Pyper and Grant (1977), Rose, Grant and Pyper (1978), Hata and Grant (1983b)). The first three papers - all of which considered heavy atoms - demonstrate (to summarize very briefly) that the transition energies examined showed little sensitivity to the method used, although the contributions from one-electron and two-electron effects varied considerably; that neither method is consistently better than the other; and that, since the EAL method is an order of magnitude faster than the OL method and also uses the same orbitals for both levels of a transition (useful when calculating oscillator strengths, for example) the EAL method is preferable. The results for bismuth in a simple single-manifold calculation (Rose, Grant and Pyper (1978)) are reproduced below:-

Level (jj label)	OL	EAL	Experiment
$(6\bar{p}^2{}_o\ 6p)_{3/2}$	0	0	0
$(6\bar{p}\ 6p^2{}_2)_{3/2}$	12676	12539	11419
$(6\bar{p}\ 6p^2{}_2)_{5/2}$	17447	17351	15438
$(6\bar{p}\ 6p^2{}_o)_{1/2}$	25069	24973	21661
$(6p^3)_{3/2}$	36312	36379	33165

The final paper (Hata and Grant (1983b)) is only concerned with the lithium isoelectronic sequence for light ($Z \leq 20$) atoms, but demonstrates that the EAL method is preferable for high-accuracy calculations; this is explained in terms of the lack of orthogonality of the atomic state functions (Ψ_a in equation (2.2.4)) when the wavefunctions are different for each atomic state. Their argument appears to be of general applicability.

It seems not unreasonable to hope that a similar result will apply in the parity non-conserving case.

The EOL method has not been discussed so far. This is mainly because, although the capacity to perform such calculations exists in theory, there is a bug in the relevant part of the published program. Since its removal involves a major change in the structure of the program, it will not be corrected until the next version of the program is published; and at the time that the calculations reported in this thesis were undertaken, it was not at all clear how the problem was to be overcome. As remarked above, if a parity conserving cal-

culation cannot be undertaken, then neither should its PNC counterpart. Also, the difference between EOL and AL/EAL calculations may be overestimated; it is worth pointing out that an EAL calculation in which all configurations are weighted equally (rather than in proportion to 2J+1 as is usual), (i.e. an AL calculation, for example) finds stationary values of the same functional as does an EOL calculation when all the levels are optimized on; thus we could expect both calculations to give identical results.

The EAL method represents a generalization of the "average of configuration" method which is used by, inter alia, Martensson et al. (1981); an EAL calculation with the usual configurational weightings produces the same wavefunctions as an average of configuration calculation, providing the former uses the same set of configurations as are averaged over in the latter; thus Martensson et al.'s jj-average of configuration calculation is equivalent to an AL calculation on the single configuration $6s^2 6\bar{p}^2 6p$, whilst their LS-average of configuration is equivalent to an EAL on the 5 CSFs of the $6s^2 6p^3$ manifold. However, the EAL method may easily be generalized itself to the OL or EOL method using little more than the techniques that follow in this chapter.

We now turn to the derivation of the functional whose stationary point we wish to determine. It may be written as

$$\boldsymbol{H}^{PM} = \sum_{r=1}^{N_c} H_{rr}^{PM} \cdot c_r^{\,2} \qquad (6.2.1)$$

where the $\{c_r\}$ are a given set of weightings subject to the normalization constraint

$$\sum_{r=1}^{N_c} c_r^2 = 1 \tag{6.2.2a}$$

and

$$H_{rs}^{PM} = \langle \Phi_r^{PM} | H^{PM} | \Phi_s^{PM} \rangle \tag{6.2.2b}$$

where Φ_r^{PM} is a parity mixed configuration state function which may be written as the usual sum of Slater determinants of one particle parity mixed wavefunctions

$$\psi_\alpha^{PM} = \psi_\alpha + iG\overline{\psi}_\alpha \tag{6.2.3}$$

where

$$\psi_\alpha = \frac{1}{r} \begin{pmatrix} P_\alpha(r)\, \chi_{\kappa_\alpha, m_\alpha}(\theta,\phi) \\ iQ_\alpha(r)\, \chi_{-\kappa_\alpha, m_\alpha}(\theta,\phi) \end{pmatrix} \tag{6.2.4}$$

and

$$\overline{\psi}_\alpha = \frac{1}{r} \begin{pmatrix} \overline{P}_\alpha(r)\, \chi_{-\kappa_\alpha, m_\alpha}(\theta,\phi) \\ i\overline{Q}_\alpha(r)\, \chi_{\kappa_\alpha, m_\alpha}(\theta,\phi) \end{pmatrix} \tag{6.2.5}$$

For simplicity we subject the ψ_α^{PM} to the orthonormality constraints

$$\langle \psi_\alpha^{PM} | \psi_\beta^{PM} \rangle = \delta_{\alpha\beta} \tag{6.2.6}$$

This is equivalent to finding the unconstrained stationary points of the functional

$$\Gamma = \boldsymbol{H}^{PM} + \sum_\alpha \overline{q}_\alpha \varepsilon_\alpha \langle \psi_\alpha^{PM} | \psi_\alpha^{PM} \rangle + \sum_{\alpha \neq \beta} \varepsilon_{\alpha\beta} \langle \psi_\alpha^{PM} | \psi_\beta^{PM} \rangle \tag{6.2.7}$$

where the ε_α and $\varepsilon_{\alpha\beta}$ are Lagrange multipliers which must be chosen such that (6.2.6) is satisfied.

The Hamiltonian

$$H^{PM} = H^{PC} + GV^{PNC} \tag{6.2.8}$$

where

$$H^{PC} = \sum_{i=1}^{N} h_i + \sum_{1\leq i<j\leq N} 1/r_{ij} \tag{6.2.9}$$

h_i is the usual single-particle Dirac Hamiltonian, and

$$V^{PNC} = \sum_{i=1}^{N} v_i{}^{PNC} \tag{6.2.10}$$

$$v_i{}^{PNC} = \gamma_5 \rho_N(r_i) \tag{6.2.11}$$

$\rho_N(r)$ is the nucleon distribution as in chapter 5, and

$$\bar{q}_\alpha = \sum_{m=1}^{N_c} c_m{}^2 q_m(\alpha) \tag{6.2.12}$$

as before.

After a considerable quantity of algebra we obtain (see Appendix 1 for a detailed derivation)

$$\begin{aligned} \Gamma = \Bigg[\sum_\alpha \bar{q}_\alpha \int_0^\infty \Bigg\{ & cQ_\alpha \left(\frac{d}{dr}+\frac{\kappa_\alpha}{r}\right) P_\alpha - cP_\alpha \left(\frac{d}{dr}-\frac{\kappa_\alpha}{r}\right) Q_\alpha \\ & -2c^2 Q_\alpha{}^2 - \frac{Z_N}{r}(P_\alpha{}^2+Q_\alpha{}^2) \Bigg\} dr + \sum_{\alpha\leq\beta,\, k\in K_0} \bar{f}^k(\alpha\beta) R^k(\alpha\beta\alpha\beta) \\ & + \sum_{\alpha<\beta,\, k\in K_+} \bar{g}^k(\alpha\beta) R^k(\alpha\alpha\beta\beta) + \sum_\alpha \varepsilon_\alpha \bar{q}_\alpha \int^\infty (P_\alpha{}^2+Q_\alpha{}^2)\, dr \\ & + \sum_{\substack{\alpha\neq\beta \\ \kappa_\alpha=\kappa_\beta}} \varepsilon_{\alpha\beta} \int_0^\infty (P_\alpha P_\beta + Q_\alpha Q_\beta)\, dr \Bigg] \end{aligned}$$

$$+ G^2 \Bigg[\sum_\alpha \bar{q}_\alpha \int_0^\infty \Big\{ c\bar{Q}_\alpha \Big(\frac{d}{dr} - \frac{\kappa_\alpha}{r} \Big) \bar{P}_\alpha$$

$$- c\bar{P}_\alpha \Big(\frac{d}{dr} + \frac{\kappa_\alpha}{r} \Big) \bar{Q}_\alpha - 2c^2 \bar{Q}_\alpha{}^2 - \frac{Z_N}{r} (\bar{P}_\alpha{}^2 + \bar{Q}_\alpha{}^2) \Big\} dr - 2 \sum_\alpha \bar{q}_\alpha \int_0^\infty \rho \{ P_\alpha \bar{Q}_\alpha - Q_\alpha \bar{P}_\alpha \} dr$$

$$+ \sum_{\alpha\beta k \in \mathbb{K}_0} \bar{f}^k(\alpha\beta) R^k(\bar{\alpha}\beta\bar{\alpha}\beta)(1+\delta_{\alpha\beta}) + \sum_{\alpha\beta k \in \mathbb{K}_+} \bar{g}^k(\alpha\beta) R^k(\alpha\bar{\alpha}\beta\bar{\beta})$$

$$+ \sum_{\alpha\beta k \in \mathbb{K}_-} \bar{g}^k(\alpha\beta) \{ R^k(\bar{\alpha}\bar{\alpha}\beta\beta) - R^k(\bar{\alpha}\alpha\beta\bar{\beta}) \}$$

$$+ \sum_\alpha \varepsilon_\alpha \bar{q}_\alpha \int_0^\infty (\bar{P}_\alpha{}^2 + \bar{Q}_\alpha{}^2) dr + \sum_{\substack{\alpha\beta \\ \kappa_\alpha = \kappa_\beta}} \varepsilon_{\alpha\beta} \int_0^\infty (\bar{P}_\alpha \bar{P}_\beta + \bar{Q}_\alpha \bar{Q}_\beta) dr$$

$$+ \sum_{\substack{\alpha\beta \\ \kappa_\alpha = -\kappa_\beta}} 2\eta_{\alpha\beta} \int_0^\infty (\bar{P}_\alpha P_\beta + \bar{Q}_\alpha Q_\beta) dr \Bigg] + G^4 \Bigg[\sum_{\alpha \le \beta k \in \mathbb{K}_0} \bar{f}^k(\alpha\beta) R^k(\overline{\alpha\beta\alpha\beta})$$

$$+ \sum_{\alpha < \beta k \in \mathbb{K}_+} \bar{g}^k(\alpha\beta) R^k(\overline{\alpha\alpha\beta\beta}) \Bigg] \qquad (6.2.13)$$

The values of k permitted in the various summations are defined by the sets $\mathbb{K}_0$, $\mathbb{K}_+$ and $\mathbb{K}_-$. These are defined in equation (A1.15), and are the usual values in the direct potential, the usual values in the exchange potentials, and the parity forbidden values in the exchange potentials respectively. The terms η_{ab} are the new Lagrange multipliers corresponding to the ε_{ab} first introduced in equation (6.2.7), and are defined in equation (A1.21).

§ 6.3 The MCDF-PNC equations

We wish to find functions which cause the functional Γ to be stationary with respect to variations in the functions on which it depends. In what follows we assume that all the derivatives and integrals exist; this will be guaranteed if

$$P_a \in \boldsymbol{L}^2(\mathbb{R})$$

$$\frac{1}{\sqrt{r}} P_a \in \boldsymbol{L}^2(\mathbb{R})$$

P_a is continuous and differentiable almost everywhere and

$$\frac{dP_a}{dr} \in \boldsymbol{L}^2(\mathbb{R}) \qquad (6.3.1)$$

with the same conditions on Q_a, $\bar{P}_a$ and $\bar{Q}_a$. In practice these conditions will be satisfied by all the functions considered, and so they will not normally be mentioned again explicitly.

Suppose we vary the function P_a, keeping all the other functions fixed:

$$P_a \to P_a + \delta P_a, \qquad (6.3.2)$$

where the variation δP_a is arbitrary except for the requirements that it must satisfy the conditions (6.3.1) and

$$\delta P_a(0) = 0$$

$$\delta P_a(\infty) = 0 \qquad (6.3.3)$$

This will cause a variation in the value of Γ:

$$\Gamma \rightarrow \Gamma + \delta\Gamma$$

where

$$\Gamma = \Gamma(P_a)$$

$$\Gamma + \delta\Gamma = \Gamma(P_a + \delta P_a) \qquad (6.3.4)$$

For clarity we may rewrite equation (6.2.13) as

$$\Gamma = \Bigg[\sum_\alpha \overline{q}_\alpha I(\alpha,\alpha) + \sum_{\alpha\leq\beta,\, k\in\mathbb{K}_o} \overline{f}^k(\alpha\beta)R^k(\alpha\beta\alpha\beta) + \sum_{\alpha<\beta,\, k\in\mathbb{K}_+} \overline{g}^k(\alpha\beta)R^k(\alpha\alpha\beta\beta)$$

$$+\sum_\alpha \varepsilon_\alpha \overline{q}_\alpha N(\alpha,\alpha) + \sum_{\substack{\alpha\neq\beta \\ \kappa_\alpha=\kappa_\beta}} \varepsilon_{\alpha\beta} N(\alpha,\beta)\Bigg]$$

$$+G^2\Bigg[\sum_\alpha \overline{q}_\alpha I(\overline{\alpha},\overline{\alpha}) - 2\sum_\alpha \overline{q}_\alpha D(\alpha) + \sum_{\alpha\beta k\in\mathbb{K}_o} \overline{f}^k(\alpha\beta)R^k(\overline{\alpha}\beta\overline{\alpha}\beta)(1+\delta_{\alpha\beta})$$

$$+ \sum_{\alpha\beta k\in\mathbb{K}_+} \overline{g}^k(\alpha\beta)R^k(\alpha\overline{\alpha}\beta\overline{\beta}) + \sum_{\alpha\beta k\in\mathbb{K}_-} \overline{g}^k(\alpha\beta)\left\{R^k(\overline{\alpha}\overline{\alpha}\beta\beta) - R^k(\overline{\alpha}\alpha\beta\overline{\beta})\right\}$$

$$+\sum_\alpha \varepsilon_\alpha \overline{q}_\alpha N(\overline{\alpha},\overline{\alpha}) + \sum_{\substack{\alpha\neq\beta \\ \kappa_\alpha=\kappa_\beta}} \varepsilon_{\alpha\beta} N(\overline{\alpha},\overline{\beta}) + \sum_{\substack{\alpha\beta \\ \kappa_\alpha=-\kappa_\beta}} 2\eta_{\alpha\beta} N(\overline{\alpha},\beta)\Bigg]$$

$$+G^4\Bigg[\sum_{\alpha<\beta,\, k\in\mathbb{K}_o} \overline{f}^k(\alpha\beta)R^k(\overline{\alpha\beta\alpha\beta}) + \sum_{\alpha<\beta,\, k\in\mathbb{K}_+} \overline{g}^k(\alpha\beta)R^k(\overline{\alpha\alpha\beta\beta})\Bigg] \qquad (6.3.5)$$

where

$$I(\alpha,\alpha) = \int_o^\infty dr\left\{cQ_\alpha\left(\frac{d}{dr}+\frac{\kappa_\alpha}{r}\right)P_\alpha - cP_\alpha\left(\frac{d}{dr}-\frac{\kappa_\alpha}{r}\right)Q_\alpha - 2c^2{Q_\alpha}^2 - \frac{Z_N}{r}({P_\alpha}^2+{Q_\alpha}^2)\right\}$$

(6.3.6)

$$N(\alpha,\beta) = \int_o^\infty dr(P_\alpha P_\beta + Q_\alpha Q_\beta) \qquad (6.3.7)$$

and

$$D(\alpha) = \int_o^\infty dr\ \rho(P_\alpha \bar{Q}_\alpha - Q_\alpha \bar{P}_\alpha) \tag{6.3.8}$$

Then, under the variation (6.3.2)

$$\delta I(\alpha,\alpha) = \int_o^\infty dr \left\{ cQ_a \left(\frac{d}{dr} + \frac{\kappa_a}{r}\right) \delta P_a - c\delta P_a \left(\frac{d}{dr} - \frac{\kappa_a}{r}\right) Q_a - \frac{Z_N}{r} 2P_a \delta P_a \right\} \delta_{a,\alpha}$$

$$= -2\int_o^\infty dr \delta P_a \left[c\left(\frac{d}{dr} - \frac{\kappa_a}{r}\right) Q_a + \frac{Z_N}{r} P_a \right] \delta_{a,\alpha} \tag{6.3.9a}$$

$$\delta I(\bar{\alpha},\bar{\alpha}) = 0 \tag{6.3.9b}$$

$$\delta R^k(a\beta a\beta) = 2(1+\delta_{a\beta}) \int_o^\infty \delta P_a P_a \frac{1}{r} Y_k(\beta\beta r) dr \tag{6.3.10a}$$

$$\delta R^k(\alpha\beta\alpha\beta) = 0 \quad \text{if } \alpha \neq a \text{ and } \beta \neq a \tag{6.3.10b}$$

$$\delta R^k(aa\beta\beta) = 2\int_o^\infty \delta P_a P_\beta \frac{1}{r} Y_k(a\beta r) dr \tag{6.3.10c}$$

$$\delta R^k(\alpha\alpha\beta\beta) = 0 \quad \text{if } \alpha \neq a \text{ and } \beta \neq a \tag{6.3.10d}$$

$$\delta N(\alpha,a) = \int_o^\infty \delta P_a . P_\alpha (1+\delta_{a\alpha}) dr \tag{6.3.11a}$$

$$\delta N(\alpha,\beta) = 0 \quad \text{if } \alpha \neq a \text{ and } \beta \neq a \tag{6.3.11b}$$

$$\delta D(\alpha) = \delta_{a\alpha} \int_o^\infty \delta P_a . \bar{Q}_a . \rho \tag{6.3.12}$$

$$\delta R^k(\bar{\alpha}\beta\bar{\alpha}\beta) = 2\delta_{a\beta} \int_o^\infty \delta P_a P_a \frac{1}{r} Y_k(\bar{\alpha}\bar{\alpha} r) dr \tag{6.3.13a}$$

$$\delta R^k(a\bar{a}\beta\bar{\beta}) = \int_o^\infty \delta P_a P_\beta \frac{1}{r} Y_k(\bar{a}\bar{\beta} r) dr \tag{6.3.13b}$$

$$\delta R^k(\bar{\alpha}\bar{\alpha}\beta\beta) = 0 \quad \text{if } \alpha \neq a \text{ and } \beta \neq a \tag{6.3.13c}$$

$$\delta R^k(\bar{\alpha}\bar{\alpha}\beta\beta) = 2\delta_{\beta a}\int_o^\infty \delta P_a \cdot \overline{P_\alpha}\,\frac{1}{r}Y_k(a\bar{\alpha}r)dr \tag{6.3.13d}$$

$$\delta R^k(\bar{a}a\beta\bar{\beta}) = \int_o^\infty \delta P_a \overline{P}_\beta \frac{1}{r}Y_k(\bar{a}\beta r)dr \tag{6.3.13e}$$

$$\delta R^k(\bar{\alpha}\alpha\beta\bar{\beta}) = 0 \quad \text{if } \alpha \neq a \text{ and } \beta \neq a \tag{6.3.13f}$$

$$\delta N(\bar{\alpha},\bar{\beta}) = 0 \tag{6.3.14a}$$

$$\delta N(\bar{\alpha},\beta) = \delta_{\beta a}\int_o^\infty \delta P_a \overline{P}_\alpha dr \tag{6.3.14b}$$

and

$$\delta R^k(\overline{\alpha\beta\gamma\delta}) = 0 \tag{6.3.15}$$

whence

$$\begin{aligned}\delta\Gamma = \int^\infty dr\ \delta P_a \Bigg\{ & -2\overline{q}_a\left[c\left\{\frac{d}{dr} - \frac{\kappa_a}{r}\right\}Q_a + \frac{Z_N}{r}P_a\right] \\ & +2\sum_{\beta,k\epsilon\mathbb{K}_o} \overline{f}^k(\alpha\beta)(1+\delta_{\alpha\beta})\frac{1}{r}Y_k(\beta\beta r)P_a \\ & +2\sum_{\beta\neq a,k\epsilon\mathbb{K}_+} \overline{g}^k(a\beta)\frac{1}{r}Y_k(a\beta r)P_\beta + 2\epsilon_a\overline{q}_a P_a + \sum_{\substack{b\neq a\\ \kappa_b=\kappa_a}} \epsilon_{ab}P_b \\ & +G^2\Bigg[-2\overline{q}_a\rho\overline{Q}_a + 2\sum_{\beta,k\epsilon\mathbb{K}_o} \overline{f}^k(a\beta)(1+\delta_{a\beta})\frac{1}{r}Y_k(\overline{\beta\beta}r)P_a \\ & +2\sum_{\beta\neq a,k\epsilon\mathbb{K}_+} \overline{g}^k(a\beta)\frac{1}{r}Y_k(\overline{a\beta}r)P_\beta + 2\sum_{\beta\neq a,k\epsilon\mathbb{K}_-} \overline{g}^k(a\beta)\frac{1}{r}\{Y_k(a\bar{\beta}r)-Y_k(\bar{a}\beta r)\}\overline{P}_\beta \\ & +2\sum_{\substack{\beta\\ \kappa_\beta=-\kappa_\alpha}} \eta_{\beta a}P_\beta\Bigg]\Bigg\}\end{aligned} \tag{6.3.16}$$

where we have exploited the symmetry of the coefficients $\bar{f}^k(ab)$ and $\bar{g}^k(ab)$ and of the Lagrange multipliers ε_{ab}, and the antisymmetry of the η_{ab}.

If the function P_a is such as to give a stationary value of the functional Γ, then we must have

$$\delta\Gamma = 0 \text{ for all variations } \delta P_a. \tag{6.3.17}$$

We know that, if

$$\int_a^b g(x)\,\delta f(x)\,dx = 0 \tag{6.3.18}$$

for all variations $\delta f(x)$, then we must have

$$g(x) = 0 \text{ on } [a,b] \tag{6.3.19}$$

as can be seen by taking $\delta f(x) = \varepsilon g(x)$ for some small ε.

From this it follows immediately that

$$\left(\frac{d}{dr} - \frac{\kappa_a}{r}\right)Q_a + \left(-\frac{\varepsilon_a}{c} + \frac{Y_a^{PM}}{cr}\right) P_a = \frac{\chi_a^{PM(Q)}}{r} \tag{6.3.20}$$

where

$$Y_a^{PM} = Z_N(r) - \frac{1}{\bar{q}_a} \sum_{bk\varepsilon K_o} (1+\delta_{ab})\bar{f}^k(ab)Y_k^{PM}(bbr) \tag{6.3.21}$$

$$\chi_a^{PM(Q)} = -r \sum_{\substack{b\neq a \\ \kappa_a=\kappa_b}} \frac{\varepsilon_{ab}}{c\bar{q}_a} P_b + G^2 r \sum_{\substack{b \\ \kappa_a=-\kappa_b}} \frac{\eta_{ab}\bar{P}_b}{c\bar{q}_a} + G^2 \frac{\bar{Q}_a \rho r}{c} + X_a^{PM(Q)} \tag{6.3.22}$$

$$X_a^{PM(Q)} = -\sum_{b\neq a;k\varepsilon K_+} \frac{\bar{g}^k(ab)}{c\bar{q}_a} Y_k^{PM}(abr)P_b + G^2 \sum_{b\neq a;k\varepsilon K_-} \frac{\bar{g}^k(ab)}{c\bar{q}_a}\left\{Y_k(\bar{a}br) - Y_k(a\bar{b}r)\right\}\bar{P}_b \tag{6.3.23}$$

and

$$Y_k^{PM}(abr) = Y_k(abr) + G^2 Y_k(\overline{abr}) \tag{6.3.24}$$

Similarly, by considering variations

$$Q_a \to Q_a + \delta Q_a \tag{6.3.25}$$

$$\overline{P}_a \to \overline{P}_a + \delta \overline{P}_a \tag{6.3.26a}$$

and

$$\overline{Q}_a \to \overline{Q}_a + \delta \overline{Q}_a \tag{6.3.26b}$$

we obtain the equations

$$\left(\frac{d}{dr}+\frac{\kappa_a}{r}\right)P_a-\left(2c-\frac{\varepsilon_a}{c}+\frac{Y_a^{PM}}{cr}\right)Q_a = -\frac{\chi_a^{PM(P)}}{r} \tag{6.3.27}$$

$$\left(\frac{d}{dr}+\frac{\kappa_a}{r}\right)\overline{Q}_a+\left(\frac{-\varepsilon_a}{c}+\frac{Y_a^{PM}}{cr}\right)\overline{P}_a = -\frac{\chi_a^{PNC(Q)}}{r} \tag{6.3.28}$$

and

$$\left(\frac{d}{dr}-\frac{\kappa_a}{r}\right)\overline{P}_a-\left(2c-\frac{\varepsilon_a}{c}+\frac{Y_a^{PM}}{cr}\right)\overline{Q}_a = -\frac{\chi_a^{PNC(P)}}{r} \tag{6.3.29}$$

respectively, where

$$\chi_a^{PM(P)} = r\sum_{\substack{b\neq a\\ \kappa_b=\kappa_a}}\frac{\varepsilon_{ab}}{c\overline{q}_a}Q_b - G^2 r\sum_{\substack{b\\ \kappa_b=-\kappa_a}}\frac{\eta_{ab}\overline{Q}_b}{c\overline{q}_a} + G^2\frac{\overline{P}_a\rho r}{c} + \chi_a^{PM(P)} \tag{6.3.30}$$

$$\chi_a^{PM(P)} = \sum_{b;k\varepsilon\mathbb{K}_+}\frac{\overline{g}^k(ab)}{c\overline{q}_a}Y_k^{PM}(abr)Q_b - G^2\sum_{b;k\varepsilon\mathbb{K}_-}\frac{\overline{g}^k(ab)}{c\overline{q}_a}\{Y_k(\overline{ab}r)-Y_k(a\overline{br})\}\overline{Q}_b \tag{6.3.31}$$

$$\chi_a^{PNC(Q)} = -r \sum_{\substack{b\neq a \\ \kappa_b=\kappa_a}} \frac{\epsilon_{ab}\bar{P}_b}{c\bar{q}_a} - r \sum_{\substack{b \\ \kappa_b=-\kappa_a}} \frac{\eta_{ab}P_b}{c\bar{q}_a} - \frac{Q_a\rho r}{c} + \chi_a^{PNC(Q)} \qquad (6.3.32)$$

$$\chi_a^{PNC(Q)} = -r \sum_{\substack{b\neq a \\ k\epsilon\mathbb{K}_+}} \frac{\bar{g}^k(ab)}{c\bar{q}_a} Y_k^{PM}(abr)\bar{P}_b - \sum_{\substack{b\neq a \\ k\epsilon\mathbb{K}_-}} \frac{\bar{g}^k(ab)}{c\bar{q}_a} \{Y_k(\bar{a}br)-Y_k(a\bar{b}r)\}P_b \qquad (6.3.33)$$

$$\chi_a^{PNC(P)} = r \sum_{\substack{b\neq a \\ \kappa_a=\kappa_b}} \frac{\epsilon_{ab}}{c\bar{q}_a}\bar{Q}_b + r \sum_{\substack{b \\ \kappa_b=-\kappa_a}} \frac{\eta_{ab}Q_b}{c\bar{q}_a} - \frac{P_a\rho r}{c} + \chi_a^{PNC(P)} \qquad (6.3.34)$$

and

$$\chi_a^{PNC(P)} = \sum_{b;k\epsilon\mathbb{K}_+} \frac{\bar{g}^k(ab)}{c\bar{q}_a} Y_k^{PM}(abr)\bar{Q}_b + \sum_{b;k\epsilon\mathbb{K}_-} \frac{\bar{g}^k(ab)}{c\bar{q}_a} \{Y_k(\bar{a}br)-Y_k(a\bar{b}r)\}Q_b \qquad (6.3.35)$$

It is perhaps worth noting that up to this point no assumption has been made about the size of G; the equations (6.3.20) to (6.3.24) and (6.3.27) to (6.3.35) will hold for any G. The above derivation therefore differs significantly from the perturbation-theoretic approach frequently adopted for this problem.

However, we now do assume that G is small, and neglect all terms of order G^2 in equations (6.3.20) to (6.3.24) and (6.3.27) to (6.3.35). Since $G \sim 10^{-14}$ this may seem to be not unreasonable, but it should be noted that G is frequently multiplied by $\rho(r) \sim 10^{12}$, and by $\bar{P}_a$ or $\bar{Q}_a$ which are unnormalized. However, in the single particle case, the G^2 terms were many orders of magnitude smaller than the others, and

there is no reason to suppose that this will not continue to be true in the many-particle case.

In the limit $G^2 \to 0$

$$Y_k^{PM}(abr) \to Y_k(abr) \tag{6.3.36}$$

$$Y_a^{PM} \to Y_a \tag{6.3.37}$$

$$\chi_a^{PM(P)} \to \chi_a^{(P)} \tag{6.3.38}$$

$$\chi_a^{PM(Q)} \to \chi_a^{(Q)} \tag{6.3.39}$$

$$\chi_a^{PM(P)} \to \chi_a^{(P)} \tag{6.3.40}$$

$$\chi_a^{PM(Q)} \to \chi_a^{(Q)} \tag{6.3.41}$$

and so we may write (6.3.20), (6.3.27), (6.3.28) and (6.3.29) as

$$\left(\frac{d}{dr} - \frac{\kappa_a}{r}\right) Q_a + \left(-\frac{\varepsilon_a}{c} + \frac{Y_a}{cr}\right) P_a = -\frac{\chi_a^{(Q)}}{r} \tag{6.3.42}$$

$$\left(\frac{d}{dr} + \frac{\kappa_a}{r}\right) P_a - \left(2c - \frac{\varepsilon_a}{c} + \frac{Y_a}{cr}\right) Q_a = -\frac{\chi_a^{(P)}}{r} \tag{6.3.43}$$

$$\left(\frac{d}{dr} + \frac{\kappa_a}{r}\right) \bar{Q}_a + \left(-\frac{\varepsilon_a}{c} + \frac{Y_a}{cr}\right) \bar{P}_a = -\frac{\bar{\chi}_a^{(Q)}}{r} \tag{6.3.44}$$

$$\left(\frac{d}{dr} - \frac{\kappa_a}{r}\right) \bar{P}_a - \left(2c - \frac{\varepsilon_a}{c} + \frac{Y_a}{cr}\right) \bar{Q}_a = -\frac{\bar{\chi}_a^{(P)}}{r} \tag{6.3.45}$$

where

$$\bar{\chi}_a^{(Q)} = - r \sum_{\substack{b \\ \kappa_b=\kappa_a}} \frac{\varepsilon_{ab}}{c\bar{q}_a} \bar{P}_b - r \sum_{\substack{b \\ \kappa_b=-\kappa_a}} \frac{\eta_{ab}}{c\bar{q}_a} P_b - \frac{Q_a}{c} \rho(r) r + \bar{X}_a^{(Q)} \tag{6.3.46}$$

$$\bar{\chi}_a^{(P)} = + r \sum_{\substack{b \\ \kappa_a=\kappa_a}} \frac{\varepsilon_{ab}}{c\bar{q}_a} \bar{Q}_b + r \sum_{\substack{b \\ \kappa_b=-\kappa_a}} \frac{\eta_{ab}}{c\bar{q}_a} Q_b - \frac{P_a}{c} \rho(r) r + \bar{X}_a^{(P)} \tag{6.3.47}$$

$$\bar{X}_a^{(P)} = \sum_{b;k\in\mathbb{K}_+} \frac{\bar{g}^k(ab)}{c\bar{q}_a} Y_k(abr)\bar{Q}_b + \sum_{b;k\in\mathbb{K}_-} \frac{\bar{g}^k(ab)}{c\bar{q}_a} \{Y_k(\bar{a}br) - Y_k(a\bar{b}r)\} Q_b \tag{6.3.48}$$

$$\bar{X}_a^{(Q)} = - \sum_{b;k\in\mathbb{K}_+} \frac{\bar{g}^k(ab)}{c\bar{q}_a} Y_k(abr)\bar{P}_b - \sum_{b;k\in\mathbb{K}_-} \frac{\bar{g}^k(ab)}{c\bar{q}_a} \{Y_k(\bar{a}br) - Y_k(a\bar{b}r)\} P_b \tag{6.3.49}$$

The equations (6.3.42) and (6.3.43) are simply the usual MCDF equations (2.2.22). The equations (6.3.44) and (6.3.45) are similar, the differences being that the sign of κ_a has been changed and that the exchange potentials have been altered to reflect the new orthogonality requirements (in the case of $\kappa_a = - \kappa_b$) and the fact that we must allow the PNC part of the Hamiltonian to introduce new k-values as discussed in Appendix 1.

§6.4 The solution of the MCDF-PNC equations

A strategy for the solution of the MCDF-PNC equations which now suggests itself may be summarized as follows:

(i) Solve the equations (6.3.42) and (6.3.43) using the MCDF package as described in §2.5.

(ii) Calculate the new MCP coefficients required. These are those of the form $V^k_{rr}(abba)$ for $k\in\mathbb{K}_-$.

(iii) Solve the equations (6.3.44) and (6.3.45) with $\bar{\chi}_a^{(Q)}$ replaced by

$$\bar{\chi}_a^{(Q)0} = -\frac{Q_a}{c}\rho(r)r \qquad (6.4.1)$$

and $\bar{\chi}_a^{(P)}$ replaced by

$$\bar{\chi}_a^{(P)0} = -\frac{P_a}{c}\rho(r)r \qquad (6.4.2)$$

This is essentially the same problem as was treated in chapter 5 except that we are now using the SCF potential and SCF eigenvalues rather than a model potential and the eigenvalues derived from it.

(iv) Use the estimates of $\bar{P}_a$ and $\bar{Q}_a$ so obtained to calculate the exchange potentials $\bar{\chi}_a^{(P)}$ and $\bar{\chi}_a^{(Q)}$ and then use these new potentials to calculate new estimates of $\bar{P}_a$ and $\bar{Q}_a$.

(v) Repeat stage (iv) until convergence is reached.

A program was written to implement this strategy, but it was found that the sequence of functions $\bar{P}_a$ and $\bar{Q}_a$ obtained at each stage of the iteration indicated in (iv) above did not converge for many orbitals, but instead the normalization

$$N_{\bar{a}} = \sqrt{\int_0^\infty (\bar{P}_a^2 + \bar{Q}_a^2)} \qquad (6.4.3)$$

increased without bound.

It was thought that this might be due to the fact that the exchange was being "switched on" all at once, and that this

might be causing one of the initial solutions to move outside the radius of convergence. It therefore seems logical to increase the exchange slowly.

If we write

$$\bar{\chi}_a^{(Q)}(\zeta) = -\frac{Q_a}{c}\rho(r).r + \zeta\left\{-r\sum\frac{\varepsilon_{ab}}{c\bar{q}_a}\bar{P}_b - r\sum\frac{\eta_{ab}}{c\bar{q}_a}P_b + \bar{X}_a^{(Q)}\right\} \tag{6.4.4}$$

and a similar expression for $\bar{\chi}_a^{(P)}(\zeta)$, in which case

$$\bar{\chi}_a^{(Q)}(1) = \bar{\chi}_a^{(Q)} \tag{6.4.5}$$

and

$$\bar{\chi}_a^{(Q)}(0) = \bar{\chi}_a^{(Q)0}$$

we may replace stages (iv) and (v) in the above strategy by

(iv') set ζ to some small (non-zero) number

(v') use the present estimates of $\bar{P}_a$ and $\bar{Q}_a$ to calculate modified exchange potentials $\bar{\chi}^{(P)}(\zeta)$ and $\bar{\chi}^{(Q)}(\zeta)$ and use these to calculate new estimates of $\bar{P}_a$ and $\bar{Q}_a$.

(vi') Repeat stage (v') until convergence is reached.

(vii') Increase ζ and go back to stage (v')

(viii') Stop when convergence has been obtained with $\zeta = 1$.

The program was modified to do this. However, it was found that there was a limiting value ζ_o of ζ beyond which ζ could not be increased; and as ζ increased towards ζ_o, however slowly, the normalizations of the orbitals became progressively larger.

§6.5 Investigation into the problems involved in the solution of the MCDF-PNC equations

The MCDF-PNC equations

$$\left(\frac{d}{dr} + \frac{\kappa_a}{r}\right)\overline{Q}_a + \left(-\frac{\varepsilon_a}{c} + \frac{Y_a}{cr}\right)\overline{P}_a = -\frac{\overline{\chi}_a^{(Q)}}{r}$$

$$\left(\frac{d}{dr} - \frac{\kappa_a}{r}\right)\overline{P}_a - \left(2c - \frac{\varepsilon_a}{c} + \frac{Y_a}{cr}\right)\overline{Q}_a = -\frac{\overline{\chi}_a^{(P)}}{r} \qquad (6.5.1)$$

subject to the boundary conditions $\overline{P}_a(0) = \overline{P}_a(\infty) = 0 = \overline{Q}_a(0) = \overline{Q}_a(\infty)$ have turned out to be very unstable. Even when the $\overline{\chi}$ are replaced by $\overline{\chi}^o$ as defined in equations (6.4.1) and (6.4.2) the solutions for some of the orbitals - notably the all-important $\overline{\overline{6p}}$ - show extreme sensitivity to the exact form of the SCF potential used. This needs to be explained.

The equations (6.5.1) are simply differential equations; they are not an eigenvalue problem. However, we consider now the associated homogeneous eigenvalue problem

$$\left(\frac{d}{dr} + \frac{\kappa_a}{r}\right) U_a + \left(-\frac{\varepsilon'_a}{c} + \frac{Y_a}{cr}\right) V_a = 0$$

$$\left(\frac{d}{dr} - \frac{\kappa_a}{r}\right) V_a - \left(2c - \frac{\varepsilon'_a}{c} + \frac{Y_a}{cr}\right) U_a = 0 \qquad (6.5.2)$$

where, as usual, we impose the boundary conditions $U_a(0) = U_a(\infty) = 0 = V_a(0) = V_a(\infty)$.

In general, the eigenvalue solutions ε'_a of this equation will not be the same as the values of ε_a employed in eq. (6.5.1) since the latter are eigenvalues of the MCDF equations which are different in that, firstly, they have non-zero right hand

sides, and secondly, that the κ-value is of the opposite sign. But we are solving the problem numerically and not analytically, and we shall see that if there exists, for some given a, an eigenvalue ε'_a of (6.5.2), close to ε_a, then the solutions $\bar{P}_a$ and $\bar{Q}_a$ of (6.5.1) will be unstable, since a small change in the eigenvalue, or one of the potentials, will cause a large change in the wavefunctions $\bar{P}_a$ and $\bar{Q}_a$.

Suppose that we have found an eigenvalue ε'_a of (6.5.2) such that $\varepsilon'_a \sim \varepsilon_a$. Then consider the functions

$$\bar{\bar{P}}_a = \bar{P}_a + \lambda U_a$$

$$\bar{\bar{Q}}_a = \bar{Q}_a + \lambda V_a \qquad (6.5.3)$$

where λ is a number, as yet undetermined. Then $\bar{\bar{P}}_a$ and $\bar{\bar{Q}}_a$ will satisfy the equations

$$\left(\frac{d}{dr} + \frac{\kappa_a}{r}\right) \bar{\bar{Q}}_a + \left(-\frac{\varepsilon_a}{c} + \frac{Y_a}{cr}\right) \bar{\bar{P}}_a = \frac{-\bar{\chi}^{(Q)}_a}{r} + \lambda \frac{\varepsilon'_a - \varepsilon_a}{c} U_a$$

$$\left(\frac{d}{dr} - \frac{\kappa_a}{r}\right) \bar{\bar{P}}_a - \left(2c - \frac{\varepsilon_a}{c} + \frac{Y_a}{cr}\right) \bar{\bar{Q}}_a = \frac{-\bar{\chi}^{(P)}_a}{r} + \lambda \frac{\varepsilon'_a - \varepsilon_a}{c} V_a \qquad (6.5.4)$$

This shows that, provided $\lambda(\varepsilon'_a - \varepsilon_a)/c$ is small, the functions $\bar{\bar{P}}_a$ and $\bar{\bar{Q}}_a$ will also approximately solve the equation (6.5.1); or, alternatively, a small error $\delta\bar{\chi}$ in the value of the $\bar{\chi}$ may result in the admixture of a large amount, of order $\frac{c}{\varepsilon'_a - \varepsilon_a} \delta\bar{\chi}$, of the function U_a and V_a into the functions $\bar{P}_a$ and $\bar{Q}_a$. Therefore, if $\varepsilon'_a - \varepsilon_a$ is small, the equations (6.5.1) are unstable.

In particular, we note that the exchange potential $\bar{\chi}_a$ depends on $\bar{P}_a$ and $\bar{Q}_a$. Suppose that in the iterative solution of (6.51) we have just obtained a new wavefunction with radial components $\bar{P}_a$ and $\bar{Q}_a$. This will cause a change in the potentials $\bar{\chi}_a^P$ and $\bar{\chi}_a^Q$ that will, in turn, cause another change in $\bar{P}_a$ and $\bar{Q}_a$ which, if $\epsilon_a' - \epsilon_a$ is small enough, will be larger than the first change. The result of this will be that the normalization of $\bar{\psi}_a$ will tend to infinity.

To test this theory the eigenvalues of the equation (6.5.2) were calculated and compared with the values of ϵ_a used in equation (6.5.1). The results are shown in table 6.1 and strongly support the above claims.

§6.6 Stabilization of solutions of the MCDF-PNC equations

There are two distinct divergence problems that we encountered in the solution of the MCDF-PNC equations; oscillatory divergence and monotonic divergence. The former may be overcome by damping, when we take as our nth iterate, not the function we obtain obtained from the solution of the MCDF-PNC equations, but a linear combination of that and the (n-1)th iterate. It was found that damping by as much as 96% was needed to prevent divergence.

Monotonic divergence was more difficult to deal with; it was found to be present for the np- orbitals. These are those for which the two eigenvalues referred to in the previous section are particularly close, and so it appears that eigensolutions of (6.5.2) are present, and are causing the problems. Therefore, it seems that we must restrict the overlap $\langle \bar{a} | \tilde{a} \rangle$,

TABLE 6.1

Comparison of eigenvalues of equations (6.5.1) and (6.5.2) and instability of solutions of (6.5.1) for bismuth

Orbital	Actual Eigenvalue (a.u.)	Eigenvalue of Homogeneous Equation (a.u.)	Linear Difference (a.u.)	Relative Difference (percent)	Instability of P N C Normalization (percent)
1s	3349.55	579.19	2770.36	478	~0
2s	607.41	570.36	+37.05	6	1
2p-	582.48	594.69	-12.21	2	100
2p	497.11	96.636	400.47	414	~0
3s	149.30	130.06	+19.24	15	3
3p-	138.10	140.86	-2.76	2	350
3p	118.75	94.56	+24.19	26	~0
3d-	100.62	112.22	-11.60	12	12
3d	96.56	unconvergable			~0
4s	35.734	26.289	+9.435	36	3
4p-	30.831	30.849	-0.018	.06	∞
4p	26.001	14.626	+11.375	78	~0
4d-	18.027	21.974	-3.947	22	10
4d	17.115	4.452	+12.663	284	~0
4f-	6.705	0.7054 13.845	+6.000 -7.140	106	40
4f	6.497	unconvergable			1
5s	6.6860	3.4124	+3.2682	96	4
5p-	4.9091	4.8829	+0.0262	.5	∞
5p	3.9769	0.7005 13.493	+3.2710	463	~0
5d-	1.3894	2.5656	-1.1762	85	12
5d	1.2711	3.1247	-2.4583	193	~0
6s	.6861	2.8115	+2.1254	310	1
6p-	.3384	.3564	-.0180	5	∞
6p	.2618	.2889	-.0238	10	70

where

$$|\tilde{a}\rangle = \frac{1}{r}\begin{pmatrix} U_a(r)\,\chi_{-\kappa_a,m_a}(\theta,\phi) \\ iV_a(r)\chi_{\kappa_a,m_a}(\theta,\phi) \end{pmatrix} \qquad (6.6.1)$$

We can do this by, at each stage in the iteration, taking as our nth iterate

$$|\bar{a}\rangle = |\bar{a}^*\rangle + [\lambda - \langle\tilde{a}|\bar{a}^*\rangle]\ |\tilde{a}\rangle \qquad (6.6.2)$$

where $|\bar{a}^*\rangle$ is the solution obtained from the MCDF-PNC equations and λ is a fixed constant. We will choose λ so that, at convergence,

$$\lambda - \langle\tilde{a}|\bar{a}^*\rangle = 0 \qquad (6.6.3)$$

In practice, it is not convenient to store or calculate the functions $|\tilde{a}\rangle$, and since a = np- in all cases in which this procedure is necessary, we will use |ns> instead of $|\widetilde{np}\text{->}$. Comparison of equations (6.3.4) and (6.3.5) with (6.5.2) and of the relevant eigenvalues in table 6.1 shows that these could reasonably be expected to be similar.

Finally, it should be noted that our exchange terms contain no diagonal contributions; all these have been transferred to the direct potentials. This is as was done in the normal MCDF theory, and should give greater stability. In practice this is not always the case, and it is sometimes advantageous to leave the diagonal terms in the exchange potentials, as has been done, for example, by Martensson et al. (1981). In this case the direct and exchange potentials take a much more symmetric form.

With these three options at our disposal, we have been able to overcome most of our convergence problems.

§6.7 Shielding

If a neutral atom in a constant electric field is considered classically, then it is clear that the atom as a whole will not move, since it is neutral; consequently, once equilibrium has been reached, the nucleus does not move (neglecting the effects on it of the electrons' motion). This can be explained by the fact that the electric field will polarize the atom so that the asymmetry of the electron distribution causes an electric field that just cancels out the external electric field acting on the nucleus.

A similar effect will occur if the atom is placed in a slowly oscillating electric field. In this context, "slowly" may be taken to include oscillations in the visible frequency range.

Thus, if an atom is irradiated with light whose frequency makes it suitable for exciting an outer electron from a lower to a higher energy state, the electron distribution will realign itself so as to shield the nucleus from the effects of the incoming radiation. This will also cause the electron which interacts with the incoming radiation to be shielded from that radiation, although the shielding will be only partial since the electron is normally at some distance from the nucleus. Thus the matrix element for the transition is reduced.

Shielding effects have been calculated for bismuth, either semi-empirically (Novikov et al. (1976)) or using the TDHF approach (Sandars (1977), Loving (1978), Harris et al. (1978),

Sandars (1980), Martennson et al. (1981)) and found to give rise to important effects on the PNC E1 matrix element.

In the MCDF model, it is more convenient to discuss things in terms of configurations, and to include shielding effects by incorporating extra configurations.

Turning for a moment to the perturbation expansion of the exchange terms, the first order contribution to the E1 matrix element due to CI may be written in terms of parity mixed single particle wavefunctions as

$$\sum_{rs} \frac{\langle fr|\Delta V|si\rangle\langle s|e1|r\rangle}{\Delta E} \qquad (6.7.1)$$

where $\Delta V = H^{PC} - H^{HF}$, H^{HF} being the Hartree-Fock Hamiltonian; e1 is a single particle operator corresponding to the many-particle operator E1; and ΔE is an energy denominator, whose precise form need not concern us here.

The matrix elements (6.7.1) must violate parity overall; thus one of the orbitals must be parity violating and the others parity conserving (at least up to an including the second order in G). Clearly the PNC orbital can be in either the one-particle or the two-particle matrix element, and it is convenient to treat the two cases separately.

If the PNC orbital is in the one-particle matrix element, then the two-particle matrix element conserves parity. The magnitude of the CI that arises between the original and new configurations of the same parity (i.e. those that give rise to two-particle matrix elements that conserve parity) is best calculated by means of the standard MCDF program. In what

follows, results including the effects of such CI will be referred to as "unshielded" results. In practice, although this is not quite the standard definition of "unshielded" (cf. Martensson et al. (1981) who discuss this problem in terms of diagrammatic perturbation theory) such CI normally makes little difference to the Babushkin gauge results (see Chapter 8) and so no real confusion is likely.

On the other hand, the PNC orbital may enter into the two particle matrix element. This will correspond, in the configurational picture, to CI between the original configurations and configurations with the opposite parity. Such CI must be determined by an essentially new computer program, whilst once the mixing coefficients have been determined, the effects on the E1 matrix element can be calculated by an almost unmodified version of the standard oscillator strengths program, since the PNC wavefunctions are not involved further. We shall refer to these effects as "shielding"; in practice, they constitute most of the shielding effects as calculated by other authors.

Rather than develop the perturbation-theoretic argument any further, we will return to the configurational approach. This is more consistent with the method of this thesis, and also has the advantage of implicitly including effects to all orders of perturbation theory within the space spanned by the set of CSF's chosen; it is developed, more or less from scratch, in the next section.

§6.8 PNC mixing with CSF's of the opposite parity

If we are to introduce configurations of the opposite parity to the initial and final states, then it is clear that, for consistency, we must assign to each new configuration a weight c_r in the functional (6.2.1) used to generate the orbitals. Since the final mixing of these configurations will be of order G, we set the relevant values of c_r to be of order G as well. This then has the advantage that their introduction does not affect $\mathcal{H}^{PM}$ or Γ to zero order in G and hence does not affect the parity conserving MCDF equations; and the second order in G change to $\mathcal{H}^{PM}$ or Γ involves only parity conserving wavefunctions, so that the PNC MCDF equations are not affected either. Of course, the new configurations must not introduce new orbitals for this to hold; otherwise, although the original equations will be unchanged, the new equations governing the new orbitals will contain terms $\frac{1}{\epsilon_a} \sim 10^{14}$ which will lead to great instabilities, as already discussed in the context of OL and EOL calculations.

Having solved the MCDF and MCDF PNC equations we must then determine the mixing coefficients $\underset{\sim}{c}_\alpha$ which are the eigenvectors of the Hamiltonian matrix $\underset{=}{H}^{PM}$ defined by equation (6.2.2b). For simplicity we assume that the first n configurations are of nominally the original parity and that last m configurations are of the opposite parity. Then we can write

$$\underset{=}{H}^{PM} = \begin{pmatrix} H_+ & iGH_x \\ -iGH_x^T & H_- \end{pmatrix} + O(G^2) \qquad (6.8.1)$$

where H_+ is a n×n matrix, H_- is m×m and H_x is n×m. The factor

iG has been included so that H_x is real and of order 1. We shall not consider further the $O(G^2)$ terms since these will lead only to terms of $O(G^2)$ in the wavefunctions, and we are interested only in terms that are O(G) or larger.

The terms H_+ and H_- are as in the parity conserving problem, at least up to and including first order in G. Thus their evaluation need not concern us further.

To calculate H_x we note that the elements of iGH_x are of the form

$$\langle r|H^{PC} + GV^{PNC}|s\rangle \qquad (6.8.2)$$

using equation (6.2.8). In what follows we must remember that the configurations r and s are created from parity mixed single-particle wavefunctions.

Expanding the first term using equation (6.2.9), and remembering that r and s have the opposite nominal parity, we can see that it may be written in the form

$$\begin{aligned}\langle r|H^{PC}|s\rangle &= \langle r|\sum_{i=1}^{N} h_i + \sum_{1\leq i<j\leq N}\frac{1}{r_{ij}}|s\rangle \\ &= \sum_{ab} T_{rs}(ab)I(a^{PM}b^{PM}) \\ &+ \sum_{\substack{abcd\\k}} V_{rs}(a^{PM}b^{PM}c^{PM}d^{PM})R^k(a^{PM}b^{PM}c^{PM}d^{PM})\end{aligned} \qquad (6.8.3)$$

where $T_{rs}(ab)$ is a MCT coefficient of magnetic monopole type where the constraint $\kappa_a = \kappa_b$ encountered in the expansion of parity

conserving Hamiltonian matrix elements has been reversed to $\kappa_a = -\kappa_b$;

$$I(a^{PM}b^{PM}) = iG \int_o^\infty dr\Big[c(Q_a\bar{P}_b'-P_a\bar{Q}_b'+\bar{P}_aQ_b' - \bar{Q}_aP_b') - 2c^2(Q_a\bar{Q}_b-\bar{Q}_aQ_b) - \frac{c\kappa_b}{r}(P_a\bar{Q}_b+Q_a\bar{P}_b+\bar{P}_aQ_b+\bar{Q}_aP_b) - \frac{Z_N(r)}{r}(P_a\bar{P}_b-\bar{P}_aP_b+Q_a\bar{Q}_b-\bar{Q}_aQ_b)\Big]\delta_{\kappa_a,-\kappa_b} \qquad (6.8.4)$$

and, by a similar argument to that used in appendix 1 to obtain equation (A1.14), the second term is

$$iG \sum_{abcd} V^k_{rs}(abcd)(R^k(abc\bar{d})-R^k(ab\bar{c}d)) \quad k\epsilon\mathbb{K}_{ac}$$

$$+iG \sum_{\substack{abcd \\ k\epsilon\mathbb{K}_{bd}}} V^k_{rs}(abcd)(R^k(ab\bar{c}d)-R^k(a\bar{b}cd)) \qquad (6.8.5)$$

where we define the range of k by

$$\mathbb{K}_{ac} = \Big\{k \,\Big|\, |j_a-j_c| \leq k \leq |j_a+j_c|;\ |j_b-j_d| \leq k \leq |j_b+j_d|;\ \kappa_a\kappa_c(-1)^{k-|j_a-j_c|} > 0;\ \kappa_b\kappa_d(-1)^{k-|j_b-j_d|} < 0\Big\} \qquad (6.8.6)$$

and

$$\mathbb{K}_{bd} = \{k \,|\, |j_a - j_c| \leq k \leq |j_a + j_c|\,;$$

$$|j_b - j_d| \leq k \leq |j_b + j_d|\,;$$

$$\kappa_b \kappa_d (-1)^{k-|j_b-j_d|} > 0$$

$$\kappa_a \kappa_c (-1)^{k-|j_a-j_c|} < 0\} \qquad (6.8.7)$$

and the usual parity restriction on k in V^k is removed.

Turning now to the second term in expression (6.8.2) we break it down into simple-particle matrix elements:

$$\langle r|V^{PNC}|s\rangle = \sum_{ab} T_{rs}(ab) \langle a|v^{PNC}|b\rangle \qquad (6.8.8)$$

where $T_{rs}(ab)$ are again MCT coefficients of the magnetic monopole type and

$$\langle a|v^{PNC}|b\rangle = i \int_o^\infty \rho_N (P_a Q_b - Q_a P_b) dr \qquad (6.8.9)$$

Thus we obtain the final result for H_x

$$(H_x)_{rs} = \sum_{\substack{ab \\ \kappa_a = -\kappa_b}} T_{rs}(ab)\, \tilde{I}(ab)$$

$$+ \sum_{\substack{abcd \\ k \in \mathbb{K}_{ac}}} V^k_{rs}(abcd)(R^k(abc\bar{d}) - R^k(a\bar{b}cd))$$

$$+ \sum_{\substack{abcd \\ k \in \mathbb{K}_{bd}}} V^k_{rs}(abcd)(R^k(ab\bar{c}d) - R^k(\bar{a}bcd))$$

$$+ \sum_{\substack{ab \\ \kappa_a = -\kappa_b}} T_{rs}(ab) \int_o^\infty \rho_N (P_a Q_b - Q_a P_b) dr \qquad (6.8.10)$$

where

$$\tilde{I}(ab) = \int_o^\infty dr\Big[c(Q_a\bar{P}_b'-P_a\bar{Q}_b'+\bar{P}_aQ_b'-\bar{Q}_aP_a')$$

$$-2c^2(Q_a\bar{Q}_b-\bar{Q}_aQ_b)$$

$$-\frac{c\kappa_b}{r}(P_a\bar{Q}_b+Q_a\bar{P}_b+\bar{P}_aQ_b+\bar{Q}_aP_b)$$

$$-\frac{Z_N}{r}(P_a\bar{P}_b-\bar{P}_aP_b+Q_a\bar{Q}_b-\bar{Q}_aQ_b)\Big] \qquad (6.8.11)$$

Now that the Hamiltonian has been set up, it must be rediagonalized. Let us write the eigenvalue equation, for eigenvectors that are nominally of the original parity, as

$$\begin{pmatrix} H_+ & iGH_x \\ -iGH_x^T & H_- \end{pmatrix}\begin{pmatrix} \underset{\sim}{c} \\ iG\underset{\sim}{\lambda} \end{pmatrix} = E\begin{pmatrix} \underset{\sim}{c} \\ iG\underset{\sim}{\lambda} \end{pmatrix} \qquad (6.8.12)$$

Then, neglecting the $O(G^2)$ terms,

$$H_+\underset{\sim}{c} = E\underset{\sim}{c} \qquad (6.8.13)$$

and

$$-iGH_x^T\underset{\sim}{c} + iGH_-\underset{\sim}{\lambda} = EiG\underset{\sim}{\lambda} \qquad (6.8.14)$$

from which we see that $\underset{\sim}{c}$ and E are the eigenvectors and eigenvalues of the original Hamiltonian H_+, whilst the $\underset{\sim}{\lambda}$'s are given in terms of these known (once the parity conserving calculation has been carried out) quantities by the equation

$$(H_- - E^{(r)})\underset{\sim}{\lambda}^{(r)} = H_x{}^T \underset{\sim}{c}^{(r)} \qquad (6.8.15)$$

where the (r) superscripts are used to denote the rth eigenvector and eigenvalue.

This is a set of m linear algebraic equations in m unknowns; to solve it is not difficult. However, it is even easier if we note that we know (from the parity conserving MCDF calculation) the eigenvalues and eigenvectors of H_-; let us denote them by $E_-{}^s$ and $c_-{}^s$ respectively. We can then expand $\underset{\sim}{\lambda}^{(r)}$ in terms of these $\underset{\sim}{c}_-{}^s$:

$$\underset{\sim}{\lambda}^{(r)} = \sum_s k^{rs}\, \underset{\sim}{c}_-{}^s \qquad (6.8.16)$$

Substitution of (6.8.16) into (6.8.15) then yields

$$\sum_s k^{rs}(H_- - E^{(r)})\underset{\sim}{c}_-{}^s = H_x{}^T c^{(r)} \qquad (6.8.17)$$

whence

$$\sum_s k^{rs}\,(E_-{}^{(s)} - E^{(r)})\underset{\sim}{c}_-{}^s = H_x{}^T \underset{\sim}{c}^{(r)} \qquad (6.8.18)$$

so that

$$k^{rs} = \frac{[\underset{\sim}{c}_-{}^s]^T\; H_x{}^T \underset{\sim}{c}^{(r)}}{E_-{}^{(s)} - E^{(r)}} \qquad (6.8.19)$$

and finally

$$\underset{\sim}{\lambda}^{(r)} = \sum_s \frac{[\underset{\sim}{c}_-{}^s]^T\; H_x{}^T \underset{\sim}{c}^{(r)}}{E_-{}^{(s)} - E^{(r)}}\; \underset{\sim}{c}_-{}^s \qquad (6.8.20)$$

The same result could, of course, have been derived by perturbation theory.

§6.9 PNC transition matrix elements

The purpose of calculating parity violating wavefunctions and mixing coefficients is to calculate the matrix elements

$$\langle f^{PM} \| T^L \| i^{PM} \rangle$$

where T^L is the same interaction Hamiltonian as in §2.4.2 and $|i^{PM}\rangle$ and $|f^{PM}\rangle$ are parity mixed wavefunctions.

If the matrix element

$\langle f \| T^L \| i \rangle$ is non-zero, then

$$\langle f^{PM} \| T^L \| i^{PM} \rangle - \langle f \| T^L \| i \rangle = O(G^2)$$

and this will be too small to concern us. However, if

$$\langle f \| T^L \| i \rangle = 0$$

then

$$\langle f^{PM} \| T^L \| i^{PM} \rangle = O(G).$$

It is such matrix elements that interest us.

The reduction of the matrix element $\langle f^{PM} \| T^L \| i^{PM} \rangle$ to a sum of one-particle matrix elements may proceed in much the same way as before. This is because the theory is jj-coupled, and so nowhere is the ℓ-value of any orbital considered.

However, as will become apparent as we proceed, it is more convenient to approach the problem in a slightly different manner.

We may write

$$|i^{PM}> = |i_+^{PM}> + iG|i_-^{PM}> \qquad (6.9.1)$$

and

$$|f^{PM}> = |f_+^{PM}> + iG|f_-^{PM}> \qquad (6.9.2)$$

where $|i_+^{PM}>$ is the contribution to the wavefunction obtained from the configurations of nominally the original parity, whilst $iG|i_-^{PM}>$ is the contribution obtained from the configurations of nominally the opposite parity; similarly for $|f_\pm^{PM}>$. Then

$$\begin{aligned} <f^{PM}||T^L||i^{PM}> &= <f_+^{PM}||T^L||i_+^{PM}> \\ &+ iG<f_+^{PM}||T^L||i_-^{PM}> \\ &- iG<f_-^{PM}||T^L||i_+^{PM}> \\ &+ G^2<f_-^{PM}||T^L||i_-^{PM}> \end{aligned} \qquad (6.9.3)$$

We neglect the last of these since it will not give rise to any terms of O(G). The second and third of these can be calculated in the usual way when the "PM" superscripts are removed so that only the parity conserving parts of the single-particle wavefunctions are used. The evaluation of the first term follows the usual technique for reduction to single particle matrix elements:

$$\langle f_+^{PM} \| T^L \| i_+^{PM} \rangle = \sum_{\substack{r,s \\ ab}} c_{fr} c_{is} \, d^L_{ab}(rs) \, \langle a^{PM} \| t^L \| b^{PM} \rangle \qquad (6.9.4)$$

exactly as in equations (2.4.9) and (2.4.10).

The single-particle matrix element may then be broken down further

$$\begin{aligned} \langle a^{PM} \| t^L \| b^{PM} \rangle &= \langle a \| t^L \| b \rangle \\ &+ G(i\langle a \| t^L \| \bar{b} \rangle - i\langle \bar{a} \| t^L \| b \rangle) \\ &+ G^2 \langle \bar{a} \| t^L \| \bar{b} \rangle . \end{aligned} \qquad (6.9.5)$$

As remarked above, we are interested in transitions for which there are no terms of order G^o. This will occur if the transition is forbidden by parity; in this case

$$\langle a \| t^L \| b \rangle = 0$$

and

$$\langle \bar{a} \| t^L \| \bar{b} \rangle = 0 \qquad (6.9.6)$$

and so

$$\langle a^{PM} \| t^L \| b^{PM} \rangle = iG(\langle a \| t^L \| \bar{b} \rangle - \langle \bar{a} \| t^L \| b \rangle) \qquad (6.9.7)$$

The reduction of these to radial integrals now takes place exactly as in §2.4.4, except that the κ value of one of the orbitals has its sign changed; otherwise everything is as before. The result is that $\langle a \| t^L \| \bar{b} \rangle$ and $\langle \bar{a} \| t^L \| b \rangle$ are expressed, as before, in terms of $\bar{M}_{a\bar{b}}$ and $\bar{M}_{\bar{a}b}$.

For convenience we write out the formulae for $\bar{M}_{a\bar{b}}$ (corresponding to the matrix element $\langle a \| t^L \| \bar{b} \rangle$):

$$\bar{M}^{m}_{a\bar{b}} = -i^{L+1}\,\frac{2L+1}{\sqrt{L(L+1)}}\,(\kappa_a-\kappa_b)\,I^{+}_{L}(\omega)$$

$$\bar{M}^{e}_{a\bar{b}}(0) = i^{L}\left(\sqrt{\frac{L}{L+1}}\,[(\kappa_a+\kappa_b)\,I^{+}_{L+1} + (L+1)\,I^{-}_{L+1}]\right.$$

$$\left. -\sqrt{\frac{L}{L+1}}\,[(\kappa_a+\kappa_b)\,I^{+}_{L-1} - L\,I^{-}_{L-1}]\right) \qquad (6.9.8)$$

$$\bar{M}^{\ell}_{a\bar{b}} = -i^{L}\left(-(2L+1)\,J^{(L)} + (\kappa_a+\kappa_b)(I^{+}_{L+1} + I^{+}_{L-1})\right.$$

$$\left. - L\,I^{-}_{L-1} + (L+1)\,I^{-}_{L+1}\right)$$

where

$$I^{\pm}_{L} = \int_{o}^{\infty} (P_a\bar{Q}_b \pm Q_a\bar{P}_b)\,j_L(\tfrac{\omega r}{c})\,dr$$

and

$$J^{(L)} = \int_{o}^{\infty} (P_a\bar{P}_b + Q_a\bar{Q}_b)\,j_L\,(\tfrac{\omega r}{c})\,dr \qquad (6.9.9)$$

Similar results hold for $\bar{M}_{-ab}$

To calculate these matrix elements, the standard oscillator strengths package has been modified. The changes were minimal and will not be reported here.

§6.10 Basis set expansion schemes

At one stage in the solution of the MCDF-PNC equations, great difficulties with convergence were encountered. These were eventually traced to a sign error in some of the exchange terms - an error which delayed this work by something like a year - but before this was discovered it was thought that these difficulties could be circumvented by use of a basis expansion

scheme, similar to that used by Roothaan (1951, 1960, 1963). The theory is independent of the source of the basis wave-functions; Roothaan used analytic functions, we used numerical functions.

Since this theory was not used for any of the results reported in this thesis, it will not be given here, but has been placed in Appendix 2 for reference.

Chapter 7

Here is wisdom. Let him that hath understood count the number of the beast: for it is the number of a man; and his number is six hundred three score and six.

John the Divine (0096)

The Parity Conserving Calculation for Atoms of Interest

CHAPTER 7

THE PARITY CONSERVING CALCULATION FOR ATOMS OF INTEREST

§7.1 Introduction

In the previous chapter we pointed out that, before parity non-conserving wavefunctions can be calculated, the normal MCDF equations must be solved for the system under consideration. This will be described in the present chapter.

The transitions of experimental and theoretical interest for investigation of PNC effects are as follows:

(i) The 876nm line in bismuth I between $[6\bar{p}(6p^2)_2]_{3/2}$ (level 2 and the ground state $6\bar{p}^2 6p$ (level 1). We refer to this as the 1-2 transition.

(ii) The 648nm line in bismuth I between $[6\bar{p}(6p^2)_2]_{5/2}$ (level 3) and the ground state. We refer to this as the 1-3 transition.

(iii) The 293nm line in thallium I between $7\bar{p}$ and $6\bar{p}$.

(iv) The 1279nm line in lead I between $(6\bar{p}^2)_0$ and $(6\bar{p}6p)_1$.

(v) The 540nm line in cesium I between 6s and 7s.

We shall consider the MCDF calculations for each atom in turn.

§7.2 Bismuth

The first calculation performed on bismuth was an EAL calculation on all the levels of the manifold $(6\bar{p}+6p)^3$. This yields five configurations, namely $(6\bar{p}^2 6p)_{3/2}$, $(6\bar{p}(6p^2)_0)_{1/2}$, $(6\bar{p}(6p^2)_2)_{3/2}$, $(6\bar{p}(6p^2)_2)_{5/2}$, and $(6p^3)_{3/2}$. We kept the

configuration $(6\bar{p}(6p^2)_0)_{1/2}$ even though it does not feature in our calculations, since experience has shown that multiplet structures are usually better described when all J-values of a manifold are included.

The results of this calculation are given in table 7.1. They are unsatisfactory for two reasons:

Firstly, the calculated energies are not in good agreement with experiment.

Secondly, the Coulomb and Babushkin results for the E2 matrix element are not very close to each other, particularly for the 1-3 transition.

This indicates that we must allow for interaction between the configurations of $(6\bar{p}+6p)^3$ and some other configurations.

It seemed a good idea to make a number of preliminary calculations in order to determine which configurations interacted significantly with the configurations of interest. Therefore, EAL-type calculations were performed in which

(i) the configurations included were the five from $(6\bar{p}+6p)^3$ plus those derived from a single other manifold with J = 3/2 or J = 5/2.

(ii) The wavefunctions from the 5 CSF calculation were kept, and not allowed to change.

(iii) Any new wavefunctions required were calculated in the SCF potential generated by the wavefunctions and a nuclear charge Z which was not fixed to be 83. This gave us a parameter which we could adjust to optimize the CI, which we found was maximized when the correlation orbital had a mean radius

TABLE 7.1

Energies and transition matrix elements calculated for bismuth in a 5 CSF calculation.

	Transition 1-2	Transition 1-3
Energy - Coulomb (cm^{-1})	12537	17317
- Coulomb & Breit (cm^{-1})	12410	17130
- Coulomb & Breit & QED (cm^{-1})	12414	17139
M1 Matrix element	1.571×10^{-6}	6.262×10^{-7}
E2 Matrix element - Coulomb	2.649×10^{-7}	8.011×10^{-7}
Babushkin	2.225×10^{-7}	5.657×10^{-7}
Experimental energy (cm^{-1})	11419	15438

of about 1.5 times that of the correlated orbital (Dyall (1980), (1981), Dyall and Larkins (1982)).

(iv) These orbitals were then used to calculate the c_{ar} of equation (2.2.4) and hence transition energies and other relevant atomic data.

The justification for this procedure is as follows. Firstly, we note that the "physical" orbitals, i.e. those out to and including 6p, that were obtained by means of the 5 CSF calculation are the best (in some sense) that are available within the EAL model. If we allow these to be varied in a CI calculation, they will not be the best possible but a compromise between those required for the $6p^3$ manifold ar those required for the interacting configurations. This is the reasoning behind steps (i) and (ii).

If we now calculate the extra correlation orbitals in the obvious way - by solving the MCDF equations using potential defined by a nuclear charge of 83 and all 83 other electrons - we obtain orbitals that are very diffuse. Thus the overlaps between the correlation and physical orbitals are small, leading to small CI effects. This is illustrated by the next calculation that will be described; but it is a problem that has long been recognised. The usual solution is to use a V^{N-1} potential (Kelly (1964), (1969)) for the correlation orbitals, which is obtained by excluding the interaction between the electron under consideration and one other electron - usually taken rather arbitrarily to be the outer-most electron with the same angular quantum numbers as the electron for which the calculation is taking place. Silver and Bartlett (1976) have generalized this to give an average

V^{N-1} potential and also a V^{N-Q} potential, where the interaction with Q electrons is excluded, and where they observe that Q need not take integer values. They experimented with different values of Q and concluded, for the system under consideration (LiH), that a value of $Q \cong 1$ was best. They also observed (see also Silver, Wilson and Bartlett (1977)) that altering the potential corresponds to a unitary transformation of the correlation function (including the continuum) space, and that a suitable potential would allow for tailoring the orbitals to the problem under consideration.

It would be possible, but not trivial, to modify our MCDF program to calculate the correlation orbitals using a V^{N-Q} potential. However, the V^{N-Q} potential is created by reducing the inter-electronic repulsion by Q while keeping the nuclear attraction fixed; a similar effect would be obtained by keeping the inter-electronic repulsion fixed and increasing the nuclear attraction by Q. This is what was done, both by Dyall (1980) and Dyall and Larkins (1982) and in the present work.

There are various criteria that may be applied to determine which configurations give rise to important CI effects. Firstly, we are trying to minimize an energy function. thus any configuration that lowers the energy of some or all of the levels under consideration may be considered important. Secondly, we want to obtain good agreement between calculated and experimental transition energies; thus any configuration that alters the transition energy of the transitions of interest is regarded as being particularly important. Thirdly,

if we have perfect wavefunctions, electric multipole matrix elements will be gauge invariant; thus any configuration that alters the ratio of Coulomb and Babushkin gauge results significantly should also be included in the final CI calculation. Following Bagus and Moser (1968) we shall place more stress on the second and third of these than on the first, since if a configuration does not affect the transition energy or E2 matrix element, both initial and final state correlations are cancelling each other out and so the E1 matrix element - which is what is of the greatest interest to the present investigation - probably will not be greatly affected either.

We describe in detail the results for the interaction with the configurations of the manifold $(6\bar{p}+6p)^2(5\bar{f}+5f)$ with J = 3/2 or 5/2. The other configurations follow a similar pattern.

It can be seen from table 7.2 that there is a definite value of Z where the effect of the configuration interaction is maximized according to all the criteria listed above - about Z = 84.3. If we note that $\langle r_{6\bar{p}} \rangle = 2.7803$ and $\langle r_{6p} \rangle = 3.1862$, then, at this value of Z, $\langle r_{5\bar{f}} \rangle = 4.01$ and $\langle r_{5f} \rangle = 4.38$, which are 1.44 and 1.37 times the value of $\langle r_{6\bar{p}} \rangle$ and $\langle r_{6p} \rangle$, in rough agreement with the assertion made above.

The importance of choosing the best value of Z should be emphasized. Had we taken Z = 83, we would have concluded that there was almost no interaction between the two manifolds.

Similar calculations have been made for a large number of interacting manifolds. The results are given in table 7.3.

TABLE 7.2

Configuration interaction between $6p^3$ and $6p^2\ 5f$ in bismuth

Z	<r> $5\bar{f}$	<r> 5f	Total energy + 21566 a.u.			Transition 1-2				Transition 1-3			
			level 1	level 2	level 3	Coulomb Energy (cm^{-1})	<E2> Coulomb $\times 10^7$	<E2> Babushkin $\times 10^7$	Ratio	Coulomb Energy (cm^{-1})	<E2> Coulomb $\times 10^7$	<E2> Babushkin $\times 10^7$	Ratio
83.0	17.85	18.07	-.078761	-.021646	+.000127	12535	2.679	2.224	1.20	17314	7.977	5.644	1.41
83.5	11.44	11.79	-.078793	-.021882	-.000219	12490	2.578	2.190	1.18	17245	7.554	5.488	1.38
83.8	8.83	9.33	-.078903	-.022592	-.001259	12359	2.330	2.103	1.11	17041	6.631	5.159	1.29
84.0	7.02	7.65	-.079105	-.023756	-.002935	12148	2.055	1.983	1.036	16717	5.688	4.803	1.18
84.2	4.94	5.51	-.079439	-.025310	-.005124	11880	1.945	1.862	1.045	16310	5.363	4.597	1.17
84.3	4.01	4.38	-.079537	-.025637	-.005599	11830	2.000	1.851	1.080	16228	5.604	4.609	1.22
84.4	3.30	3.49	-.079531	-.025510	-.005443	11856	2.077	1.877	1.11	16261	5.936	4.707	1.26
85.0	1.85	1.85	-.079106	-.023386	-.002443	12229	2.473	2.083	1.19	16826	7.362	5.271	1.40

TABLE 7.3

Configuration interaction with the $6p^3$ manifold in bismuth I

Interacting Manifold	No. of CSF's	Maximum shift in total energy a.u. × 10^{-4}		
		level 1	level 2	level 3
$6p^2 5f$	13	8	40	58
$[6s]6p^3 6d$	38	235	253	273
$6p^2 7p$	13	12	8	3
$[6s^2]6p^5$	1	16	12	0
$6p6d^2$	22	114	112	104
$6p5f^2$	23	16	15	13
$6p7p^2$	13	26	30	31
$[6s]6p^3 7s$	13	16	6	5
$[5d][6s]6p^5$	14	2	10	16
$[5p]6p^4$	18	0	0	0
$[5s^2]6p^5$	18	0	0	0
$[5p^2]6p^5$	6	0	0	0
$[5d^2]6p^5$	27	2	2	2
$[5s]6p^3 6d$	43	0	0	0
$[5s]\ 6p^3 7s$	18	0	0	0
$[5d]\ 6p^3 7s$	43	3	5	6
$6p5f7p$	30	1	1	2
$[6s^2]6p^3 6d^2$	66	17	17	17
$[5p]6p^3 7p$	83	4	4	4
$[5p]6p^3 5f$	91	2	4	5
$[5d]6p^3 5g$	99	9	15	18
$[5s^2]6p^3 6d^2$	66	6	6	6
$[5s^2]6p^3 5f^2$	72	8	8	8
$[5p^2]6p^3 7s^2$	37	3	3	3
$[5p^2]6p^3 7s^2$	66	4	4	4
$[6s^2]6p^3 7s^2$	4	6	6	6
$[6s^2]6p^3 5f^2$	72	6	6	6
$6p5g^2$	72	2	2	2
$[4f]6p^4$	13	0	0	0

TABLE 7.3

Configuration interaction with the $6p^3$ manifold in bismuth I

Interacting Manifold	No. of C&F's	Transition 1-2 Maximum change in energy cm^{-1}	Transition 1-2 Maximum change in Coulomb/Bab ratio for <E2> %	Transition 1-3 Maximum change in energy cm^{-1}	Transition 1-3 Maximum change in Coulomb/Bab ratio for <E2> %
$6p^2 5f$	13	-700	-17	-1090	-25
$[6s]6p^3 6d$	38	-400	+19	-830	+26
$6p^2 7p$	13	+110	-7	+220	-17
$[6s^2]6p^5$	1	+90	-8	+340	-11
$6p6d^2$	22	+140	-6	+290	-9
$6p5f^2$	23	+40	-2	+90	-3
$6p7p^2$	13	-110	-1	-120	-2
$[6s]6p^3 7s$	13	+150	-1	+180	0
$[5d][6s]6p^5$	14	-180	+1	-310	+2
$[5p]6p^4$	18	0	0	0	0
$[5s^2]6p^5$	18	0	0	0	0
$[5p^2]6p^5$	6	0	0	0	0
$[5d^2]6p^5$	27	-10	0	-10	0
$[5s]6p^3 6d$	43	0	0	0	0
$[5s]6p^3 7s$	18	0	0	0	0
$[5d]6p^3 7s$	43	-50	0	-70	0
$6p5f7p$	30	-20	0	-40	0
$[6s^2]6p^3 6d^2$	66	0	0	0	0
$[5p]6p^3 7p$	83	0	0	0	0
$[5p]6p^3 5f$	91	-40	0	-50	0
$[5d]6p^3 5g$	99	-140	±1	-200	±1
$[5s^2]6p^3 6d^2$	66	0	0	0	0
$[5s^2]6p^3 5f^2$	72	0	0	0	0
$[5p^2]6p^3 7s^2$	37	0	0	0	0
$[5d^2]6p^3 7s^2$	66	0	0	0	0
$[6s^2]6p^3 7s^2$	4	0	0	0	0
$[6s^2]6p^3 5f^2$	72	0	0	0	0
$6p5g^2$	72	0	0	0	0
$[4f]6p^4$	13	0	0	0	0

The size of computer storage available limits the number of configurations of a given parity and J-value allowed in a calculation to 165. We therefore chose out of the list in Table 7.3 the manifolds

$6p^2 5f$ $6p6d^2$ $6p^2 7p$ $[6s]6p^3 6d$ $[6s^2]6p^5$

$6p5f^2$ $6p7p^2$ $[6p]6p^3 7s$ and $[5d]$ $[6s]6p^5$

These are the ones that make the greatest contribution after allowing for the number of configurations in each. This gives us a total of 150 configurations.

To get a feel for how things behaved, a subset of these was chosen - namely

$6p^2 5f$ $6p6d^2$ and $6p^2 7p$.

These are the manifolds which reduce the Coulomb-Babushkin discrepancy the most, and give, with the $6p^3$ manifold, a total of 53 configurations.

We consider first the results of the 53 CSF calculations. These are shown in figures 7.0, 7.1, 7.2 and 7.3 and table 7.4. There is no reason why the same Z value should be used for each correlation orbital, but for simplicity we have done so. We may identify four values of Z which are of interest:

(a) Z = 83.85 and Z = 84.50. At these points the discrepancy between the Coulomb and Babushkin results for the E2 matrix elements is approximately zero.

(b) Z = 84.20. At this point the effect of configuration interaction on transition energies and E2 matrix elements is

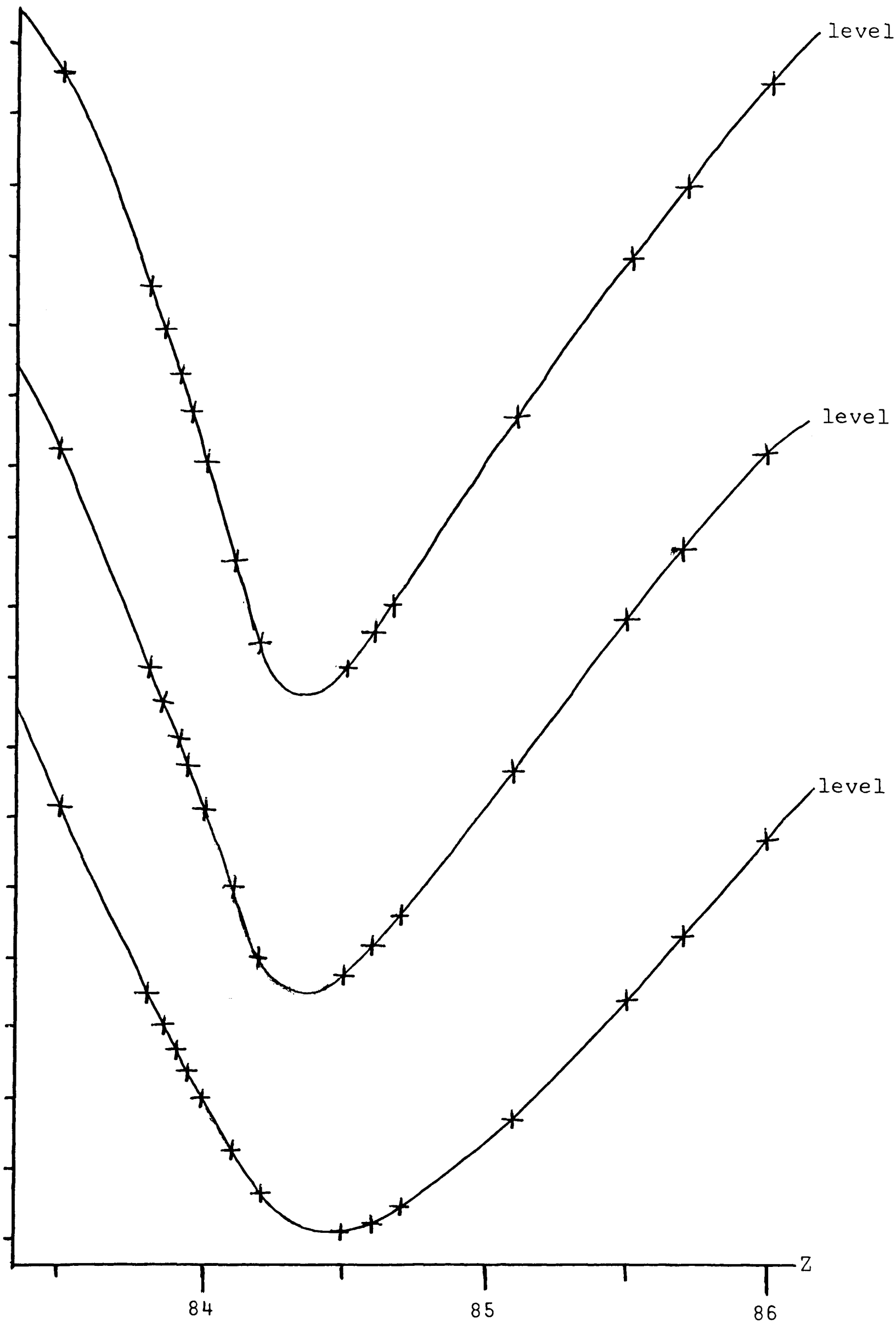

Figure 7.0 Dependence of total energies (in arbitrary units) on the value of Z used for the correlation orbitals in the 53 CSF bismuth calculation.

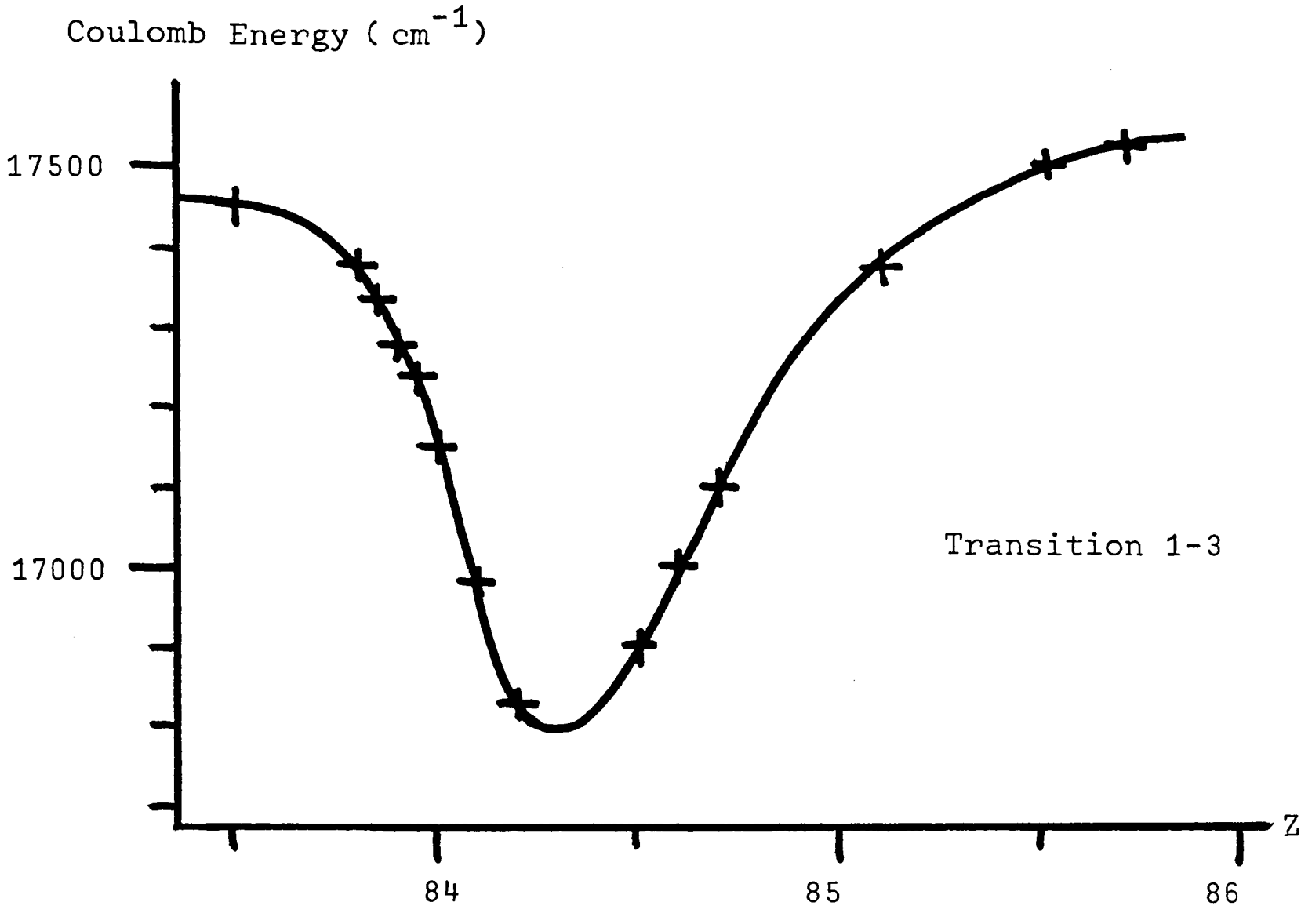

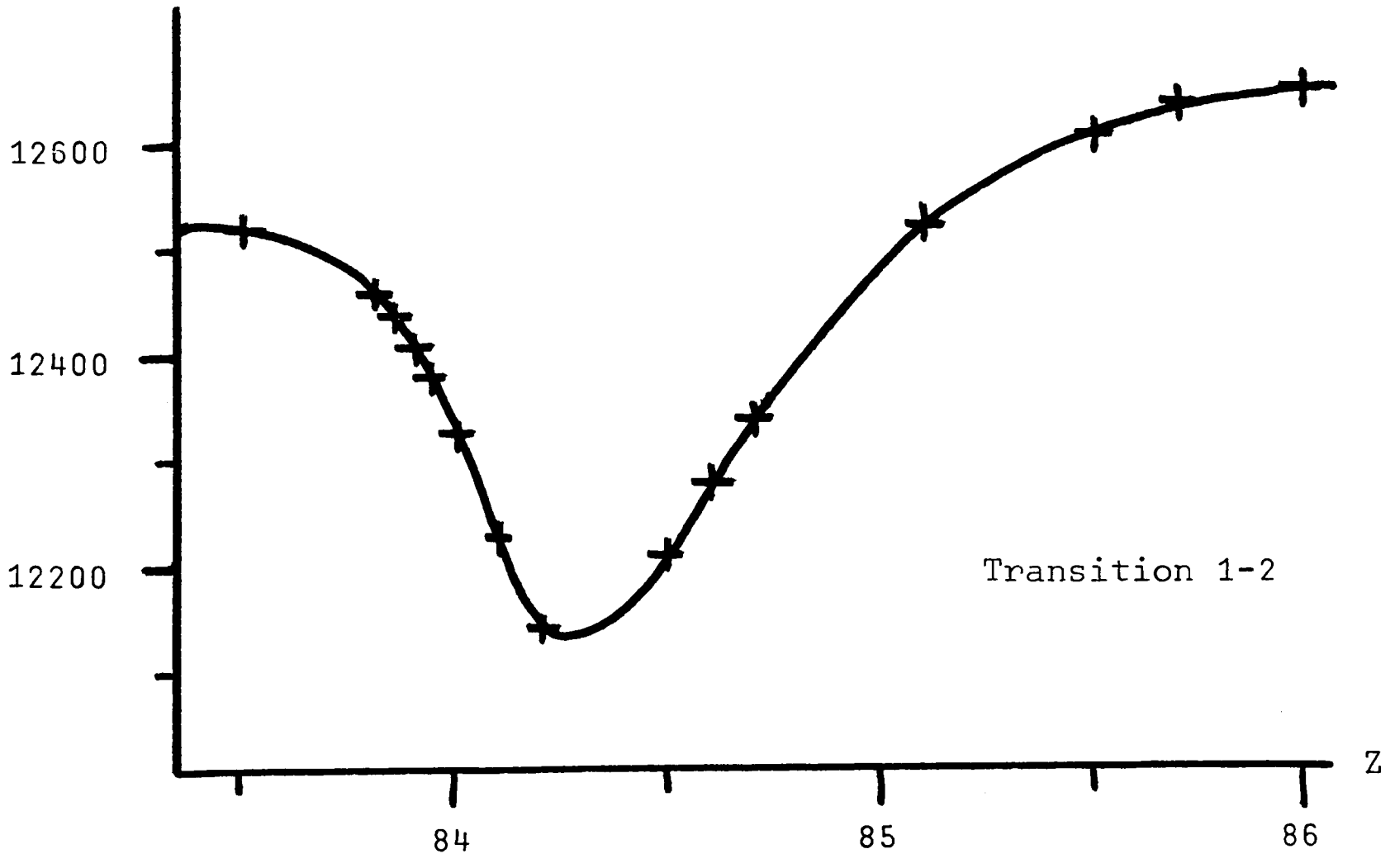

Figure 7.1. Dependence of transition energies on the value of Z used for the correlation orbitals in the 53 CSF bismuth calculation.

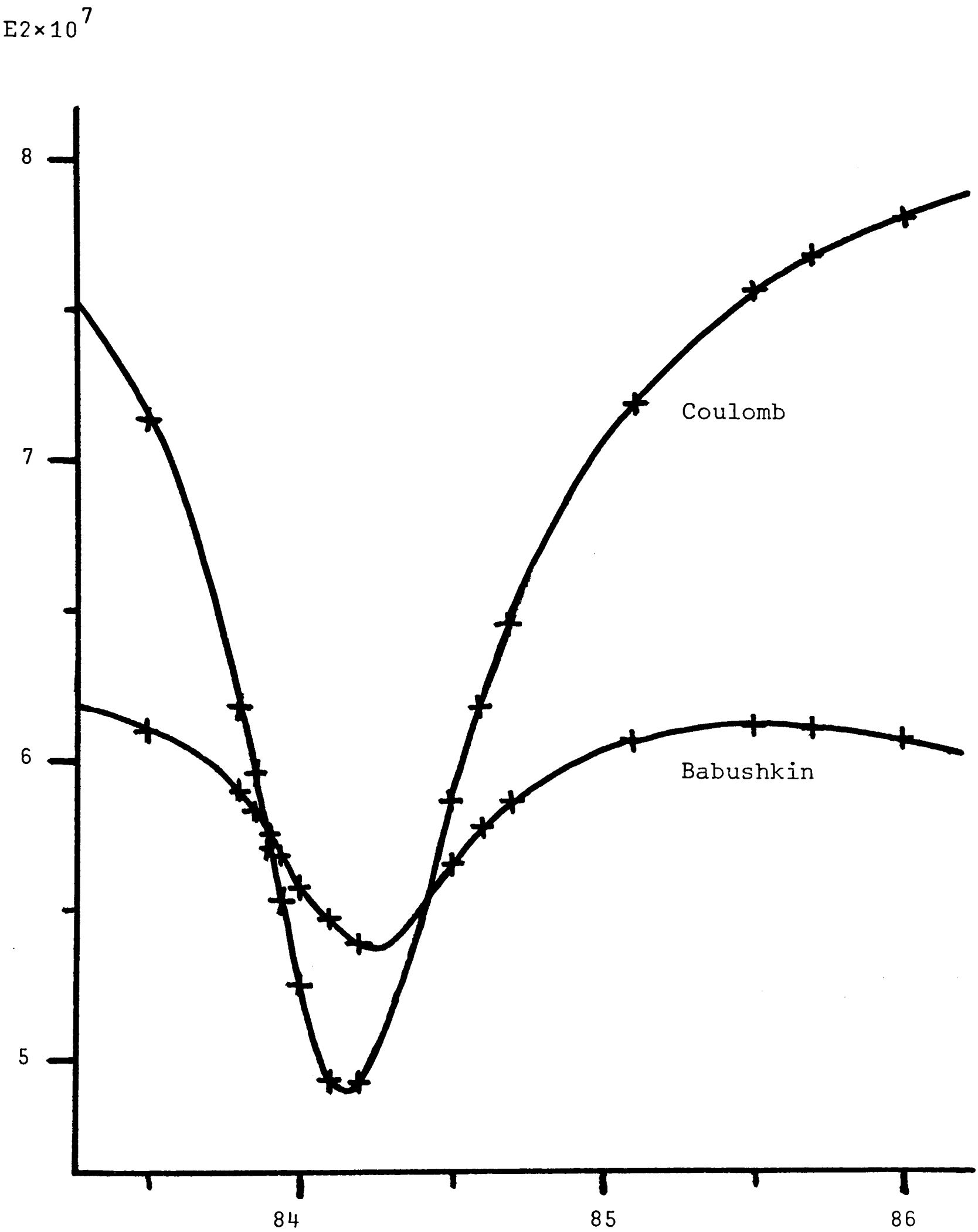

Figure 7.2. Dependence of the E2 matrix element for the 1-3 transition on the value of Z used for the correlation orbitals in the 53 CSF bismuth calculation.

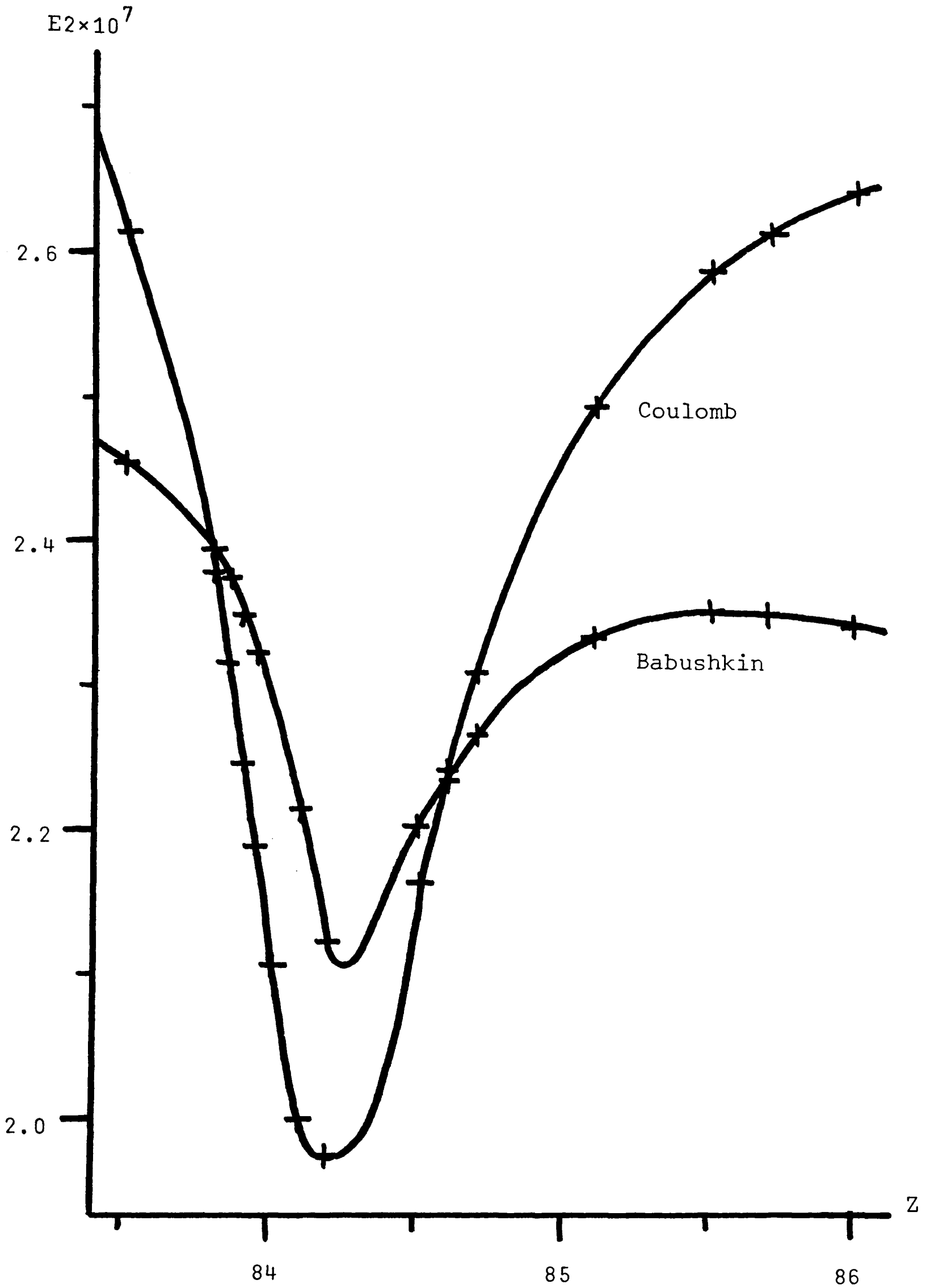

Figure 7.3. Dependence of the E2 matrix element for the 1-2 transition on the value of Z used for the correlation orbitals in the 53 CSF bismuth calculation.

TABLE 7.4

The 53 CSF bismuth calculation

Correlation Z	Transition 1 - 2 Energy Coulomb (cm^{-1})	Energy Coul+Breit+QED (cm^{-1})	<E2> Coul gauge Coul energy $\times 10^7$	<E2> Bab gauge Coul energy $\times 10^7$	<E2> Coul gauge Coul+Breit+QED energy $\times 10^7$	<E2> Bab gauge Coul+Breit+QED energy $\times 10^7$
83.5	12521	12392	2.617	2.453	2.565	2.408
83.8	12461	12333	2.379	2.397	2.320	2.357
83.9	12407	12280	2.247	2.350	2.187	2.310
84.0	12327	12201	2.106	2.286	2.046	2.248
84.1	12228	12102	2.000	2.217	1.942	2.181
84.2	12143	12018	1.976	2.164	1.920	2.130
84.5	12209	12091	2.166	2.203	2.111	2.172
84.6	12278	12162	2.242	2.238	2.186	2.206
84.7	12343		2.311	2.268		
85.1	12525		2.497	2.336		
85.5	12614		2.590	2.353		
85.7	12637		2.618	2.352		
86.0	12654		2.647	2.344		

Correlation Z	Transition 1 - 3 Energy Coulomb (cm^{-1})	Energy Coul+Breit+QED (cm^{-1})	<E2> Coul gauge Coul energy $\times 10^7$	<E2> Bab gauge Coul energy $\times 10^7$	<E2> Coul gauge Coul+Breit+QED energy $\times 10^7$	<E2> Bab gauge Coul+Breit+QED energy $\times 10^7$
83.5	17450	17273	7.140	6.099	6.986	5.974
83.8	17374	17200	6.188	5.904	6.021	5.796
83.9	17287	17114	5.724	5.760	5.558	5.657
84.0	17155	16983	5.255	5.592	5.093	5.495
84.1	16989	16819	4.935	5.447	4.780	5.356
84.2	16841	16673	4.921	5.385	4.770	5.299
84.5	16907	16748	5.868	5.660	5.712	5.578
84.6	17009	16853	6.189	5.774	6.029	5.691
84.7	17106		6.467	5.868		
85.1	17375		7.204	6.077		
85.5	17497		7.585	6.121		
85.7	17524		7.705	6.112		
86.0	17539		7.831	6.079		

The value of Z is that which is used to obtain the correlating orbitals

Experimental energies 11419 and 15437

Table 7.4 continued

Correlation Z	Total energies† a.u.			$M1 \times 10^7$ a.u.	
	level 1	level 2	level 3	Transition 1-2	Transition 1-3
83.5	-.121784	-.064732	-.042276		
83.8	-.124547	-.067772	-.045386		
83.85	-.124958	-.068290	-.045968	16.16	-6.687
83.9	-.125343	-.068813	-.046579		
83.94	-.125643	-.069243	-.047094	16.17	-6.717
84.0	-.126072	-.069904	-.047909		
84.1	-.126728	-.071012	-.049321	16.17	-6.777
84.2	-.127280	-.071954	-.050546	16.18	-6.818
84.5	-.127855	-.072223	-.050818	16.29	-6.858
84.6	-.127761	-.071817	-.050260		
84.7	-.127593	-.071355	-.049650	16.36	-6.845
85.1	-.126349	-.069281	-.047181		
85.5	-.124621	-.067146	-.044900		
85.7	-.123704	-.066125	-.043860		
86.0	-.122361	-.064704	-.042448		

†Energies are relative to $(6p^2)\,^3P_0\,6p\ J=\frac{1}{2}$ which is not correlated in these calculations and therefore has constant energy. This has been done for numerical stability reasons.

maximized.

(c) Z = 84.40. At this point the effect of configuration interaction on the absolute energies is maximized. We note that this is close to (b).

These will be referred to later when we consider the results of the PNC calculations.

It should also be noted that the results for the E2 matrix element in the Babushkin gauge show less variation than those in the Coulomb gauge.

The analysis of the results of the 155 CSF bismuth calculations (see figures 7.4, 7.5, 7.6 and 7.7 and table 7.5) leads to the value of $Z \sim 84.2$ being best. For such a value we have good agreement between the Coulomb and Babushkin gauge values for the E2 matrix element (to $\lesssim$ 5%) and good agreement between the calculated and measured transition energies. This is also the point of maximum correlation as measured by the effect on the transition energies. However, we note that the effects on the total energies are maximized at Z = 84.50.

These considerations lead us to hope that we have a good description of the relevant states of bismuth when the value $Z \sim 84.2$ is used in the 155-CSF bismuth calculation.

As before, we note that the Babushkin gauge results are more stable than the Coulomb gauge ones.

§7.3 Thallium

We repeated the procedure for thallium. A calculation using only the two CSF's $6\bar{p}$ and $7\bar{p}$ gives a transition energy

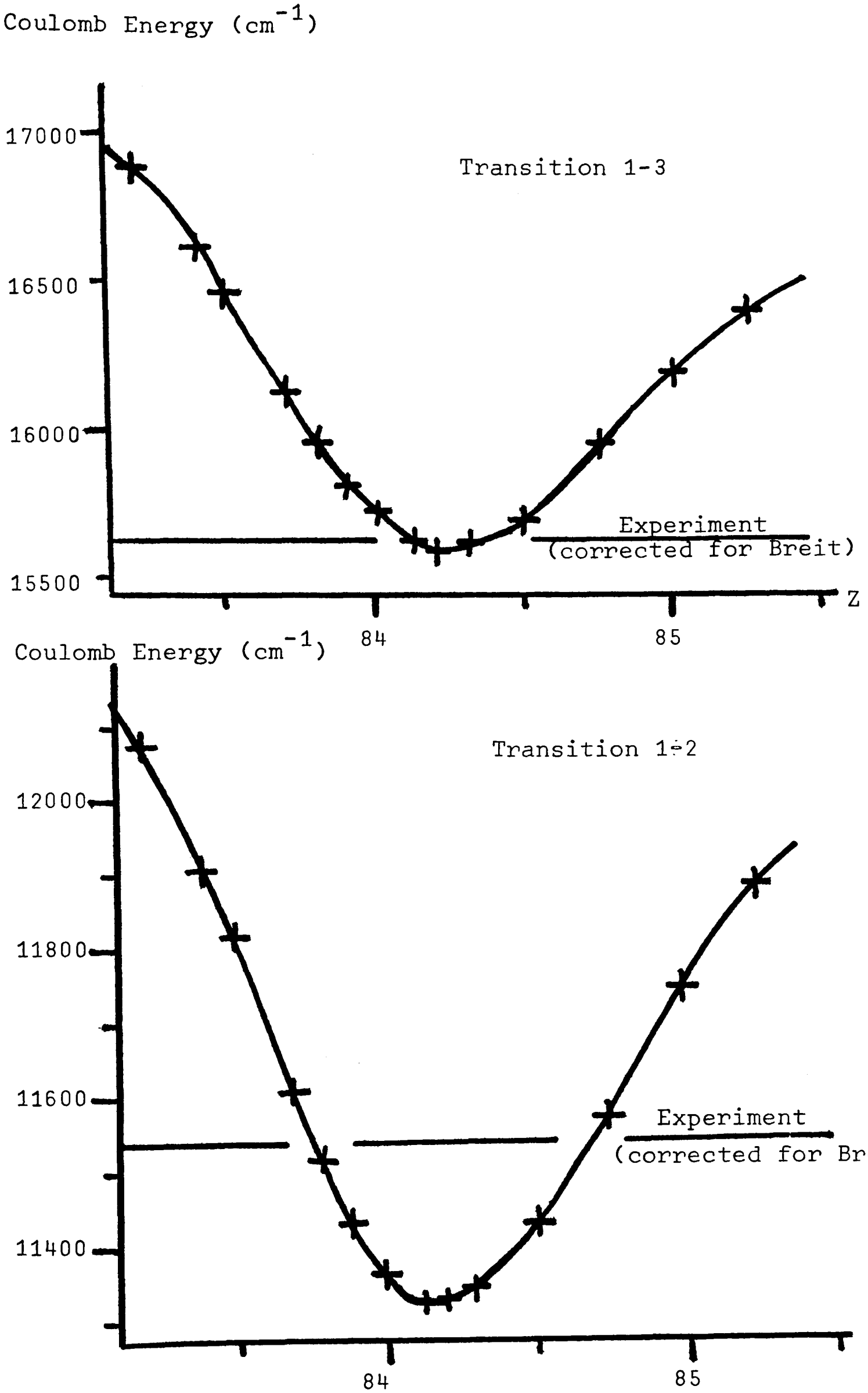

Figure 7.4. Dependence of transition energies on the value of Z used for the correlation orbitals in the bismuth 155 CSF calculation.

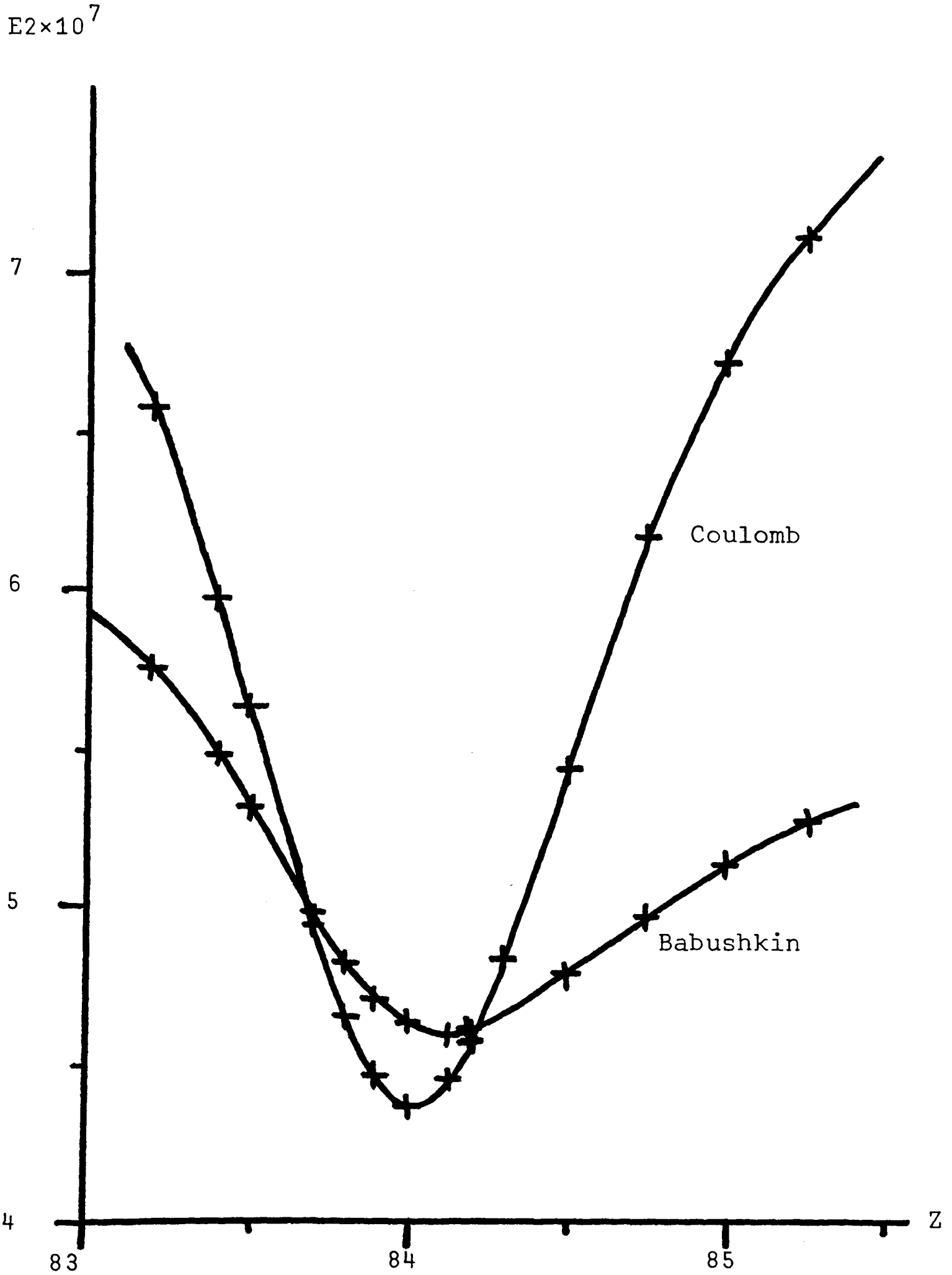

Figure 7.5. Dependence of the E2 matrix element for the 1-3 transition on the value of Z used for the correlation orbitals in the bismuth 155 CSF calculation.

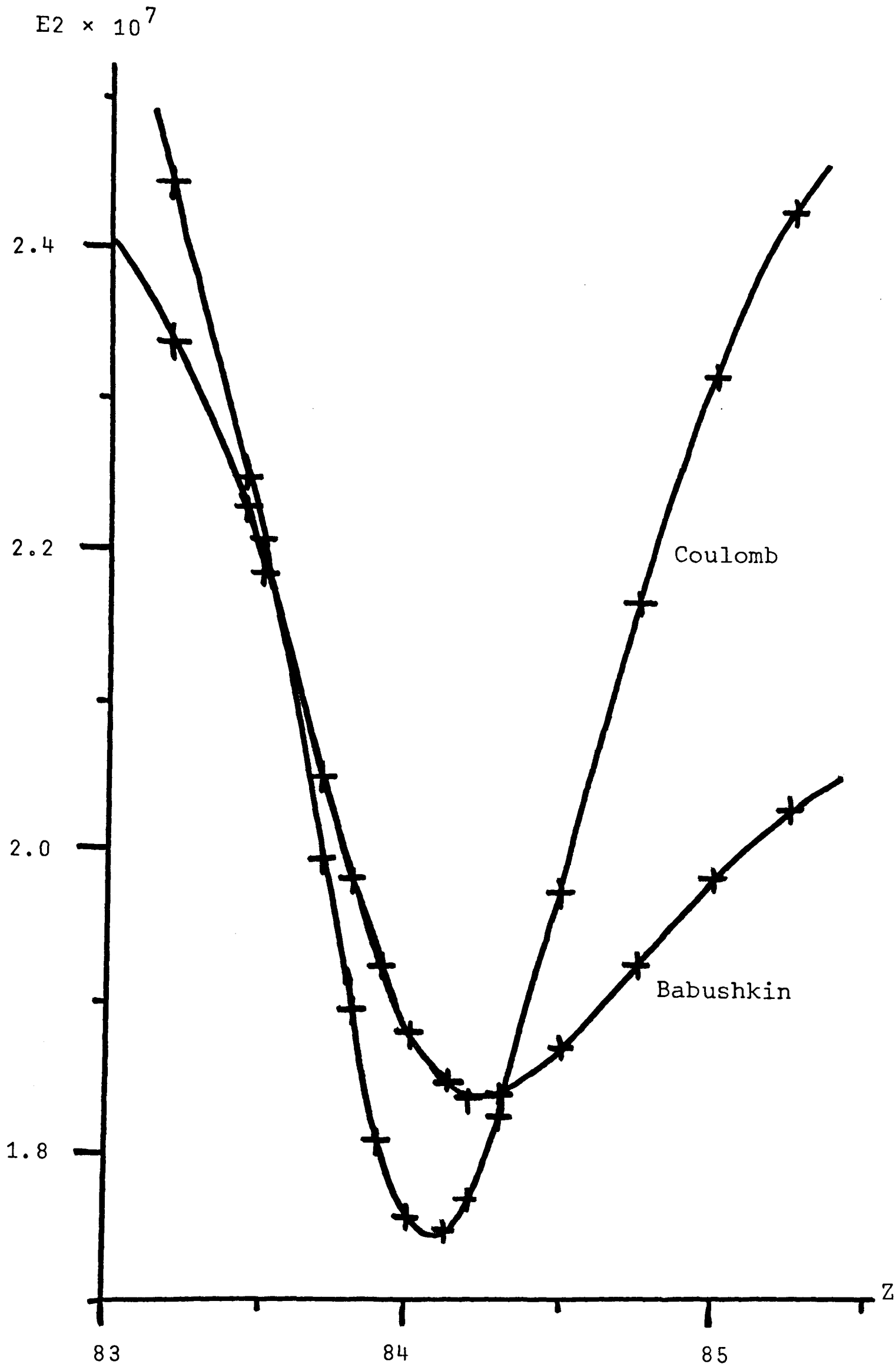

Figure 7.6. Dependence of the E2 matrix element for the 1-2 transition on the value of Z used for the correlation orbitals in the bismuth 155 CSF calculation.

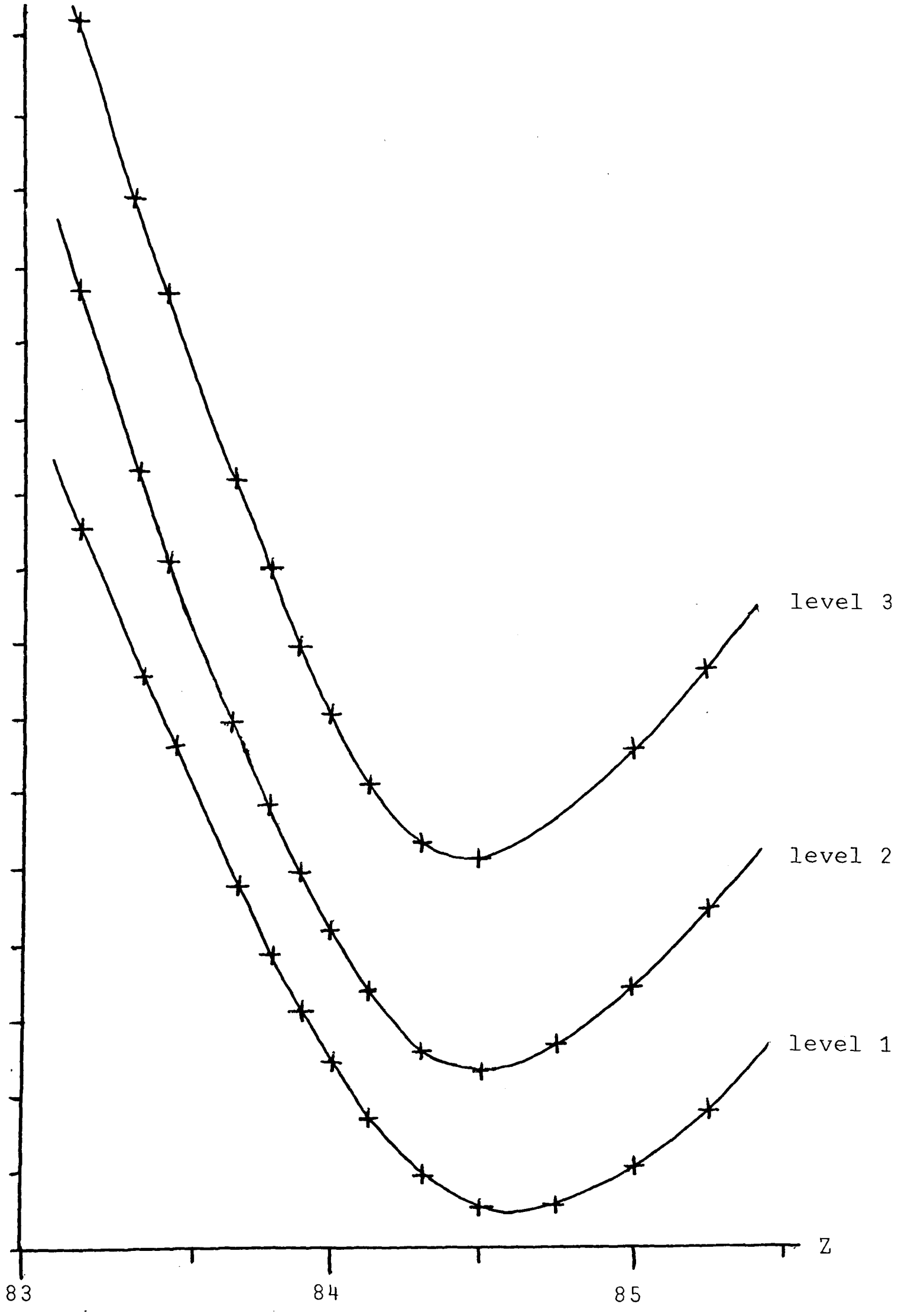

Figure 7.7 Dependence of total energies (in arbitrary units) on the value of Z used for the correlation orbitals in the bismuth 155 CSF calculation.

TABLE 7.5

The 155 CSF bismuth calculation

Correlation Z	Transition 1 - 2 Energy Coulomb (cm^{-1})	Coulomb+Breit (cm^{-1})	<E2> Coul gauge Coul energy $\times 10^7$	Bab gauge Coul energy $\times 10^7$	Coul gauge Coul+Breit energy $\times 10^7$	Bab gauge Coul+Breit energy $\times 10^7$
83.2	12082	11947	2.445	2.342	2.396	2.293
83.4	11913	11781	2.299	2.247	2.247	2.201
83.5	11819		2.207	2.181		
83.7	11616	11488	1.997	2.050	1.944	2.007
83.8	11518	11392	1.894	1.983	1.843	1.943
83.9	11434	11310	1.810	1.924	1.760	1.887
84.0	11371		1.758	1.879		
84.128	11331	11212	1.747	1.846	1.700	1.812
84.2	11329		1.769	1.838		
84.3	11347	11232	1.823	1.840	1.776	1.808
84.5	11434		1.976	1.870		
84.75	11590	11485	2.169	1.928	2.122	1.898
85.0	11748		2.321	1.984		
85.25	11887	11791	2.431	2.031	2.384	2.002

Correlation Z	Transition 1 - 3 Energy Coulomb (cm^{-1})	Energy Coulomb+Breit (cm^{-1})	E2 Coul gauge Coul energy $\times 10^7$	E2 Bab gauge Coul energy $\times 10^7$	E2 Coul gauge Coul+Breit energy $\times 10^7$	E2 Bab gauge Coul+Breit energy $\times 10^7$
83.2	16876	16694	6.578	5.751	6.440	5.621
83.4	16611	16434	5.975	5.474	5.833	5.355
83.5	16458		5.636	5.309		
83.7	16120	15949	4.951	4.970	4.813	4.868
83.8	15952	15784	4.661	4.820	4.526	4.724
83.9	15803	15637	4.457	4.703	4.326	4.611
84.0	15717		4.372	4.629		
84.128	15602	15444	4.451	4.600	4.325	4.516
84.2	15587		4.580	4.612		
84.3	15601	15448	4.829	4.654	4.702	4.574
84.5	15687		5.444	4.786		
84.75	15947	15804	6.173	4.970	6.035	4.892
85.0	16177		6.733	5.128		
85.25	16383	16252	7.131	5.257	6.987	5.175

Experimental energies 11419 and 15437

Table 7.5 continued

Correlation Z	Total energies† a.u.			$M1 \times 10^7$ a.u.	
	level 1	level 2	level 3	Transition 1-2	Transition 1-3
83.2	.128706	.073657	.051815	15.77	-6.548
83.4	.133505	.079224	.057817	15.68	-6.553
83.5	.135916	.082065	.060926	15.63	-6.558
83.7	.140509	.087583	.067060		
83.8	.142633	.090142	.069950	15.55	-6.582
83.9	.144603	.092506	.072600	15.47	-6.594
84.0	.146385	.094574	.074910	15.46	-6.607
84.128	.148322	.096693	.077235	15.45	-6.624
84.2				15.48	-6.631
84.3	.150200	.098500	.079118	15.51	-6.638
84.5	.151242	.099144	.079629	15.57	-6.633
84.75	.151122	.098316	.078479	15.63	-6.600
85.0	.149901	.096375	.076194	15.67	-6.556
85.25	.148055	.093893	.073409	15.71	-6.518

†Energies are relative to $(6p^2)_0 6\bar{p}$ $J=\frac{1}{2}$ which is not correlated in these calculations and therefore has constant energy. This has been done for numerical stability reasons.

of 31631 cm^{-1} (experiment 34165) and a M1 matrix element -1.361×10^{-10}. The E2 matrix elements are zero. As in the case of bismuth we will try and reduce the discrepancy between theory and experiment by means of configuration interaction. We will assess the importance of a configuration by calculating the change it produces in the calculated transition energy, total energy of the $6P_{\frac{1}{2}}$ and $7P_{\frac{1}{2}}$ levels and M1 matrix elements, since E2 = 0 by virtue of the conservation of angular momentum.

The results are shown in table 7.6. They lead us to take as correlating configurations those from the manifolds [6s] (6p+7p)6d, [5d] (6p+7p)7s, [$6s^2$] $(6p+7p)^3$, [6s] (6p+7p)7s, [5p] (6p+7p)5f, [$5d^2$] $6p^3$ and [5d] (6p+7p)5g - a total of 75.

This calculation leads to results that are shown in table 7.7. They do not show a clear value of Z that gives the maximum correlation, since the maximum change in the M1 matrix element occurs at $Z \simeq 82.5$ but the maximum change in the transition energy at $Z \simeq 83.0$, whilst the total energy of $6P_{\frac{1}{2}}$ is minimized at $Z \simeq 82.5$ but of $7P_{\frac{1}{2}}$ at $Z \simeq 82.0$. Even the energy obtained with Z = 83.0 (33277 cm^{-1}) is not in very good agreement with experiment.

These results could be improved by taking a different value of Z for each orbital, but we would not expect an improvement of more than one or two hundred cm^{-1}, and did not consider this worth the investment of computer time that it would involve.

§7.4 Lead

A calculation using the five configurations of $6p^2$

TABLE 7.6

Configuration interaction in thallium: effects on the λ = 293nm transition

Interacting Manifold	Maximum change in energy (cm^{-1})	Maximum change in <M1> %	Number of CSF's	Shift in total energy of levels $\times 10^4$ a.u.	
				lower	upper
8p	0	0	1	0	0
[6s](6p+7p)6d	+2300	+91	8	117	3
[5d][6s](6p+7p)^3	0	0	85		
[5d](6p+7p)7s	+50	0	8	8	0
[6s^2](6p+7p)^3	-1080	-2	14	139	197
[6s](6p+7p)7s	+190	-2	6	21	12
[6s^2](6p+7p)6d^2	+10	0	14	13	12
[5p](6p+7p)^2	0	+1	25	0	0
[5s^2](6p+7p)^3	0	0	14	1	1
[5s](6p+7p)6d	0	0	8	0	0
[5s](6p+7p)7s	0	-1	6	0	0
[5p^2](6p+7p)5f^2	0	0	8	0	0
[5p](6p+7p)5f	+30	+2	10	8	0
[5d^2] 6p^3	+130	0	19	6	0
[5d^2]6p^{2}7p	-180	0	76	2	10
[5d^2]6p7p^2	-30	0	76	0	1
[5d^2]7p^3	0	0	19	0	0
[4f](6p+7p)^2	0	0	9	0	0
[5d](6p+7p)5g	+180	+2	10	8	1
[6s^2](6p+7p)6d7s	0	0	8	0	0
[5d6s](6p+7p)7s^2	0	0	8	0	0

TABLE 7.7

The 77 CSF thallium calculation: effects of correlation on the λ = 293nm transition

Z for correlation orbitals	E (Coulomb) cm^{-1}	M1 × 10^{10} a.u.	Energy level change a.u. × 10^6	
			level 1	level 2
81.5	32040	-2.051	23634	21770
82.0	32654	-2.964	28276	23613
82.5	33125	-3.413	28846	22038
83.0	33277	-2.978	27638	20139
83.5	33179	-2.381	25612	18558

yields, for the 1279nm transition in lead, an energy of 6937 cm^{-1} (experiment 7819) and a M1 matrix element 1.558 $\times 10^{-6}$. The Breit correction to the energy is -167 cm^{-1}. Again, the agreement between experiment and theory is not very good, and so we will again attempt to reduce this discrepancy by means of configuration interaction.

The results of interaction with the configurations derived from a number of manifolds are shown in table 7.8. We have also included the effects on the level $(6p^2)_o$ since the transition $(6\bar{p}^2)_o \rightarrow (6p^2)_o$ has been the subject of some theoretical work; such work is, however, outside the scope of this thesis.

We again select the main contributing manifolds; these are

$6d^2$ $[5d]6p^2 7s$ $[6s^2]6p^4$ $[5s]6p^2 6d$ $7p^2$ $5f^2$

$6p7p$ $[6s]6p^2 7s$ $[6s]6p^2 6d$ and $[5d]6p^2 5g$

(the $[5s]6p^2 6d$ being included due to an error in an earlier CI calculation) which, with the basic $6p^2$, give us a 115 CSF calculation.

The results of this calculation with various values of Z are shown in table 7.9. They indicate that the effects on the transition energies and M1 values reach a plateau at Z = 82.85, whilst the level energies are minimized at about Z = 83.4. At these values of Z the calculated transition energy for the λ = 1279nm transition is 7033 cm^{-1} and 7065 cm^{-1} respectively, and the M1 value is 1.571×10^{-6} and 1.579×10^{-6}.

TABLE 7.8

Configuration interaction in lead:

effects on the J = 0 and J = 1 states

Interacting manifold	No. of CSF's	Change in level energy (a.u.×10^6) level 1 $(6\bar{p}^2)_0$	level 2 $(6\bar{p}6p)_1$	level 5 $(6p^2)_0$	Change in transition energy (a.u.×10^6) transition 1-2	1-5	Change in M1 % 1-2 transition
[6s]$6p^2$6d	18	15395	17954	2870	-2559	12525	-6.9
[$6s^2$]$6p^4$	3	4947	4148	18970	799	-14023	+1.2
$6d^2$	3	3727	3035	15281	692	-11554	+1.4
[$6s^2$]$6p^3$7p	13	4497	4358	4085	139	412	+0.4
[$6s^2$]$6p^2$$7p^2$	22	2238	2242	2247	-4	9	0
$7p^2$	3	1126	791	3376	335	-2250	+0.8
[5d6s]$6p^4$	18	1304	1616	1909	-312	-605	-0.9
$5f^2$	3	706	227	2013	479	-1307	+2.0
[$6s^2$]$6p^2$$6d^2$	29	932	922	912	10	20	0
[5d]$6p^2$5g	29	1095	808	2462	287	-1367	+0.7
6p7p	6	1093	53	1059	1040	34	+3.6
[5d]$6p^2$7s	18	252	232	798	20	-546	+0.1
[6s]$6p^2$7s	9	716	997	424	-281	292	-0.8
[$5s^2$]$6p^2$$6d^2$	29	696	697	696	-1	0	0
[$5d^2$]$6p^4$	29	382	417	821	-35	-439	-0.1
[$5d^2$]$6p^2$$7s^2$	29	496	495	494	1	2	0
[5p]$6p^2$5f	29	306	215	674	91	-368	+0.2
[$5p^2$]$6p^4$	22	67	68	96	-1	-29	0
[5p] $6p^3$	13	15	13	24	+2	-9	0
[5s]$6p^2$6d	18	13	12	6	1	7	0
[$5s^2$]$6p^4$	3	3	0	9	3	-6	0
[5s]$6p^2$7s	9	5	5	1	0	4	0
5f7p	1	2	3	2	-1	0	0
6p5f	1	1	4	3	-3	-2	0
[5s]$6p^2$5g	2	0	0	0	0	0	0
[6s]$6p^2$5g	2	0	0	0	0	0	0

TABLE 7.9

The 115 CSF lead calculation: effects of correlation

Correlation Z	Change in level energy (a.u. × 10^6)			Change in transition energy (a.u. × 10^6) transition		Change in M1 % 1-2 transition
	level 1 $(6\overline{p}^2)_0$	level 2 $(6\overline{p}6p)_1$	level 5 $(6p^2)_0$	1-2	1-5	
82.7	21935	21473	38280	+462	-16345	+.9
82.85	23874	23436	40460	+438	-16586	+.8
83.0	25382	24936	41929	+444	-16547	+.9
83.2	26738	26238	42861	+500	-16123	+1.0
83.4	27389	26807	42735	+582	-15346	+1.3
83.5	27469	26847	42325	+622	-15478	+1.4
83.6	27400	26744	41719	+656	-14975	+1.5
83.8	26874	26174	40060	+700	-13886	+1.6

A larger calculation, selecting the correlating manifolds

$6d^2$ $[6s^2]6p^4$ $7p^2$ $5f^2$ $6p7p$ $[6s]6p^27s$

$[6s]6p^26d$ $[5d]6p^25g$ $[6s^2]6p^37p$ $[6s^2]6p^27p^2$

$[5d6s]6p^4$ and $[6s^2]6p^26d^2$

according to a slightly different criterion for important contributions (namely, putting more weight on the effects on total energies of the levels of interest) gives rise to a 161 CSF calculation; the results obtained with different values of Z are shown in table 7.10. Qualitatively, these are much the same as for the 115 CSF calculation, showing stationary points of the transition energies and M1 value at Z = 82.85 and of the total energy at $Z \simeq 83.5$. Again, the effects of correlation on the M1 matrix element and 1279nm transition energy are small.

Despite the disappointingly small effects of CI on these calculated values, we will not attempt to improve the calculation further since this transition is of less interest than those in bismuth and thallium.

§7.5 Cesium

We made a 2-CSF calculation on the configurations 6s and 7s. The result we obtained for the transition energy was 15959 cm^{-1}. The Breit interaction reduces this by 24 cm^{-1}. The M1 matrix element showed severe numerical instability when the gridsize and inner grid point were varied and will not be considered further.

TABLE 7.10

The 161 CSF lead calculation: effects of correlation

Correlation Z	Change in level energy (a.u.× 10^6) Level 1 $(6\bar{p}^2)_0$	level 2 $(6\bar{p}6p)_1$	level 5 $(6p^2)_0$	Change in transition energy (a.u.× 10^6) Transition 1-2	1-5	Change in M1 % 1-2 transition
82.5	26103	26201	42492	-98	-16389	-0.7
82.85	31262	31461	49445	-199	-18183	-1.0
83.2	34517	34691	50222	-174	-15705	-0.9
83.5	35664	35793	50092	-129	-14428	-0.6
83.55	35709	35767	49878	-58	-14169	-0.6
83.6	35713	35755	49614	-42	-13901	-0.5
83.8	35357	35353	48142	+4	-12785	-0.4

The calculated transition energy is not in very good agreement with the experimental value of 18536 cm^{-1}, so we attempted to improve this by means of interaction with the configurations of the manifolds 8s, [5s](6s+7s)5d, [5p](6s+7s)5f, [5p](6s+7s)6p, [5s](6s+7s)^2, [5s](6s+7s)8s, [4d](6s+7s)^2, [4d](6s+7s)6d, [4d](6s+7s)5g, [5p^2](6s+7s)5d^2, [4d]6p^2, [5p^2](6s+7s)6p^2, [5s^2](6s+7s)6d^2, [4d^2](6s+7s)6p^2, [4d](6s+7s)5d, [5p^2](6s+7s)4f^2, [5s^2](6s^{2}7s+6s7s^2), [5s^2](6s+7s)8s^2, [5p^2](6s^{2}7s+6s7s^2), [5p](6s+7s)4f, [5s^2](6s+7s)5d^2, [5s]6p^2, [4d](6s+7s)8s, and [5p^2](6s+7s)6p^2.

The results were disappointing; in no case did the transition energy change by more than 120 cm^{-1}, and in most cases the change was far less than this. Therefore, we will not attempt to calculate further the correlation for cesium.

Chapter 8

The Moving Finger writes; and, having writ,
Moves on: nor all thy Piety nor Wit
Shall lure it back to cancel half a line,
Nor all thy Tears wash out a Word of it.

Khayyám (1100a)

Results of the PNC MCDF Calculations

CHAPTER 8

RESULTS OF THE PNC MCDF CALCULATIONS

§8.1 Introduction

In this chapter we report the results of the numerical solution of the PNC MCDF equations (6.3.44) and (6.3.45). The computer programs used to perform these calculations are described in appendix 4 and listed in appendix 5.

To start with, we will make some general remarks on the calculations. We will then report the calculations for each atom (bismuth, thallium, cesium and lead) in turn.

§8.2 General considerations

It is convenient to divide the right hand sides of the MCDF PNC equations into five parts:

$$\bar{X}_a^{(P)} = D_a^{(P)} + X_a^{(P)HF} + X_a^{(P)PV} + r \sum_{\substack{b \neq a \\ \kappa_b = \kappa_a}} \frac{\varepsilon_{ab}}{c\bar{q}_a} \bar{Q}_b + r \sum_{\substack{b \\ \kappa_b = -\kappa_a}} \frac{\eta_{ab}}{c\bar{q}_a} Q_b \qquad (8.2.1)$$

where

$$D_a^{(P)} = - \frac{P_a}{c} \rho_N(r) r \qquad (8.2.2)$$

is the driving term;

$$X_a^{(P)HF} = \sum_{\substack{b \\ k \in K_-}} \frac{\bar{g}^k(ab)}{c\bar{q}_a} Y_k(\bar{a}b;r)\, Q_b \qquad (8.2.3)$$

is the Hartree-Fock exchange; and

$$X_a^{(P)PV} = \sum_{\substack{b \\ k\varepsilon \boldsymbol{K}_+}} \frac{\bar{g}^k(ab)}{c\bar{q}_a} Y_k(ab;r)\bar{Q}_b - \sum_{\substack{b \\ k\varepsilon \boldsymbol{K}_-}} \frac{\bar{g}^k(ab)}{c\bar{q}_a} Y_k(a\bar{b};r)Q_b \quad (8.2.4)$$

is the parity violating exchange. A similar division of $\bar{\chi}_a^{(Q)}$ may be made.

The evaluation of the off-diagonal multipliers presents a number of problems. Those between orbitals of the same parity are calculated by the MCDF package. This works for the simple cases, where no orbitals are fixed; but for parameters between a fixed and an unfixed orbital, unsatisfactory results are obtained; this is the situation for the correlation calculations, where all except the extra correlation orbitals are fixed. In practice, therefore, we Schmidt orthogonalize the parity conserving wavefunctions at the end of a run and set the multipliers ε_{ab} to zero. Since their effect on the final E1 matrix element is small this is not expected to lead to any appreciable errors.

Work is in progress to circumvent these problems by exploiting the fact that the solution of the MCDF equations should be linear in the Lagrange multipliers using methods similar to those of Smith (1971).

Formulae for the PNC Lagrange multipliers may be derived (see appendix 3), but the inclusion of multipliers calculated in this way leads to instabilities and does not seem to improve orthogonality. This is probably a consequence of the nature of the formulae in appendix 3, in which a great deal of cancellation is likely to occur. Instead we have treated them as variable parameters and set them by hand, choosing their values so that orthogonality is obtained. This is not as

depend linearly on the multipliers. Alternatively, a method based on Smith's approach mentioned above could have been used.

Finally, we come to the calculation of the components of $|ns\rangle$ in $|\overline{np}\rangle$ in order to overcome the instabilities discussed in §6.5. If the $n\bar{p}$ and ns shells are full, we only include the Hartree-Fock exchange, and there are no Lagrange multipliers, then it may be shown that, writing $a = n\bar{p}$ and $b = ns$,

$$\langle b|\bar{a}\rangle = \frac{\int_o^\infty \rho_N(r)(P_b Q_a - Q_b P_a)}{\varepsilon_b - \varepsilon_a} \qquad (8.2.5)$$

which is quite easy to calculate; however, as we remove the above restrictions, the equation (8.2.5) assumes progressively more complex forms, and it soon becomes more practical to treat these as adjustable parameters and set them by hand as well.

The values of these parameters are given in appendix 6.

It will be convenient to refer to the non-correlation orbitals at some points. We shall call these "physical" orbitals, since they are calculated in a truly self-consistent manner, as opposed to the correlation orbitals, which are artificially contracted.

All the results reported have used $\sin^2\theta_W = 0.25$ for easy comparison with other calculations. The results for $\sin^2\theta_W = 0.23$ may be obtained by multiplication of the present numbers by 0.947 (bismuth), 0.948 (lead), 0.946 (thallium) or 0.920 (cesium).

8.3 Bismuth

The results of the calculations performed on bismuth without taking shielding into account are shown in table 8.1.

The first point that should be made is that the M1 and E2 matrix elements are of approximately the same magnitude for the 1-3 transition, in contrast to the assumption sometimes made (e.g. Henley and Wilets (1976)) that E2 is negligible compared to M1. It is therefore important to ensure that this has been accounted for when experimental and theoretical values for the PNC ratio are compared. For the 1-2 transition the E2 matrix element is small enough to be neglected if desired.

The second point is that we can obtain reasonable gauge invariance. This is in marked contrast to the results of Carter and Kelly (1979) and Rose (1979), and gives us greater confidence in our results. The Babushkin gauge results are far more stable than those in the Coulomb gauge, and so are the ones used in the calculation of the PNC ratio.

The first four calculations use experimental transition energies (Moore (1958)) and the mixing coefficients derived from hyperfine structure measurements by Landman and Lurio (1970), in which we have changed the signs of the mixing coefficients for some levels to keep them consistent with phase conventions in the MCDF program. However, use of MCDF energies and mixing coefficients improves the gauge invariance, and so it is these that are used in all subsequent calculations on bismuth. In any case, use of experimental energies will not change the

TABLE 8.1

The PNC ratio for bismuth

Orbitals	Exchange	Correlation Z PC	Correlation Z PNC	No. of CSF	Nucleus	Are ϵ_{ab} included?	PM Orthog-onality	Energy	Mixing Coeffs.	Transition 1-2 M1 × 10^6	Transition 1-3 M1 × 10^7	Transition 1-2 $\frac{E1\ (Coul)}{G}$
$j=\frac{1}{2}$ only	H-F	-	-	1	U	no	no	Expt	L-L	1.658	-7.480	.4716
$j=\frac{1}{2}$ only	H-F	-	-	1	F	no	no	Expt	L-L	1.658	-7.480	.4480
$j=\frac{1}{2}$ only	H-F	-	-	5	F	no	no	Expt	L-L	1.661	-7.502	.0867
$j=\frac{1}{2}$ only	full	-	-	5	F	no	no	Expt	L-L	1.661	-7.502	.3779
$j=\frac{1}{2}$ only	full	-	-	5	F	no	no	MCDF	MCDF	1.567	-6.261	.3105
all	full	-	-	5	F	no	no	MCDF	MCDF	1.567	-6.261	.2598
all	full	-	-	5	F	yes	no	MCDF	MCDF	1.567	-6.261	.2595
all	full	-	-	5	F	yes	yes	MCDF	MCDF	1.567	-6.261	.2036
all except 7p	full	84.2	83.0	53	F	no	no	MCDF	MCDF	1.618	-6.818	.2554
all except 7p	full	84.2	84.2	53	F	no	no	MCDF	MCDF	1.618	-6.818	.2474
all	full	84.2	86.0	53	F	no	no	MCDF	MCDF	1.618	-6.818	.2523
all except 7p	full	84.2	84.2	53	F	no	Physical orbitals only	MCDF	MCDF	1.618	-6.818	.1835
all except 7p	full	84.2	84.2	53	F	no	yes	MCDF	MCDF	1.618	-6.818	.1908
all except 7p 5f	full	84.5	84.5	53	F	no	Physical orbitals only	MCDF	MCDF	1.629	-6.858	.1799
all except 7p $5\bar{f}$	full	83.85	83.85	53	F	no	Physical orbtials only	MCDF	MCDF	1.616	-6.687	.1876
all except 7p	full	84.2	84.2	155	F	no	no	MCDF	MCDF	1.548	-6.631	.2747
all except 7p	full	84.2	84.2	155	F	no	Physical orbitals only	MCDF	MCDF	1.548	-6.631	.2070
all except 7p	full	84.2	84.2	155	F	no	incomplete for correlation orbitals	MCDF	MCDF	1.548	-6.631	.2257
all except 7p	full	84.2	84.2	155	F	no	yes	MCDF	MCDF	1.548	-6.631	.2207
all except 7p	full	84.0	84.0	155	F	no	Physical orbitals only	MCDF	MCDF	1.546	-6.607	.2007
all eccept 7p	full	84.5	84.5	155	F	no	Physical orbitals only	MCDF	MCDF	1.557	-6.633	.1802

U Nucleus: uniform nuclear density distribution

F Nucleus: Fermi nuclear density distribution

L-L Mixing Coeffs: Mixing coefficients as determined by Landman and Lurio (1970)

- shielding omitted

Transition 1-2 $\frac{E1}{G}$ (Bab)	Transition 1-3 $\frac{E1}{G}$ (Coul)	Transition 1-3 $\frac{E1}{G}$ (Bab)	Transition 1-2 R (Bab) (exc. E2)	Transition 1-3 R (Bab) (exc. E2)	Transition 1-2 E2 (Coul) $\times 10^7$	Transition 1-2 E2 (Bab) $\times 10^7$	Transition 1-3 E2 (Coul) $\times 10^7$	Transition 1-3 E2 (Bab) $\times 10^7$
.2193	-.3340	-.1344	-12.6	-17.1	2.427	2.038	7.402	5.472
.2047	-.3230	-.1255	-11.8	-16.0	2.427	2.038	7.402	5.472
.1836	.0884	-.1125	-10.5	-14.3	2.369	1.970	7.228	5.317
.2871	-.2005	-.1759	-16.5	-22.4	2.369	1.970	7.228	5.317
.2950	-.1924	-.1669	-17.9	-26.6	2.685	2.225	8.010	5.656
.2916	-.1673	-.1650	-17.7	-25.1	2.685	2.225	8.010	5.656
.2909	-.1668	-.1645	-17.7	-25.0	2.685	2.225	8.010	5.656
.2793	-.0639	-.1580	-17.0	-24.1	2.685	2.225	8.010	5.656
.2766	-.1451	-.1666	-16.3	-23.3	1.976	2.164	4.921	5.384
.2952	-.1431	-.1710	-17.4	-23.9	1.976	2.164	4.921	5.384
.2843	-.1457	-.1686	-16.8	-23.6	1.976	2.164	4.921	5.384
.2839	-.0451	-.1644	-16.7	-23.0	1.976	2.164	4.921	5.384
.2787	-.0493	-.1615	-16.4	-22.6	1.976	2.164	4.921	5.384
.2876	-.0393	-.1673	-16.8	-23.3	2.167	2.203	5.869	5.660
.2888	-.0483	-.1654	-17.0	-23.6	2.316	2.375	5.963	5.836
.2745	-.2939	-.1588	-16.9	-22.8	1.769	1.838	4.580	4.612
.2641	-.1950	-.1527	-16.3	-22.0	1.769	1.838	4.580	4.612
.2488	-.1669	-.1493	-15.3	-21.5	1.769	1.838	4.580	4.612
.2547	-.02435	-.1127	-15.7	-16.3	1.769	1.838	4.580	4.612
.2633	-.1860	-.1540	-16.2	-22.2	1.758	1.879	4.372	4.629
.2658	-.1973	-.1569	-16.3	-22.5	1.976	1.870	5.444	4.786

results of the fully correlated calculation significantly, since in that case the calculated and experimental energies are almost the same.

The nucleon density is assumed to be a Fermi distribution (eq. (3.2.4)) except in the first calculation. The uniform nucleus calculation was put in to give an indication of its accuracy - only about 10% with the gridsize (h=0.06) used. For this reason alone it should not be used.

When the exchange is limited to the Hartree-Fock part only, the only orbitals of large normalization are those with $j = \frac{1}{2}$. In the first few calculations, therefore, we have included only these. When we include all the exchange terms, all orbitals acquire a non-negligible normalization, causing a change of about 50% to the Babushkin gauge matrix elements.

The imposition of the orthogonality constraints for orbitals of opposite κ-value by means of Lagrange multipliers increases the gauge dependence of the results by a considerable amount. This can be reduced by the inclusion of correlation.

When we try and include correlation, the question that immediately arises is, what is the correct value of Z to use? Is it the same as in the parity conserving case, or the physical value of 83, or something else?

There are three reasons for taking the first alternative. Firstly, the division of the parity mixed wavefunction into a parity conserving and a parity non-conserving part is rather artificial, and we would like to treat both parts in the same way. Secondly, increasing Z had the effect of drawing

in orbitals that would otherwise have been too diffuse to have correlated the valence orbitals to any extent; we would like to draw in the PNC orbitals in a similar way, otherwise their effects are likely to be small. Thirdly, it is found empirically that the E1 matrix element is stationary for this choice of Z.

The results of varying Z with 53 CSF lead us to take as optimal the value of Z = 84.20. This maximizes the effects of correlation on the E1 matrix elements. It is also the point at which the effects on the E2 matrix element are maximized, so we take this in preference to Z = 83.85 or Z = 84.50, at which points we had the most gauge invariant values for E2.

Use of an orthogonal core again increases the gauge dependence, which is decreased slightly when the orthogonality is extended to the correlation orbitals.

In the 155 CSF calculation, the correlation effects are again maximized at $Z \simeq 84.2$. This is the same as the preferred value for the PC calculation on all criteria other than total energies of the levels of interest. At this value we find that the best gauge invariance for the 1-2 transition occurs when we do not include the orthogonality constraints, and for the 1-3 transition when we orthogonalize the physical orbitals completely and the correlation orbitals partially.

The value of the E1 matrix element for the 1-3 transition changes drastically when we put in the final touches to the orthogonalization. It looks suspicious for two reasons: firstly, it shows a very marked gauge dependence, and secondly, it is very different from the other values.

Examination of the PNC wavefunctions whows that this is due to a violent change in the $\overline{5f}$ and $\overline{6d}$ wavefunctions. The orthogonality integrals $\langle nd|\overline{5f}\rangle$ and $\langle n\overline{f}|\overline{6d}\rangle$ are small, and so we do not include $\eta_{5\overline{f},nd}$ and $\eta_{6d,n\overline{f}}$ until a late stage. But when we do, the normalizations of $|\overline{5f}\rangle$ and $|\overline{6d}\rangle$ change from 22.80 and 7.73 to 350.0 and 315.4 respectively - values far in excess of those obtained for any other orbitals of such high angular momentum - whilst the $\langle\overline{6d}|5\overline{f}\rangle$ and $\langle 6d|\overline{5f}\rangle$ overlaps increase from -5.9 and -9.4 to -314.6 - the highest values by far obtained for orbitals with $j > \frac{1}{2}$. The other overlaps are relatively unaffected. Since configurations containing $5\overline{f}$ and 6d interact strongly with $6p^3$, this causes a large change to the E1 matrix element. The main effects are introduced by $\eta_{6d,5\overline{f}}$, with $\eta_{5d,5\overline{f}}$ making a smaller contribution.

It is not clear at this stage whether this is a real physical effect, or the manifestation of a numerical instability in the computer program. The observation may be made that, in the parity conserving case, orbitals with high angular momentum are frequently difficult or impossible to converge due to numerical instabilities; however, such orbitals also show substantial sensitivity to the precise form of the potential used (and, it should be remembered, the Lagrange multipliers enter via the exchange potential), and thus, there seems to be no a priori reason for preferring one explanation rather than the other. Since this problem was not discovered until towards the end of the time available for performing the calculations reported here, it has not been investigated further; however, it is clear that further work in this area

would be beneficial at some stage.

However, a choice must be made as to whether to take the results with or without the final orthogonalization as the preferred results. Since the normalization of the correlating PNC orbitals can be taken (very crudely) as a measure of the amount of correlation, and working on the principle of "better too little than too much" (it is perhaps worth noting that the contribution from $|5\overline{f}\rangle$ to the E1 matrix element is negligible (<<1%) in the partially orthogonalized case, and the fully orthogonalized results are approximately equal to the partially orthogonalized results (to $\sim$ 1%) if we neglect the contribution from $|5\overline{f}\rangle$); since the final normalizations are atypically large; and bearing in mind all the comments given above, it was decided to reject the fully orthogonalized value of E1. In table 8.2, therefore, we have given the normalizations of the orbitals, where the physical orbitals have been orthogonalized, but not the correlation orbitals.

The effects of correlation may be seen to be minimal - the E1 matrix element may be reduced but only by a few percent. This is in agreement with the results of Henley et al. (1977), but is more general as there are many more configurations in this work, and greater flexibility (due to the variability of Z) has been incorporated in the orbitals.

For bismuth, we put forward unshielded values of R of -15.3×10^{-8} and -21.5×10^{-8} for the 1-2 and 1-3 transitions respectively. We consider that these numbers are good to about 5%, excluding the effects of shielding.

TABLE 8.2

Orbital normalization: bismuth 155 CSF calculation

orthogonal physical orbitals, nonorthogonal correlation orbitals

1s	321.377
2s	1942.810
2p-	1939.200
2p	0.076484
3s	1075.379
3p-	1074.201
3p	0.249801
3d-	0.245259
3d	0.017563
4s	640.925
4p-	641.067
4p	0.407931
4d-	0.442429
4d	0.062205
4f-	0.090155
4f	0.021975
5s	370.880
5p-	372.738

5p	0.821710
5d-	2.89919
5d	0.466720
6s	217.718
6p-	233.598
6p	5.52946
6d-	13.8503
6d	5.98959
5f-	22.8021
5f	1.16824
7p-	530.234
7p	0.012233
7s	694.864

As described in sections 6.7 and 6.8, we take shielding into account by allowing for CI with configurations of even parity. In order to determine which configurations should be included, we first performed a series of calculations, incorporating one manifold at a time, for all manifolds which were thought likely to make a reasonable contribution and which did not contain too many configurations. The results are shown in table 8.3, where in all cases both the parity conserving and the PNC correlation orbitals were those with Z = 84.2, and parity mixed orthogonality was "incomplete for correlation orbitals" (i.e. the preferred orbitals). It can be seen that the largest contributions (bearing in mind the numbers of configurations in each) come from the manifolds $6s^26p^4$, $6s^26p^27s$, $6s^26p^26d$, $[5d]6s^26p^4$ and $6s6p^37p$ which between them yield a further 74 configurations to add to the 155 odd-parity functions used already.

A CI calculation on these 229 configurations gives rise to mixing coefficients up to 46 and a shielding contribution to the E1 matrix elements as follows:-

Transition 1-2 Coulomb gauge	.09677G
Transition 1-2 Babushkin gauge	-.07138G
Transition 1-3 Coulomb gauge	.07111G
Transition 1-3 Babushkin gauge	.08586G

The discrepancy between the Coulomb and Babushkin gauge results should not give too much cause for alarm, since the comparable results of Rose (1979) show that a CI calculation involving just a few configurations does not lead to gauge invariance, and that in this case the Coulomb gauge values are not reliable

TABLE 8.3

Shielding: Effects on Bismuth of various manifolds: CI with 155 CSF's of odd parity

Manifold	No. of CSF	Max $\lvert c_{ij} \rvert$	$E1/_G$ 1-2 Coul	1-2 Bab	1-3 Coul	1-3 Bab
$6s6p^4$	5	36	.0441	-.0373	-.1129	-.0515
$6s^26p^27s$	5	37	.0974	.0078	-.0634	.0619
$6s6p^37p$	32	15	-.0216	-.0020	.0197	.0003
$[5p]6s^26p^37s$	32	2.4	-.0052	-2×10^{-5}	.0064	2×10^{-5}
$[5s]6s^26p^4$	5	.1	-5×10^{-5}	4×10^{-7}	-4×10^{-5}	2×10^{-6}
$[4s]6s^26p^4$	5	.005	4×10^{-6}	-6×10^{-10}	6×10^{-6}	-3×10^{-8}
$6p^46d$	16	11	.0053	-.0002	.0040	-.0003
$6s^26p^26d$	16	41	.0064	-.0553	.1665	.0758
$6s6p^27s6d$	58	13	-.0033	.0008	.0059	-.0009
$6s^26d^27s$	8	2	-.0001	.0001	.0005	3×10^{-5}
$6s6p^35f$	33	6	.0003	.0006	-.0015	.0002
$6s^26p7s5f$	11	7	-.0007	8×10^{-5}	4×10^{-5}	-.0002
$6s6p^27p^2$	55	11	.0020	.0004	-.0032	.0001
$6s6p7p^3$	32	.6	2×10^{-5}	-2×10^{-6}	-4×10^{-5}	1×10^{-6}
$6s^27s7p^2$	5	2	.0002	-5×10^{-5}	-.0002	3×10^{-5}
$6s^26p7p7s$	11	10	-.0011	-.0005	.0006	-.0003
$6s^27s5f^2$	8	.2	5×10^{-6}	3×10^{-6}	1×10^{-5}	4×10^{-6}
$[5d]6s6p^47s$	58	8.6	.0005	-5×10^{-5}	-.0005	.0002
$6p^47s$	5	4	.0001	-9×10^{-5}	-.0002	-3×10^{-5}
$6p^37s7p$	32	13	-5×10^{-5}	2×10^{-8}	4×10^{-5}	-5×10^{-8}
$6s6p^27s^2$	5	6	.0003	-7×10^{-5}	-7×10^{-6}	-9×10^{-5}
$[5d]6p^6$	2	.2	-4×10^{-5}	1×10^{-6}	8×10^{-6}	-2×10^{-6}
$[5d]6p^57p$	36	.3	4×10^{-6}	-2×10^{-7}	1×10^{-5}	9×10^{-7}
$[5d]6s^26p^4$	16	9	-.0144	-.0034	.0151	.0007
$[3s]6s^26p^4$	5	.0007	-5×10^{-7}	-1×10^{-9}	3×10^{-6}	-9×10^{-10}
$[2s]6s^26p^4$	5	6×10^{-5}	7×10^{-8}	-9×10^{-12}	-1×10^{-7}	-5×10^{-11}
$[1s]6s^26p^4$	5	3×10^{-6}	2×10^{-8}	1×10^{-13}	-2×10^{-8}	-2×10^{-13}
$[4s]6s^26p^37p$	32	.013	3×10^{-5}	-5×10^{-8}	-5×10^{-5}	3×10^{-8}
$[5s]6s^26p^37p$	32	39	.0008	-2×10^{-6}	-.0002	1×10^{-6}
$6s^26p6d5f$	42	7	.0004	.0013	.0039	-.0022
$6s^26p6d7p$	36	15	.0009	-.0006	-.0022	.0012

but the Babushkin gauge values are acceptable. This preference for the Babushkin gauge, whish is adopted here, is confirmed by the choice of the length form of the matrix element by other authors; by our earlier experience of parity conserving E2 matrix elements and unshielded PNC E1 matrix elements, which showed that the Babushkin gauge results are far more stable than those in the Coulomb gauge; and by the fact that choosing the Coulomb gauge would lead, for the first transition, to shielding increasing the magnitude of the E1 matrix element , which is counter to intuition. Accordingly, the final result for the shielded E1 matrix element

Transition 1-2 .1774G

Transition 1-3 -.0634G

is obtained, whence the value for R is

Transition 1-2 $R = -10.9 \times 10^{-8}$

Transition 1-3 $R = -9.1 \times 10^{-8}$

§8.4 Thallium

The unshielded results for the thallium $6p \rightarrow 7p$ $\lambda = 292nm$ transition are presented in table 8.4. We have drawn on our experience from bismuth to reduce the number of calculations to a minimum; thus we have always taken the same value of Z for PC and PNC orbitals, and restricted this to 82.5 or 83.0. For all calculations we have used a Fermi nuclear distribution, full exchange, and MCDF mixing coefficients.

We may see at once that the Babushkin gauge results are far steadier than the Coulomb providing we keep to either MCDF or experimental energies; so we take the former to be

TABLE 8.4

The PNC calculation for thallium: no shielding

Correlation Z	No. of CSF	PM orthogonality	Energy used for E1	M1 × 10^{10} (MCDF energy)	$E1/_G$ Coul	$E1/_G$ Bab	R × 10^3 Bab
	2	no	MCDF	-1.361	-.1880	-.2420	1.668
	2	no	Expt	-1.361	-.1877	-.2023	1.394
	2	yes	MCDF	-1.361	-.1984	-.2375	1.637
	2	yes	Expt	-1.361	-.1984	-.1988	1.370
82.5	77	physical orbitals only	MCDF	-3.413	-.1503	-.2457	.6754
82.5	77	physical orbitals only	Expt	-3.413	-.1502	-.1964	.5399
82.5	77	yes	MCDF	-3.413	-.1277	-.2431	.6683
82.5	77	yes	Expt	-3.413	-.1277	-.1943	.5341
83.0	77	physical orbitals only	MCDF	-2.978	-.1420	-.2461	.7753
83.0	77	physical orbitals only	Expt	-2.978	-.1420	-.1958	.6168

more reliable. The gauge dependence is reduced when we orthogonalize the orbitals of opposite parity, but is made worse when we include correlation and worse still if we orthogonalize the correlation orbitals. Also, the use of the experimental transition energy reduces the gauge dependence, so we prefer these results.

The M1 matrix element is so variable that we are not very confident of the accuracy of the preferred result, -3.413×10^{-10}. Certainly, this seems to be much less certain than the E1 element.

We give the final unshielded result for thallium, $E1 = -1.80 \times 10^{-13}$, which we expect to be accurate to about 5%, excluding the effects of shielding. This corresponds to using the experimental transition energy.

The shielding calculation proceeds in much the same way as for bismuth. The results of allowing for CI with various even manifolds are shown in table 8.5; in this case we have taken our source of parity conserving and PNC orbitals to be the Z = 82.5 calculations, the latter being fully orthogonalized.

Again, we take the manifolds that give the largest contribution per configuration, namely

$$7s \quad 6s(6p^2+6p7p+7p^2) \quad [5d]6s^2(6p^2+6p7p+7p^2)$$
$$6s7s^2 \ (6p^2+6p7p+7p^2)7s \quad 6s7s6d$$
$$[5d]6s^2(6p+7p)5f \quad \text{and} \quad 6s6d^2$$

and perform a CI calculation on these 73 configurations along with the original 77. This gives rise to a reduction of the E1 matrix due to shielding of magnitude:

TABLE 8.5

Shielding: Effects on thallium of various manifolds: CI with 77 CSF's of odd parity

Manifold	No. of CSF's	max $\|c_{ij}\|$	$E1/_G$	
			Coul	Bab
7s	1	7.9	.0271	.0183
$6s(6p^2+6p7p+7p^2)$	12	24	-.0261	.0275
$[5p]6s^2(6p+7p)7s$	12	6.7	.0028	9×10^{-5}
$[5p]6s^2(6p+7p)6d$	22	.86	.0011	-1×10^{-5}
$[5d]6s^2(6p^2+6p7p+7p^2)$	21	105	.2198	-.0622
$[5d]6s^2(6p+7p)5f$	22	10.4	.0019	.0033
$[4f]6s^2(6p+7p)6d$	22	.18	-3×10^{-5}	1×10^{-6}
$[4f]6s^2(6p+7p)5g$	22	.0036	-2×10^{-8}	3×10^{-10}
$(6p^2+6p7p+7p^2)6d$	21	6.7	.0008	-.0001
$[5s]6s^2(6p^2+6p7p+7p^2)$	12	.10	5×10^{-5}	7×10^{-7}
6s7s6d	1	28	.0002	.0002
$6s6d^2$	3	3.6	-.0005	-.0003
6s(6p+7p)5f	2	1.1	7×10^{-7}	-2×10^{-7}
$(6p^2+6p7p+7p^2)7s$	12	52	-.0044	-.0056
$6s7s^2$	1	23.30	.0015	-.0033
$[5p]6s^27s5f$	1	1.842	4×10^{-6}	-1×10^{-9}
$[5d^2]6s6p^4$	29	.35	-1×10^{-7}	2×10^{-8}
$[5d]6s6p^27s$	18	26	-.0003	-6×10^{-5}
$[4d]6s^2(6p^2+6p7p+7p^2)$	21	.035	-1×10^{-5}	2×10^{-7}
$[5d]\ 6s7p^27s$	18	5.9	1×10^{-5}	3×10^{-6}
$[5d]6s^27s5g$	1	.64	2×10^{-7}	3×10^{-8}
$[5d]6s6p^25g$	29	.64	4×10^{-7}	-2×10^{-7}
$[5d]6s7p^25g$	29	.047	5×10^{-9}	1×10^{-9}
$[5d^2]6s^26p^27s$	29	13.80	.0005	-.0001

Coulomb gauge .0002087G

Babushkin gauge .02077G ·

and therefore the shielded value of the E1 matrix element becomes, in the Babushkin gauge,

$$E1 = -1.61 \times 10^{-13}$$

§8.5 Cesium

A calculation on the 6s → 7s transition in cesium in which we use a Fermi nucleus, full exchange, and MCDF energies and mixing coefficients, gives E1 matrix elements of -1.034×10^{-14} (Coulomb gauge) and -1.149×10^{-14} (Babushkin gauge). This calculation gave good orthogonality even when none was forced explicitly. The near equality of these numbers and our experience with other elements leads us to take the Babushkin gauge results of -1.15×10^{-14} for the unshielded matrix element.

Once again we evaluate the CI and resulting E1 matrix elements for a number of odd-parity manifolds. However, in this case there is a difference, namely that in all cases except one it is necessary to incorporate new wavefunctions to allow for the correlation orbitals. Parity conserving wavefunctions can be obtained in the usual way; however, PNC wavefunctions cannot, as mentioned in §6.8. Therefore, the latter are obtained by starting with a Slater function and then making it orthogonal - in the parity mixed sense - to all the other orbitals by a Schmidt-type orthogonalization process. Since the final E1 matrix element shows little sensitivity to the initial Slater function - provided it is of a

reasonable normalization - it is taken to be zero in all the figures given here. Table 8.6 shows the results of these calculations.

As can be seen from table 8.6, the only manifold to make any worth-while contribution is [5p](6s+7s)5d. If the value of Z used to determine the parity conserving wave-function is chosen to maximize E1 in the Babushkin gauge (the only reasonable criterion) then we obtain the shielding contribution to E1 of

$$E1 = -.0006492\ G \quad \text{Coulomb gauge}$$
$$= -.0008334\ G \quad \text{Babushkin gauge}$$

from which we derive the shileded value of E1 (in the Babushkin gauge)

$$E1 = -1.098 \times 10^{-14}.$$

§8.6 Lead

The results for the calculations on lead without shielding are shown in table 8.7, where we have again used a Fermi nucleus, MCDF mixing coefficients, and full exchange. The value of Z chosen is that which causes a stationary value of the transition energy and M1 matrix element rather than that which minimizes the total energy; this choice was made for historical reasons. They are the least satisfactory, since the E1 matrix elements show great gauge dependence and vary a great deal as the correlation orbitals are orthogonalized. Inclusion of the correlation improves the gauge dependence, but this is lost when we orthogonalize the correlation orbitals.

TABLE 8.6

Sheilding: Effects on cesium of various manifolds

Manifold	No.of CSF's	P.C correlation Z	Max $\lvert c_{ij} \rvert$	E1/G Coul	E1/G Bab
$6\overline{p}$	1	any	<.01	$<10^{-5}$	$<10^{-5}$
[4d](6s+7s)4f	8	55.5	.016	7×10^{-6}	-4×10^{-5}
[4d](6s+7s)6p	8	56.0	.012	5×10^{-5}	-1×10^{-6}
		58.0	.013	.0001	-3×10^{-6}
		59.5	.010	9×10^{-5}	-2×10^{-6}
		62.0	.004	3×10^{-5}	-8×10^{-7}
		65.0	.0005	-6×10^{-6}	-2×10^{-8}
		70.0	.003	1×10^{-6}	-3×10^{-7}
[5p](6s+7s)8s	6	68.0	.015	6×10^{-6}	-1×10^{-6}
		73.0	.019	8×10^{-6}	-5×10^{-6}
		78.0	.013	3×10^{-5}	-3×10^{-6}
[5p](6s+7s)5d	8	54.5	.43	-.0011	-.00016
		54.8	.87	-.0017	-.00047
		55.0	.50	-.0016	-.00064
		56.6	.40	-.0006	-.00083
		55.7	.94	-.0005	-.00083
		55.8	.89	-.0005	-.00082
		56.0	.31	-.0005	-.00079
[5p]($6s^2$+6s7s+$7s^2$)	5	-	.112	.0003	-5×10^{-5}
[5s](6s+7s)6p	6	57.5	.125	.0001	-6×10^{-7}

TABLE 8.7

The PNC calculation for lead: no shielding

Correlation Z	No. of CSF	PM orthogonality	Energy used for E1	$M1 \times 10^6$ (MCDF energy)	$E1/_G$ Coul	$E1/_G$ Bab	$R \times 10^7$ Bab
	5	no	MCDF	1.558	.5631	.2283	-1.40
	5	no	Expt	1.558	.5631	.2573	-1.57
	5	yes	MCDF	1.558	.4296	.2205	1.35
	5	yes	Expt	1.558	.4296	.2485	1.52
82.85	115	no	MCDF	1.571	.5826	.2480	-1.50
82.85	115	no	Expt	1.571	.5826	.2758	-1.67
82.85	115	physical orbitals only	MCDF	1.571	.4500	.2401	-1.46
82.85	115	physical orbitals only	Expt	1.571	.4500	.2670	-1.62
82.85	115	yes	MCDF	1.571	1.0474	.1234	-.748
82.85	115	yes	Expt	1.571	1.0474	.1372	-.832

TABLE 8.8

Shielding: effects on lead of various manifolds:

CI with 115 CSF's of even parity

Configuration	No. of CSF	Max $\lvert c_{ij} \rvert$	E1 Coul	E1 Bab
$[6s]6p^3$	1	43.81	-.2953	-.0446
$[6s]6p^2 7p$	20	52.1	-.0307	-.0043
6p7s	3	196	1.0385	-.1213
6p6d	4	39	.1429	-.0362
$[5d]6p^3$	13	8.7	-.0548	-.0031
$[6s^2]6p^3 6d$	13	5.4	.0057	.0004
$[6s]6p6d7s$	15	17.9	-.0064	.0005
$[6s]6p6d^2$	25	7.6	.0046	.0006
$[6s^2]6p^3 7s$	5	19.6	.0021	.0004
$[5d\ 6s^2]6p^5$	4	.73	-4×10^{-5}	-5×10^{-6}
6d7p	4	2.6	.0002	.0002
6d5f	4	8.2	.0015	.0009
$[4f]6d^3$	32	.025	1×10^{-6}	-7×10^{-9}
$[6s]6p7p^2$	20	5.9	.0006	-6×10^{-5}
$[6s]7p^3$	5	.93	4×10^{-5}	1×10^{-6}
7s7p	3	27.80	.0006	.0006
$[6s]6p5f^2$	25	1.707	.0001	7×10^{-6}
5f5g	4	.34	9×10^{-6}	8×10^{-6}
$[5d]6p^2 7p$	47	8.06	-.0083	-.0024
$[5d]6p7p^2$	47	1.67	.0004	-2×10^{-6}
$[6s]6p7s^2$	3	9.5	-.0010	.0001
$[5d]6p7s^2$	4	2.007	1×10^{-5}	4×10^{-6}
$[4f]6p^2 7s$	9	.017	-2×10^{-7}	-4×10^{-10}
$[5p]6p^2 7s$	20	8.704	-.0020	-.0001

The extreme variation of the matrix elements may be traced to instabilities in the $\overline{7s}$ and $\overline{7\bar{p}}$ wavefunctions, whose normalizations increase by a factor of 20 when the Lagrange multipliers are included. Since the main contribution from the correlation orbitals comes from these two orbitals, the results are unstable. The instability of the $\overline{n\bar{p}}$ orbitals has already been dealt with in §6.5; the instability of the $\overline{7s}$ is a consequence of the linking of the $\overline{7s}$ and $\overline{7\bar{p}}$ orbitals by the Lagrange multiplier $\eta_{7s7\bar{p}}$.

We note also that the E1 matrix elements calculated with experimental energies are more stable than those with MCDF energies, so we prefer the former. This is in accord with the procedure for thallium.

In view of the above considerations, we give an unshielded value of $R = -1.62 \times 10^{-7}$.

A series of CI and oscillator strengths calculations were carried out once again to determine the most important configurations contributing to the shielding effects on this value. The results, using non-orthogonal PNC correlation orbitals, are shown in table 8.8, and lead us to take the manifolds

$$[6s]6p^3 \quad 6p7s \quad 6p6d \quad [6s]6p^2 7p \quad [5d]6p^3$$
$$6d5f \quad 7s7p \quad [6s^2]6p^3 7s$$

which together contain 53 configurations.

When the final 168-CSF CI calculation is performed, the result obtained for the shielding effects on lead (using the MCDF energy) is

E1 = .7906G Coulomb gauge

-.1836G Babushkin gauge

A smaller result is obtained for the shielding if we PM-Schmidt orthogonalize the orbitals:-

E1 = -.3351G Coulomb gauge

-.0724G Babushkin gauge

PM-orthogonalization also reduces the unshielded value of the E1 matrix element by

.0003G Coulomb gauge

.0037G Babushkin gauge.

If we assume that the shielding effect scales with energy in the same way as the unshielded E1 matrix element, then we obtain for the shielded E1 matrix element, using experimental energies and PM-Schmidt orthogonalized wavefunctions, in the Babushkin gauge

E1 = .1824G

whence

$$R = -1.106 \times 10^{-7}.$$

Chapter 9

It is more important to have beauty in one's equations than to have them fit experiment.

Dirac

Conclusions

CHAPTER 9

CONCLUSIONS

§9.1 Novel features of these calculations

The single particle calculations reported in chapter 5 have revealed a number of disturbing numerical problems, all of which are associated with the use of a uniform nucleon distribution. This is hardly surprising, since the use of a grid to tabulate functions and algorithms which make assumptions about continuity and differentiability cannot be expected to cope satisfactorily with sudden changes in those functions unless the changes are taken into account explicitly (which was not done in this case). The use of a Fermi nucleus is ideal for overcoming these problems since all derivatives of the nucleon density distribution exist; however, this is the first work, as far as is known, in which it has been used in this context.

Exchange terms have been included in a fully consistent manner for the first time in this work; previous calculations have treated them - if they have treated them at all - by perturbation theory, or, in Martensson's (1981) calculations, have not included contributions from all orbitals. No other calculations published so far have included any exchange in the case of lead; we have included all the exchange terms for all atoms considered.

The problem of orthogonality of parity mixed orbitals of the opposite κ-value is one that has not been tackled properly before; here it is introduced naturally by means of Lagrange multipliers. This is the most consistent way

of doing so; certainly it is much more acceptable than Schmidt orthogonalization. However, it must be treated with care; we have shown that instabilities can arise in the use of this method.

Configuration interaction has been used to treat both correlation and shielding on a far greater scale than ever before. Unshielded results for the E1 matrix elements determined using correlated wavefunctions have been shown to be much the same as those using uncorrelated functions, providing we use the Babushkin gauge; shielding leads to substantial reductions in the PNC ratio in bismuth and lead, and smaller diminutions in thallium and cesium.

Finally, we have given the value of the E1 matrix element calculated in both Coulomb and Babushkin gauges. Previous results showed that these differed by a large amount - typically a factor of four - but we have shown that, in the unshielded case, gauge invariance can be obtained to a reasonable degree for thallium, bismuth and cesium. All results given are in the Babushkin gauge, since these show far greater stability. The present preference shown for the Babushkin gauge over the Coulomb is in accordance with that of almost all authors who have considered the problem (e.g. Commins and Bucksbaum (1980), Bouchiat (1980), Hiller et al. (1980), Fortson and Wilets (1980), Carter and Kelley (1979)).

§9.2 Comparison of results with other calculations and experime

To facilitate comparison, we have given the results of other calculations, of our calculations, and of experiment,

for each of the transitions of interest, in tables 9.1 to 9.5.

For bismuth, the present results are in broad agreement with results calculated by other authors, provided of course that we compare unshielded results with unshielded and shielded with shielded. In particular, the extent of the shielding is approximately as determined by other methods.

Comparison with experiment is more difficult, since it is difficult for a theoretician to know which of the experimental results (if any!) he should believe. Certainly the agreement between our final (shielded) results and the experimental results of Baird (1980) (λ = 648nm transition) and of Hollister et al. (1981) (λ = 876nm), which seem to be the generally preferred results, is quite striking.

For thallium, our results - provided we take the uncorrelated value of the M1 matrix element - are broadly consistent with both experiment and other calculations. Again, the magnitude of the shielding effect is in reasonable agreement with Sandars' approximate estimate of 8% (see Bouchiat (1980)).

The situation is similar for cesium, where the present results are in broad agreement with, although smaller than, other calculated results. The present calculations also give a result that is within the experimental error range. The 5% reduction due to shielding accords with the value given by Bouchiat (1980, 1983).

For lead, the present results are in good agreement with those of Novikov et al.,

TABLE 9.1

The PNC ratio for bismuth

λ=648nm $6\bar{p}^2 6p \rightarrow (6\bar{p}(6p^2)_2)_{5/2}$ transition

	R	Reference
Other calculations	-32×10^{-8}	Brimicombe et al. (1976)
	$\sim -10 \times 10^{-8}$	Moskalev (1976)
	-24×10^{-8} (U)	Novikov et al. (1976)
	-18×10^{-8} (S)	
	-12×10^{-8}	Harris et al. (1978)
	-15×10^{-8}	Loving (1978)
	-23×10^{-8} (L)	Carter and Kelly (1979)
	-3×10^{-8} (V)	
	-38×10^{-8} (U)(B)	Rose (1979)
	-160×10^{-8} (U)(C)	
	-27×10^{-8} (G)(U)(B)	
	-13×10^{-8} (G)(S)(B)	
	-11.1×10^{-8}	Martensson et al. (1981)
These calculations	-21.5×10^{-8} (U)	This work
	-9.1×10^{-8} (S)	
Experiment	$(\sim 5 \pm 5) \times 10^{-8}$	Baird et al. (1976)
	$(+2.7 \pm 1.7) \times 10^{-8}$	Baird et al. (1977)
	$(-20 \pm 5) \times 10^{-8}$	Barkov and Zolotorev (1978a) Barkov et al. (1979)
	$(-25 \pm 5) \times 10^{-8}$	Barkov and Zolotorev (1978b)
	$(-10.7 \pm 1.5) \times 10^{-8}$	Baird (1980)
	$(-0.22 \pm 1.0) \times 10^{-8}$	Bogdanov et al. (1980a)
	$(+0.4 \pm 2) \times 10^{-8}$	Bogdanov et al. (1980b)

The symbols (U) etc. are explained after table 9.5.

TABLE 9.2

The PNC ratio for bismuth

λ=876nm $6\bar{p}^2 6p \rightarrow (6\bar{p}(6p^2)_2^{\cdot})_{3/2}$ transition

	R	Reference
Other calculations	-24×10^{-8}	Brimicombe et al. (1976)
	-28×10^{-8}	Henley and Wilets (1976)
	$\sim -10 \times 10^{-8}$	Moskalev (1976)
	-18×10^{-8} (U)	Novikov et al. (1976)
	-14×10^{-8} (S)	
	-9×10^{-8}	Harris et al. (1978)
	-13×10^{-8}	Loving (1978)
	-17×10^{-8} (L)	Carter and Kelly (1979)
	-14×10^{-8} (V)	
	-15×10^{-8} (U)(B)	Rose (1979)
	-77×10^{-8} (U)(C)	
	-13×10^{-8} (G)(U)(B)	
	-6×10^{-8} (G)(S)(B)	
	-8.3×10^{-8}	Martensson et al. (1981)
These Calculations	-15.3×10^{-8} (U)	This work
	-10.9×10^{-8} (S)	
Experiment	$(-0.7 \pm 3.2) \times 10^{-8}$	Lewis et al. (1977)
	$(+0.2 \pm 1.5) \times 10^{-8}$	Fortson (1978)
	$(-10.4 \pm 1.7) \times 10^{-8}$	Hollister et al. (1981)

The symbols (U) etc. are explained after table 9.5

TABLE 9.3

The PNC ratio for thallium

λ=293nm $6\bar{p} \rightarrow 7\bar{p}$ transition

	R	Reference
Other calculations	1.0×10^{-3}	Bouchiat & Bouchiat (1975)
	1.2×10^{-3}	Sushkov et al. (1976)
	1.5×10^{-3}	Chu et al. (1977)
	1.1×10^{-3}	Neuffer & Commins (1977)
	1.11×10^{-3} (L)(A)	Bardsley & Norcross (1980)
	1.00×10^{-3} (M)(E)	
	1.06×10^{-3} (M)(T)	
	1.46×10^{-3} (L)(F)	
	1.5×10^{-3}	Kelly & Carter (1980)
	0.89×10^{-3}	Das (1981),Das et al.(1982)
These calculations	-1.80×10^{-13}/M1 (U)(X)	This work
	-1.61×10^{-13}/M1 (S)(X)	
	1.46×10^{-3} †(U)(A)	
	1.30×10^{-3} †(S)(A)	
Experiment	$(2.6 \pm 1.2)\ 10^{-3}$	Conti et al. (1979)
	$(1.4 \pm 0.5)\ 10^{-3}$	Bucksbaum et al. (1981a,b)

The symbols (U) etc. are explained after table 9.5

TABLE 9.4

The PNC ratio for cesium

λ=540nm 6s→7s transition

	R		Reference
Other calculations	$\sim 10^{-4}$		Bouchiat & Bouchiat (1974)
	-2.0×10^{-14}/M1	(X)	Bouchiat & Bouchiat (1975)
	$\sim 10^{-4}$		Khriplovich (1975)
	-2.44×10^{-14}/M1	(X)	Loving & Sandars (1975)
	$\sim 10^{-4}$		Moskalev (1976)
	-6.5×10^{-5}		Neuffer & Commins (1977b)
	-1.72×10^{-14}/M1	(P)(U)(X)	Bouchiat (1980), Bouchiat et al. (1983)
	-1.58×10^{-14}/M1	(P)(S)(X)	
	-1.58×10^{-14}/M1	(N)(U)(X)	
	-1.47×10^{-14}/M1	(N)(U)(X)	
	-1.60×10^{-14}/M1	(X)	Das (1981)
These calculations	-1.15×10^{-14}/M1	(U)	This Work
	-1.10×10^{-14}/M1	(S)	
Experiment	$(5.6 \pm 18) \times 10^{-4}$		Bouchiat & Pottier (1977)
	$(-1.07 \pm .26) \times 10^{-14}$/M1	(X)	Bouchiat et al. (1982)

The symbols (U) etc. are explained after table 9.5.

Bouchiat et al. (Phys. Lett. 134B 463 (1984)) have just published a revised experimental value for E1 = $(-1.25 \pm .21) \times 10^{-14}$

TABLE 9.5

The PNC ratio for lead:

λ=1279nm $6p^2\,^3P_0 \rightarrow 6p^2\,^3P_1$ transition

	R	Reference
Other calculations	$\sim 4 \times 10^{-8}$	Bouchiat & Bouchiat (1974)
	$\sim 10^{-7}$	Moskalev (1976)
	-1.4×10^{-7}	Novikov et al. (1976)
These calculations	-1.62×10^{-7} (U)	This work
	-1.11×10^{-7} (S)	
Experiment	$-9.9 \pm 2.5 \times 10^{-8}$	Emmons et al. (1983)

The symbols (U) etc. are explained on the next page.

NOTES ON TABLES 9.1 to 9.5

(A) Assuming M1 = -2.11×10^{-5} μ_B (standard definition of M1) (experimental value)

(B) Babushkin gauge for E1.

(C) Coulomb gauge for E1.

(E) Using experimental energy.

(F) Using calculated value of M1.

(G) Values derived from mixing coefficients chosen to give correct G-factors.

(L) Length form for E1.

(M) Using matrix elements of α for E1.

(N) Norcross potential.

(P) Stone potential.

(S) Screened values.

(T) Using theoretical energy.

(U) Unscreened values.

(V) Velocity form for E1.

(X) The M1 matrix element must be given as a reduced matrix element of the operator used in chapter 2.

the only other results that make any claim to be accurate; and they are also in excellent agreement with the experimental value (this was published too recently to be discussed elsewhere in this thesis). They show that shielding is important, although less so than in bismuth, giving a 30% reduction in the E1 matrix element.

§9.3 Deficiencies of the present calculations

Possibly the major problem left unsolved by this investigation is that of the instability of some of the PNC orbitals. The reason for this is not fully understood at present. Fortunately, the orbitals affected are those with $j > \frac{1}{2}$ and hence with relatively small normalizations (before the instability sets in), and so it is hoped that the practice of fixing them at zero or their pre-instability values will not lead to great inaccuracies.

Another important problem highlighted by the present investigation is that of calculating M1 matrix elements in cesium and, to a lesser extent, in thallium. This problem has been known for some time (Fortson and Wilets (1980)).

The lack of gauge invariance in the final, shielded results for bismuth and lead, the atoms in which shielding is important, is disappointing, especially in view of the generally good gauge invariance obtained when shielding was omitted. As discussed elsewhere, gauge invariance does not guarantee correctness, although observable quantities must have this property. Thus the lack of gauge invariance must cast a cloud over the quality of the results.

Finally, the Lagrange multipliers (both parity conserving and parity non-conserving varieties) have not been calculated *ab initio* in all cases, as would have been liked, because of the problems discussed in section 8.2.

§9.4 Suggestions for further work

To state a problem is to suggest a field for further work. Thus, one question that needs to be answered is why some of the PNC orbitals are unstable. Perhaps there are problems associated with the component of $|n\text{-}\kappa\rangle$ in $|\overline{n_\kappa}\rangle$, as is the case for $|\overline{np}\rangle$. If so, the overlap $\langle n\text{-}\kappa|\overline{n\kappa}\rangle$ can be constrained suitably, in the same way as the $\langle ns|\overline{np}\rangle$ overlap was constrained. Otherwise - or if this alone is not enough - it may turn out to be impracticable to solve the MCDF-PNC equations numerically, in which case one of the basis set expansion schemes described in appendix 2 may prove a suitable alternative.

The reason for the instability of the M1 matrix elements for cesium and thallium is better understood. The problem here is that, if $\frac{\omega}{c} \ll 1$ (a reasonable approximation: $\frac{\omega}{c} \sim 10^{-3}$) then

$$\langle a||M1||b\rangle = (\text{angular factors}) \times \int_o^\infty (P_a P_b + Q_a Q_b)(1+0(\frac{\omega^2}{c^2})) \quad (9.4.1)$$

and, in the case of cesium, a = 6s and b = 7s, but

$$\int_o^\infty (P_{6s} P_{7s} + Q_{6s} Q_{7s}) = 0 \quad (9.4.2)$$

This means that we are calculating a very small quantity which may easily be swamped by errors in the orthogonality integral, a behaviour not allowed for in a general purpose computer program. This difficulty could be overcome in a relatively straightforward fashion by subtracting off the leading 1 from the series expansion in powers of $\frac{\omega}{c}$.

The gauge invariance, although good in many cases, is not perfect, particularly in the case of shielded matrix elements. As suggested in section 8.3, this is thought to be due to an inadequate basis of configurations. Since the main contributions to the E1 matrix elements are from the $j = \frac{1}{2}$ orbitals, due to the huge normalization factors associated with them, the gauge dependence may well be reduced by allowing for interaction with more configurations containing such orbitals. The amount of mixing with these will almost certainly be small, and so will not greatly effect the transition energies or parity conserving matrix elements, but should have a far greater effect on the E1 PNC matrix element. The effect of allowing for interaction with manifolds like those already used but with $ns \rightarrow (n+1)s$ or $n\bar{p} \rightarrow (n+1)\bar{p}$ should be investigated, possibly also including the effect that these have on the PNC E1 matrix elements as a criterion for their importance - an effect not used as a criterion for the selection of parity conserving CSF's, and have the correlation orbitals, so far. Since the extra correlation orbitals introduced in this way will be naturally even more diffuse than the correlation orbitals introduced so far, it will probably be necessary to artificially contract them (by increasing Z) still further. Indeed, there is no need to restrict ourselves to bound state orbitals; continuum-type orbitals, or even pseudo-orbitals which have no physical meaning, could be considered for use in the configurations which are to be added to the basis sets.

As described in section 8.2, work is under way to improve the method used to calculate the parity conserving Lagrange

multipliers. This should allow them to be calculated in a relatively simple way that should be free of the instabilities that accompany their evaluation at present, since they will be determined by an essentially non-iterative method; furthermore, no extra problems should arise due to one of the orbitals being fixed, or both orbitals having equal occupations, or orbitals having very small occupations.

The application of the method to PNC Lagrange multipliers is not expected to present any problems.

The suggestions given so far point to an important feature of any further work on calculating optical activity in heavy atoms: any improvements are as likely to come from an improved understanding of the parity conserving aspects of the problem as of its parity violating aspects. Indeed, for heavy atoms, it would appear that the PNC side of atomic physics is as well understood as the conventional, parity conserving, side. This is in spite of the advances in atomic theory made over the last two years or so, since these have been mainly confined to atoms with only a few electrons (see the recent series of articles by Hata and Grant in J.Phys.B. and the references given by them). However, corresponding advances in heavy atoms can be hoped for in the not too distant future, particularly since recent modifications to the MCDF package of programs should enable it to operate an order of magnitude faster, whilst bigger modern computers that have become available of late allow much larger programs, and hence a substantial increase in the number of configurations and orbitals that can be used. Perhaps it would be a good idea to get a really good theoretical description of the parity conserving problem in heavy atoms - including

correlation - as a pre-requisite for tackling the PNC problem.

A different approach to the problem of correlation from that used in this thesis might be to use Slater functions for the correlation orbitals; in this case, the time-consuming business of calculating the extra orbitals variationally could be avoided. However, there then arises the question of what value of Z to use when generating the PNC wavefunctions. If the PNC wavefunctions are also determined by means of Slater functions, an approach such as that of appendix 2 will be necessary. The use of Slater functions in the shielding calculations is simple - indeed this was done in the shielding calculation for cesium presented in this thesis.

Alternatively, we could try to get the best possible orbitals by performing "extended optimal level" (EOL) calculations. These are a generalization of the optimal level technique described in §2.2, in which more than one level is optimized simultaneously, in the present case the upper and lower levels of the transitions of interest. At present there is a fault in the published MCDF program which causes all such calculations to fail, but when it is fixed, it could be a good thing to try some such runs, provided that they will converge. A further advantage of this is that we will not have to fix the physical orbitals or raise the value of Z for the correlation orbitals.

All the results in this thesis have been obtained using eigenvalues and eigenvectors of the Hamiltonian matrix without the Breit interaction being included, because Breit calculations on complex systems were very timeconsuming at the time that most of the work reported here was carried out; however,

with improvements to the Breit package, such calculations should now be practicable. In most cases, we do not expect the use of Breit eigenvalues and eigenvectors to make much difference, the exceptions being M1 matrix elements in cesium and thallium where the Breit interaction is known to introduce substantial effects (Neuffer and Commins (1977a,1977b)). However, it would be useful to know for certain.

Finally, the techniques developed in this thesis have not made use of the powerful methods of many body perturbation theory (MBPT). It may be possible to combine the MCDF and MBPT approaches so as to utilize the strengths of both methods and to cover their weaknesses, perhaps in a way analogous to the way that Hata and Grant (1983a) recently used the MCDF program to improve results that accounted for correlation very well but only included approximate relativistic correction This in itself would be a substantial project.

§9.5 Numerical accuracy of the calculations

At the end of a complex calculation, especially one involving the use of computers, the question inevitably arises: "Is the answer right?" It would be a very confident (or foolish) man who gave to such a question, as answer, an unqualified "Yes".

As associated question that also arises is "How accurate are the results?" In what follows we shall be mainly concerned with the numerical accuracy of the results; inaccuracies introduced by the model used are much more difficult to assess quantitatively. We shall discuss the accuracy of the results with reference to a number of tests.

§9.5.1 Test 1: dependence on gridsize and inner integration point

As stated in §2.5, we calculate the wavefunctions at points on a logarithmic grid

$$r_i = r_o \, e^{h(i-1)} \qquad (9.5.1)$$

where r_o and h are the inner integration point and gridsize respectively. For the calculations reported in this thesis the values used are 10^{-7} and 0.06 respectively, but clearly any figure finally quoted should be independent of these to a reasonable extent.

We have performed a series of calculations on the bismuth $6p^3$ manifold (5 CSF) problem, where parity mixed orthogonality has not been constrained by means of Lagrange multipliers. The results are given in table 9.6, and are most encouraging. They indicate that the figures quoted in chapter 8 have four-figure numerical accuracy.

Incidentally, the dependence on h and r_o of these results is far less than that of the single-particle results discussed in chapter 5. This is due to the use of a Fermi nucleon distribution.

§9.5.2 Test 2: orthogonality

If $\kappa_a = -\kappa_b$ and the orbitals a and b are full, then we should have $\langle \bar{a}|b\rangle = \langle a|\bar{b}\rangle$, no matter what Lagrange multipliers are used.

In table 9.7, we give results for $\langle \bar{a}|b\rangle$ and $\langle \bar{a}|b\rangle - \langle a|\bar{b}\rangle$ for the full orbitals, again in the bismuth $6p^3$ manifold cal-

TABLE 9.6

Dependence of results on h and r_o: bismuth 5 CSF calculation

no shielding or orthogonality

h	r_o (a.u)	overlaps	E1 (a.u.)			
			1-2 transition		1-3 transition	
			Coul.	Bab.	Coul.	Bab.
.06	10^{-5}	(2)	.2592	.2910	-.1659	-.1646
		(1)	.2593	.2906	-.1667	-.1644
.06	10^{-6}	(2)	.2594	.2909	-.1663	-.1646
		(1)	not expected to be significantly different from the figures below.			
.06	10^{-7}	-	.2595	.2909	-.1668	-.1645
.08	10^{-7}	(2)	.2593	.2909	-.1666	-.1645
		(1)	.2593	.2909	-.1666	-.1645
.10	10^{-7}	(2)	.2590	.2909	-.1668	-.1645
		(1)	.2589	.2911	-.1665	-.1647

The overlaps referred to above are the values of $\langle ns|\overline{np}\rangle$, which either may be redetermined (1) or values given in Table A6.1 may be retained (2).

Table 9.7

Orthogonality of full orbitals in bismuth

a	b	$\langle\bar{a}\|b\rangle$	$\langle\bar{a}\|b\rangle-\langle a\|\bar{b}\rangle$	Ratio
1s	2p-	43.96	6.201×10^{-8}	1.411×10^{-9}
1s	3p-	19.36	8.869×10^{-9}	4.581×10^{-10}
1s	4p-	9.442	5.388×10^{-9}	5.706×10^{-10}
1s	5p-	4.053	-1.638×10^{-9}	4.041×10^{-10}
2s	2p-	1936.	9.152×10^{-5}	4.727×10^{-8}
2s	3p-	52.56	4.112×10^{-7}	7.823×10^{-9}
2s	4p-	21.59	6.849×10^{-8}	3.172×10^{-9}
2s	5p-	8.948	8.336×10^{-9}	9.316×10^{-10}
2p-	3s	-53.70	3.505×10^{-7}	6.527×10^{-9}
2p-	4s	-21.57	1.809×10^{-8}	8.387×10^{-10}
2p-	5s	-9.322	2.241×10^{-8}	2.404×10^{-9}
2p-	6s	-3.253	3.640×10^{-7}	1.119×10^{-7}
2p	3d-	.009552	2.185×10^{-10}	2.287×10^{-8}
2p	4d-	.005361	1.813×10^{-10}	3.382×10^{-8}
2p	5d-	.001980	1.260×10^{-8}	6.364×10^{-6}
3s	3p-	1086.	5.989×10^{-5}	5.608×10^{-8}
3s	4p-	51.06	6.080×10^{-7}	1.191×10^{-8}
3s	5p-	18.19	4.218×10^{-8}	2.319×10^{-9}
3p-	4s	-59.35	9.981×10^{-8}	1.682×10^{-9}
3p-	5s	-21.10	4.181×10^{-6}	1.982×10^{-7}
3p-	6s	-7.128	4.286×10^{-9}	6.013×10^{-8}
3p	3d-	.2177	4.000×10^{-9}	1.837×10^{-8}
3p	4d-	.03058	1.458×10^{-7}	4.768×10^{-5}
3p	5d-	.01019	1.664×10^{-10}	1.633×10^{-8}
3d-	4p	-.03762	2.551×10^{-10}	6.781×10^{-8}
3d-	5p	-.01387	8.569×10^{-11}	6.178×10^{-8}
3d	4f-	.001212	-2.171×10^{-5}	2.242×10^{-8}
4s	4p-	630.9	2.937×10^{-7}	4.655×10^{-8}
4s	5p-	43.86	5.755×10^{-6}	1.312×10^{-8}
4p-	5s	-58.78	1.477×10^{-5}	2.513×10^{-6}
4p-	6s	-16.75	7.790×10^{-8}	4.651×10^{-7}
4p	4d-	.2638	7.884×10^{-6}	2.989×10^{-4}
4p	5d-	.02705	3.497×10^{-7}	1.293×10^{-6}
4d-	5p	-.04237	3.678×10^{-10}	8.681×10^{-8}
4d	4f-	-.007288	-2.569×10^{-9}	3.525×10^{-7}
4f-	5d	.03849	-4.256×10^{-4}	1.106×10^{-7}
5s	5p-	355.0	1.056×10^{-3}	2.975×10^{-5}
5p-	6s	-54.48	4.278×10^{-4}	7.852×10^{-4}
5p	5d-	-.3258	$2.914 \times 10^{}$	$8.944 \times 10^{}$

culations, without parity mixed orthogonality being constrained by use of appropriate Lagrange multipliers. The wavefunctions were converged to one part in 10^8. It can be seen that, in general, $\langle\bar{a}|b\rangle = \langle a|\bar{b}\rangle$ to about one part in 10^7, the exceptions to this being almost entirely integrals involving the loosely bound 5d- and 6s electrons. Again, the figures are consistent with the hope that the final E1 matrix elements are accurate numerically to about four significant figures.

§9.5.3 Test 3: $\langle ns|\bar{np}\rangle$ overlaps

We have shown in section 8.2 that, if the $a = \bar{np}$ and $b = ns$ shells are full, we only include the Hartree-Fock exchange, and there are no Lagrange multipliers, then

$$\langle b|\bar{a}\rangle = \frac{\int_o^\infty \rho_N(r)\ (P_b Q_a - Q_b P_a)}{\varepsilon_b - \varepsilon_a} \qquad (9.5.2)$$

The values of $\langle b|\bar{a}\rangle$ obtained from the PNC wavefunctions can be compared with the values obtained using the above formula. The results of such a comparison, again for the 5 CSF bismuth calculation, are given in table 9.8. The comparison shows that the PNC wavefunction gives overlaps that are good to a few parts per million; and so once again the numerical accuracy of the wavefunctions is vindicated.

§9.5.4 Test 4: gauge invariance

The three previous tests have tested only the numerical accuracy of the algorithms used to solve the equations. They have indicated that the numerical accuracy of the E1 matrix

TABLE 9.8

$\langle ns|n\bar{p}\rangle$ overlaps in bismuth

n	$\langle ns\|n\bar{p}\rangle$ using eq. (9.5.2)	discrepancy between eq. (9.5.2) and using PNC wavefunctions
2	1987.18	5.59×10^{-3}
3	1088.40	1.54×10^{-3}
4	633.597	4.26×10^{-4}
5	343.543	2.23×10^{-4}
6	179.556	7.95×10^{-5}

Notes

(i) The nuclear radius used for these calculations was incorrectly set; hence the overlaps differ slightly from those given in table A6.1.

(ii) For n = 6, equation (9.5.2) does not hold in its present unmodified form, since $6\bar{p}$ is not full. The requisite modifications have been made to derive the number given above.

elements is, in general, probably good to about one part in a thousand.

The situation with gauge invariance is more complex. Some models (e.g. single-particle models, RPA, TDHF) are such that gauge invariance follows automatically; in these cases any gauge dependence is an indication of numerical inaccuracies, and not an indication of the accuracy of the model. For instance, the difference between the Coulomb and Babushkin gauge results shown in table 5.3 - typically a few parts in a million, providing the "difference corrections" are included - are numerical in origin.

However, gauge invariance is not a feature of the MCDF model. In the parity conserving case this is well-known (Grant 1974), and the fact that this is true in the PNC case as well can be seen from table 8.1, where the gauge variation is, in some cases, substantial - and, in almost all cases, far larger than can be accounted for by mere numerical inaccuracies.

Previous attempts to calculate the PNC E1 matrix element from wavefunctions obtained in a Hartree-Fock model in both Coulomb (or velocity) and Babushkin (or length) gauges (Carter and Kelley (1979), Rose (1979)) lead to results that were widely different - typically a factor of four apart. As far as the author of this thesis is aware, there are no other results obtained in a simple Hartree-Fock model that show anything like gauge invariance.

What does this gauge insensitivity mean? It does not mean that the present model necessarily is superior to other

ones, but it is an indication that it may be, and as such forms one test of the quality of the wavefunctions (Sandars (1980)). Certainly the improvement in gauge invariance when the correlation orbitals were added is a consequence of better atomic wavefunctions.

§9.5.5 The E2/M1 ratio for bismuth

An overall "feel" for the accuracy of the parity conserving wavefunctions can be obtained by comparing the ratio of the E2 and M1 transition probabilities in bismuth with those obtained experimentally (Roberts et al. (1980)), semi-empirically (Garstang (1964)) and theoretically (present work). The results are as follows:

	1-2 transition	1-3 transition
Roberts et al.		0.21 ± .02
Garstang	6.8×10^{-3}	0.25
Present	8.46×10^{-3}	0.29
Other theory (Rose (1979))	11.1×10^{-3}	0.47

The present results, although not spectacularly good, are in broad agreement with both the semi-empirical and experimental ones. Furthermore, comparison of transition probabilities effectively doubles the discrepancy between matrix elements, since the former depend on the square of the latter.

§9.5.6 G-factors

A similar comparison of Lande g-factors for bismuth may

be made. The results in this case are encouraging; they show that the CI is pulling the calculated results steadily towards the experimental values, and also that they are pulled furthest when the preferred value of Z (84.2) is used in the 155 CSF calculation.

		level 1	level 2	level 3
Experiment		$^4S_{3/2}$	$^2D_{3/2}$	$^2D_{5/2}$
Moore (1958)		1.6433	1.225	1.11
Semi-empirical				
Landman & Lurio (1970)		1.6371	1.2473	1.2005
Theoretical				
Rose (1979)		1.77	1.26	1.26
Present calculations				
5 CSF		1.757	1.124	1.200
53 CSF correlation	Z=83.85	1.737	1.152	1.200
	Z=84.2	1.722	1.162	1.201
	Z=84.5	1.721	1.165	1.201
155 CSF correlation	Z=84.0	1.710	1.171	1.200
	Z=84.2	1.705	1.175	1.200
	Z=84.5	1.708	1.173	1.200

§9.5.7 Conclusions

It is notoriously difficult to specify the accuracy of a complex numerical calculation; extra sources of error have the tendency to appear - for instance, shielding that was neglected in the earlier calculations. However, the preceding arguments - and a certain amount of "feeling" - lead us to suggest that the present results are probably accurate to

about 10% or so; possibly in lead the accuracy is a little worse due to the problems encountered during the orthogonalization process.

§9.6 Final remarks

This thesis has described the self-consistent theory of the parity non-conserving interaction in atoms, in which shielding, exchange and orthogonality are taken into account rigorously; and has applied it to the atoms of experimental interest, to produce answers with remarkably little gauge dependence; and the folly of using a uniform nucleon distribution has been exposed.

It is hoped that this work has deepended our understanding of parity non-conservation in atoms.

Appendix 1

It does not do to leave a live dragon out of your calculations.

Tolkien (1937)

Detailed Derivation of the Parity Mixed Energy Functional

APPENDIX 1

DETAILED DERIVATION OF THE PARITY MIXED ENERGY FUNCTIONAL

The energy functional with which we wish to work is defined in equation (6.2.7) as

$$\Gamma = \boldsymbol{H}^{PM} + \sum_{\alpha} \bar{q}_{\alpha}\varepsilon_{\alpha} \langle\psi_{\alpha}^{PM}|\psi_{\alpha}^{PM}\rangle + \sum_{\substack{\alpha\beta \\ \alpha\neq\beta}} \varepsilon_{\alpha\beta} \langle\psi_{\alpha}^{PM}|\psi_{\beta}^{PM}\rangle \qquad (A1.1)$$

where, combining equations (6.2.1) and (6.2.2),

$$\boldsymbol{H}^{PM} = \sum_{r=1}^{N_c} \langle\Phi_r{}^{PM}|H^{PM}|\Phi_r^{PM}\rangle\, c_r{}^2 \qquad (A1.2)$$

We first evaluate the second and third terms on the right hand side of equation (A1.1):

$$\begin{aligned}
\langle\psi_{\alpha}^{PM}|\psi_{\beta}^{PM}\rangle &= \langle\psi_{\alpha}+iG\bar{\psi}_{\alpha}|\psi_{\beta}+iG\bar{\psi}_{\beta}\rangle \\
&= \langle\psi_{\alpha}|\psi_{\beta}\rangle + iG\langle\psi_{\alpha}|\bar{\psi}_{\beta}\rangle - iG\langle\bar{\psi}_{\alpha}|\psi_{\beta}\rangle \\
&\quad + G^2\langle\bar{\psi}_{\alpha}|\bar{\psi}_{\beta}\rangle \\
&= \delta_{\kappa_{\alpha},\kappa_{\beta}}\left\{\int_0^{\infty}(P_{\alpha}P_{\beta}+Q_{\alpha}Q_{\beta})dr + G^2\int_0^{\infty}(\bar{P}_{\alpha}\bar{P}_{\beta}+\bar{Q}_{\alpha}\bar{Q}_{\beta})dr\right\} \\
&\quad + iG\delta_{\kappa_{\alpha},-\kappa_{\beta}}\left\{\int_0^{\infty}(P_{\alpha}\bar{P}_{\beta}+Q_{\alpha}\bar{Q}_{\beta})dr - \int_0^{\infty}(\bar{P}_{\alpha}P_{\beta}+\bar{Q}_{\alpha}Q_{\beta})\right\}
\end{aligned} \qquad (A1.3)$$

We observe that the above expression has two different forms depending on the relative values of κ_{α} and κ_{β}. It therefore seems a good idea to write

$$\sum_{\substack{\alpha\beta \\ \alpha\neq\beta}} \varepsilon_{\alpha\beta} \langle \psi_\alpha^{PM} | \psi_\beta^{PM} \rangle = \sum_{\substack{\alpha\beta \\ \kappa_\alpha = \kappa_\beta \\ \alpha\neq\beta}} \varepsilon_{\alpha\beta} \langle \psi_\alpha^{PM} | \psi_\beta^{PM} \rangle + \sum_{\substack{\alpha\beta \\ \kappa_\alpha = -\kappa_\beta}} \varepsilon_{\alpha\beta} \langle \psi_\alpha^{PM} | \psi_\beta^{PM} \rangle \qquad \text{(A1.4)}$$

Considering only the first term for the moment, we exploit the fact that, from (A1.3),

$$\langle \psi_\alpha^{PM} | \psi_\beta^{PM} \rangle = \langle \psi_\beta^{PM} | \psi_\alpha^{PM} \rangle \quad \text{if } \kappa_\alpha = \kappa_\beta$$

to write it in the form

$$\sum_{\substack{\alpha\beta \\ \kappa_\alpha = \kappa_\beta \\ \alpha<\beta}} (\varepsilon_{\alpha\beta} + \varepsilon_{\beta\alpha}) \langle \psi_\alpha^{PM} | \psi_\beta^{PM} \rangle$$

$$= \sum_{\substack{\alpha\beta \\ \kappa_\alpha = \kappa_\beta \\ \alpha<\beta}} (\varepsilon'_{\alpha\beta} + \varepsilon'_{\beta\alpha}) \langle \psi_\alpha^{PM} | \psi_\beta^{PM} \rangle$$

$$= \sum_{\substack{\alpha\beta \\ \kappa_\alpha = \kappa_\beta \\ \alpha\neq\beta}} \varepsilon'_{\alpha\beta} \langle \psi_\alpha^{PM} | \psi_\beta^{PM} \rangle$$

where $\varepsilon'_{\alpha\beta} = \frac{1}{2}(\varepsilon_{\alpha\beta} + \varepsilon_{\beta\alpha}) = \varepsilon'_{\beta\alpha}$

Therefore we may assume without loss of generality that

$$\varepsilon_{\alpha\beta} = \varepsilon_{\beta\alpha} \quad (\kappa_\alpha = \kappa_\beta) \qquad \text{(A1.5a)}$$

Considering now the second term, we obtain in the same way that

$$\langle \psi_\alpha^{PM} | \psi_\beta^{PM} \rangle = -\langle \psi_\beta^{PM} | \psi_\alpha^{PM} \rangle \quad \text{if } \kappa_\alpha = -\kappa_\beta$$

and hence it may be written as

$$\sum_{\substack{\alpha\beta \\ \kappa_\alpha = -\kappa_\beta}} \varepsilon'_{\alpha\beta} \langle \psi_\alpha^{PM} | \psi_\beta^{PM} \rangle$$

where

$$\varepsilon'_{\alpha\beta} = \tfrac{1}{2}(\varepsilon_{\alpha\beta} - \varepsilon_{\beta\alpha}) = -\varepsilon'_{\beta\alpha}$$

and so, without loss of generality, we may assume that

$$\varepsilon_{\alpha\beta} = -\varepsilon_{\beta\alpha} \qquad (\kappa_\alpha = -\kappa_\beta) \tag{A1.5b}$$

We next turn our attention to the evaluation of $\boldsymbol{H}^{PM}$. We use the equations (6.2.8) to (6.2.10) to write

$$\begin{aligned}
\langle \Phi_r^{PM} | H^{PM} | \Phi_r^{PM} \rangle &= \langle \Phi_r^{PM} | \sum_{i=1}^{N} h(i) | \Phi_r^{PM} \rangle \\
&\quad + G \ \langle \Phi_r^{PM} | \sum_{i=1}^{N} v_i^{PNC} | \Phi_r^{PM} \rangle \\
&\quad + \langle \Phi_r^{PM} | \sum_{1 \leq i < j \leq N} 1/r_{ij} | \Phi_r^{PM} \rangle \\
&= \sum_a q_r(a) \ \langle \psi_a^{PM} | h | \psi_a^{PM} \rangle \\
&\quad + G \sum_a q_r(a) \ \langle \psi_a^{PM} | v^{PNC} | \psi_a^{PM} \rangle \\
&\quad + \langle \Phi_r^{PM} | \sum_{1 \leq i < j \leq N} 1/r_{ij} | \Phi_r^{PM} \rangle
\end{aligned} \tag{A1.6}$$

Calculating each of these terms in turn we find that

$$\langle\psi_a^{PM}|h|\psi_a^{PM}\rangle=\langle\psi_a|h|\psi_a\rangle+G^2\langle\bar{\psi}_a|h|\bar{\psi}_a\rangle$$

$$=\int_o^\infty dr\left\{cQ_a\left(\frac{d}{dr}+\frac{\kappa_a}{r}\right)P_a-cP_a\left(\frac{d}{dr}-\frac{\kappa_a}{r}\right)Q_a-2c^2Q_a{}^2-\frac{Z_N}{r}(P_a{}^2+Q_a{}^2)\right\}$$

$$+G^2\int_o^\infty dr\left\{cQ_a\left(\frac{d}{dr}-\frac{\kappa_a}{r}\right)\bar{P}_a-c\bar{P}_a\left(\frac{d}{dr}+\frac{\kappa_a}{r}\right)\bar{Q}_a-2c^2\bar{Q}_a{}^2-\frac{Z_N}{r}(\bar{P}_a{}^2+\bar{Q}_a{}^2)\right\} \tag{A1.7}$$

$$\langle\psi_a^{PM}|v^{PNC}|\psi_a^{PM}\rangle=\langle\psi_a|v^{PNC}|iG\bar{\psi}_a\rangle+\langle iG\bar{\psi}_a|v^{PNC}|\psi_a\rangle$$

$$=iG.i\int_o^\infty\rho\{P_a\bar{Q}_a-Q_a\bar{P}_a\}dr-iG.i\int_o^\infty\rho\{\bar{P}_aQ_a-\bar{Q}_aP_a\}dr$$

$$=-2G\int_o^\infty\rho\{P_a\bar{Q}_a-Q_a\bar{P}_a\}dr \tag{A1.8}$$

To calculate the third term in equation (A1.6) is more difficult. To do so we must go back to the basic definition of an MCP coefficient (Grant (1973)). There we find that

$$\langle TM|\sum_{i<j}1/r_{ij}|T'M'\rangle=\delta_{MM'}\sum_{\substack{\alpha_1\beta_1\\ \alpha_2\beta_2}}\left\{\gamma^k_{TT'}(\alpha_1\beta_1\alpha_2\beta_2)X^k(\alpha_a\beta_1\alpha_2\beta_2)\right.$$

$$\left.+\Xi^k_{TT'}(\alpha_1\beta_1\beta_2\alpha_2)X^k(\alpha_1\beta_1\beta_2\alpha_2)\right\} \tag{A1.9}$$

where $\gamma_{TT'}(\alpha_1\beta_1\alpha_2\beta_2)$ and $\Xi_{TT'}(\alpha_1\beta_1\beta_2\alpha_2)$ are angular factors dependent only on j and m values and occupation numbers and not on any parity considerations, and

$$X^k(\alpha\beta\gamma\delta)=\langle\alpha||C^k||\gamma\rangle\langle\beta||C^k||\delta\rangle R^k(\alpha\beta\gamma\delta) \tag{A1.10}$$

R^k is as defined in equation (2.2.19)

It is now clear how this is to be generalized to the parity mixed case. The quantities $\gamma^k_{TT'}(\alpha_1\beta_1\alpha_2\beta_2)$ and $\Xi^k_{TT'}(\alpha_1\beta_1\beta_2\alpha_2)$

remain unchanged, while $X^k(\alpha\beta\gamma\delta)$ is replaced by

$$X^k(\alpha\,\underline{PM}_\beta PM_\gamma PM_\delta PM) = \langle\alpha\|\, C^k \,\|\gamma\rangle\langle\beta\|\, C^k \,\|\delta\rangle R^k(\alpha\beta\gamma\delta)$$

$$-G\Big\{+i\langle\bar{\alpha}\|\, C^k \,\|\gamma\rangle\langle\beta\|\, C^k \,\|\delta\rangle R^k(\bar{\alpha}\beta\gamma\delta)$$

$$+i\langle\alpha\|\, C^k \,\|\gamma\rangle\langle\bar{\beta}\|\, C^k \,\|\delta\rangle R^k(\alpha\bar{\beta}\gamma\delta)$$

$$-i\langle\alpha\|\, C^k \,\|\bar{\gamma}\rangle\langle\beta\|\, C^k \,\|\delta\rangle R^k(\alpha\beta\bar{\gamma}\delta)$$

$$-i\langle\alpha\|\, C^k \,\|\gamma\rangle\langle\beta\|\, C^k \,\|\bar{\delta}\rangle R^k(\alpha\beta\gamma\bar{\delta})\Big\}$$

$$+\,G^2\Big\{+\langle\bar{\alpha}\|\, C^k \,\|\bar{\gamma}\rangle\langle\beta\|\, C^k \,\|\delta\rangle R^k(\bar{\alpha}\beta\bar{\gamma}\delta)$$

$$+\langle\alpha\|\, C^k \,\|\gamma\rangle\langle\bar{\beta}\|\, C^k \,\|\bar{\delta}\rangle R^k(\alpha\bar{\beta}\gamma\bar{\delta})$$

$$-\langle\bar{\alpha}\|\, C^k \,\|\gamma\rangle\langle\bar{\beta}\|\, C^k \,\|\delta\rangle R^k(\overline{\alpha\beta}\gamma\delta)$$

$$+\langle\alpha\|\, C^k \,\|\bar{\gamma}\rangle\langle\bar{\beta}\|\, C^k \,\|\delta\rangle R^k(\alpha\overline{\beta\gamma}\delta)$$

$$+\langle\bar{\alpha}\|\, C^k \,\|\gamma\rangle\langle\beta\|\, C^k \,\|\bar{\delta}\rangle R^k(\bar{\alpha}\beta\gamma\bar{\delta})$$

$$-\langle\alpha\|\, C^k \,\|\bar{\gamma}\rangle\langle\beta\|\, C^k \,\|\bar{\delta}\rangle R^k(\alpha\beta\overline{\gamma\delta})\Big\}$$

$$-\,G^3\Big\{+i\langle\alpha\|C^{\,k} \,\|\bar{\gamma}\rangle\langle\bar{\beta}\|C^{\,k} \,\|\bar{\delta}\rangle R^k(\alpha\overline{\beta\gamma\delta})$$

$$+i\langle\bar{\alpha}\|C^{\,k} \,\|\bar{\gamma}\rangle\langle\beta\|C^{\,k} \,\|\bar{\delta}\rangle R^k(\bar{\alpha}\beta\gamma\bar{\delta})$$

$$-i\langle\bar{\alpha}\|C^{\,k} \,\|\gamma\rangle\langle\bar{\beta}\|C^{\,k} \,\|\bar{\delta}\rangle R^k(\overline{\alpha\beta}\gamma\bar{\delta})$$

$$-i\langle\bar{\alpha}\|C^{\,k} \,\|\bar{\gamma}\rangle\langle\bar{\beta}\|C^{\,k} \,\|\delta\rangle R^k(\overline{\alpha\beta\gamma}\delta)\Big\}$$

$$+\,G^4\,\langle\bar{\alpha}\|\, C^k\|\bar{\gamma}\rangle\langle\bar{\beta}\|\, C^k \,\|\bar{\delta}\rangle R^k(\overline{\alpha\beta\gamma\delta}) \qquad \text{(A1.11)}$$

At present we are only interested in diagonal elements, in which case T = T', M = M'. Then the matrix elements take

one of two simpler forms; either

$$\alpha = \delta \quad \text{and} \quad \beta = \gamma \quad \text{(case (a))} \tag{A1.12a}$$

or

$$\alpha = \gamma \quad \text{and} \quad \beta = \delta \quad \text{(case (b))} \tag{A1.12b}$$

For simplicity we will consider separately the terms in each power of G.

(i) Terms of order G^o. These appear exactly as in the parity conserving case, and so the k-values are determined as before: the elements $\langle\alpha||C^k||\gamma\rangle$ and $\langle\beta||C^k||\delta\rangle$ must be allowed by parity considerations i.e. $\ell_\alpha+\ell_\gamma+k$ must be even, and $\ell_\beta+\ell_\delta+k$ must also be even.

(ii) Terms of order G. We take the first term as typical. Then the terms $\langle\bar{\alpha}||C^k||\gamma\rangle$ and $\langle\beta||C^k||\delta\rangle$ must be parity allowed, i.e. $\ell_{\bar{\alpha}}+k+\ell_\gamma$ and $\ell_\beta+k+\ell_\delta$ must both be even
i.e. $\ell_\alpha+k+\ell_\gamma$ must be odd and $\ell_\beta+k+\ell_\delta$ must be even. In case (a) this implies that $\ell_\alpha+k+\ell_\beta$ must be odd and $\ell_\beta+k+\ell_\alpha$ must be even. There are clearly no values of k that satisfy this condition. In case (b) we must have that $\ell_\alpha+k+\ell_\alpha$ is odd $\ell_\beta+k+\ell_\beta$ is even. Since ℓ_α and ℓ_β are integral, this can never be satisfied.

The same argument will hold for all terms of order G; hence we conclude that there are no terms of order G.

(iii) Terms of order G^2. These fall into two distinct categories: (A) the first two terms and (B) the last four.

We take the first term as typical of category (A). Here $\ell_\alpha+k+\ell_\beta$ must be even as must $\ell_\beta+k+\ell_\delta$.

In case (a) this becomes that $\ell_\alpha+k+\ell_\beta$ must be even, and

we get coefficients with the usual values of k.

In case (b) this becomes $\ell_\alpha+k+\ell_\alpha$ and $\ell_\beta+k+\ell_\beta$ must both be even, i.e. k must be even. This also yields coefficients with the usual values of k. Thus the coefficients of the first two terms of order G^2 have the usual k-values.

We take the third term as typical of category (B). Here $\ell_\alpha+k+\ell_\beta$ and $\ell_\alpha+k+\ell_\beta$ must both be odd.

In case (a) this becomes $\ell_\alpha+k+\ell_\beta$ must be odd, and in case (b) $\ell_\alpha+k+\ell_\alpha$ and $\ell_\beta+k+\ell_\beta$ must both be odd.

Thus the coefficients of the last four terms correspond to the "wrong" calues of k.

(iv) Terms of order G^3. By exactly the same argument as (ii) we conclude that there are none.

(v) Terms of order G^4. We require $\ell_\alpha+\ell_\gamma+k$ and $\ell_\beta+\ell_\delta+k$ to be even, so these have the same coefficients as the terms of order G^o.

Thus we obtain

$$\langle TM^{PM}|\textstyle\sum 1/r_{ij}|TM^{PM}\rangle = \sum_{\substack{\alpha\beta\gamma\delta,k \\ \alpha=\delta\,\&\,\beta=\gamma \\ \text{or } \alpha=\gamma\,\&\,\beta=\delta}} \left\{\gamma^k_{TT}(\alpha\beta\gamma\delta)X^k_{PM}(\alpha\beta\gamma\delta)+\Xi^k_{TT}(\gamma\beta\gamma\delta)X^k_{PM}(\alpha\beta\gamma\delta)\right\}$$

$$= \sum_{\substack{\alpha=\gamma\,\&\,\beta=\delta \\ \text{or } \alpha=\delta\,\&\,\gamma=\beta \\ k}} \Omega^k_{TT}(\alpha\beta\gamma\delta)X^k_{PM}(\alpha\beta\gamma\delta) \qquad \text{(A1.13)}$$

(where $\Omega^k_{TT}(\alpha\beta\gamma\delta)=\gamma^k_{TT}(\alpha\beta\gamma\delta)+\Xi^k_{TT}(\alpha\beta\gamma\delta)$)

$$= \sum_{\substack{\alpha\beta \\ k}} \left\{\Omega^k_{TT}(\alpha\beta\beta\alpha)X^k_{PM}(\alpha\beta\beta\alpha)+\Omega^k_{TT}(\alpha\beta\alpha\beta)X^k_{PM}(\alpha\beta\alpha\beta)\right\}$$

$$= \sum_{\substack{\alpha\beta \\ k\in \mathbb{K}_+}} V^k_{TT}(\alpha\beta\beta\alpha)R^k(\alpha\beta\beta\alpha) + \sum_{\substack{\alpha\beta \\ k\in \mathbb{K}_o}} V^k_{TT}(\alpha\beta\alpha\beta)R^k(\alpha\beta\alpha\beta)$$

$$+ G^2\Bigg(\sum_{\substack{\alpha\beta \\ k\in \mathbb{K}_+}} V^k_{TT}(\alpha\beta\beta\alpha)[R^k(\bar{\alpha}\beta\bar{\beta}\alpha) + R^k(\alpha\bar{\beta}\beta\bar{\alpha})]$$

$$+ \sum_{\substack{\alpha\beta \\ k\in \mathbb{K}_o}} V^k_{TT}(\alpha\beta\alpha\beta)[R^k(\bar{\alpha}\beta\bar{\alpha}\beta) + R^k(\alpha\bar{\beta}\alpha\bar{\beta})]\Bigg)$$

$$+ G^2\Bigg(\sum_{\substack{\alpha\beta \\ k\in \mathbb{K}_-}} V^k_{TT}(\alpha\beta\beta\alpha)[-R^k(\overline{\alpha\beta}\beta\alpha)+R^k(\alpha\overline{\beta\beta}\alpha)+R^k(\bar{\alpha}\beta\beta\bar{\alpha})-R^k(\alpha\beta\overline{\beta\alpha})]$$

$$+ \sum_{\substack{\alpha\beta \\ k\in \mathbb{K}_*}} V_{TT}(\alpha\beta\alpha\beta)[-R^k(\overline{\alpha\beta}\alpha\beta)+R^k(\alpha\overline{\beta\alpha}\beta)+R^k(\bar{\alpha}\beta\alpha\bar{\beta})-R^k(\alpha\beta\overline{\alpha\beta})]\Bigg)$$

$$+ G^4\Bigg(\sum_{\substack{\alpha\beta \\ k\in \mathbb{K}_+}} V^k_{TT}(\alpha\beta\beta\alpha)R^k(\overline{\alpha\beta\beta\alpha})+\sum_{\substack{\alpha\beta \\ k\in \mathbb{K}_o}} V^k_{TT}(\alpha\beta\alpha\beta)R^k(\overline{\alpha\alpha\beta\beta})\Bigg) \qquad \text{(A1.14)}$$

where the $\mathbb{K}$ are sets of indices defined for each α and β by

$$\mathbb{K}_o = \{k|\ k \geq 0,\ k \text{ is even},\ k \leq (j_\alpha+j_\beta)\delta_{\alpha\beta}\} \qquad \text{(A1.15a)}$$

$$\mathbb{K}_* = \{k|\ k \geq 0,\ k \text{ is odd},\ k \leq (j_\alpha+j_\beta)\delta_{\alpha\beta}\} \qquad \text{(A1.15b)}$$

$$\mathbb{K}_+ = \{k||j_\alpha-j_\beta| \leq k \leq j_\alpha+j_\beta,\ \kappa_\alpha\kappa_\beta(-1)^{k-|j_\alpha-j_\beta|} > 0\} \qquad \text{(A1.15c)}$$

$$\mathbb{K}_- = \{k||j_\alpha-j_\beta| \leq k \leq j_\alpha+j_\beta,\ \kappa_\alpha\kappa_\beta(-1)^{k-|j_\alpha-j_\beta|} < 0\} \qquad \text{(A1.15d)}$$

The $V^k_{TT'}(\alpha\beta\gamma\delta)$ are MCP coefficients in which the usual parity restriction has been lifted. They reduce to 3-j symbols in the case of one of the orbitals being full as before.

As usual we set

$$f_r^k(\alpha\beta) = V_{rr}^k(\alpha\beta\alpha\beta) \qquad \text{(A1.16a)}$$

$$g_r^k(\alpha\beta) = V_{rr}^k(\alpha\beta\beta\alpha) \qquad \text{(A1.16b)}$$

Then we may write (A1.14) as

$$\langle\Phi_r^{PM}|\sum_{i<j} 1/r_{ij}|\Phi_r^{PM}\rangle = \sum_{\substack{b\geq a\\ k}} f_r^k(ab)F_{PM}^k(ab) + \sum_{\substack{b>a\\ k}} g_r^k(ab)G_{PM}^k(ab) \qquad \text{(A1.17)}$$

where the k are no longer restricted by parity considerations. The restrictions on the range of a and b are a consequence of the fact that the MCP coefficients are such that $f_r^k(ab)=0$ if $a>b$ and $g_r^k(ab)=0$ if $a\geq b$.

Comparison of (A1.14) and (A1.17) gives

$$F_{PM}^k(ab)=R^k(abab)+G^2\left[R^k(a\bar{b}a\bar{b})+R^k(\bar{a}b\bar{a}b)\right]+G^4R^k(\overline{abab}) \qquad \text{(A1.18a)}$$

$$k\varepsilon K_o$$

$$F_{PM}^k(ab)=G^2\left[-R^k(\overline{a\bar{b}}ab)+R^k(a\overline{\bar{a}b}a\bar{b})+R^k(\bar{a}ba\bar{b})-R^k(ab\overline{a\bar{b}})\right]$$

$$=0 \qquad k\varepsilon K_* \qquad \text{(A1.18b)}$$

$$G_{PM}^k(ab)=R^k(aabb)+G^2\left[R^k(\bar{a}a\bar{b}b)+R^k(a\bar{a}b\bar{b})\right]+G^4R^k(\overline{aabb})$$

$$=R^k(aabb)+2G^2R^k(\bar{a}a\bar{b}b)+G^4R^k(\overline{aabb}) \quad k\varepsilon K_+ \qquad \text{(A1.18c)}$$

$$G_{PM}^k(ab)=G^2\left[-R^k(\overline{a\bar{b}}ba)+R^k(a\overline{\bar{b}b}a)+R^k\overline{(\bar{a}abb\bar{a})}-R^k(ab\overline{\bar{b}a})\right]$$

$$=G^2\left[-2R^k(\bar{a}ab\bar{b})+R^k(\overline{\bar{a}a}bb)+R^k(aa\overline{\bar{b}b})\right] \quad k\varepsilon K_- \qquad \text{(A1.18d)}$$

We now bring together the foregoing results to yield

$$\Gamma = \sum_{r=1}^{N_c} c_r{}^2 \Bigg\{ \sum_a q_r(a) \int_o^\infty dr \Big[cQ_a \Big(\frac{d}{dr}+\frac{\kappa_a}{r}\Big) P_a - cP_a \Big(\frac{d}{dr}-\frac{\kappa_a}{r}\Big) Q_a$$

$$-2c^2 Q_a{}^2 - \frac{Z_N}{r}(P_a{}^2+Q_a{}^2)\Big] + G^2 \int_o^\infty dr \Big[c\bar{Q}_a \Big(\frac{d}{dr}-\frac{\kappa_a}{r}\Big) \bar{P}_a - c\bar{P}_a \Big(\frac{d}{dr}+\frac{\kappa_a}{r}\Big) \bar{Q}_a$$

$$-2c^2 \bar{Q}_a{}^2 - \frac{Z_N}{r}(\bar{P}_a{}^2+\bar{Q}_a{}^2)\Big] - G \sum_a q_r(a) 2G \int_o^\infty \rho\{P_a\bar{Q}_a - Q_a\bar{P}_a\}dr$$

$$+ \sum_{\substack{b\geq a \\ k\in K_o}} f_r^k(ab)\Big[R^k(abab)+G^2\{R^k(a\bar{b}a\bar{b})+R^k(\bar{a}b\bar{a}b)\}$$

$$+G^4 R^k(\bar{a}\bar{b}ab)\Big]$$

$$\sum_{\substack{b>a \\ k\in K_+}} g_r^k(ab)\Big[R^k(aabb)+2G^2 R^k(\bar{a}a\bar{b}b)+G^4 R^k(\bar{a}\bar{a}\bar{b}b)\Big]$$

$$+ \sum_{\substack{b>a \\ k\in K_-}} g_r^k(ab)\Big[G^2(-2R^k(\bar{a}ab\bar{b})+R^k(\bar{a}\bar{a}bb)+R^k(aa\bar{b}\bar{b}))\Big]\Bigg\}$$

$$+ \sum_a \bar{q}_a \varepsilon_a \Big[\int_o^\infty (P_a{}^2+Q_a{}^2)dr + G^2 \int_o^\infty (\bar{P}_a{}^2+\bar{Q}_a{}^2)dr\Big]$$

$$+ \sum_{\substack{ab \\ \kappa_a\neq\kappa_b \\ a\neq b}} \varepsilon_{ab} \Big[\int_o^\infty (P_aP_b+Q_aQ_b)dr + G^2 \int_o^\infty (P_aP_b+Q_aQ_b)dr\Big]$$

$$+ \sum_{\substack{ab \\ \kappa_a=-\kappa_b}} iG\varepsilon_{ab} \Big[\int_o^\infty (P_a\bar{P}_b+Q_a\bar{Q}_b-\bar{P}_aP_b-\bar{Q}_aQ_b)dr\Big] \qquad \text{(A1.19)}$$

Collecting together terms in each power of G

$$\Gamma = \Bigg[\sum_a \bar{q}_a \int^\infty dr \Big(cQ_a\Big(\frac{d}{dr}+\frac{\kappa_a}{r}\Big)P_a - cP_a\Big(\frac{d}{dr}-\frac{\kappa_a}{r}\Big) Q_a - 2c^2Q_a{}^2 - \frac{Z_N}{r}(P_a{}^2+Q_a{}^2)\Big)$$

$$+ \sum_{\substack{b\geq a \\ k\in K_o}} \bar{f}^k(ab)R^k(abab) + \sum_{\substack{b>a \\ k\in K_+}} \bar{g}^k(ab)R^k(aabb) + \sum_a \bar{q}_a\varepsilon_a \int^\infty (P_a{}^2+Q_a{}^2)dr$$

$$+\sum_{\substack{ab\\ \kappa_a=\kappa_b\\ a\neq b}}\varepsilon_{ab}\int_o^\infty (P_aP_b+Q_aQ_b)dr\Bigg]$$

$$+G^2\Bigg[\sum_a \bar{q}_a\int_o^\infty dr\left(c\bar{Q}_a\left(\frac{d}{dr}-\frac{\kappa_a}{r}\right)\bar{P}_a-c\bar{P}_a\left(\frac{d}{dr}+\frac{\kappa_a}{r}\right)\bar{Q}_a-2c^2\bar{Q}_a{}^2-\frac{Z}{r}\frac{N}{}(\bar{P}_a{}^2+\bar{Q}_a{}^2)\right)$$

$$+2\sum_a \bar{q}_a\int^\infty \rho\{P_a\bar{Q}_a-Q_a\bar{P}_a\}dr+\sum_{\substack{b>a\\ k\varepsilon K_o}}\bar{f}^k(ab)\{R^k(a\bar{b}a\bar{b})+R^k(\bar{a}b\bar{a}b)\}$$

$$+\sum_{\substack{b>a\\ k\varepsilon K_+}}\bar{g}^k(ab)2R^k(\bar{a}a\bar{b}b)+\sum_{\substack{b>a\\ k\varepsilon K_-}}\bar{g}^k(ab)\{-2R^k(\bar{a}ab\bar{b})+R^k(\overline{a\bar{a}}bb)+R^k(aa\overline{b\bar{b}})\}$$

$$+\sum_a \bar{q}_a\varepsilon_a\int_o^\infty(\bar{P}_a^2+\bar{Q}_a^2)dr+\sum_{\substack{ab\\ a\neq b\\ \kappa_a=\kappa_b}}\varepsilon_{ab}\int_o^\infty(\bar{P}_a\bar{P}_b+\bar{Q}_a\bar{Q}_b)dr$$

$$+\sum_{\substack{ab\\ \kappa_a=-\kappa_b}}\eta_{ab}\int_o^\infty(\bar{P}_aP_b+\bar{Q}_aQ_b-P_a\bar{P}_b-Q_a\bar{Q}_b)\Bigg]$$

$$+G^4\Bigg[\sum_{\substack{a\leq b\\ k\varepsilon K_o}}\bar{f}^k(ab)R^k(\overline{abab})+\sum_{\substack{a<b\\ k\varepsilon K_+}}\bar{g}^k(ab)R^k(\overline{aabb})\Bigg] \qquad (A1.20)$$

where we have written, for simplicity

$$\eta_{ab}=-iG^{-1}\varepsilon_{ab}\quad(\kappa_a=-\kappa_b) \qquad (A1.21)$$

$$\bar{f}^k(ab)\sum_r c_r{}^2 f_r{}^k(ab) \qquad (A1.22)$$

and

$$\bar{g}^k(ab)=\sum_r c_r{}^2 f_r{}^k(ab) \qquad (A1.23)$$

The equation (A1.20) will now yield equation (6.2.13) when the symmetry of the coefficients $\bar{g}^k(ab)$ and $\bar{f}^k(ab)$ and the antisymmetry of η_{ab} are exploited, where we redefine

$$\bar{g}^k(ab) = \bar{g}^k(ba) \quad a > b$$

$$\bar{f}^k(ab) = \bar{f}^k(ba) \quad a > b \tag{A1.24}$$

Appendix 2

Through me you pass into the city of woe.....

All hope abandon, ye who enter here.

Danté (1320)

Basis Set Expansion Schemes

APPENDIX 2

BASIS SET EXPANSION SCHEMES

The parity conserving parts of the wavefunction, P_a and Q_a, satisfy the normal MCDF equations. We can solve these with the MCDF package as described in chapter 3. The details of that calculation, although interesting, do not concern us her we will merely assume that the functions P_a and Q_a, the eigenvalues ε_a and the Lagrange multipliers ε_{ab} have been calculated to an arbitrary accuracy and are readily available. This is the case in practice.

We therefore turn our attention to the problem of calculating the parity violating parts of the wavefunction, $\overline{P}_a$ and $\overline{Q}_a$. To do this we shall follow the procedure first used by Roothaan (1951, 1960, 1963), but, as will be explained, the resulting equations are much simpler.

Firstly, we return to the energy functional as defined in equation (6.2.13). Certain features are apparent on an examination of it. Firstly, the terms that are independent of G are also independent of the parity violating part of the wavefunction (indeed, something would be seriously wrong if they were not), and therefore, when we vary the parity violating wavefunctions, the change in these terms will be zero. We may therefore forget about them, since we require only equations for the PNC wavefunctions.

Secondly, the terms of order G^4 will disappear in the limit $G \to 0$ and, since $G \sim 10^{-14}$, may safely be ignored. We are then left with the problem of finding stationary values of the functional

$$G=\sum_\alpha \bar{q}_\alpha \int_0^\infty dr\left(c\bar{Q}_\alpha\left(\frac{d}{dr}-\frac{\kappa_\alpha}{r}\right)\bar{P}_\alpha - c\bar{P}_\alpha\left(\frac{d}{dr}+\frac{\kappa_\alpha}{r}\right)\bar{Q}_\alpha - 2c^2\bar{Q}_\alpha{}^2 - \frac{Z_N}{r}(\bar{P}_\alpha{}^2+\bar{Q}_\alpha{}^2)\right)$$

$$-2\sum_\alpha \bar{q}_\alpha \int_0^\infty \rho\{P_\alpha\bar{Q}_\alpha - Q_\alpha\bar{P}_\alpha\} + \sum_{\alpha\beta,k\in\mathbb{K}_0} \bar{f}^k(\alpha\beta)(1+\delta_{\alpha\beta})R^k(\bar{\alpha}\beta\bar{\alpha}\beta)$$

$$+\sum_{\alpha\beta k\in\mathbb{K}_+} \bar{g}^k(\alpha\beta)R^k(\alpha\bar{\alpha}\beta\bar{\beta}) - \sum_{\alpha\beta k\in\mathbb{K}_-} \bar{g}^k(\alpha\beta)[R^k(\bar{\alpha}\alpha\beta\bar{\beta}) - R^k(\bar{\alpha}\bar{\alpha}\beta\beta)]$$

$$+\sum_\alpha \varepsilon_\alpha \bar{q}_\alpha \int_0^\infty (\bar{P}_\alpha{}^2+\bar{Q}_\alpha{}^2) + \sum_{\substack{\alpha\neq\beta \\ \kappa_\alpha=\kappa_\beta}} \varepsilon_{\alpha\beta}\int_0^\infty (\bar{P}_\alpha\bar{P}_\beta+\bar{Q}_\alpha\bar{Q}_\beta) + \sum_{\substack{\alpha\beta \\ \kappa_\alpha=-\kappa_\beta}} 2\eta_{\alpha\beta}\int_0^\infty (\bar{P}_\alpha P_\beta+\bar{Q}_\alpha Q_\beta)$$

(A2.1)

In an iterative basis set expansion scheme we obtain a sequence of functions $\bar{P}_a^{(n)}$ and $\bar{Q}_a^{(n)}$ which, we hope , will converge. In the first case we require that

$$\bar{P}_a^{(n)} = \lambda_a \bar{P}_a^{(n-1)} + \mu_a \Pi_a^{(n-1)} \qquad n \geq 1$$

$$\bar{Q}_a^{(n)} = \nu_a \bar{Q}_a^{(n-1)} + \tau_a \Omega_a^{(n-1)} \qquad \text{(A2.2)}$$

where the $\Pi_a^{(n-1)}$ and $\Omega_a^{(n-1)}$ are functions which will be defined later, and $P_a^{(o)}$ and $Q_a^{(o)}$ are the solutions of the MCDF-PNC equations with $\chi = \chi^{(0)}$. We then find stationary values of G as a function of the real variables λ_a, μ_a, ν_a, τ_a.

Substitution of (A2.2) in (A2.1), and the dropping of the '(n-1)' superscripts, yields

$$G=\sum_\alpha \bar{q}_\alpha \int_0^\infty \Bigg[c(\nu_\alpha\bar{Q}_\alpha+\tau_\alpha\Omega_\alpha)\left(\frac{d}{dr}-\frac{\kappa_\alpha}{r}\right)(\lambda_\alpha\bar{P}_\alpha+\mu_\alpha\Pi_\alpha) - c(\bar{P}_\alpha\lambda_\alpha+\mu_\alpha\Pi)_\alpha\left(\frac{d}{dr}+\frac{\kappa_\alpha}{r}\right)(\nu_\alpha\bar{Q}_\alpha+\tau_\alpha\Omega)_\alpha$$

$$-2c^2(\nu_\alpha\bar{Q}_\alpha+\tau_\alpha\Omega_\alpha)^2 - \frac{Z_N}{r}((\lambda_\alpha\bar{P}_\alpha+\mu_\alpha\Pi_\alpha)^2+(\nu_\alpha\bar{Q}_\alpha+\tau_\alpha\Omega_\alpha)^2)\Bigg]$$

$$-2\sum_\alpha \bar{q}_\alpha \int_0^\infty \rho\left[P_\alpha(\nu_\alpha\bar{Q}_\alpha+\tau_\alpha\Omega_\alpha) - Q_\alpha(\lambda_\alpha\bar{P}_\alpha+\mu_\alpha\Pi_\alpha)\right]$$

$$
\begin{aligned}
&- \sum_{\substack{\alpha\neq\beta \\ k\in \underline{\mathbb{K}}}} \overline{g}^{k}(\alpha\beta)\Big[\lambda_\alpha\lambda_\beta \boldsymbol{L}^k(\overline{P}_\alpha P_\beta;P_\alpha\overline{P}_\beta)+\lambda_\alpha\mu_\beta \boldsymbol{L}^k(\overline{P}_\alpha P_\beta;P_\alpha\Pi_\beta)+\lambda_\alpha\nu_\beta \boldsymbol{L}^k(\overline{P}_\alpha P_\beta;Q_\alpha\overline{Q}_\beta) \\
&\qquad +\lambda_\alpha\tau_\beta \mathbb{L}^k(\overline{P}_\alpha P_\beta;Q_\alpha\Omega_\beta) \\
&\quad +\mu_\alpha\lambda_\beta \boldsymbol{L}^k(\Pi_\alpha P_\beta;P_\alpha\overline{P}_\beta)+\mu_\alpha\mu_\beta \boldsymbol{L}^k(\Pi_\alpha P_\beta;P_\alpha\Pi_\beta)+\mu_\alpha\nu_\beta \boldsymbol{L}^k(\Pi_\alpha P_\beta;Q_\alpha\overline{Q}_\beta) \\
&\qquad +\mu_\alpha\tau_\beta \mathbb{L}^k(\Pi_\alpha P_\beta;Q_\alpha\Omega_\beta) \\
&\quad +\nu_\alpha\lambda_\beta \boldsymbol{L}^k(\overline{Q}_\alpha Q_\beta;P_\alpha\overline{P}_\beta)+\nu_\alpha\mu_\beta \boldsymbol{L}^k(\overline{Q}_\alpha Q_\beta;P_\alpha\Pi_\beta)+\nu_\alpha\beta_\beta \boldsymbol{L}^k(\overline{Q}_\alpha Q_\beta;Q_\alpha\overline{Q}_\beta) \\
&\qquad +\nu_\alpha\tau_\beta \mathbb{L}^k(\overline{Q}_\alpha Q_\beta;Q_\alpha\Omega_\beta) \\
&\quad +\tau_\alpha\lambda_\beta \boldsymbol{L}^k(\Omega_\alpha Q_\beta;P_\alpha\overline{P}_\beta)+\tau_\alpha\mu_\beta \boldsymbol{L}^k(\Omega_\alpha Q_\beta;P_\alpha\Pi_\beta)+\tau_\alpha\nu_\beta \boldsymbol{L}^k(\Omega_\alpha Q_\beta;Q_\alpha\overline{Q}_\beta) \\
&\qquad +\tau_\alpha\tau_\beta \mathbb{L}^k(\Omega_\alpha Q_\beta;Q_\alpha\Omega_\beta)\Big] \\
&+ \sum_{\substack{\alpha\neq\beta \\ k\in \underline{\mathbb{K}}}} \overline{g}^{k}(\alpha\beta)\Big[\lambda_\alpha^2 \boldsymbol{L}^k(\overline{P}_\alpha P_\beta;\overline{P}_\alpha P_\beta)+2\lambda_\alpha\mu_\alpha \boldsymbol{L}^k(\overline{P}_\alpha P_\beta;\Pi_\alpha P_\beta)+2\lambda_\alpha\nu_\alpha \boldsymbol{L}^k(\overline{P}_\alpha P_\beta;\overline{Q}_\alpha Q_\beta) \\
&\qquad +2\lambda_\alpha\tau_\alpha \mathbb{L}^k(\overline{P}_\alpha P_\beta;\Omega_\alpha Q_\beta) \\
&\quad +\mu_\alpha^2 \boldsymbol{L}^k(\Pi_\alpha P_\beta;\Pi_\alpha P_\beta)+2\mu_\alpha\nu_\alpha \boldsymbol{L}^k(\Pi_\alpha P_\beta;\overline{Q}_\alpha Q_\beta)+2\mu_\alpha\tau_\alpha \boldsymbol{L}^k(\Pi_\alpha P_\beta;\Omega_\alpha Q_\beta) \\
&\qquad +\nu_\alpha^2 \mathbb{L}^k(\overline{Q}_\alpha Q_\beta;\overline{Q}_\alpha Q_\beta) \\
&\quad +2\nu_\alpha\tau_\alpha \boldsymbol{L}^k(\overline{Q}_\alpha Q_\beta;\Omega_\alpha Q_\beta)+\tau_\alpha^2 \boldsymbol{L}^k(\Omega_\alpha Q_\beta;\Omega_\alpha Q_\beta)\Big] \\
&+ \sum_{\substack{\alpha\neq\beta \\ k\in \underline{\mathbb{K}}_+}} \overline{g}^{k}(\alpha\beta)\Big[\lambda_\alpha\lambda_\beta \boldsymbol{L}^k(\rho_{\alpha\beta};\overline{P}_\alpha\overline{P}_\beta)+\lambda_\alpha\mu_\beta \boldsymbol{L}^k(\rho_{\alpha\beta};\overline{P}_\alpha\Pi_\beta)+\mu_\alpha\lambda_\beta \boldsymbol{L}^k(\rho_{\alpha\beta};\Pi_\alpha\overline{P}_\beta)+\mu_\alpha\mu_\beta \boldsymbol{L}^k(\rho_{\alpha\beta};\Pi_\alpha\Pi \\
&\qquad +\nu_\alpha\nu_\beta \boldsymbol{L}^k(\rho_{\alpha\beta};\overline{Q}_\alpha\overline{Q}_\beta)+\nu_\alpha\tau_\beta \boldsymbol{L}^k(\rho_{\alpha\beta};\overline{Q}_\alpha\Omega_\beta)+\tau_\alpha\nu_\beta \boldsymbol{L}^k(\rho_{\alpha\beta};\Omega_\alpha\overline{Q}_\beta)+\tau_\alpha\tau_\beta \boldsymbol{L}^k(\rho_{\alpha\beta};\Omega_o \\
&+ \sum_{\substack{\alpha\beta \\ k\in \boldsymbol{K}_o}} \overline{f}^{k}(\alpha\beta)(1+\delta_{\alpha\beta})\Big[\lambda_\beta^2 \boldsymbol{L}^k(\rho_{\alpha\alpha};\overline{P}_\beta\overline{P}_\beta)+2\lambda_\beta\mu_\beta \boldsymbol{L}^k(\rho_{\alpha\alpha};\overline{P}_\beta\Pi_\beta)+\mu_\beta^2 \boldsymbol{L}^k(\rho_{\alpha\alpha};\Pi_\beta\Pi_\beta) \\
&\qquad +\nu_\beta^2 \boldsymbol{L}^k(\rho_{\alpha\alpha};\overline{Q}_\beta\overline{Q}_\beta)+2\nu_\beta\tau_\beta \boldsymbol{L}^k(\rho_{\alpha\alpha};\overline{Q}_\beta\Omega_\beta)+2\tau_\beta^2 \boldsymbol{L}^k(\rho_{\alpha\alpha};\Omega_\beta\Omega_\beta)\Big] \\
&+ \sum_\alpha \epsilon_\alpha\overline{q}_\alpha \int_o^\infty \Big[\lambda_\alpha^2\overline{P}_\alpha^2+2\lambda_\alpha\mu_\alpha\overline{P}_\alpha\Pi_\alpha+\mu_\alpha^2\Pi_\alpha^2+\nu_\alpha^2\overline{Q}_\alpha^2+2\nu_\alpha\tau_\alpha\overline{Q}_\alpha\Omega_\alpha+\tau_\alpha^2\Omega_\alpha^2\Big]
\end{aligned}
$$

$$+\sum_{\substack{\alpha\neq\beta\\ \kappa_\alpha=\kappa_\beta}} \varepsilon_{\alpha\beta}\int_0^\infty\Big(\lambda_\alpha\lambda_\beta\bar{P}_\alpha\bar{P}_\beta+\lambda_\alpha\mu_\beta\bar{P}_\alpha\Pi_\beta+\mu_\alpha\lambda_\beta\Pi_\alpha\bar{P}_\beta+\mu_\alpha\mu_\beta\Pi_\alpha\Pi_\beta+\nu_\alpha\nu_\beta\bar{Q}_\alpha\bar{Q}_\beta$$

$$+\nu_\alpha\tau_\beta\bar{Q}_\alpha\Omega_\beta+\tau_\alpha\nu_\beta\Omega_\alpha\bar{Q}_\beta+\tau_\alpha\tau_\beta\Omega_\alpha\Omega_\beta\Big)$$

$$-\sum_{\substack{\alpha\beta\\ \kappa_\alpha=-\kappa_\beta}} 2\eta_{\alpha\beta}\int_0^\infty\Big(\lambda_\beta P_\alpha\bar{P}_\beta+\nu_\beta Q_\alpha\bar{Q}_\beta+\mu_\beta P_\alpha\Pi_\beta+\tau_\beta Q_\alpha\Omega_\beta\Big) \qquad \text{(A2.3)}$$

where we have used the notation

$$\rho_{ab} = P_aP_b + Q_aQ_b$$

$$\rho_{\bar{a}b} = \bar{P}_aP_b + \bar{Q}_aQ_b$$

$$\rho_{\bar{a}\bar{b}} = \bar{P}_a\bar{P}_b+\bar{Q}_a\bar{Q}_b$$

which should not be confused with the nuclear density ρ, and

$$L^k(f;g) = \int_0^\infty\int_0^\infty \frac{r_<^k}{r_>^{k+1}}\, f(r_1)g(r_2)\, dr_1\, dr_2 \qquad \text{(A2.4)}$$

in analogy with the more conventional R^k integral. Then the condition that λ_a, μ_a, ν_a, τ_a be such as to make G stationary may be written

$$\frac{\partial G}{\partial\lambda_a} = 0 \qquad \text{(A2.5)}$$

$$\frac{\partial G}{\partial\mu_a} = 0 \qquad \text{(A2.6)}$$

$$\frac{\partial G}{\partial\nu_a} = 0 \qquad \text{(A2.7)}$$

$$\frac{\partial G}{\partial\tau_a} = 0 \qquad \text{(A2.8)}$$

Equation (A2.5) yields

$$\lambda_a\{\bar{q}_a\int_o^\infty -\frac{Z_N}{r}\bar{P}_a^2 + \sum_{c,k\epsilon K_-}\bar{g}^k(ac)L^k(\bar{P}_aP_c;\bar{P}_aP_c)+\sum_{c,k\epsilon K_0}\bar{f}^k(ac)(1+\delta_{ac})L^K(\rho_{cc};\bar{P}_a\bar{P}_a)$$

$$+\varepsilon_a\bar{q}_a\int_o^\infty \bar{P}_a^2\}$$

$$+\mu_a\{\bar{q}_a\int_o^\infty -\frac{Z_N}{r}\bar{P}_a\Pi_a+\sum_{c,k\epsilon K_-}\bar{g}^k(ac)L^k(\bar{P}_aP_c;\Pi_aP_c)+\sum_{c,k\epsilon K_0}\bar{f}^k(ac)(1+\delta_{ac})L^k(\rho_{cc};\bar{P}_a\Pi_a)$$

$$+\varepsilon_a\bar{q}_a\int_o^\infty \bar{P}_a\Pi_a\}$$

$$+\nu_a\{c\bar{q}_a\int_o^\infty \bar{Q}_a\left(\frac{d}{dr}-\frac{\kappa_a}{r}\right)\bar{P}_a+\sum_{c,k\epsilon K_-}\bar{g}^k(ac)L^k(\bar{P}_aP_c;\bar{Q}_aQ_c)\}$$

$$+\tau_a\{c\bar{q}_a\int_o^\infty \Omega_a\left(\frac{d}{dr}-\frac{\kappa_a}{r}\right)\bar{P}_a+\sum_{c,k\epsilon K_-}\bar{g}^k(ac)L^k(\bar{P}_aP_c;\Omega_aQ_c)\}$$

$$+\sum_b\lambda_b\{-\sum_{k\epsilon K_-}\bar{g}^k(ab)L^k(\bar{P}_aP_b;P_a\bar{P}_b)+\sum_{k\epsilon K_+}\bar{g}^k(ab)L^k(\rho_{ab};\bar{P}_a\bar{P}_b)+\varepsilon_{ab}\int_o^\infty \bar{P}_a\bar{P}_b\}$$

$$+\sum_b\mu_b\{-\sum_{k\epsilon K_-}\bar{g}^k(ab)L^k(\bar{P}_aP_b;P_a\Pi_b)+\sum_{k\epsilon K_+}\bar{g}^k(ab)L^k(\rho_{ab};\bar{P}_a\Pi_b)+\varepsilon_{ab}\int_o^\infty \bar{P}_a\Pi_b\}$$

$$+\sum_b\nu_b\{-\sum_{k\epsilon K_-}\bar{g}^k(ab)L^k(\bar{P}_aP_b;Q_a\bar{Q}_b)\}$$

$$+\sum_b\tau_b\{-\sum_{k\epsilon K_-}\bar{g}^k(ab)L^k(\bar{P}_aP_b;Q_a\Omega_b)\}$$

$$+\bar{q}_a\int_o^\infty \rho(r)Q_a\bar{P}_a+\sum_{\substack{b\\ \kappa_b=-\kappa_a}}\eta_{ab}\int_o^\infty \bar{P}_aP_b = 0 \qquad \text{(A2.9)}$$

while from equation (A2.6) we obtain

$$\lambda_a\{-\int_o^\infty\frac{Z_N}{r}\bar{P}_a\Pi_a\bar{q}_a+\sum_{\beta,k\epsilon K_-}\bar{g}^k(a\beta)L^k(\bar{P}_aP_\beta;\Pi_aP_\beta)+\sum_{\beta,k\epsilon K_0}\bar{f}^k(a\beta)(1+\delta_{a\beta})L^k(\rho_{\beta\beta},\bar{P}_a\Pi_a)$$

$$+\varepsilon_a\bar{q}_a\int_o^\infty \bar{P}_a\Pi_a\}$$

$$+\mu_a\{-\int_o^\infty \frac{Z_N}{r}\Pi_a\Pi_a\bar{q}_a+\sum_{\beta,k\epsilon K_-}\bar{g}^k(a\beta)L^k(\Pi_aP_\beta;\Pi_aP_\beta)+\sum_{\beta,k\epsilon K_0}\bar{f}^k(a\beta)(1+\delta_{a\beta})L^k(\rho_{\beta\beta};\Pi_a\Pi_a)$$

$$+\epsilon_a\bar{q}_a\int_o^\infty \Pi_a{}^2\}$$

$$+\nu_a\{c\bar{q}_a\int_o^\infty \bar{Q}_a\left(\frac{d}{dr}-\frac{\kappa_a}{r}\right)\Pi_a+\sum_{\beta,k\epsilon K_-}\bar{g}^k(a\beta)L^k(\Pi_aP_\beta;\bar{Q}_aQ_\beta)\}$$

$$+\tau_a\{c\bar{q}_a\int_o^\infty \Omega_a\left(\frac{d}{dr}-\frac{\kappa_a}{r}\right)\Pi_a+\sum_{\beta,k\epsilon K_-}\bar{g}^k(a\beta)L^k(\Pi_aP_\beta;\Omega_aQ_\beta)\}$$

$$+\sum_b\lambda_b\{-\sum_{k\epsilon K_-}\bar{g}^k(ab)L^k(\Pi_aP_b;P_a\bar{P}_b)+\sum_{k\epsilon K_+}\bar{g}^k(ab)L^k(\rho_{ab};\Pi_a\bar{P}_b)+\epsilon_{ab}\int_o^\infty \Pi_a\bar{P}_b\}$$

$$+\sum_b\mu_b\{-\sum_{k\epsilon K_-}\bar{g}^k(ab)L^k(\Pi_aP_b;P_a\Pi_b)+\sum_{k\epsilon K_+}\bar{g}^k(ab)L^k(\rho_{ab};\Pi_a\Pi_b)+\epsilon_{ab}\int_o^\infty \Pi_a\Pi_b\}$$

$$+\sum_b\nu_b\{-\sum_{k\epsilon K_-}\bar{g}^k(ab)L^k(\Pi_aP_b;Q_a\bar{Q}_b)\}$$

$$+\sum_b\tau_b\{-\sum_{k\epsilon K_-}\bar{g}^k(ab)L^k(\Pi_aP_b;Q_a\Omega_b)\}$$

$$+\bar{q}_a\int_o^\infty \rho Q_a\Pi_a+\sum_{\substack{\beta\\ \kappa_\beta=-\kappa_\alpha}}\eta_{a\beta}\int_o^\infty \Pi_aP_\beta=0 \qquad \text{(A2.10)}$$

Equation (A2.7) gives us

$$\lambda_a\{c\bar{q}_a\int_o^\infty \bar{Q}_a\left(\frac{d}{dr}-\frac{\kappa_a}{r}\right)\bar{P}_a+\sum_{\beta,k\epsilon K_-}\bar{g}^k(a\beta)L^k(\bar{P}_aP_\beta;\bar{Q}_aQ_\beta)\}$$

$$+\mu_a\{c\bar{q}_a\int_o^\infty \bar{Q}_a\left(\frac{d}{dr}-\frac{\kappa_a}{r}\right)\Pi_a+\sum_{\beta,k\epsilon K_-}\bar{g}^k(a\beta)L^k(\Pi_aP_\beta;\bar{Q}_aQ_\beta)\}$$

$$+\nu_a\{-2c^2\bar{q}_a\int_o^\infty \bar{Q}_a{}^2-\bar{q}_a\int_o^\infty \frac{Z_N}{r}\bar{Q}_a\bar{Q}_a+\sum_{\beta,k\epsilon K_-}\bar{g}^k(a\beta)L^k(\bar{Q}_aQ_\beta;\bar{Q}_aQ_\beta)$$

$$+\sum_{\beta,k\epsilon K_0}\bar{f}^k(a\beta)(1+\delta_{a\beta})L^k(\rho_{\beta\beta};\bar{Q}_a\bar{Q}_a)+\epsilon_a\bar{q}_a\int_o^\infty \bar{Q}_a{}^2\}$$

$$+\tau_a\{-2c^2\,\bar{q}_a\int_o^\infty \Omega_a\bar{Q}_a - \bar{q}_a\int_o^\infty \frac{Z_N}{r}\Omega_a\bar{Q}_a + \sum_{\beta,k\epsilon K_-} \bar{g}^k(a\beta)L^k(\bar{Q}_aQ_\beta;\Omega_aQ_\beta)$$

$$+ \sum_{\beta,k\epsilon K_o} \bar{f}^k(a\beta)(1+\delta_{a\beta})L^k(\rho_{\beta\beta};\bar{Q}_a\Omega_a)+\epsilon_a\bar{q}_a\int_o^\infty \bar{Q}_a\Omega_a\}$$

$$+\sum_b \lambda_b\{-\sum_{k\epsilon K_-} \bar{g}^k(ab)L^k(\bar{Q}_aQ_b;P_a\bar{P}_b)\}$$

$$+\sum_b \mu_b\{-\sum_{k\epsilon K_-} \bar{g}^k(ab)L^k(\bar{Q}_aQ_b;P_a\Pi_b)\}$$

$$+\sum_b \nu_b\{-\sum_{k\epsilon K_-} \bar{g}^k(ab)L^k(\bar{Q}_aQ_b;Q_a\bar{Q}_b)+\sum_{k\epsilon K_+} \bar{g}^k(ab)L^k(\rho_{ab};\bar{Q}_a\bar{Q}_b)+\epsilon_{ab}\int_o^\infty \bar{Q}_a\bar{Q}_b\}$$

$$+\sum_b \tau_b\{-\sum_{k\epsilon K_-} \bar{g}^k(ab)L^k(\bar{Q}_aQ_b;Q_a\Omega_b)+\sum_{k\epsilon K_+} \bar{g}^k(ab)L^k(\rho_{ab};\bar{Q}_a\Omega_b)+\epsilon_{ab}\int_o^\infty \bar{Q}_a\Omega_b\}$$

$$-\bar{q}_a\int_o^\infty \rho P_a\bar{Q}_a + \sum_{\substack{\beta \\ \kappa_\beta=-\kappa_\alpha}} \eta_{ab}\int_o^\infty \bar{Q}_aQ_\beta = 0 \qquad (A2.11)$$

and finally from (A2.8) we derive

$$\lambda_a\{c\bar{q}_a\int_o^\infty \Omega_a\left(\frac{d}{dr}-\frac{\kappa_a}{r}\right)\bar{P}_a+\sum_{\beta,k\epsilon K_-} \bar{g}^k(a\beta)L^k(\bar{P}_aP_\beta;\Omega_aQ_\beta)\}$$

$$+\mu_a\{c\bar{q}_a\int_o^\infty \Omega_a\left(\frac{d}{dr}-\frac{\kappa_a}{r}\right)\Pi_a+\sum_{\beta,k\epsilon K_-} \bar{g}^k(a\beta)L^k(\Pi_aP_\beta;\Omega_aQ_\beta)\}$$

$$+\nu_a\{-2c^2\bar{q}_a\int_o^\infty \bar{Q}_a\Omega_a-\bar{q}_a\int_o^\infty \frac{Z_N}{r}\bar{Q}_a\Omega_a+\sum_{\beta,k\epsilon K_-} \bar{g}^k(a\beta)L^k(\bar{Q}_aQ_\beta;\Omega_aQ_\beta)$$

$$+\sum_{\beta,k\epsilon K_o} \bar{f}^k(a\beta)(1+\delta_{a\beta})L^k(\rho_{\beta\beta};\bar{Q}_a\Omega_a)+\epsilon_a\bar{q}_a\int_o^\infty \bar{Q}_a\Omega_a\}$$

$$+\tau_a\{-2c^2\bar{q}_a\int_o^\infty \Omega_a\Omega_a-\bar{q}_a\int_o^\infty \frac{Z_N}{r}\Omega_a\Omega_a+\sum_{\beta,k\epsilon K_-} \bar{g}^k(a\beta)L^k(\Omega_aQ_\beta;\Omega_aQ_\beta)$$

$$+\sum_{\beta,k\epsilon K_o} \bar{f}^k(a\beta)(1+\delta_{a\beta})L^k(\rho_{\beta\beta};\Omega_a\Omega_a)+\epsilon_a\bar{q}_a\int_o^\infty \Omega_a{}^2\}$$

$$+\sum_b \lambda_b \{- \sum_{k\epsilon \mathbb{K}_-} \bar{g}^k(ab) L^k(\Omega_a Q_b; P_a \bar{P}_b)\} + \sum_b \mu_b \{- \sum_{k\epsilon K_-} \bar{g}^k(ab) L^k(\Omega_a Q_b; P_a \pi_b)\}$$

$$+\sum_b \nu_b \{- \sum_{k\epsilon \mathbb{K}_-} \bar{g}^k(ab) L^k(\Omega_a Q_b; Q_a \bar{Q}_b) + \sum_{k\epsilon \mathbb{K}_+} \bar{g}^k(a\beta) L^k(\rho_{ab}; \Omega_a \bar{Q}_b) + \epsilon_{ab} \int_o^\infty \Omega_a \bar{Q}_b\}$$

$$+\sum_b \tau_b \{- \sum_{k\epsilon \mathbb{K}_-} \bar{g}^k(ab) L^k(\Omega_a Q_b; Q_a \Omega_b) + \sum_{k\epsilon \mathbb{K}_+} \bar{g}^k(a\beta) L^k(\rho_{ab}; \Omega_a \Omega_b) + \epsilon_{ab} \int_o^\infty \Omega_a \Omega_b\}$$

$$-\bar{q}_a \int_o^\infty \rho P_a \Omega_a + \sum_{\substack{\beta \\ \kappa_\beta = -\kappa_\alpha}} \eta_{a\beta} \int_o^\infty \Omega_a Q_\beta = 0 \qquad \text{(A2.12)}$$

We must also include the orthogonality condition

$$\int_o^\infty \{\bar{P}_a^{(n)} P_b + \bar{Q}_a^{(n)} Q_b\} = \int_o^\infty \{P_a \bar{P}_b^{(n)} + Q_a \bar{Q}_b^{(n)}\} \quad (\kappa_a = -\kappa_b) \qquad \text{(A2.13)}$$

from which we obtain

$$\lambda_a \int_o^\infty \bar{P}_a^{(n-1)} P_b + \mu_a \int_o^\infty \Pi_a^{(n-1)} P_b + \nu_a \int_o^\infty \bar{Q}_a^{(n-1)} Q_b + \tau_a \int_o^\infty \Omega_a^{(n-1)} Q_b$$

$$= \lambda_b \int_o^\infty P_a \bar{P}_b^{(n-1)} + \mu_b \int_o^\infty P_a \Pi_b^{(n-1)} + \nu_b \int_o^\infty Q_a \bar{Q}_b^{(n-1)} + \tau_b \int_o^\infty Q_a \Omega_b^{(n-1)} \qquad \text{(A2.14)}$$

This yields us $4N_w + N_\eta$ linear equations in $4N_w + N_\eta$ unknowns, where N_w is the number of wavefunctions, and N_η is the number of orthogonality constraints. They may be solved without difficulty once the coefficients of the λ_a, μ_a, ν_a, τ_a and η_{ab} have been calculated. This is much simpler than in the parity conserving case, when the equations to be solved are all cubics.

The $\Pi_a^{(n)}$ and $\Omega_a^{(n)}$ are defined as

$$\Pi_a^{(n)} = \overset{\gamma}{P}_a^{(n)}$$

$$\Omega_a^{(n)} = \overset{\gamma}{Q}_a^{(n)} \qquad \text{(A2.15)}$$

where $\overset{\gamma}{P}_a^{(n)}$ and $\overset{\gamma}{Q}_a^{(n)}$ are solutions of the MCDF-PNC equations with $\bar{\chi}$ calculated using $\bar{P}_a = \bar{P}_a^{(n-1)}$ and $\bar{Q}_a = \bar{Q}_a^{(n-1)}$.

A simpler scheme is to define the functions $\bar{P}_a^{(n)}$ and $\bar{Q}_a^{(n)}$ not by equation (A2.2) but by

$$\bar{P}_a^{(n)} = \bar{P}_a^{(n-1)} + \lambda_a \Pi_a^{(n-1)}$$

$$\bar{Q}_a^{(n)} = \bar{Q}_a^{(n-1)} + \lambda_a \Omega_a^{(n-1)} \qquad \text{(A2.16)}$$

where

$$\Pi_a^{(n)} = \overset{\gamma}{P}{}^{(n)} - \bar{P}^{(n)}$$

and

$$\Omega_a^{(n)} = \overset{\gamma}{Q}_a^{(n)} - \bar{Q}_a^{(n)} \qquad \text{(A2.17)}$$

and $\overset{\gamma}{P}_a^{(n)}$ and $\overset{\gamma}{Q}_a^{(n)}$ are defined as before. We will refer to the variations Π_a and Ω_a collectively as "$\bar{a}$'". Again we drop the '(n-1)' superscripts to obtain the functional

$$G = \sum_\alpha \bar{q}_\alpha \int_0^\infty \left[c(\bar{Q}_\alpha + \lambda_\alpha \Omega_\alpha)\left(\frac{d}{dr} - \frac{\kappa_\alpha}{r}\right)(\bar{P}_\alpha + \lambda_\alpha \Pi_\alpha) 2 - 2c^2(\bar{Q}_\alpha + \lambda_\alpha \Omega_\alpha)^2 \right.$$

$$\left. - \frac{Z_N}{r}((\bar{P}_\alpha + \lambda_\alpha \Pi_\alpha)^2 + (\bar{Q}_\alpha + \lambda_\alpha \Omega_\alpha)^2) \right]$$

$$-2\sum_\alpha \bar{q}_\alpha \int_0^\infty \rho (P_\alpha(\bar{Q}_\alpha + \lambda_\alpha \Omega_\alpha) - Q_\alpha(\bar{P}_\alpha + \lambda_\alpha \Pi_\alpha))$$

$$- \sum_{\substack{\alpha\beta \\ k \in \boldsymbol{K}}} \bar{g}^k(\alpha\beta)\{R^k(\bar{\alpha}\alpha\beta\bar{\beta}) + 2\lambda_a R^k(\bar{\alpha}'\alpha\beta\bar{\beta})$$

$$+\lambda_\alpha\lambda_\beta R^k(\bar\alpha'\alpha\beta\bar\beta')-R^k(\bar\alpha\bar\alpha\beta\beta)\qquad -2\lambda_\alpha R^k(\bar\alpha\bar\alpha'\beta\beta)\quad -\lambda_\alpha^2 R^k(\bar\alpha'\bar\alpha'\beta\beta)\Big\}$$

$$+\sum_{\alpha\beta,\,k\epsilon K_+}\bar g^k(\alpha\beta)\left(R^k(\alpha\bar\alpha\beta\bar\beta)+2R^k(\alpha\bar\alpha'\beta\bar\beta)\lambda_\alpha+\lambda_\alpha^2R^k(\alpha\bar\alpha'\beta\bar\beta')\right)$$

$$+\sum_{\substack{\alpha\beta\\ k\epsilon K_0}}\bar f^k(\alpha\beta)(1+\delta_{\alpha\beta})\left(R^k(\alpha\bar\beta\alpha\bar\beta)+2\lambda_\beta R^k(\alpha\bar\beta\alpha\bar\beta')+\lambda_\beta{}^2R^k(\alpha\bar\beta'\alpha\bar\beta')\right)$$

$$+\sum_\alpha\ \epsilon_\alpha\bar q_\alpha\int_0^\infty\{\rho_{\bar\alpha\bar\alpha}+2\lambda_\alpha\rho_{\bar\alpha\bar\alpha'}+\lambda_\alpha^2\rho_{\bar\alpha'\bar\alpha'}\}$$

$$+\sum_{\substack{\alpha\neq\beta\\ \kappa_\alpha=\kappa_\beta}}\epsilon_{\alpha\beta}\int_0^\infty\{\rho_{\bar\alpha\bar\beta}+2\lambda_\alpha\rho_{\bar\alpha'\bar\beta}+\lambda_\alpha^2\rho_{\bar\alpha'\bar\beta'}\}\qquad -\sum_{\substack{\alpha\beta\\ \kappa_\alpha=-\kappa_\beta}}2\eta_{\alpha\beta}\int_0^\infty(\rho_{\alpha\bar\beta}+\lambda_\beta\rho_{\alpha\bar\beta'})$$

(A2.18)

The condition that this be stationary now reads

$$\frac{\partial G}{\partial\lambda_a}=0 \qquad \text{(A2.19)}$$

from which we obtain the equation

$$\lambda_a\Bigg(\int_0^\infty\left[2c\Omega_a\left(\frac{d}{dr}-\frac{\kappa_a}{r}\right)\Pi_a-2c^2\Omega_a{}^2-\frac{Z_N}{r}(\Pi_a{}^2+\Omega_a{}^2)\right]$$

$$+\sum_{b,\,k\epsilon K_-}\frac{\bar g^k(ab)}{\bar q_a}R^k(\bar a'\bar a'bb)\qquad +\sum_{b,\,k\epsilon K_+}\frac{\bar g^k(ab)}{\bar q_a}R^k(a\bar a'b\bar b')$$

$$+\sum_{b,\,k\epsilon K_0}\frac{\bar f^k(ab)(1+\delta_{ab})}{\bar q_a}R^k(b\bar a'b\bar a')+\epsilon_a\int_0^\infty\rho(\bar a'\bar a'_{\cdot})+\sum_{\substack{b\neq a\\ \kappa_b=\kappa_a}}\frac{\epsilon_{ab}}{\bar q_a}\int_0^\infty\rho(\bar a',\bar b)\Bigg)$$

$$+\sum_b\lambda_b\{-\sum_{k\epsilon K_-}\frac{\bar g^k(ab)}{\bar q_a}R^k(\bar a'ab\bar b')\ +\sum_{\substack{b\\ \kappa_b=-\kappa_a}}\frac{\eta_{ab}}{\bar q_a}\int_0^\infty\rho(\bar a',b)$$

$$=-\int_o^\infty\left[c\bar{Q}_a\left(\frac{d}{dr}-\frac{\kappa_a}{r}\right)\Pi_a+c\Omega_a\left(\frac{d}{dr}-\frac{\kappa_a}{r}\right)\bar{P}_a-2c^2\bar{Q}_a\Omega_a-\frac{Z_N}{r}(\bar{P}_a\Pi_a+\bar{Q}_a\Omega_a)\right]+\int_o^\infty\rho\,(P_a\Omega_a-Q_a\Pi_a)$$

$$+\sum_{b,k\in K_-}\frac{\bar{g}^k(ab)}{\bar{q}_a}\left[R^k(\bar{a}'abb)-R^k(\bar{a}'\bar{a}bb)\right]-\sum_{b,k\in K_+}\frac{\bar{g}^k(ab)}{\bar{q}_a}R^k(a\bar{a}'\,b\bar{b})-\sum_{\substack{b\\k\in K_o}}\frac{\bar{f}^k(ab)(1+\delta_{ab})}{\bar{q}_a}R^k(b\bar{a}b$$

$$-\varepsilon_a\int_o^\infty\rho(\bar{a}\bar{a}')-\sum_{\substack{b\neq a\\ \kappa_b=\kappa_a}}\frac{\varepsilon_{ab}}{\bar{q}_a}\int_o^\infty\rho(\bar{a}'\bar{b}) \qquad \text{(A2.20)}$$

where we have written, for clarity, $\rho(ab)$ in place of ρ_{ab}

This yields $N_w + N_\eta$ linear equations in $N_w + N_\eta$ unknowns, which can again be solved easily.

Another variation on this latter scheme is to take

$$\Pi_a^{(n)}=\left(\frac{d}{dr}-\frac{\kappa_a}{r}\right)\bar{P}_a^{(n)}-\left(2c-\frac{\varepsilon_a}{c}+\frac{Y_a}{cr}\right)\bar{Q}_a^{(n)}+\frac{\bar{\chi}_a^{(P)(n)}}{r}$$

$$\Omega_a^{(n)}=\left(\frac{d}{dr}-\frac{\kappa_a}{r}\right)\bar{Q}_a^{(n)}+\left(\frac{-\varepsilon_a}{c}+\frac{Y_a}{cr}\right)\bar{P}_a^{(n)}+\frac{\bar{\chi}_a^{(Q)(n)}}{r} \qquad \text{(A2.21)}$$

This is suggested since then we cannot get zero on the right-hand side of equation (A2.20) unless $\bar{P}_a$ and $\bar{Q}_a$ satisfy the MCDF-PNC equations.

We again include the orthogonality condition (A2.12); this time it yields

$$\lambda_a\int_o^\infty\rho(\bar{a}'^{(n)},b)-\lambda_b\int_o^\infty\rho(\bar{b}'^{(n)},a)=\int_o^\infty\rho(a,\bar{b}^{(n)})-\int_o^\infty\rho(\bar{a}^{(n)},b) \qquad \text{(A2.22)}$$

For $n \geq 1$ we already have $\bar{a}^{(n)}$ and $\bar{b}^{(n)}$ suitably orthogonalized; in this case the equation (A2.22) reduces to

$$\lambda_a\int_o^\infty\rho(\bar{a}'^{(n)},b)-\lambda_b\int_o^\infty\rho(\bar{b}'^{(n)},a)=0 \qquad \text{(A2.23)}$$

The above schemes described above are all iterative. A non-iterative scheme - more in the spirit of Roothaan's method - follows.

A considèration of the generalized exchange potentials $\bar{\chi}^{(P)}$ and $\bar{\chi}^{(Q)}$ as defined in equations (6.3.46) and (6.3.47) shows that there are two distinct regions. In the region $r \lesssim r_N$, where r_N is the nuclear radius, we have

$$\bar{\chi}_a^{(P)} \sim - \frac{P_a}{c} \rho(r).r = \bar{\chi}_a^{(P)(0)}$$

$$\bar{\chi}^{(q)} \sim - \frac{Q_a}{r} \rho(r).r = \bar{\chi}_a^{(Q)(0)} \qquad \text{(A2.24)}$$

by virtue of the large value of $\rho(r)$ ($\sim 10^{12}$). In the region $r \gtrsim r_N$ we have $\rho(r) \sim 0$, and in this case the exchange potentials will take the more conventional form

$$\bar{\chi}_a^{(P)} \sim r \sum_{\substack{b \neq a \\ \kappa_b = \kappa_a}} \frac{\varepsilon_{ab}}{c\bar{q}_a} Q_b + r \sum_{\kappa_b = -\kappa_a} \frac{\eta_{ab}}{c\bar{q}_a} Q_b + \bar{\chi}_a^{(P)} \qquad \text{(A2.25)}$$

with a similar expression for $\bar{\chi}_a^{(Q)}$.

Therefore, it may be that the solution of the MCDF-PNC equations (6.3.44) and (6.3.45) with $\bar{\chi} = \bar{\chi}^{(0)}$ will yield reliable solutions to the MCDF-PNC equations in the region $r \lesssim r_N$; and then we can attempt to allow for the effects of the exchange potentials by mixing this with multiples of parity conserving wavefunctions of the opposite κ (which will be solutions of similar equations, with similar exchanges and the same κ as the MCDF-PNC equations in $r \gtrsim r_N$).

We write, therefore,

$$\bar{\bar{P}}_a = \sum_{\substack{b \\ \kappa_a=\kappa_b}} \lambda_a^b \bar{\bar{P}}_b + \sum_{\substack{b \\ \kappa_a=-\kappa_b}} \mu_a^b P_b$$

$$\bar{\bar{Q}}_a = \sum_{\substack{b \\ \kappa_a=\kappa_b}} \lambda_a^b \bar{\bar{Q}}_b + \sum_{\substack{b \\ \kappa_a=-\kappa_b}} \mu_a^b Q_b \qquad \text{(A2.26)}$$

where $\bar{\bar{P}}$ and $\bar{\bar{Q}}$ are solutions of the MCDF-PNC equations with $\bar{\chi} = \chi^{(0)}$. We then vary λ_a^b and μ_a^b so as to minimize the functional $\mathcal{G}$ of equation (A2.1).

There is, of course, no reason why coefficients λ_a^b and μ_a^b should be included for all orbital pairs (a,b); in fact, the number will frequently need to be reduced for computational reasons.

Substitution of equation (A2.26) into equation (A2.1) gives

$$\mathcal{G} = \sum_\alpha \bar{q}_\alpha \int_0^\infty \Big\{ 2c \sum_\gamma (\lambda_\alpha^\gamma \bar{\bar{Q}}_\gamma + \mu_\alpha^\gamma Q_\gamma) \left(\frac{d}{dr} - \frac{\kappa_\alpha}{r}\right) \sum_\delta (\lambda_\alpha^\delta \bar{\bar{P}}_\delta + \mu_\alpha^\delta P_\delta)$$

$$-2c^2 \sum_\gamma (\lambda_\alpha^\gamma \bar{\bar{Q}}_\gamma + \mu_\alpha^\gamma Q_\gamma) \sum_\delta (\lambda_\alpha^\delta \bar{\bar{Q}}_\delta \mu_\alpha^\delta Q_\delta)$$

$$- \frac{Z_N}{r} \sum_{\gamma\delta} \Big[(\lambda_\alpha^\gamma \bar{\bar{P}}_\gamma + \mu_\alpha^\gamma P_\gamma)(\lambda_\alpha^\delta \bar{\bar{P}}_\delta + \mu_\alpha^\delta P_\delta) + (\lambda_\alpha^\gamma \bar{\bar{Q}}_\gamma + \mu_\alpha^\gamma Q_\gamma)(\lambda_\alpha^\delta \bar{\bar{Q}}_\delta + \mu_\alpha^\delta Q_\delta) \Big] \Big\}$$

$$-2 \sum_\alpha \bar{q}_\alpha \int_0^\infty \rho \sum_\gamma \{ P_\alpha (\lambda_\alpha^\gamma \bar{\bar{Q}}_\gamma + \mu_\alpha^\gamma Q_\gamma) - Q_\alpha (\lambda_\alpha^\gamma \bar{\bar{P}}_\gamma + \mu_\alpha^\gamma P_\gamma) \}$$

$$\sum_\alpha \varepsilon_\alpha \bar{q}_\alpha \int_0^\infty \sum_{\gamma\delta} \{ \lambda_\alpha^\gamma \lambda_\alpha^\delta \rho(\bar{\bar{\gamma}}\bar{\bar{\delta}}) + 2\lambda_\alpha^\gamma \mu_\alpha^\delta \rho(\bar{\bar{\gamma}}\delta) + \mu_\alpha^\gamma \mu_\alpha^\delta \rho(\gamma\delta) \}$$

$$
\begin{aligned}
&- \sum_{\substack{k\in\mathbb{K}_- \\ \alpha\beta\gamma\delta}} \bar{g}^k(\alpha\beta)\{\lambda_\alpha^\gamma\lambda_\beta^\delta R^k(\bar{\bar{\gamma}}\alpha\beta\bar{\bar{\delta}})+2\lambda_\alpha^\gamma\mu_\beta^\delta R^k(\bar{\bar{\gamma}}\alpha\beta\delta)+\mu_\alpha^\gamma\mu_\beta^\delta R^k(\gamma\alpha\beta\delta) \\
&\qquad -\lambda_\alpha^\gamma\lambda_\alpha^\delta R^k(\bar{\bar{\gamma}}\bar{\bar{\delta}}\beta\beta)-2\lambda_\alpha^\gamma\mu_\alpha^\delta R^k(\bar{\bar{\gamma}}\delta\beta\beta)-\mu_\alpha^\gamma\mu_\alpha^\delta R^k(\gamma\delta\beta\beta)\} \\
&+ \sum_{\substack{k\in\mathbb{K}_+ \\ \alpha\beta\gamma\delta}} \bar{g}^k(\alpha\beta)\{\lambda_\alpha^\gamma\lambda_\beta^\delta R^k(\alpha\bar{\bar{\gamma}}\beta\bar{\bar{\delta}})+2\lambda_\alpha^\gamma\mu_\beta^\delta R^k(\alpha\bar{\bar{\gamma}}\beta\delta)+\mu_\alpha^\gamma\mu_\beta^\delta R^k(\alpha\gamma\beta\delta)\} \\
&+ \sum_{\substack{k\in\mathbb{K}_o \\ \alpha\beta\gamma\delta}} (1+\delta_{\alpha\beta})\bar{f}^k(\alpha\beta)\{\lambda_\alpha^\gamma\lambda_\alpha^\delta R^k(\bar{\bar{\gamma}}\beta\bar{\bar{\delta}}\beta)+2\lambda_\alpha^\gamma\mu_\alpha^\delta R^k(\bar{\bar{\gamma}}\beta\delta\beta)+\mu_\alpha^\gamma\mu_\alpha^\delta R^k(\gamma\beta\delta\beta)\} \\
&+ \sum_{\substack{\alpha\beta\gamma\delta \\ \kappa_\alpha=\kappa_\beta}} \varepsilon_{\alpha\beta}\int_o^\infty\{\lambda_\alpha^\gamma\lambda_\beta^\delta\rho(\bar{\bar{\gamma}}\bar{\bar{\delta}})+2\lambda_\alpha^\gamma\mu_\beta^\delta\rho(\bar{\bar{\gamma}}\delta)+\mu_\alpha^\gamma\mu_\beta^\delta\rho(\gamma\delta)\} \\
&-2 \sum_{\substack{\alpha\beta\delta \\ \kappa_\alpha=-\kappa_\beta}} \eta_{\alpha\beta}\int_o^\infty\{\lambda_\beta^\delta\rho(\alpha\bar{\bar{\delta}})+\mu_\beta^\delta\rho(\alpha\delta)\} \qquad \text{(A2.27)}
\end{aligned}
$$

The requirement that λ_b^d and μ_b^d should give a stationary value of G is written, as before as

$$\frac{\partial G}{\partial \lambda_b^d} = 0 \qquad \text{(A2.28)}$$

$$\frac{\partial G}{\partial \mu_b^d} = 0 \qquad \text{(A2.29)}$$

Then from equation (A2.28) we obtain

$$
\begin{aligned}
\sum_a \lambda_b^a \Bigg\{ &\int_o^\infty \Big(c\bar{\bar{Q}}_d\Big(\frac{d}{dr}-\frac{\kappa_b}{r}\Big)\bar{\bar{P}}_a+c\bar{\bar{Q}}_a\Big(\frac{d}{dr}-\frac{\kappa_b}{r}\Big)\bar{\bar{P}}_d-2c^2\bar{\bar{Q}}_a\bar{\bar{Q}}_d-\frac{Z_N}{r}\rho(\bar{\bar{d}}\bar{\bar{a}})+\varepsilon_b\rho(\bar{\bar{d}}\bar{\bar{a}})\Big) \\
&+ \sum_{c,k\in\mathbb{K}_-} \frac{\bar{g}^k(ab)}{\bar{q}_b} R^k(\bar{\bar{d}}\bar{\bar{a}}cc)+ \sum_{c,k\in\mathbb{K}_o} \frac{(1+\delta_{bc})\bar{f}^k(bc)}{\bar{q}_b} R^k(\bar{\bar{d}}c\bar{\bar{a}}c)\Bigg\}
\end{aligned}
$$

$$+\sum_a \mu_b^a \left\{ \int_o^\infty (c\bar{\bar{Q}}_d \left(\frac{d}{dr} - \frac{\kappa_b}{r}\right) P_a + cQ_a \left(\frac{d}{dr} - \frac{\kappa_b}{r}\right) \bar{\bar{P}}_d - 2c^2 Q_a \bar{\bar{Q}}_d - \frac{Z_N}{r} \rho(\bar{\bar{da}}) + \varepsilon_b \rho(\bar{\bar{da}}) \right.$$

$$\left. + \sum_{c,k\in K_-} \frac{\bar{g}^k(ab)}{\bar{q}_b} R^k(\bar{\bar{dacc}}) + \sum_{c,k\in K_o} \frac{(1+\delta_{bc})\bar{f}^k(bc)}{\bar{q}_b} R^k(\bar{\bar{dcac}}) \right\}$$

$$+\sum_{ac} \lambda_c^a \{ -\sum_{k\in K_-} \frac{\bar{g}^k(bc)}{\bar{q}_b} R^k(\bar{\bar{dbca}}) + \sum_{k\in K_+} \frac{\bar{g}^k(bc)}{\bar{q}_b} R^k(b\bar{\bar{d}}\bar{\bar{c}}a) + \frac{\varepsilon_{bc}}{\bar{q}_b} \int_o^\infty \rho(\bar{\bar{da}}) \}$$

$$\sum_{ac} \mu_c^a \{ -\sum_{k\in K_-} \frac{\bar{g}^k(bc)}{\bar{q}_b} R^k(\bar{\bar{dbca}}) + \sum_{k\in K_+} \frac{\bar{g}^k(bc)}{\bar{q}_b} R^k(b\bar{\bar{d}}ca) + \frac{\varepsilon_{bc}}{\bar{q}_b} \int_o^\infty \rho(\bar{\bar{da}}) \}$$

$$- \sum_{\substack{a \\ \kappa_a = -\kappa_b}} \frac{\eta_{ab}}{\bar{q}_b} \int_o^\infty \rho(\bar{\bar{ad}}) = \int_o^\infty \rho(P_b \bar{\bar{Q}}_d - Q_b \bar{\bar{P}}_d) \qquad \text{(A2.30)}$$

and equation (A2.29) gives us

$$\sum_a \lambda_b^a \left\{ \int_o^\infty \left[c\{Q_d \left(\frac{d}{dr} - \frac{\kappa_b}{r}\right) \bar{\bar{P}}_a + \bar{\bar{Q}}_a \left(\frac{d}{dr} - \frac{\kappa_b}{r}\right) P_d\} - 2c^2 Q_d \bar{\bar{Q}}_a - \frac{Z_N}{r} (Q_d \bar{\bar{Q}}_a + P_d \bar{\bar{P}}_a) + \varepsilon_b \rho(\bar{\bar{ad}}) \right] \right.$$

$$\left. + \sum_{c,k\in K_-} \frac{\bar{g}^k(bc)}{\bar{q}_b} R^k(\bar{\bar{adcc}}) + \sum_{c,k\in K_o} \frac{(1+\delta_{bc})}{\bar{q}_b} \bar{f}^k(bc)\, R^k(\bar{\bar{acdc}}) \right\}$$

$$+\sum_a \mu_b^a \left\{ \int_o^\infty \left[c\{Q_d \left(\frac{d}{dr} - \frac{\kappa_b}{r}\right) P_a + Q_a \left(\frac{d}{dr} - \frac{\kappa_b}{r}\right) P_d\} - 2c^2 Q_d Q_a - \frac{Z_N}{r} (P_a P_d + Q_a Q_d) + \varepsilon_b \rho(ad) \right] \right.$$

$$\left. + \sum_{c,k\in K_-} \frac{\bar{g}^k(bc)}{\bar{q}_b} R^k(adcc) + \sum_{c,k\in K_+} \frac{(1+\delta_{bc})}{\bar{q}_b} \bar{f}^k(bc)\, R^k(acdc) \right\}$$

$$+\sum_{ac} \lambda_c^a \{ -\sum_{k\in K_-} \frac{\bar{g}^k(bc)}{\bar{q}_b} R^k(\bar{\bar{acbd}}) + \sum_{k\in K+} \frac{\bar{g}^k(bc)}{\bar{q}_b} R^k(\bar{\bar{cabd}}) + \frac{\varepsilon_{bc}}{\bar{q}_b} \int_o^\infty \rho(\bar{\bar{ad}}) \}$$

$$+\sum_{ac} \mu_c^a \{ -\sum_{k\in K_-} \frac{\bar{g}^k(bc)}{\bar{q}_b} R^k(acbd) + \sum_{k\in K_+} \frac{\bar{g}^k(bc)}{\bar{q}_b} R^k(cabd) + \frac{\varepsilon_{bc}}{\bar{q}_b} \int_o^\infty \rho(ad) \}$$

$$- \sum_{\substack{a \\ \kappa_a = -\kappa_b}} \eta_{ab} \int_o^\infty \frac{\rho(ad)}{\bar{q}_b} = \int_o^\infty \rho(P_b Q_d - Q_b P_d) \qquad \text{(A2.31)}$$

The orthogonality condition (A2.13) now takes the form

$$\sum_c \{\lambda_a^c \int_0^\infty (\bar{\bar{P}}_c \; P_b + \bar{\bar{Q}}_c \; Q_b) - \mu_b^c \int_o^\infty (P_a P_c + Q_a Q_c)\}$$

$$- \sum_d \{\lambda_b^d \int_o^\infty (\bar{\bar{P}}_d \; P_a + \bar{\bar{Q}}_d \; Q_a) - \mu_a^d \int_o^\infty (P_b P_d + Q_b Q_d)\} = 0 \qquad \text{(A2.32)}$$

This scheme has the advantage over those outlined earlier not only of speed, but that the basis functions used are more reasonable on physical grounds than the numerical ones used in the iterative schemes.

Appendix 3

And be fruitful, and multiply upon the earth.

The Lord (-2348)

Formulae for the PNC Lagrange Multipliers

APPENDIX 3

FORMULAE FOR THE P N C LAGRANGE MULTIPLIERS

We may write the MCDF equations (2.2.22) as

$$\left(\mathbb{L} - \varepsilon_a + \frac{Y_a}{r}\right) U_a = V_a \qquad \text{(A3.1)}$$

where

$$U_a = \begin{Bmatrix} P_a \\ Q_a \end{Bmatrix} \qquad \text{(A3.2)}$$

$$V_a = \begin{Bmatrix} -\frac{c}{r}\chi_a^{(Q)} \\ \\ +\frac{c}{r}\chi_a^{(P)} \end{Bmatrix} \qquad \text{(A3.3)}$$

and the operator $\mathbb{L}$ contains the derivative, κ_a and $-2c^2$ terms, and the MCDF-PNC equations (6.3.44) and (6.3.45) for an orbital b with $\kappa_b = -\kappa_a$ as

$$\left(\mathbb{L} - \varepsilon_b + \frac{Y_b}{r}\right) \bar{U}_b = \bar{V}_b + \sum_c \frac{\eta_{bc}}{\bar{q}_b} U_c \qquad \text{(A3.4)}$$

where

$$\bar{V}_a = \begin{Bmatrix} -\frac{c}{r}\chi_a^{(Q)} \Big|_{\eta = 0} \\ \\ \frac{c}{r}\chi_a^{(P)} \Big|_{\eta = 0} \end{Bmatrix} \qquad \text{(A3.5)}$$

Then

$$\langle a|\mathbb{L}|\bar{b}\rangle = \langle a|\bar{V}_b + \sum_c \frac{\eta_{bc}}{\bar{q}_b} U_c + \varepsilon_b \bar{U}_b - \frac{Y_b}{r}\bar{U}_b\rangle$$

$$= \langle a|V_b\rangle + \frac{\eta_{ba}}{-} + \varepsilon_b \langle a|\bar{b}\rangle - \langle a|\frac{Y_b}{r}|\bar{b}\rangle \qquad \text{(A3.6)}$$

We also exploit the fact that $\mathbb{L}$ is Hermitian to write

$$\langle a|\mathbb{L}|\bar{b}\rangle = \langle \varepsilon_a U_a - \frac{Y_a}{r} U_a + V_a|\bar{b}\rangle$$

$$= \varepsilon_a \langle a|\bar{b}\rangle - \langle a|\frac{Y_a}{r}|\bar{b}\rangle + \langle V_a|\bar{b}\rangle \qquad \text{(A3.7)}$$

Combining (A3.6) and (A3.7) we obtain

$$\langle a|\bar{b}\rangle\ (\varepsilon_a-\varepsilon_b) = \langle a|\bar{V}_b\rangle + \frac{\eta_{ba}}{\bar{q}_a} - \langle a|\frac{Y_b}{r}|\bar{b}\rangle + \langle a|\frac{Y_a}{r}|\bar{b}\rangle - \langle V_a|\bar{b}\rangle$$

(A3.8)

Similarly

$$\langle b|\bar{a}\rangle\ (\varepsilon_b-\varepsilon_a) = \langle b|\bar{V}_a\rangle + \frac{\eta_{ab}}{\bar{q}_b} - \langle b|\frac{Y_a}{r}|\bar{a}\rangle + \langle b|\frac{Y_b}{r}|\bar{a}\rangle - \langle V_b|\bar{a}\rangle$$

(A3.9)

We wish to choose η_{ab} such that

$$\langle a|\bar{b}\rangle = \langle b|\bar{a}\rangle \qquad \text{(A3.10)}$$

If this is so, then (providing $\bar{q}_a \neq \bar{q}_b$)

$$\langle a|\bar{V}_b\rangle - \langle V_a|\bar{b}\rangle + \langle b|\bar{V}_a\rangle - \langle V_b|\bar{a}\rangle + \langle a|\frac{Y_a-Y_b}{r}|\bar{b}\rangle + \langle b|\frac{Y_b-Y_a}{r}|\bar{a}\rangle$$

$$+ \frac{\eta_{ba}}{\bar{q}_b} + \frac{\eta_{ab}}{\bar{q}_a} = 0 \qquad \text{(A3.11)}$$

Whence, using the definitions of V_a and V_b and the anti-symmetry of the η_{ab}

$$\eta_{ab}=\int_o^\infty\Big[\frac{-c}{r}\,P_a\bar{\chi}_b^{(Q)}+\frac{c}{r}\,Q_a\bar{\chi}_b^{(P)}+\frac{c}{r}\,\chi_a^{(Q)}\bar{P}_b-\frac{c}{r}\,\chi_a^{(P)}\bar{Q}_a-P_b\,\frac{c}{r}\,\bar{\chi}_a^{(Q)}+Q_b\,\frac{c}{r}\,\bar{\chi}_a^{(P)}$$

$$+\bar{P}_a\,\frac{c}{r}\,\chi_b^{(Q)}-\bar{Q}_a\,\frac{c}{r}\,\chi_b^{(P)}+\frac{(Y_a-Y_b)}{r}\,(P_a\bar{P}_b+Q_a\bar{Q}_b-P_b\bar{P}_a-Q_b\bar{Q}_a)\Big]\,dr$$

$$\Big/\;\frac{1}{\bar{q}_b}-\frac{1}{\bar{q}_a} \qquad\qquad (A3.12)$$

where the $\bar{\chi}$ are calculated taking $\eta = 0$.

If the orbital a is fixed, as in a correlation calculation (Chapter 8), then the above analysis does not hold. But in this case we know $\langle\bar{a}|b\rangle$. Thus, if we have $\langle a|\bar{b}\rangle = \langle b|\bar{a}\rangle$, then from (A3.8)

$$\eta_{ba}=\bar{q}_b\left(\langle\bar{a}|b\rangle(\varepsilon_a-\varepsilon_b)-\langle a|\bar{V}_b\rangle+\langle a|\frac{Y_b-Y_a}{r}|\bar{b}\rangle+\langle V_a|\bar{b}\rangle\right)$$

$$=\bar{q}_b\int_o^\infty\Big((\varepsilon_a-\varepsilon_b)(\bar{P}_aP_b+\bar{Q}_aQ_b)+\frac{c}{r}P_a\bar{\chi}_b^{(Q)}\Big|_{\eta=0}-\frac{c}{r}Q_a\bar{\chi}_b^{(P)}\Big|_{\eta=0}-\frac{c}{r}\bar{P}_b\chi_a^{(Q)}+\frac{c}{r}\bar{Q}_b\chi_a^{(P)}$$

$$+\frac{Y_b-Y_a}{r}\;(P_a\bar{P}_b+Q_a\bar{Q}_b)\Big)dr \qquad\qquad (A3.13)$$

providing that the potentials Y_a and χ_a are those used to calculate the orbital a and are not calculated in the obvious way.

Appendix 4

And Joshua charged them that went to describe the land, saying

"Go and walk through the land, and describe it, and come again to me, that I may here cast lots for you before the LORD at Shiloh"

Joshua (-1433)

Description of the Computer Programs

APPENDIX 4

DESCRIPTION OF THE COMPUTER PROGRAMS

§A4.1 Introduction

A listing of the computer programs used to generate the results reported in chapter 8 is given in appendix 5.

There are five separate programs: firstly, the routines that are modified to produce MCP coefficients diagonal in the configurations for the "wrong" values of k, which are used in the PNC MCDF equations (6.3.44) and (6.3.45); secondly, the main program that solved the PNC-MCDF equations; thirdly, the PNC oscillator strengths program; fourthly, the modifications to the MCP program needed to make it generate coefficients for the PNC mixing coefficients program; and finally the PNC mixing coefficients program itself.

§A4.2 The modified MCP routines as used for diagonal coefficients

These are given for completeness only, since the modifications to the standard routines (Grant et al. (1980)) are trivial. MCP has been altered so that only the coefficients $V^k_{rr}(abcd)$ are calculated, since in an EAL-type calculation the coefficients $V^k_{rs}(abcd)$ $(r \neq s)$ are used only to determine mixing coefficients and energies, and not to evaluate wavefunctions, and the former are known already from the parity conserving MCDF calculation.

The changes to SKRC are similarly trivial; they are reflected in the redefinition of the quantities KD1 and KE1.

§A4.3 The MCDF-PNC program

This is an essentially new program, although several of the routines have been taken from the standard MCDF package The general structure is represented in figure A4.1.

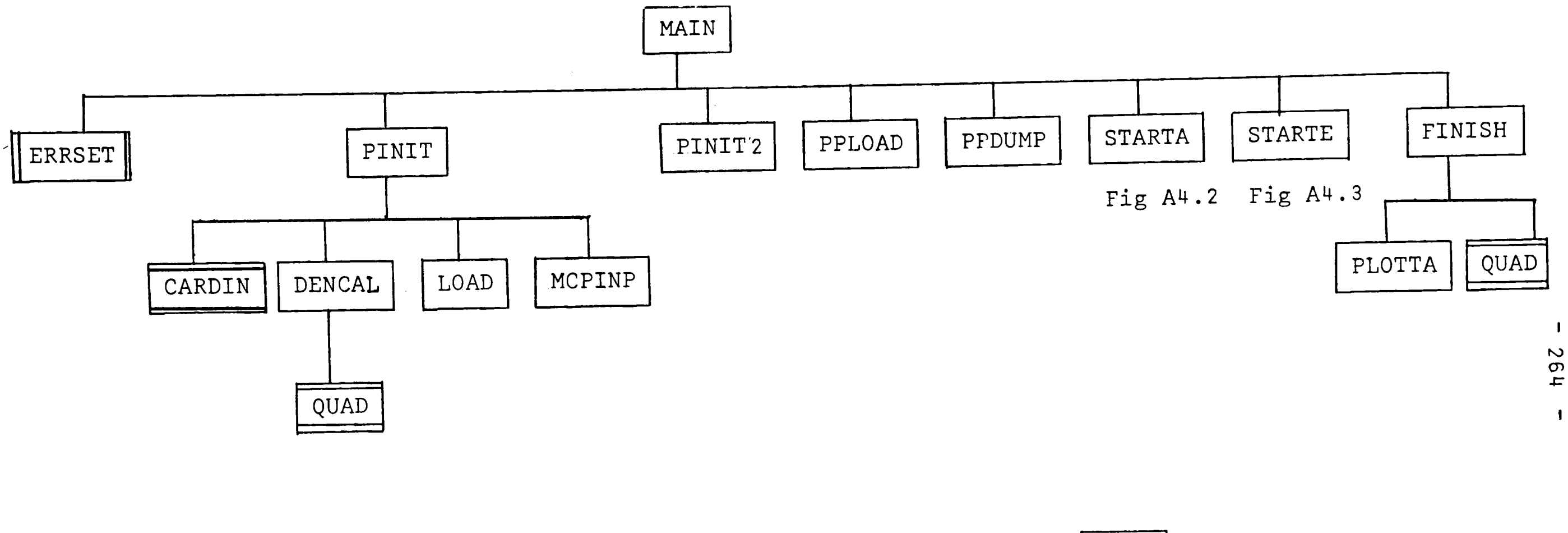

ERRSET IBM supplied local routine

QUAD Routine taken without significant modification from MCDF package

Figure A4.1 Structure of the MCDF PNC program

The MAIN routine controls the sequence of the calculation and is varied from run to run.. The example given is for demonstration purposes only.

ERRSET is an IBM routine used here to suppress underflow error messages.

PINIT initializes the problem by setting the fortran stream numbers and reading the data using the free-format card reader CARDIN. A call to LOAD supplies all the relevant MCDF data; the off-diagonal MCP coefficients are not needed and so are rejected to save computer space. A radial grid is set up, which saves time later and enables the code to be optimized better by the compiler. Since we are interested in the value of the PC wavefunctions near the origin and the standard MCDF program sets these to zero if they are less than 10^{-10}, they are reconstructed assuming a simple power series expansion. MCPINP - similar to the standard MCPIN - reads in the PNC MCP coefficients, while DENCAL calculates the nuclear density corresponding to either a Fermi or a uniform nucleus. Finally, we change the values of kappa and ℓ, since this will enable us to use some routines from the MCDF package without modification.

PINIT2, which is not always called, decides which PNC Lagrange multipliers should be included, and sets them to the required values.

PPLOAD loads the PNC wavefunctions from a previous run into core. These are dumped to disk by PPDUMP at frequent intervals.

STARTA, whose structure is shown in figure A4.2, calculates the PNC wavefunctions, without the inclusion of exchange or

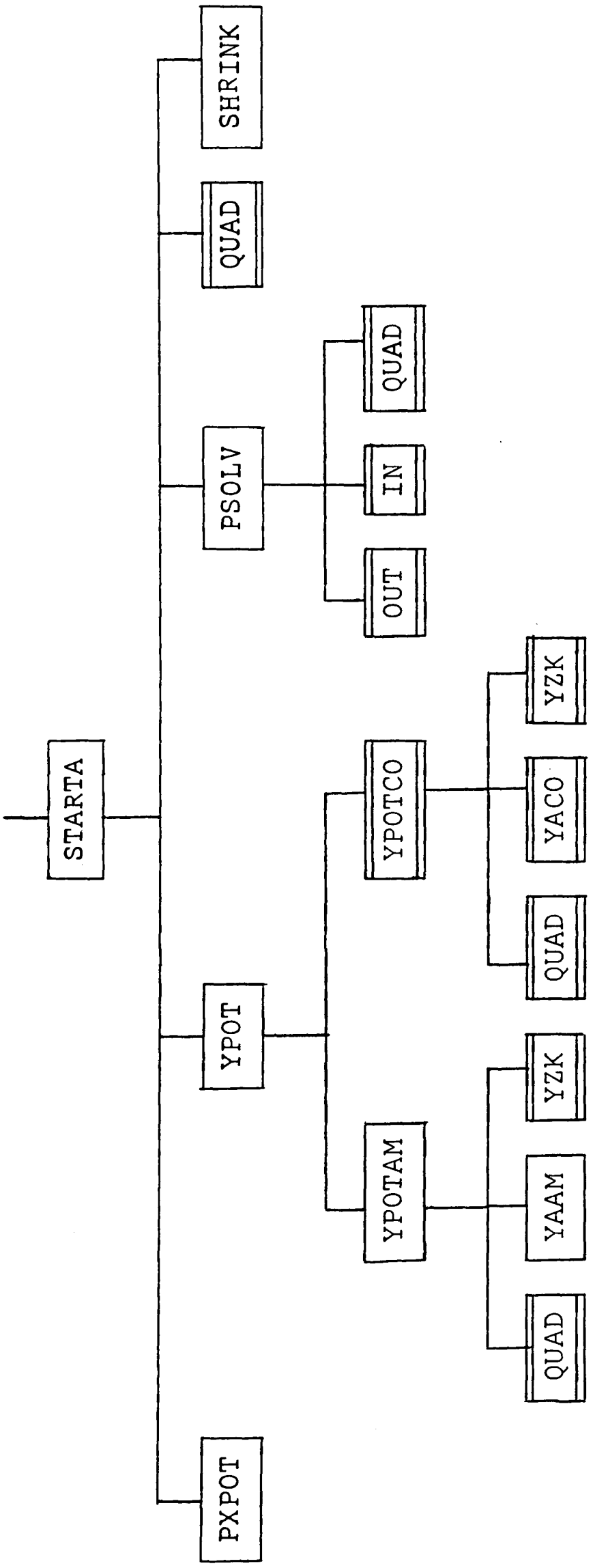

Figure A4.2 Routines called from STARTA in the MCDF FNC program

For explanation of boxing, see Fig. A4.1

difference corrections. For each orbital an estimate of the initial slope of the $\overline{P}$-wavefunction and the normalization is made, the underlying philosophy being that $|\overline{n\kappa}\rangle$ should look something like $|m\ -\kappa\rangle$ for $m \sim n$. If no such $|m\ -\kappa\rangle$ exists we just guess. In practice, this always seems to give acceptable initial estimates. We calculate the driving terms and direct potentials by calls to PXPOT and YPOT, and then solve the MCDF-PNC by a call to PSOLV.

The routine PSOLV solves the MCDF-PNC equations (6.3.44) and (6.3.45) by using a four-point formula for $\frac{d\overline{P}}{dr}$. Corrections may be included to allow for the differences between this and a six-point formula. The routine follows, to a great extent, the routine SOLV of the MCDF package. Many of its features have already been described in § 5.3; others worthy of note are that the wavefunctions are rescaled to unit norm for stability - they are set to zero if they fall to less than 10^{-10} at large distances - in the main iterative section, which we require to be passed through at least four times - this being the number necessary for the normalization to settle down. The outward integration is performed by OUT, the inward by IN.

STARTE is similar to STARTA, except that it must have initial estimates for the wavefunctions to start from. For each orbital, we repeatedly

(i) calculate the driving terms and exchange and direct potentials by calling PXPOT3 and YPOT.

(ii) solve the MCDF-PNC equations by SOLV,

(iii) change the component of $|ns\rangle$ in $|\overline{np}\rangle$ if necessary,

and

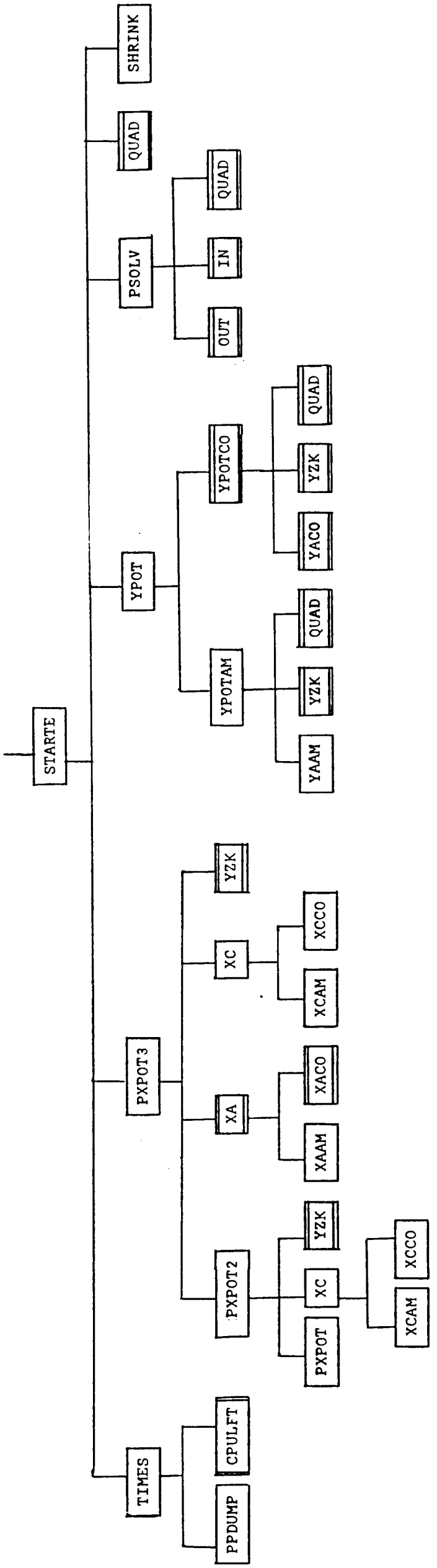

Figure A4.3. Routines called for STARTE in the MCDF PNC program.
For explanation of boxing, see fig. A4.1.

(iv) damp the change in the wavefunctions if we can improve convergence in this way, and

(v) continue until

$$\frac{\max\left(|\bar{P}_{new}-\bar{P}_{old}|+|\bar{Q}_{new}-\bar{Q}_{old}|\right)}{\text{normalization}} < \text{AXXE}$$

where $\bar{P}_{new}$ and $\bar{Q}_{new}$ are the undamped functions obtained from PSOLV and AXXE is a convergence criterion. A diagram of STARTE is given in Figure A4.3.

The routine YPOT calls YPOTCO or YPOTAM depending on whether the normal or the symmetric forms of the direct potential are required. Similarly, XA is equal to XACO or XAAM and XC equals XCCO or XCAM for an exchange potential without or with diagonal terms included.

PXPOT calculates the driving terms; PXPOT2 adds on the Hartree-Fock exchange, and PXPOT3 adds to this the PNC exchange.

Finally FINISH writes out the parity mixed orthogonalities, and the normalizations of the PNC wavefunctions. If required the wavefunctions can be written out or drawn by a call to PLOTTA.

The program in its present form takes several minutes to run on the IBM 360/195 for the atoms considered.

§A4.4 The PNC oscillator strengths program

This is basically the same as the oscillator strengths routines of the MCDF package. It calculates the matrix elements $\langle f_+^{PM} \| T^L \| i_+^{PM} \rangle$ defined in equation (6.9.4), the other contributions to $\langle f^{PM} \| T^L \| i^{PM} \rangle$ being calculated separately by the standard oscillator strengths program which has only had trivial modifications made to it. The main differences between this and the standard routines are:

(i) only E1 matrix elements can be calculated

(ii) the information on configurations, etc., is read from the MCDF dump rather than being input as data.

The MAIN routine reads in the relevant data using CARDIN, loads the MCDF dump with LOAD, the PNC dump with PPLOAD, and the MCT dump with MCTIN. For each pair of levels requested the requisite Bessel functions are evaluated by BESSJ and then CSFM calculates the matrix elements.

This is done by calls to PSPME, which calculates the single particle matrix elements, with either the bra or the ket being PNC, the orbitals being determined by each MCT coefficient in turn. Multiplication by the MCT coefficient and the relevant mixing coefficient gives the contribution due to each, which are summed as in equation (6.9.4). Once a single particle matrix element has been calculated it is stored in case it is needed again.

Figure A4.4 shows the sequence of routines in this program.

The program takes a few seconds to run.

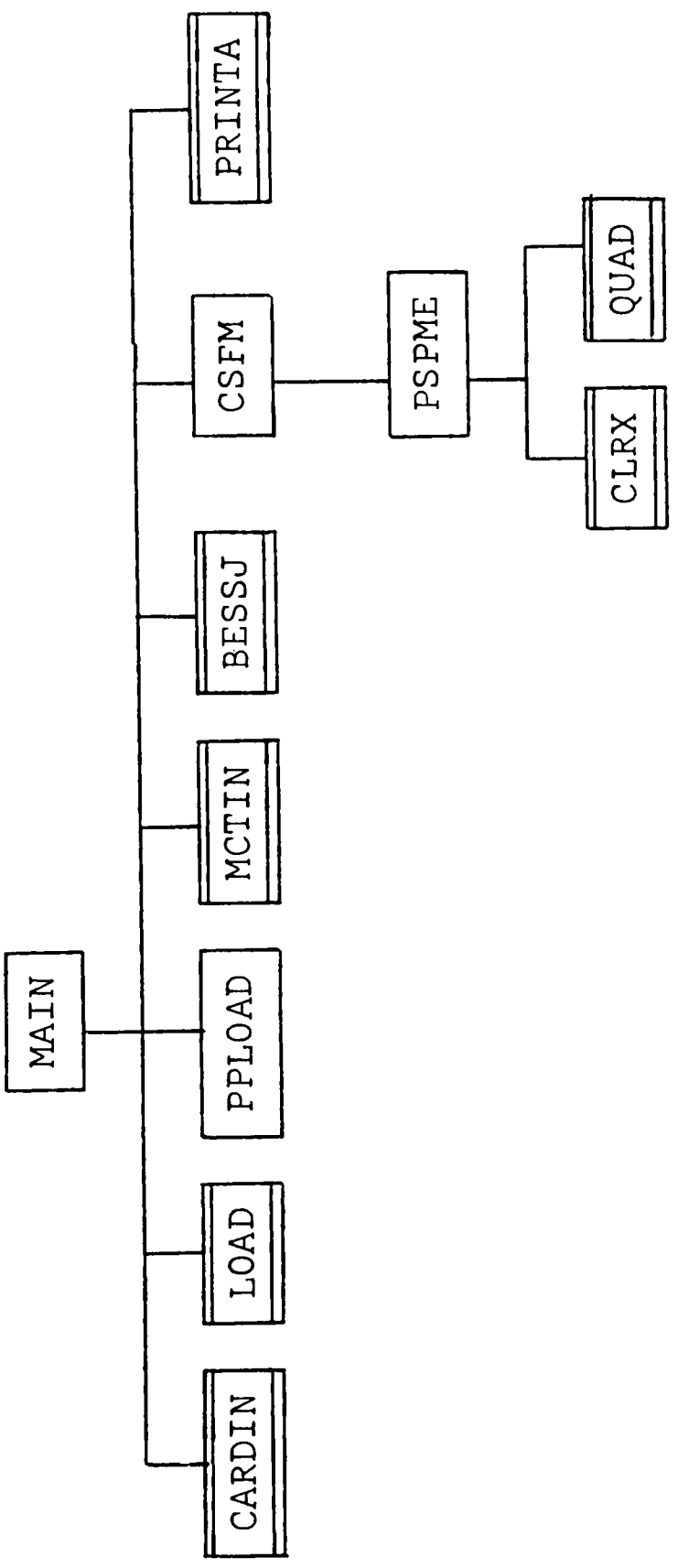

Figure A4.4 The PNC oscillator strengths program. For explanation of boxing see Figure A4.1

§A4.5 Modifications to the MCP program so that it generates coefficients for PNC mixing coefficients program

These modifications to the MCP program are even more trivial than those which were incorporated to allow the calculation of diagonal coefficients; they comprise merely the reversal of a few parity checks in MCP, RKCO and SKRC to reflect the fact that now $k\varepsilon\mathbb{K}_{ac}$ or $k\varepsilon\mathbb{K}_{bd}$ rather than $k\varepsilon\mathbb{K}_{o}$ (for the definitions of these see equations (6.8.6), (6.8.7) and (A1.15a)).

§A4.6 The PNC mixing coefficients program

The sequence of routines which together make up this program is shown in figure A4.5.

The MAIN routine starts with a call to ERRSET. It then calls PART1 which loads and sets up the initial data and also loads the parity conserving wavefunctions. Any mixing coefficients of order G (i.e. any left from a previous calculation) are set to zero and a radial grid is set up.

PART2A then loads the magnetic monopole-type MCT coefficients, calculates the nuclear density, and evaluates the contribution to H_x from V^{PNC} and the parity conserving wavefunctions according to the last term of equation (6.8.10).

This is followed by PART2B that loads the PNC wavefunctions. The PM wavefunctions are then orthogonalized by a Schmidt process if requested. The MCP coefficients corresponding to $k\varepsilon\mathbb{K}_{ac}$ (equation (6.8.6)) and $k\varepsilon\mathbb{K}_{bd}$ (equation (6.8.7)) are next loaded by INVKAC and INVKBD respectively. Finally the remaining terms of H_x are evaluated by MATO. The subroutine

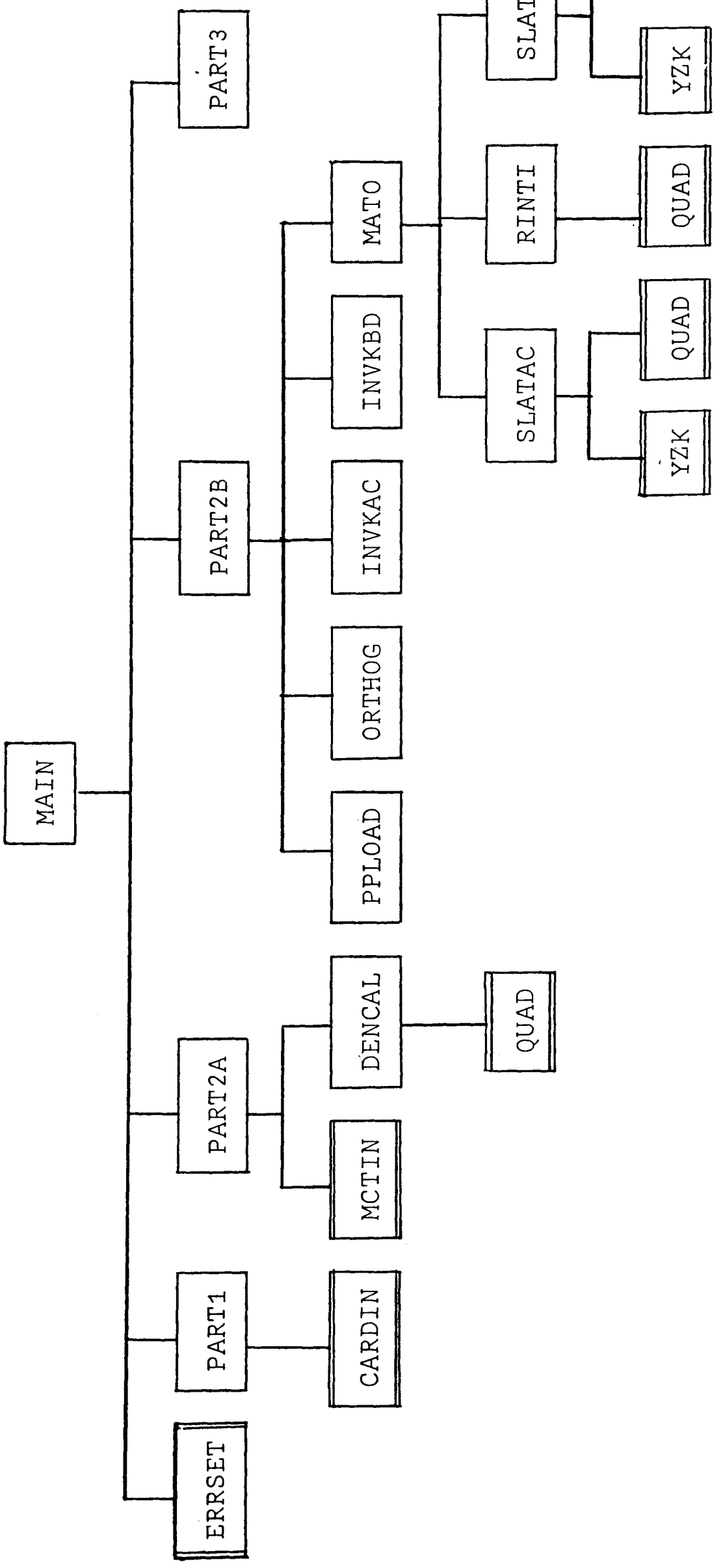

Figure A4.5 The PNC mixing coefficients program. Boxing as in figure A4.1

MATO is based on the routine of the same name in the standard MCDF package., but duplicated to allow for the calculation of the second and third terms in equation(6.8.10). Duplication, rather than quadruplication, occurs, because SLATAC and SLATBD calculate the first two and last two respectively of the Slater integrals simultaneously. RINTI is called to evaluate the integral $\tilde{I}(ab)$ of equations (6.8.10) and (6.8.11)

Finally, PART3 loads the Hamiltonians that have been calculated and dumped by the parity conserving MCDF program and which corresponds to H_+ and H_- in equation (6.8.12). It then diagonalizes the full Hamiltonian by applying the equation (6.8.20) and rewrites the MCDF dump with the new mixing coefficients.

Appendix 5

And now, my son, I have shown thee everything,
and the law of all the stars of the heaven is completed.

"Enoch" (-110)

Listing of the Computer Programs

APPENDIX 5

LISTING OF THE COMPUTER PROGRAMS

The first three computer programs have been listed on microfiche to save paper. The first column contains the modifications to the MCP program to produce the extra MCP coefficients required by the PNC MCDF program; columns two to five contain the complete PNC MCDF program, including the routines taken from the standard MCDF program; and columns six and seven contain the PNC oscillator strengths program, again including the routines taken from the standard MCDF program.

The following pages contain, firstly, the modifications to the MCP program needed to generate the MCP coefficients used in the shielding calculation and the modification to the oscillator strengths program necessary to enable it to calculate the effect of shielding on the E1 matrix element. These are followed by a listing of the program used to calculate PNC mixing coefficients between configurations of opposite parity; it is necessary to supplement this with the routines CARDIN, QUAD, YZK and BLOCKDATA taken from the standard MCDF program and the routines DENCAL and PPLOAD from the PNC MCDF program. As listed, the program will not PM orthogonalize functions or generate Slater functions, although orthogonalization may be brought about by inserting

```
CALL ORTHOG
```

after

```
CALL PPLOAD
```

in subroutine PART2B. Slater functions were generated in PPLOAD when required. The microfiche has been glued onto the inside back cover of the thesis.

I Modifications to the MCP program to generate coefficients required for shielding calculations:

1. Subroutine MCP:

Line 161 - for

```
IOPAR = 1
```

read

```
IOPAR = -1
```

2. Subroutine RKCO:

i) insert after line 33

```
IF (ISPAR(JA).EQ.ISPAR(JB))RETURN
```

ii) line 163 - for

```
IF(NCORE.EQ.0.OR.NAK(IT1).NE.NAK(IT2))RETURN
```

read

```
IF(NCORE.EQ.0.OR.NAK(IT1).NE.-NAK(IT2))RETURN
```

3. Subroutine SKRC:

a) for coefficients with $k \varepsilon \mathbb{K}_{ac}$

i) line 17 - for

```
IF(KAPS(2)*KAPS(4).LT.0)ISD2 = -1
```

read

```
IF(KAPS(2)*KAPS(4).GT.0)ISD2 = -1
```

ii) line 38 - for

```
IF(KAPS(2)*KAPS(3).LT.0)ISE2 = -1
```

read

```
IF(KAPS(2)*KAPS(3).GT.0)ISE2 = -1
```

b) for coefficients with $k \varepsilon \mathbb{K}_{bd}$

i) line 15 - for

```
IF(KAPS(1)*KAPS(3).LT.0)ISD1 = -1
```

read

```
IF(KAPS(1)*KAPS(3).GT.0)ISD1 = -1
```

ii) line 36 - for

```
IF(KAPS(1)*KAPS(4).LT.0)ISE1 = -1
```

read

```
IF(KAPS(1)*KAPS(4).GT.0)ISE1 = -1
```

II Modifications to the oscillator strengths program so as to calculate the effect of shielding on matrix elements

Subroutine OSCL: delete line 146

```
IF(ITEST.LT.0) GO TO 21
```

```
1.//XXOEH222  JOB  (AF18,OBH,0-30,1,,,,,,0),PLUMMER
2.//  EXEC FGCLG,CPRINT=NO,PARM.L='NOMAP,OVLY',REGICN.G=210K
3.//C.SYSIN DD *
4.        IMPLICIT REAL*8(A-H,O-Z)
5.        CALL ERRSET (208,0,-1,1)
6.        CALL PART1
7.        CALL PART2A
8.        CALL PART2B
9.        CALL PART3
10.       STOP
11.       END
```

```
      SUBROUTINE PART1
      IMPLICIT REAL*8(A-H,O-Z)
      COMMON/INFORM/IRD,IPD,IR1,IR2,IP2,IR3
      COMMON/ORB1/E(25)
      COMMON/DEF1/Z,RNT,H,EPH,ACCY,C,N,NWA
      COMMON/CONS/ZERO,HALF,TENTH,ONE,TWO,THREE,TEN
      COMMON/ORB4/NW,NCF,NH(25),NP(25),NAK(25)
      COMMON/OFFD/ECV(100),IECV(100),NEC
      COMMON/HMAT/EAV,CCF(20),UCF(25)
      COMMON/WAVE/PF(350,25),QF(350,25)
      COMMON/NPOT/ZZ(350)
      COMMON/NPAR/PARM(4),Z1,NUCTYP,NPARM
      COMMON/LEVS/NLEV,LEV(20)
      COMMON/KNTR/ITC(40)
      COMMON/GRID/R(350)
      COMMON/MIXMAT/CIJ(20,20)
      COMMON/EEEEEE/ENERGY(20)
      COMMON/PARITY/IPARTY(20)
      COMMON/OSC1/IATJPO(20),IASPAR(20)
      COMMON/SYM/ITJPO(20),ISPAR(20)
      COMMON/JUNK/EPS,NCFP,NCFM,NCFPP1,NCMIN,NMCP,NCFTT
      DIMENSION RT(20),IT(20)
C
C     INITIAL DATA
C
      IPD=6
      IRD=5
      IR2=9
      IR3=17
      EPS=1.0D-10
      ITC(7)=0
      ITC(12)=0
      ITC(13)=0
      ITC(14)=0
      ITC(15)=0
      ITC(16)=0
      ITC(17)=0
      ITC(18)=0
      ITC(19)=0
      CALL CARDIN(0,XX,XXX,NN,RT,IT,20)
      NCFP=IT(1)
      NCFM=IT(2)
      NCFPP1=NCFP+1
      CALL CARDIN(0,XX,XXX,NN,RT,IT,20)
      NLEV=NN
      DO 104 I=1,NN
  104 LEV(I)=IT(I)
C
C     LOAD UP WITH EVERYTHING
C
      IF (ITC(19).EQ.1) WRITE (6,1001) IR2
 1001 FORMAT (/' ++++++++++ LOAD STARTED ++++++++++  ON STREAM NUMBER'
     X       ,I4)
      REWIND IR2
      READ(IR2)
      IF (ITC(16).EQ.1) WRITE (6,5656)
 5656 FORMAT (' READ ON STREAM 9 OK')
      READ (IR2) NCMIN,NW,NCF,N
      WRITE (6,5432) NW,NCF,N
 5432 FORMAT (/' NW =',I5,5X,'NCF =',I5,5X,'N =',I5/)
      IF (ITC(16).EQ.1) WRITE (6,5656)
      READ (IR2) ZX,RNT,H,C
      IF (ITC(16).EQ.1) WRITE (6,5656)
      Z=DABS(ZX)
      EPH=DEXP(H)
C
      DO 1 I=1,NW
      READ (IR2) NH(I),NP(I),NAK(I),E(I)
      IF (ITC(16).EQ.1) WRITE (6,5656)
      READ (IR2)
      IF (ITC(16).EQ.1) WRITE (6,5656)
      READ (IR2) (PF(J,I),J=1,N),(QF(J,I),J=1,N)
      IF (ITC(16).EQ.1) WRITE (6,5656)
    1 CONTINUE
C
      READ (IR2) NMCP
      IF (ITC(16).EQ.1) WRITE (6,5656)
      IF (NMCP.EQ.0) GO TO 2
      READ (IR2)
      IF (ITC(16).EQ.1) WRITE (6,5656)
      READ (IR2)
      IF (ITC(16).EQ.1) WRITE (6,5656)
      READ (IR2)
      IF (ITC(16).EQ.1) WRITE (6,5656)
      READ (IR2)
      IF (ITC(16).EQ.1) WRITE (6,5656)
```

```
C
    2 READ (IR2) (CCF(I),I=1,NCF)
      IF (ITC(16).EQ.1) WRITE (6,5656)
      READ (IR2) (UCF(I),I=1,NW) .
      IF (ITC(16).EQ.1) WRITE (6,5656)
      IF (NCMIN.EQ.0) GO TO 3
      NCFTT=NCF*NCMIN
      READ (IR2)
      IF (ITC(16).EQ.1) WRITE (6,5656)
C
    3 READ (IR2)
      IF (ITC(16).EQ.1) WRITE (6,5656)
      READ (IR2) EAV,((CIJ(I,J),J=1,NCF),I=1,NCF),(ENERGY(I),I=1,NCF)
      IF (ITC(16).EQ.1) WRITE (6,5656)
      IF (ITC(19).EQ.1) WRITE (6,6666) EAV,((CIJ(I,J),J=1,NCF),I=1,NCF
     X      (ENERGY(I),I=1,NCF)
 6666 FORMAT (/' EAV/CIJ/ENERGY'/(1P5D20.10))
C
      READ (IR2) NEC
      IF (ITC(16).EQ.1) WRITE (6,5656)
      IF (NEC.EQ.0) GO TO 4
      READ (IR2) (IECV(I),I=1,NEC),(ECV(I),I=1,NEC)
      IF (ITC(16).EQ.1) WRITE (6,5656)
C
    4 READ (IR2) NUCTYP
      IF (ITC(16).EQ.1) WRITE (6,5656)
      READ (IR2) (ZZ(I),I=1,N)
      IF (ITC(16).EQ.1) WRITE (6,5656)
      READ (IR2) Z1
      IF (ITC(16).EQ.1) WRITE (6,5656)
      READ (IR2) NPARM
      IF (ITC(16).EQ.1) WRITE (6,5656)
      IF (NPARM.EQ.0) GO TO 5
      READ (IR2) (PARM(I),I=1,NPARM)
      IF (ITC(16).EQ.1) WRITE (6,5656)
    5 CONTINUE
      READ(IR2)
      IF (ITC(16).EQ.1) WRITE (6,5656)
      READ(IR2)
      IF (ITC(16).EQ.1) WRITE (6,5656)
      READ(IR2) (IATJPO(J),J=1,NCF)
      IF (ITC(16).EQ.1) WRITE (6,5656)
      READ(IR2) (ISPAR(J),J=1,NCF)
      IF (ITC(16).EQ.1) WRITE (6,5656)
      IF (ITC(19).EQ.1) WRITE (6,1003)
 1003 FORMAT (/' ++++++++++ LOAD FINISHED ++++++++++'/)
C
C     IF ANY ORDER G CIJ'S HAVE BEEN CALCULATED SET THEM BACK TO ZERO
C
      DO 50 J=1,NCF
      X=ZERO
      DO 51 I=1,NCFP
   51 X=X+CIJ(I,J)*CIJ(I,J)
      IF (X.LT.TENTH) GOTO 50
      DO 52 I=NCFPP1,NCF
   52 CIJ(I,J)=ZERO
   50 CONTINUE
      REWIND 14
      WRITE (14) ((CIJ(I,J),I=1,NCF),J=1,NCF)
C
C     RADIAL GRID
C
      R(1)=RNT
      DO 101 I=2,N
  101 R(I)=R(I-1)*EPH
      RETURN
      END
```

```
      SUBROUTINE PART2A
      IMPLICIT REAL*8(A-H,O-Z)
      INTEGER*2 ISTOR(25,25)
      COMMON/OSC4/NNLDR(20,20),NSLDF(20,20)
      COMMON/INFORM/IRD,IPD,IR1,IR2,IP2,IR3
      COMMON/ORB1/E(25)
      COMMON/DEF1/Z,RNT,H,EPH,ACCY,C,N,NWA
      COMMON/CONS/ZERO,HALF,TENTH,ONE,TWO,THREE,TEN
      COMMON/KNTR/ITC(40)
      COMMON/ORB4/NW,NCF,NH(25),NP(25),NAK(25)
      COMMON/HMAT/EAV,CCF(20),UCF(25)
      COMMON/WAVE/PF(350,25),QF(350,25)
      COMMON/HAMC/HAMX(10,10)
      COMMON/NUCDEN/RHO(350)
      COMMON/TATB/TA(360),TB(360)
      COMMON/GRID/R(350)
      COMMON/MIXMAT/CIJ(20,20),ENERGY(20)
      COMMON/PARITY/IPARTY(20)
      COMMON/OSC1/IATJPO(20),IASPAR(20)
      COMMON/SYM/ITJPO(20),ISPAR(20)
      COMMON/OSC3/XSLDR(500),ISLDR(500)
      COMMON/JUNK/EPS,NCFP,NCFM,NCFPP1,NCMIN,NMCP,NCFTT
      DIMENSION STOR(100)
      CALL MCTIN
      CALL DENCAL
C
C     CALCULATE THE CROSS-TERMS IN THE HAMILTONIAN
C     INVOLVING ONLY THE P.C. WAVEFUNCTIONS & THE P.N.C. HAMILTONIAN
C
      NWA=NW+1
      IX=0
      IXMAX=100
      IF (ITC(19).EQ.1) WRITE (6,4444) NW
 4444 FORMAT (/' NW',I12)
      DO 102 I=1,NW
      DO 102 J=1,NW
  102 ISTOR(I,J)=0
      IF (ITC(19).EQ.1) WRITE (6,4445) NCFP,NCFPP1,NCF
 4445 FORMAT (/' NCFP,NCFPP1,NCF',3I12)
      DO 109 ITR=1,NCFP
      DO 108 JTR=1,NCFM
      HAMX(ITR,JTR)=ZERO
      JTRP=JTR+NCFP
      ILDN=NNLDR(ITR,JTRP)
      IF (ILDN.EQ.0) GOTO 108
      ILDA=NSLDF(ITR,JTRP)
      ILDB=ILDA+ILDN-1
      IF (ITC(19).EQ.1) WRITE (6,4446) ILDA,ILDB
 4446 FORMAT (/' ILDA,ILDB',2I12)
      DO 107 IL=ILDA,ILDB
      IC=ISLDR(IL)/NWA
      ID=ISLDR(IL)-IC*NWA
      IF (ITC(19).EQ.1) WRITE (6,4447) NP(IC),NH(IC),NP(ID),NH(ID)
 4447 FORMAT (/' IC,ID',2(I12,A2))
      IXX=ISTOR(IC,ID)
      IF (ITC(19).EQ.1) WRITE(6,2001) ITR,JTRP,ILDN,ILDA,ILDB,IL,
     X          ISLDR(IL),IXX,IX,NP(IC),NH(IC),NP(ID),NH(ID)
 2001 FORMAT (/' 2001',9I10,2(I8,A2))
      IF (IXX.EQ.0) GOTO 112
      HSP=STOR(IXX)
      GOTO 103
  112 IX=IX+1
      IF (IX.GT.IXMAX) STOP 23
      IF ((NAK(IC)+NAK(ID)).EQ.0) GOTO 99
      HSP=ZERO
      GOTO 98
   99 DO 97 I=1,N
   97 TA(I)=RHO(I)*R(I)*(PF(I,IC)*QF(I,ID)-QF(I,IC)*PF(I,ID))
      CALL QUAD(HSP)
   98 ISTOR(IC,ID)=IX
      STOR(IX)=HSP
  103 HAMX(ITR,JTR)=HAMX(ITR,JTR)+XSLDR(IL)*HSP
      IF (ITC(19).EQ.1) WRITE (6,2002) HSP,HAMX(ITR,JTR),XSLDR(IL)
 2002 FORMAT (/' 2002',1P3D20.10)
  107 CONTINUE
  108 CONTINUE
  109 CONTINUE
      IF (ITC(12).EQ.0) RETURN
      DO 77 I=1,NCFP
   77 WRITE (6,5555) (HAMX(I,J),J=1,NCFM)
 5555 FORMAT (' HAM',1P10D12.4)
      RETURN
      END
```

```
      SUBROUTINE PART2B
      IMPLICIT REAL*8(A-H,O-Z)
      COMMON/JUNK/EPS,NCFP,NCFM,NCFPP1,NCMIN,NMCP,NCFTT
      COMMON/HAMC/HAMX(10,10)
      COMMON/KNTR/ITC(40)
C
C     CALCULATE CROSS-TERMS IN THE HAMILTONIAN
C     INVOLVING PNC WAVEFUNCTIONS
C
      CALL PPLOAD
      IFTEEN=15
      ISTEEN=16
      CALL INVKAC(IFTEEN)
      CALL INVKBD(ISTEEN)
      CALL MATO
      WRITE (14) ((HAMX(I,J),I=1,NCFP),J=1,NCFM)
      REWIND 14
      IF (ITC(12).EQ.0) RETURN
      DO 10 I=1,NCFP
   10 WRITE (6,1001) (HAMX(I,J),J=1,NCFM)
 1001 FORMAT (/' HAM'/(1P10D13.5))
      RETURN
      END
```

```
      SUBROUTINE INVKAC(IN)
      IMPLICIT REAL*8(A-H,O-Z)
C
C     THIS SUBROUTINE READS ANY MCP COEFFICIENTS WHICH ARE REQUIRED
C      OF THE "AC" TYPE
C     A PRINT OUT IS MADE IF OPTION 7 IS SET
C
C     NO SUBROUTINES CALLED.
C
      COMMON/DEF1/Z,RNT,H,EPH,ACCY,C,N,NWA
      COMMON/DEF2/NCFX,NMAX,NFMAX,NMCPX,NECX,NSCFX
      COMMON/MCPKAC/NNAC(10,10),NSAC(10,10),XSAC(500),ISAC(500),
     X       NMCPAC
      COMMON/JUNK/EPS,NCFP,NCFM,NCFPP1,NCMIN,NMCP,NCFTT
      COMMON/INFORM/IRD,IPD
      COMMON/KNTR/ITC(40)
      COMMON/ORB4/NW,NCF,NH(25),NP(25),NAK(25),IQ(25,20)
C
      MCPACX=500
      NMCPAC=0
      IF (IN.EQ.0) RETURN
      REWIND IN
      READ (IN)
      READ (IN)
      READ (IN)
      READ (IN)
      READ (IN)
      READ (IN)
      READ (IN)
      READ (IN)
      READ (IN)
C
      IF (ITC(7).EQ.1) WRITE (IPD,301)
C
      DO 1 IR=1,NCFP
      DO 1 IS=1,NCFM
    1 NNAC(IR,IS)=0
C
    2 READ (IN) IR,IS,IA,IB,IC,ID,IK,X
      IF (IR.EQ.0) GO TO 5
      IF (ITC(7).EQ.0) GO TO 4
C
      IF (IA.EQ.0) GO TO 3
      WRITE (IPD,302) IR,IS,
     X    NP(IA),NH(IA),NP(IB),NH(IB),NP(IC),NH(IC),NP(ID),NH(ID),
     X    IK,X
      GO TO 4
    3 WRITE (IPD,304) IR,IS,NP(IC),NH(IC),NP(ID),NH(ID),X
C
    4 CONTINUE
      IF (IR.GT.NCFP) GOTO 2
      IF (IS.LE.NCFP) GOTO 2
      NMCPAC=NMCPAC+1
      IF (NMCPAC.GT.NMCPX) GO TO 7
      ISM=IS-NCFP
      NNAC(IR,ISM)=NNAC(IR,ISM)+1
      ISAC(NMCPAC)=(((IK*NWA+IA)*NWA+IB)*NWA+IC)*NWA+ID
      XSAC(NMCPAC)=X
      GO TO 2
C
    5 IC=1
      DO 6 IR=1,NCFP
      DO 6 IS=1,NCFM
      NSAC(IR,IS)=IC
    6 IC=IC+NNAC(IR,IS)
C
      REWIND IN
      WRITE (IPD,303) NMCPAC
      RETURN
C
    7 WRITE (IPD,300)
      STOP 5
C
  300 FORMAT (/1X,26HDIMENSION ERROR FOR NMCPAC)
  301 FORMAT (/1X,16HMCP COEFFICIENTS//4X,1HR,3X,1HS,31X,1HK/)
  302 FORMAT (1X,2I4,4(3X,I2,A2),I4,3X,1PD14.7)
  303 FORMAT (/1X,I5,25H MCP AC COEFFICIENTS READ)
  304 FORMAT (1X,2I4,14X,2(3X,I2,A2),7X,1PD14.7)
      END
```

```
      SUBROUTINE INVKBD(IN)
      IMPLICIT REAL*8(A-H,O-Z)
C
C     THIS SUBROUTINE READS ANY MCP COEFFICIENTS WHICH ARE REQUIR
C      OF THE "BD" TYPE
C     A PRINT OUT IS MADE IF OPTION 7 IS SET
C
C     NO SUBROUTINES CALLED.
C
      COMMON/DEF1/Z,RNT,H,EPH,BDCY,C,N,NWA
      COMMON/DEF2/NCFX,NMAX,NFMAX,NMCPX,NECX,NSCFX
      COMMON/MCPKBD/NNBD(10,10),NSBD(10,10),XSBD(500),ISBD(500),
     X      NMCPBD
      COMMON/JUNK/EPS,NCFP,NCFM,NCFPP1,NCMIN,NMCP,NCFTT
      COMMON/INFORM/IRD,IPD
      COMMON/KNTR/ITC(40)
      COMMON/ORB4/NW,NCF,NH(25),NP(25),NAK(25),IQ(25,20)
C
      MCPBDX=500
      NMCPBD=0
      IF (IN.EQ.0) RETURN
      REWIND IN
      READ (IN)
      READ (IN)
      READ (IN)
      READ (IN)
      READ (IN)
      READ (IN)
      READ (IN)
      READ (IN)
      READ (IN)
C
      IF (ITC(7).EQ.1) WRITE (IPD,301)
C
      DO 1 IR=1,NCFP
      DO 1 IS=1,NCFM
    1 NNBD(IR,IS)=0
C
    2 READ (IN) IR,IS,IA,IB,IC,ID,IK,X
      IF (IR.EQ.0) GO TO 5
      IF (ITC(7).EQ.0) GO TO 4
C
      IF (IA.EQ.0) GO TO 3
      WRITE (IPD,302) IR,IS,
     X   NP(IA),NH(IA),NP(IB),NH(IB),NP(IC),NH(IC),NP(ID),NH(ID)
     )   IK,X
      GO TO 4
    3 WRITE (IPD,304) IR,IS,NP(IC),NH(IC),NP(ID),NH(ID),X
C
    4 CONTINUE
      IF (IR.GT.NCFP) GOTO 2
      IF (IS.LE.NCFP) GOTO 2
      NMCPBD=NMCPBD+1
      IF (NMCPBD.GT.NMCPX) GO TO 7
      ISM=IS-NCFP
      NNBD(IR,ISM)=NNBD(IR,ISM)+1
      ISBD(NMCPBD)=(((IK*NWA+IA)*NWA+IB)*NWA+IC)*NWA+ID
      XSBD(NMCPBD)=X
      GO TO 2
C
    5 IC=1
      DO 6 IR=1,NCFP
      DO 6 IS=1,NCFM
      NSBD(IR,IS)=IC
    6 IC=IC+NNBD(IR,IS)
C
      REWIND IN
      WRITE (IPD,303) NMCPBD
      RETURN
C
    7 WRITE (IPD,300)
      STOP 5
C
  300 FORMAT (/1X,26HDIMENSION ERROR FOR NMCPBD)
  301 FORMAT (/1X,16HMCP COEFFICIENTS//4X,1HR,3X,1HS,31X,1HK/)
  302 FORMAT (1X,2I4,4(3X,I2,A2),I4,3X,1PD14.7)
  303 FORMAT (/1X,I5,25H MCP BD COEFFICIENTS READ)
  304 FORMAT (1X,2I4,14X,2(3X,I2,A2),7X,1PD14.7)
      END
```

```
      SUBROUTINE PART3
      IMPLICIT REAL*8(A-H,O-Z)
      COMMON/INFORM/IRD,IPD,IR1,IR2,IP2,IR3
      COMMON/ORB1/E(25)
      COMMON/DEF1/Z,RNT,H,EPH,ACCY,C,N,NWA
      COMMON/CONS/ZERO,HALF,TENTH,ONE,TWO,THREE,TEN
      COMMON/ORB4/NW,NCF,NH(25),NP(25),NAK(25)
      COMMON/HMAT/EAV,CCF(20),UCF(25)
      COMMON/NPAR/PARM(4),Z1,NUCTYP,NPARM
      COMMON/LEVS/NLEV,LEV(20)
      COMMON/KNTR/ITC(40)
      COMMON/HAMP/HAM1(10,10)
      COMMON/HAMM/HAM2(10,10)
      COMMON/HAMCC/HAMX(10,10)
      COMMON/MIXING/CIJ(20,20)
      COMMON/EEEEEE/ENERGY(20)
      COMMON/OFFD/ECV(100),IECV(100),NEC
      COMMON/NPOT/ZZ(350)
      COMMON/PARITY/IPARTY(20)
      COMMON/OSC1/IATJPO(20),IASPAR(20)
      COMMON/SYM/ITJPO(20),ISPAR(20)
      COMMON/JUNK/EPS,NCFP,NCFM,NCFPP1,NCMIN,NMCP,NCFTT
      DIMENSION HL(20)
C
C      LOAD UP WHAT HAS BEEN DUMPED
C
      REWIND 14
      READ(14) ((CIJ(I,J),I=1,NCF),J=1,NCF)
      READ(14) ((HAMX(I,J),I=1,NCFP),J=1,NCFM)
      REWIND 14
C
C     LOAD UP THE DIAGONAL TERMS
C
      IF (ITC(19).EQ.1) WRITE (6,3333) NCFP
 3333 FORMAT (/' NCFP',I12)
      REWIND 12
      READ(12) NCFPX
      WRITE (6,3737) NCFPX
 3737 FORMAT (/' NCFP FROM HAMILTONIAN DUMP',I4)
      IF (NCFP.NE.NCFPX) STOP 29
      READ(12) ((HAM1(I,J),I=1,NCFP),J=1,NCFP)
      REWIND 12
      REWIND 13
      IF (ITC(19).EQ.1) WRITE (6,7080) NCFM
 7080 FORMAT (/' NCFM =',I12)
      READ(13) NCFMX
      WRITE (6,3738) NCFMX
 3738 FORMAT (/' NCFM FROM HAMILTONIAN DUMP',I4)
      IF (NCFM.NE.NCFMX) STOP 29
      READ(13) ((HAM2(I,J),I=1,NCFM),J=1,NCFM)
      REWIND 13
      DO 70 I=1,NCFP
      DO 70 J=I,NCFP
   70 HAM1(J,I)=HAM1(I,J)
      DO 71 I=1,NCFM
      DO 71 J=I,NCFM
   71 HAM2(J,I)=HAM2(I,J)
      IF (ITC(15).EQ.1) WRITE (6,7081)
 7081 FORMAT (/' HAM')
      DO 80 I=1,NCFP
   80 IF (ITC(15).EQ.1) WRITE (6,2004) (HAM1(I,J),J=1,NCFP)
     X                 ,(HAMX(I,J),J=1,NCFM)
 2004 FORMAT(/(1P8D16.7))
      DO 79 I=1,NCFM
   79 IF (ITC(15).EQ.1) WRITE (6,2004) (HAMX(J,I),J=1,NCFP)
     X                 ,(HAM2(I,J),J=1,NCFM)
      IF (ITC(19).EQ.1) WRITE (6,7082)
 7082 FORMAT (/' CIJ')
      DO 81 I=1,NCF
   81 IF (ITC(19).EQ.1) WRITE(6,2004) (CIJ(I,J),J=1,NCF)
C
C      DETERMINE PARITY OF EACH LEVEL
C
      DO 10 LEVEL=1,NCF
      PARTYP=ZERO
      DO 11 J=1,NCFP
   11 PARTYP=PARTYP+CIJ(J,LEVEL)*CIJ(J,LEVEL)
      DO 12 J=NCFPP1,NCF
   12 PARTYP=PARTYP-CIJ(J,LEVEL)*CIJ(J,LEVEL)
      IF (ITC(19).EQ.1) WRITE(6,1999) PARTYP
 1999 FORMAT (/' PARTYP ',1PD20.10)
      IF (PARTYP.LE.ZERO) IPARTY(LEVEL)=-1
      IF (PARTYP.GT.ZERO) IPARTY(LEVEL)=+1
   10 CONTINUE
      IF (ITC(19).EQ.1) WRITE (6,2003) (IPARTY(I),I=1,NCF)
 2003 FORMAT (/' IPARTY',10I10)
```

```
87.C
88.C      CALCULATE PNC MIXING COEFFICIENTS
89.C      =================================
90.C
91.C      THESE ARE ZERO AT THE PRESENT
92.C
93.       DO 13 LEVI=1,NLEV
94.       LEVEL=LEV(LEVI)
95.       IR=LEVEL
96.       IF (IPARTY(LEVEL).EQ.+1) GOTO 14
97.       WRITE (6,1002) LEVEL
98. 1002  FORMAT (//' WRONG LEVEL',I3)
99.       STOP 19
100.  14  CONTINUE
101.C
102.C                    T        R
103.C     CALCULATE   H    LAMBDA
104.C                    X        +
105.C
106.      DO  15 I=NCFPP1,NCF
107.      IM=I-NCFP
108.      HL(I)=ZERO
109.      DO 16 J=1,NCFP
110.  16  HL(I)=HL(I)+HAMX(J,IM)*CIJ(J,LEVEL)
111.  15  CONTINUE
112.      IF (ITC(19).EQ.1) WRITE (6,2006) (HL(I),I=NCFPP1,NCF)
113. 2006 FORMAT (/' HL',1P10D13.4)
114.C
115.C     FROM WHICH WE GET THE MIXING COEFFS
116.C
117.      DO 17 ITT=1,NCF
118.      IF (IPARTY(ITT).NE.-1) GOTO 17
119.      CHL=ZERO
120.      DO 18 I=NCFPP1,NCF
121.  18  CHL=CHL+CIJ(I,ITT)*HL(I)
122.      CHLDE=CHL/(ENERGY(ITT)-ENERGY(IR))
123.      IF (ITC(19).EQ.1) WRITE(6,2007) CHL,CHLDE
124. 2007 FORMAT(/' CHL,CHLDE',1P2D20.10)
125.      DO 19 I=NCFPP1,NCF
126.  19  CIJ(I,LEVEL)=CIJ(I,LEVEL)+CHLDE*CIJ(I,ITT)
127.  17  CONTINUE
128.  13  CONTINUE
129.      JMAX=NCF
130.      IF (NCF.GT.10.AND.ITC(15).NE.1) JMAX=10
131.      DO 82 I=1,NCF
132.  82  WRITE (6,2008) (CIJ(I,J),J=1,JMAX)
133. 2008 FORMAT (' CIJ',1P10D12.3)
134.C
135.C     REVERSE THE SIGN OF THE PNC CIJ FOR THE GROUND STATE SO THAT
136.C     WE CALCULATE  < R / T / S PNC > - < R PNC / T / S >
137.C
138.      DO 23 I=NCFPP1,NCF
139.  23  CIJ(I,1)=-CIJ(I,1)
140.C
141.C     CHANGE THE MCDF DUMP ACCORDINGLY
142.C
143.      REWIND 9
144.      IMAX=3*NW+4
145.      DO 20 I=1,IMAX
146.  20  READ(9) II
147.      IF(II.EQ.0) GOTO 21
148.      DO 22 I=1,4
149.  22  READ(9)
150.  21  READ(9)
151.      READ(9)
152.      READ(9)
153.      WRITE (9) EAV,((CIJ(I,J),J=1,NCF),I=1,NCF),
154.     X          (ENERGY(I),I=1,NCF)
155.      IF (ITC(19).EQ.1) WRITE (6,6666) EAV,((CIJ(I,J),J=1,NCF),I=1,NCF
156.     X          (ENERGY(I),I=1,NCF)
157. 6666 FORMAT (/' EAV/CIJ/ENERGY'/(1P5D20.10))
158.      WRITE(9) NEC
159.      IF(NEC.NE.0) WRITE(9)(IECV(I),I=1,NEC),(ECV(I),I=1,NEC)
160.      WRITE (9) NLCTYP
161.      WRITE (9) (ZZ(I),I=1,N)
162.      WRITE (9) Z1
163.      WRITE (9) NPARM
164.      IF (NPARM.NE.0) WRITE(9)(PARM(I),I=1,NPARM)
165.      WRITE(9)
166.      WRITE(9)
167.      WRITE(9)
168.      WRITE(9) (IATJPO(J),J=1,NCF)
169.      WRITE(9) (ISPAR(J),J=1,NCF)
170.      REWIND 9
171.      RETURN
172.      END
```

```
      SUBROUTINE MCTIN
      IMPLICIT REAL*8(A-H,O-Z)
      DIMENSION HEDIN(12)
      COMMON/ORB4/NW,NCF,NH(25),NP(25),NAK(25)
      COMMON/INFORM/IRD,IPD
      COMMON/MCTA/KA,IOPAR
      COMMON/OSC3/XSLDR(500),ISLDR(500)
      COMMON/OSC4/NNLDR(20,20),NSLDF(20,20)
      COMMON/KNTR/ITC(40)
C
C  READ BASIC INFORMATION REGARDING TENSOR OPERATOR
C
      NFILE=11
      REWIND NFILE
      READ (NFILE) HEDIN
      READ (NFILE) NCFIN,NWIN
      WRITE (6,9676) NCFIN,NWIN
 9676 FORMAT (/' MCT DUMP : NCF =',I5,5X,' NW =',I5/)
      IF (NW.NE.NWIN.OR.NCF.NE.NCFIN) GO TO 7
      READ (NFILE)
      READ (NFILE)
      READ (NFILE)
      READ (NFILE)
      READ (NFILE)
      READ (NFILE)
      READ (NFILE)
      READ (NFILE)
      READ (NFILE) KA,IOPAR
      IF (KA.EQ.0) WRITE(IPD,301)
      NWA=NW+1
C
      DO 2 I=1,NCF
      DO 1 J=1,NCF
      NNLDR(I,J)=0
    1 CONTINUE
    2 CONTINUE
C
C  BEGIN READING MCT COEFFICIENTS.
C
      ICMAX=500
      IC=0
    3 READ (NFILE) ITR,JTR,IA,IB,COEFF
      IF (ITC(19).EQ.1) WRITE (6,1234) ITR,JTR,IA,IB,COEFF
 1234 FORMAT (/' MCT COEFF : ',I8,I6,I8,I6,1PD18.5)
      IF (ITR.EQ.0) GO TO 4
      IC=IC+1
      IF (IC.GT.ICMAX) GO TO 9
      NNLDR(ITR,JTR)=NNLDR(ITR,JTR)+1
      ISLDR(IC)=NWA*IA+IB
      XSLDR(IC)=COEFF
      GO TO 3
C
C  STORE START AND NUMBER OF COEFFICIENTS READ FOR EACH
C  CONFIGURATION.
C
    4 CONTINUE
      WRITE (IPD,302) HEDIN,IC,KA,IOPAR
      IC=1
      DO 6 ITR=1,NCF
      DO 5 JTR=1,NCF
      NSLDF(ITR,JTR)=IC
      IC=IC+NNLDR(ITR,JTR)
    5 CONTINUE
    6 CONTINUE
      IF (ITC(18).NE.1) GOTO 99
      WRITE (6,310)
  310 FORMAT (//' MATRIX NNLDR ')
      DO 98 II=1,NCF
      WRITE (6,311) (NNLDR(II,JJ),JJ=1,NCF)
  311 FORMAT (/(20I6))
   98 CONTINUE
      WRITE (6,312)
  312 FORMAT (//' MATRIX NSLDF')
      DO 97 II=1,NCF
   97 WRITE (6,313) (NSLDF(II,JJ),JJ=1,NCF)
  313 FORMAT (/(20I6))
   99 CONTINUE
      RETURN
C
    7 WRITE (IPD,300)
      STOP  20
    9 WRITE (IPD,303)
      STOP  22
C
  300 FORMAT (/1X,'INCONSISTENT MCT DUMP')
  301 FORMAT (/1X,'TENSOR RANK IS ZERO')
  302 FORMAT (//1X,'MCT DUMP : ',12A8//
     X    1X,I4,' MCT COEFFICIENTS READ'//
     X    1X,'TENSOR RANK ',I2,6X,'PARITY ',I2//)
  303 FORMAT (/1X,'DIMENSION ERROR FOR MCT COEFFICIENTS IN MCTIN')
      END
```

```
      SUBROUTINE MATO
      IMPLICIT REAL*8(A-H,O-Z)
C
C     THIS SUBROUTINE ADDS TO THE OFF-DIAGONAL MATRIX ELEMENTS
C     THE CONTRIBUTIONS FROM INTERACTIONS WITHIN OPEN SHELLS
C
C  SUBROUTINES CALLED: RINTI,SLATAC,SLATBD
C
      COMMON/DEF1/Z,RNT,H,EPS,ACCY,C,N,NWA
      COMMON/KNTR/ITC(40)
      COMMON/MCPKAC/NNAC(10,10),NSAC(10,10),XSAC(500),ISAC(500),
     X       NMCPAC
      COMMON/MCPKBD/NNBD(10,10),NSBD(10,10),XSBD(500),ISBD(500),
     X       NMCPBD
      COMMON/JUNK/EPS,NCFP,NCFM,NCFPP1,NCMIN,NMCP,NCFTT
      COMMON/HAMC/HAMX(10,10)
      COMMON/ORB4/NW,NCF,NH(25),NP(25),NAK(25),IQ(25,20)
C
      IF (ITC(16).EQ.1) WRITE (6,1095)
 1095 FORMAT (//)
      IF (ITC(12).EQ.0) GOTO 88
      DO 99 I=1,NCFP
   99 WRITE (6,1099) (HAMX(I,J),J=1,NCFM)
 1099 FORMAT (' MATO :HAM ',1P10D12.4)
   88 CONTINUE
      IF (ITC(13).EQ.0) GOTO 9
      WRITE (6,1095)
      DO 92 I=1,NCFP
   92 WRITE (6,1092) (NSAC(I,J),J=1,NCFM)
 1092 FORMAT (' NSAC',10I10)
      DO 93 I=1,NCFP
   93 WRITE (6,1093) (NNAC(I,J),J=1,NCFM)
 1093 FORMAT (' NNAC',10I10)
      WRITE (6,1095)
    9 CONTINUE
      IF (NMCPAC.EQ.0.AND.NMCPBD.EQ.0) RETURN
      IF (NCF.EQ.1) RETURN
      DO 3 ITR=1,NCFP
C
C     CYCLE OVER THE OFF-DIAGONAL ELEMENTS
C     USING MCP COEFFS OF THE "AC" TYPE
C
      DO 3 JTR=1,NCFM
      JA=NSAC(ITR,JTR)
      ILDN=NNAC(ITR,JTR)
      IF (ITC(14).EQ.1) WRITE (6,1094) ITR,JTR,JA,ILDN
 1094 FORMAT (' ITR,JTR,JA,ILDN',4I10)
      IF (ILDN.LE.0) GOTO 3
C
C     SKIP IF NO TERMS IN THIS ELEMENT
C
      JB=JA+ILDN-1
C
C     EXTRACT CORRESPONDING ENTRIES FROM TABLE
C
      DO 2 JJ=JA,JB
C      WRITE (6,1001) NWA,NCF,NCFM,NCFP,ITR,JTR,NMCPAC,NMCPBD,JA,JB,JJ
C1001 FORMAT (13I10)
      KX=ISAC(JJ)
      ID=MOD(KX,NWA)
      KX=KX/NWA
      IC=MOD(KX,NWA)
      KX=KX/NWA
      IB=MOD(KX,NWA)
      KX=KX/NWA
      IA=MOD(KX,NWA)
      KK=KX/NWA
C
C     TEST FOR I(A,B) INTEGRAL
C
      IF (IA+IB.LE.0) GOTO 1
      WA=SLATAC(IA,IB,IC,ID,KK)
      WB=XSAC(JJ)
      GOTO 22
```

```
C
C       EVALUATE I(A,B) INTEGRAL.
C
      1 WA=RINTI(IC,ID)
        WB=XSAC(JJ)
   22   CONTINUE
        WAWB=WA*WB
        IF (ITC(14).EQ.1) WRITE (6,1090) JJ,WA,WB,WAWB
 1090 FORMAT (' MCP NO.',I5,' WA, WB IN STATEMENT 2 ',1P2D20.10
     X       '     PRODUCT',D20.10)
        HAMX(ITR,JTR)=HAMX(ITR,JTR)+WA*WB
     2  CONTINUE
     3  CONTINUE
        DO 13 ITR=1,NCFP
C
C       CYCLE OVER THE OFF-DIAGONAL ELEMENTS
C
        DO 13 JTR=1,NCFM
        JA=NSBD(ITR,JTR)
        ILDN=NNBD(ITR,JTR)
        IF (ILDN.LE.0) GOTO 13
C
C       SKIP IF NO TERMS IN THIS ELEMENT
C
        JB=JA+ILDN-1
C
C       EXTRACT CORRESPONDING ENTRIES FROM TABLE
C
        DO 12 JJ=JA,JB
        KX=ISBD(JJ)
        ID=MOD(KX,NWA)
        KX=KX/NWA
        IC=MOD(KX,NWA)
        KX=KX/NWA
        IB=MOD(KX,NWA)
        KX=KX/NWA
        IA=MOD(KX,NWA)
        KK=KX/NWA
C
C       TEST FOR I(A,B) INTEGRAL
C
        IF (IA+IB.LE.0) GOTO 12
        WA=SLATBD(IA,IB,IC,ID,KK)
        WB=XSBD(JJ)
        WAWB=WA*WB
        IF (ITC(14).EQ.1) WRITE (6,1091) JJ,WA,WB,WAWB
 1091 FORMAT (' MCP NO.',I5,' WA, WB, PRODUCT ::: ',1P3D20.10)
        HAMX(ITR,JTR)=HAMX(ITR,JTR)+WA*WB
   12   CONTINUE
    13  CONTINUE
        IF (ITC(16).EQ.1) WRITE (6,1097)
 1097 FORMAT (///)
        IF (ITC(12).EQ.0) GOTO 89
        DO 98 I=1,NCFP
   98   WRITE (6,1098) (HAMX(I,J),J=1,NCFM)
 1098 FORMAT (' MATO :HAM ',1P10D12.4)
        WRITE (6,1097)
   89   CONTINUE
        RETURN
        END
```

```
      DOUBLE PRECISION FUNCTION RINTI (J,K)
      IMPLICIT REAL*8(A-H,O-Z)
C
C     THE VALUE OF THIS FUNCTION IS THE ONE-ELECTRON INTEGRAL
C     I(J,K) FOR ORBITALS J,K.
C     A CENTRAL DIFFERENCE FORMULA IS USED TO APPROXIMATE THE
C     DERIVATIVE.
C
C     SUBROUTINE CALLED : QUAD
C
      COMMON/CONS/ZERO,HALF,TENTH,ONE,TWO,THREE,TEN
      COMMON/INFORM/IRD,IPD
      COMMON/ORB4/NW,NCF,NH(25),NP(25),NAK(25),IQ(25,20)
      COMMON/DEF1/Z,RNT,H,EPH,ACCY,C,N,NWA
      COMMON/WAVE/PF(350,25),QF(350,25)
      COMMON/PNCWF/PPF(350,25),PQF(350,25)
      COMMON/NPOT/ZZ(350)
      COMMON/TATB/TA(360),TB(360)
      COMMON/GRID/R(350)
C
C     STOP IF ORBITALS J AND K HAVE DIFFERENT KAPPA VALUES
C
      IF (NAK(J).EQ.(-NAK(K))) GO TO 1
      WRITE (IPD,300) NP(J),NH(J),NP(K),NH(K)
      STOP 6
C
    1 CONTINUE
      M=4
      DO 2 I=1,M
      TA(I)=ZERO
      L=N+1-I
    2 TA(L)=ZERO
      NN=N-M
      M=M+1
      CD=C/(840.0D 00*H)
      CA= 672.0D 00*CD
      CB=-168.0D 00*CD
      CC=  32.0D 00*CD
      CD=  -3.0D 00*CD
      WA=C*C
      WA=WA+WA
      WB=C*DFLOAT(NAK(K))
      DO 3 I=M,NN
      TA(I)=
     X    +QF(I,J)*(-(WA*R(I)+ZZ(I))*PQF(I,K)-WB*PPF(I,K)
     X     +CA*(PPF(I+1,K)-PPF(I-1,K))+CB*(PPF(I+2,K)-PPF(I-2,K))
     X     +CC*(PPF(I+3,K)-PPF(I-3,K))+CD*(PPF(I+4,K)-PPF(I-4,K)))
     X   -PQF(I,J)*(-(WA*R(I)+ZZ(I))*QF(I,K)+WB*PF(I,K)
     X     +CA*(PF(I+1,K)-PF(I-1,K))+CB*(PF(I+2,K)-PF(I-2,K))
     X     +CC*(PF(I+3,K)-PF(I-3,K))+CD*(PF(I+4,K)-PF(I-4,K)))
     X   -PF(I,J)*(ZZ(I)*PPF(I,K)+WB*PQF(I,K)
     X     +CA*(PQF(I+1,K)-PQF(I-1,K))+CB*(PQF(I+2,K)-PQF(I-2,K))
     X     +CC*(PQF(I+3,K)-PQF(I-3,K))+CD*(PQF(I+4,K)-PQF(I-4,K)))
     X   +PPF(I,J)*(ZZ(I)*PF(I,K)-WB*QF(I,K)
     X     +CA*(QF(I+1,K)-QF(I-1,K))+CB*(QF(I+2,K)-QF(I-2,K))
     X     +CC*(QF(I+3,K)-QF(I-3,K))+CD*(QF(I+4,K)-QF(I-4,K)))
    3 CONTINUE
      CALL QUAD (RESULT)
      RINTI=RESULT
      RETURN
C
  300 FORMAT (/1X,40HATTEMPT TO CALCULATE I(J,K) FOR ORBITALS,
     X   I4,A2,' &',I3,A2,'  WHICH HAVE NONE-OPPOSITE KAPPAS')
      END
```

```
      DOUBLE PRECISION FUNCTION SLATAC(IA,IB,IC,ID,K)
      IMPLICIT REAL*8(A-H,O-Z)
C
C        THE VALUE OF THIS FUNCTION IS THE SLATER INTEGRAL
C        AS NORMALLY DEFINED IN TERMS OF THE FOUR SETS OF
C        QUANTUM NUMBERS  A,B,C,D
C
C        SUBROUTINES CALLED: YZK,QUAD
C
      COMMON/DEF1/Z,RNT,H,EPS,ACCY,C,N,NWA
      COMMON/WAVE/PF(350,25),QF(350,25)
      COMMON/PNCWF/PPF(350,25),PQF(350,25)
      COMMON/TATB/TA(360),TB(360)
      COMMON/GRID/R(350)
C
C        TABULATE INTEGRAND FOR COMPUTATION OF  YK(R)
C
C       WRITE (6,1002) IA,IB,IC,ID,K
 1002 FORMAT (' SLATAC ( ',5I5,'  )')
C       WRITE(6,1010) (R(I),I=1,N)
 1010 FORMAT (' R(I)'/(1P10D13.4))
C       WRITE (6,1011) (PF(I,IB),I=1,N)
 1011 FORMAT (' PF(I,IB)'/(1P10D13.4))
C       WRITE (6,1012) (PPF(I,ID),I=1,N)
 1012 FORMAT (' PPF(I,ID)'/(1P10D13.4))
C       WRITE (6,1013) (QF(I,IB),I=1,N)
 1013 FORMAT (' QF(I,IB)'/(1P10D13.4))
C       WRITE (6,1014) (PQF(I,ID),I=1,N)
 1014 FORMAT (' PQF(I,ID)'/(1P10D13.4))
C       WRITE (6,1015) (PPF(I,IB),I=1,N)
 1015 FORMAT (' PPF(I,IB)'/(1P10D13.4))
C       WRITE (6,1016) (PF(I,ID),I=1,N)
 1016 FORMAT (' PF(I,ID)'/(1P10D13.4))
C       WRITE (6,1017) (PQF(I,IB),I=1,N)
 1017 FORMAT (' PQF(I,IB)'/(1P10D13.4))
C       WRITE (6,1018) (QF(I,ID),I=1,N)
 1018 FORMAT (' QF(I,ID)'/(1P10D13.4))
      DO 1 I=1,N
    1 TA(I)=R(I)*(PF(I,IB)*PPF(I,ID)+QF(I,IB)*PQF(I,ID)
     )       -PPF(I,IB)*PF(I,ID)-PQF(I,IB)*QF(I,ID))
C       WRITE (6,1003) (TA(I),I=1,N)
 1003 FORMAT (' TA INPUT TO YZK'/(1P10D13.4))
C
C       CALL YZK TO TABULATE YK(R)
C
      CALL YZK (K)
C
C          MULTIPLY BY SECOND TERM, AND OBTAIN RESULT BY INTEGRATION
C
C       WRITE (6,1004) (TB(I),I=1,N)
 1004 FORMAT (' TB RETURNED FROM YZK'/(1P10D13.4))
      DO 2 I=1,N
    2 TA(I)=(PF(I,IA)*PF(I,IC)+QF(I,IA)*QF(I,IC))*TB(I)
C       WRITE (6,1005) (TA(I),I=1,N)
 1005 FORMAT (' TA INPUT TO QUAD'/(1P10D13.4))
      CALL QUAD (RESULT)
      SLATAC=RESULT
      RETURN
      END
```

```
      DOUBLE PRECISION FUNCTION SLATBD(IA,IB,IC,ID,K)
      IMPLICIT REAL*8(A-H,O-Z)
C
C        THE VALUE OF THIS FUNCTION IS THE SLATER INTEGRAL
C        AS NORMALLY DEFINED IN TERMS OF THE FOUR SETS OF
C        QUANTUM NUMBERS  A,B,C,D
C
C        SUBROUTINES CALLED: YZK,QUAD
C
      COMMON/DEF1/Z,RNT,H,EPS,ACCY,C,N,NWA
      COMMON/WAVE/PF(350,25),QF(350,25)
      COMMON/PNCWF/PPF(350,25),PQF(350,25)
      COMMON/TATB/TA(360),TB(360)
      COMMON/GRID/R(350)
C
C        TABULATE INTEGRAND FOR COMPUTATION OF  YK(R)
C
      DO 1 I=1,N
    1 TA(I)=R(I)*(PF(I,IB)*PF(I,ID)+QF(I,IB)*QF(I,ID))
C
C     CALL YZK TO TABULATE YK(R)
C
      CALL YZK (K)
C
C        MULTIPLY BY SECOND TERM, AND OBTAIN RESULT BY INTEGRATION
C
      DO 2 I=1,N
    2 TA(I)=(PF(I,IA)*PPF(I,IC)+QF(I,IA)*PQF(I,IC)
     X        -PPF(I,IA)*PF(I,IC)-PQF(I,IA)*QF(I,IC))*TB(I)
      CALL QUAD (RESULT)
      SLATBD=RESULT
      RETURN
      END
```

```
      SUBROUTINE CRTHOG
      IMPLICIT REAL*8(A-H,O-Z)
C
C     F. M. ORTHOGONALIZE EVRYTHING
C
C      SUBROUTINES CALLED : QUAD
C
      COMMON/ORB4/NW,NCF,NH(25),NP(25),NAK(25),IQ(25,20)
      COMMON/PNCWF/PPF(350,25),PQF(350,25)
      COMMON/DEF1/Z,RNT,H,EPH,ACCY,C,N,NWA
      COMMON/CONS/ZERO,HALF,TENTH,ONE,TWO,THREE,TEN
      COMMON/WAVE/PF(350,25),QF(350,25)
      COMMON/GRID/RAD(350)
      COMMON/TATB/TA(360),TB(360)
C
      DO 69 ITIME=1,3
C
C     FOR EACH ORBITAL
C
      DO 44 JJ=1,NW
C
C     NOW PNC ORTHOGONALIZE TO THE NECCESARY FUNCTIONS
C
      DO 77 J=JJ,NW
      IF (NAK(J).NE.-NAK(JJ)) GOTO 77
      DO 71 I=1,N
   71 TA(I)=(PPF(I,JJ)*PF(I,J)+PQF(I,JJ)*QF(I,J))*RAD(I)
      CALL QUAD(PRECOM)
      DO 72 I=1,N
   72 TA(I)=(PF(I,JJ)*PPF(I,J)+QF(I,JJ)*PQF(I,J))*RAD(I)
      CALL QUAD(CORCOM)
      DELCOM=CORCOM-PRECOM
      WRITE (6,1111) NP(JJ),NH(JJ),NP(J),NH(J),PRECOM,CORCOM,DELCOM
 1111 FORMAT (' ORTHOGONALITY OF',I4,A2,' WITH',I4,A2,1P3D15.6)
      DO 73 I=1,N
      PPF(I,JJ)=PPF(I,JJ)+DELCOM*PF(I,J)
   73 PQF(I,JJ)=PQF(I,JJ)+DELCOM*QF(I,J)
   77 CONTINUE
   44 CONTINUE
   69 CONTINUE
      RETURN
      
```

Appendix 6

Here is my journey's end

Shakespeare (1606)

Numerical Parameters Used in the Solution of the PNC MCDF Equations

APPENDIX 6

NUMERICAL PARAMETERS USED IN THE SOLUTION OF THE PNC MCDF EQUATIONS

In this appendix we shall list the various numerical parameters that had to be determined, usually by trial and error, for the PNC MCDF equations.

Firstly, even when all the techniques described in §6.6 were applied, we still experienced convergence problems with a few orbitals. We therefore fixed the troublesome orbitals, either to zero or to the zero-exchange values. Since these all have $j \geq 3/2$, and so would not be expected to give a very large contribution, even when all the exchange terms are included, we do not expect this to lead to errors that are too substantial.

We then list the projections $\langle ns|\overline{np}\rangle$ which need to be constrained. If any such projection is not listed, it need not be constrained to any value to ensure convergence - indeed, it must not.

Finally, we list the PNC Lagrange multipliers. For the bismuth 5 and 155 CSF calculations, these will give excellent orthogonality; for the others, they are such that the E1 matrix elements are good to at least 1 part in 10^3. Any multipliers that are not specified should be set to zero.

TABLE A6.0

Fixed orbitals

Atom	No. of CSF	Correlation Z PC	Correlation Z PNC	Orbitals fixed
Bi	5	-	-	none
	53	84.2	83.0	7p
	53	84.2	84.2	7p
	53	84.2	86.0	none
	53	84.5	84.5	7p 5f
	53	83.85	83.85	7p $5\bar{f}$
	155	84.2	84.2	7p
	155	84.0	84.0	7p
	155	84.5	84.5	7p
Tl	2	-	-	none
	77	82.5	82.5	6p 5g
	77	83.0	83.0	6p 5g
Cs	2	-	-	none
Pb	5	-	-	6p
	115	82.85	82.85	7p $5\bar{g}$ 5g

TABLE A6.1

$\langle ns|\bar{\bar{np}}\rangle$ overlaps for bismuth: no PNC

Lagrange multipliers

n	$\langle ns\|\bar{\bar{np}}\rangle$
2	1936.212154
3	1068.260521
4	630.866786
5	354.955747
6	202.027571

TABLE A6.2

PNC Lagrange multipliers used in the 5 CSF bismuth calculation

$1s\ 6\bar{p}$	0
$2s\ 6\bar{p}$	0
$3s\ 6\bar{p}$	.1392
$4s\ 6\bar{p}$	.01174
$5s\ 6\bar{p}$	.30968
$6s\ 6\bar{p}$	.103300
$3\bar{d}\ 6p$	.905783
$4\bar{d}\ 6p$	1.122394
$5\bar{d}\ 6p$	7.177524

TABLE A6.3

$\langle ns|\bar{n}\bar{p}\rangle$ for bismuth: PNC Lagrange multipliers included

n	$\langle ns\|\bar{n}\bar{p}\rangle$
2	1936.212193
3	1068.260595
4	630.867055
5	354.957009
6	187.730559

TABLE A6.4

PNC Lagrange multipliers used for the correlation orbitals in the 53 CSF bismuth calculation

$4s\ 7\bar{p}$	-1.811
$4p\ 6\bar{d}$	-35.15
$4\bar{f}\ 6d$	2.00
$5s\ 7\bar{p}$	-2.788
$5p\ 6\bar{d}$	-30.48
$6s\ 7\bar{p}$	-3.887
$6p\ 6\bar{d}$	-22.45
$6d\ 5\bar{f}$	.13528

TABLE A6.5

PNC Lagrange multipliers used for the correlation orbitals in the 155 CSF bismuth calculation

1s $7\bar{p}$	69.8014253
2s $7\bar{p}$	39.4200350
$2\bar{p}$ 7s	-44.3299794
2p $6\bar{d}$	-28.9756817
3s $7\bar{p}$	25.9593584
$3\bar{p}$ 7s	-33.6258150
3p $6\bar{d}$	-25.3198832
3d $5\bar{f}$	23.6610514
4s $7\bar{p}$	18.6847471
$4\bar{p}$ 7s	-26.2190602
4p $6\bar{d}$	-21.8427226
4d $5\bar{f}$	24.5302123
$4\bar{f}$ 6d	20.6190273
5s $7\bar{p}$	13.5202385
$5\bar{p}$ 7s	-20.2412053
5p $6\bar{d}$	-18.8886936
5d $5\bar{f}$	24.1718271
6s $7\bar{p}$	10.2619484
$6\bar{p}$ 7s	-11.4436770
6p $6\bar{d}$	-14.4181481
6d $5\bar{f}$	11.8671101
$7\bar{p}$ 7s	-7.2863419

TABLE A6.6

$\langle ns|\overline{np}\rangle$ overlaps for thallium: no PNC

Lagrange multipliers

n	$\langle ns\|\overline{\overline{np}}\rangle$
2	1645.068
3	904.05
4	531.2
5	293.01

TABLE A6.7

PNC Lagrange multipliers for thallium:

2 CSF calculation

$6s\ 6\overline{p}$	1.16
$6s\ 7\overline{p}$	.351

TABLE A6.8

$\langle ns|\overline{np}\rangle$ overlaps for thallium: PNC

Lagrange multipliers included

n	$\langle ns\|\overline{np}\rangle$
2	1645.1132
3	904.1942
4	531.9412
5	293.1644

TABLE A6.9

PNC Lagrange multipliers for thallium:

correlation orbitals

$2\bar{p}$ 7s	105.271
2p $6\bar{d}$	.02282
$3\bar{p}$ 7s	89.457
$4\bar{p}$ 7s	76.9298
$5\bar{p}$ 7s	70.1709
5d $5\bar{f}$	1.0864
$6\bar{p}$ 7s	42.0256
$7\bar{p}$ 7s	19.1715
7p $6\bar{d}$	-.001794
6d $5\bar{f}$	.1011

TABLE A6.10

$\langle ns|\overline{\overline{np}}\rangle$ overlaps for cesium

n	$\langle ns\|\overline{\overline{np}}\rangle$
2	196.9182
3	101.106
4	57.676
5	28.970

TABLE A6.11

$\langle ns|\overline{\overline{np}}\rangle$ overlaps for lead:

no PNC Lagrange multipliers

n	$\langle ns\|\overline{\overline{np}}\rangle$
2	1783.5931
3	982.1583
4	578.8798
5	322.2545
6	182.882

TABLE A6.12

PNC Lagrange multipliers for lead:

5 CSF calculation

6s $6\bar{p}$	3.937

TABLE A6.13

$\langle ns|\overline{n\bar{p}}\rangle$ overlaps for lead: PNC

Lagrange multipliers included

n	$\langle ns|\overline{n\bar{p}}\rangle$
2	1783.59298
3	982.15843
4	578.87973
5	322.25530
6	169.61993

TABLE A6.14

PNC Lagrange multipliers for lead correlation orbitals

2s $7\bar{p}$	59.37
$2\bar{p}$ 7s	255.6
3s $7\bar{p}$	41.991
$3\bar{p}$ 7s	207.274
4s $7\bar{p}$	32.568
$4\bar{p}$ 7s	173.622
5s $7\bar{p}$	26.449
$5\bar{p}$ 7s	167.824
5d $5\bar{f}$	-.189
6s $7\bar{p}$	28.081
$6\bar{p}$ 7s	151.275
6d $5\bar{f}$	-.0411
7s $7\bar{p}$	14.9711

References

Of making many books there is no end;

  and much study is a weariness of the flesh.

Solomon (-950)

REFERENCES

Abbot, L.F. and Barnett, R.M. Phys. Rev. 19D 3250 (1979).

Arnison, G. et al. Phys. Lett. 122B 103 (1983).

Arnison, G. et al. Phys. Lett. 126B 398 (1983).

Bagus, P.S. and Moser, C.M. Phys. Rev. 167 14 (1968).

Baird, P.E.G., Brimicombe, M.W.S.M., Roberts, G.J., Sandars, P.G.H and Stacey, D.N. Proc. 5th Int. Conf. At. Phys. (1976), pub. Plenum (1977) page 27.

Baird, P.E.G., Brimicombe, M.W.S.M., Hunt, R., Roberts, G.J., Sandars, P.G.H. and Stacey, D. Phys. Rev. Lett. 39 789 (1977).

Baird, P.E.G. International Workshop on Neutral Current Interactions in Atoms 1979, ed. Williams, W.L. (1980).

Banner, G. et al. Phys. Lett. 122B 476 (1983).

Bardsley, J.N. and Norcross, D.W. J. Quant. Spect. and Rad. Trans. 23 575 (1980).

Barish, S.J. et al. Phys. Rev. Lett. 33 448 (1974).

Barkov, L.M. and Zolotorev, M.C. J.E.T.P. Letters 27 357 (1978).

Barkov, L.M. and Zolotorev, M.C. J.E.T.P. Letters 28 503 (1978).

Barkov, L.M., Khriplovich, I.B. and Zolotorev, M.C. Comments At. Mol. Phys. 8 79 (1979).

Barkov, L.M. and Zolotorev, M.C. J.E.T.P. Letters 31 523 (1980).

Bauche, J. Comments At. Mol. Phys. 10 57 (1981).

Benvenuti, A. et al. Phys. Rev. Lett. 32 800 (1973).

Bethe, H.A. and Salpeter, E.E. Quantum Mechanics of One and Two Electron Systems (1957), publ. Springer-Verlag, Berlin.

Blaise, J. and Radziemski, L.J. J. Opt. Soc. America 66 644 (1976).

Blin-Stoyle, R.J. Phys. Rev. 120 181 (1960).

Bogdanov, Y.V., Sobelman, I.I., Sorokin, V.N. and Struk, I.I. J.E.T.P. Letters 31 214 (1980).

Bogdanov, Y.V., Sobelman, I.I., Sorokin, V.N. and Struk, I.I. J.E.T.P. Letters 31 522 (1980).

Bouchiat, C.C. J. Phys. G 3 183 (1977).

Bouchiat, C.C., Piketty, C.A. and Pignon, D. Nuclear Physics B221, 68 (1983).

Bouchiat, M.A. and Bouchiat, C.C. J. Phys. 35 899 (1974).

Bouchiat, M.A. and Bouchiat, C.C. Phys. Lett. 48B 111 (1974).

Bouchiat, M.A. and Bouchiat, C.C. J. Phys. 36 493 (1975).

Bouchiat, M.A. and Pottier, L. Unification of Elementary Forces and Gauge Theories, ed. Cline, D.B. and Mills, F.F. (1977); also Laser Spectroscopy III, ed. Hall, J.L. and Carlsten, J.L., pub. Springer-Verlag Berlin (1977) page 8.

Bouchiat, M.A., Guena, J., Hunter, L. and Pottier, L. Phys. Lett. 117B 358 (1982).

Breit, G. Phys. Rev. 34 553 (1929).

Breit, G. Phys. Rev. 36 383 (1930).

Breit, G. Phys. Rev. 39 616 (1932).

Brimicombe, M.W.S.M., Loving, C.E. and Sandars, P.G.H. J. Phys. B 9 L1 (1976).

Brimicombe, M.W.S.M., Loving, C.E. and Sandars, P.G.H. J. Phys. B 9 L237 (1976).

Broch, E.K. Arch. Math. Naturvidenski 48 25 (1945).

Bucksbaum, P.H., Commins, E.D. and Hunter L.R. Phys. Rev. Lett. 46 640 (1981).

Bucksbaum, P.H., Commins, E.D. and Hunter L.R. Phys. Rev. 24D 1134 (1981).

Carter, S.L. and Kelly, H.P. Phys. Rev. Lett. 42 966 (1979).

Chu, S., Conti, R. and Commins, E.D. Phys. Lett. 60A 96 (1977).

Commins, E.D. Proc. 7th Int. Conf. At. Phys. (1979), pub. Plenum (1980), page 121.

Commins, E.D. and Bucksbaum, P.H. Ann. Rev. Nuc. Part. Sci., 30 1 (1980).

Condon, E.U. and Shortley, G.H. The Theory of Atomic Spectra pub. C.U.P. (1935).

Conti, R., Bucksbaum, P.H., Chu, S., Commins, E.D. and Hunter, L.I Phys. Rev. Lett. 42 343 (1979).

Coveney, P.V. and Sandars, P.G.H. J. Phys. B 16 3726 (1983)

Cowan, R.D. Phys. Rev. 163 54 (1967).

Dalgarno, A. and Lewis, J.T. Proc. Roy. Soc. 233A 70 (1955).

Danté Alighieri The Divine Comedy, part 1: Inferno (1320) Translated by Cary, H.F. (1888).

Das, B.P. Ph.D. Thesis, University of New York at Albany, (1981).

Das, B.P., Andriessen, J., Vajed-Samii,M., Ray, S.N. and Das, T.P. Phys. Rev. Lett. 49 32 (1982).

Desclaux, J.P., Mayers, D.F. and O'Brien, F. J. Phys. B 4 632 (1971).

Desclaux, J.P. Comp. Phys. Comm. 9 31 (1975).

Dyall, K.G. Ph.D. Thesis, Monash (1980).

Dyall, K.G. Private Communication (1981).

Dyall, K.G. and Larkins, F.P. J. Phys. B 15 1021 (1982).

Emmons, T.P., Reeves, J.M. and Fortson, E.N. Phys. Rev. Lett 51 2089 (1983).

Enoch The First Book of Enoch (-110).

Fischer, C.F. The Hartree-Fock Method for Atoms (1977) publ. Wiley, New York.

Fortson, E.N. Proc. 8th Int. Neutrino Conf., ed. Fowler E.C. (1978), publ. Perdue Univ.

Fortson, E.N. and Wilets, L. Adv. At. Mol. Phys. 16 319 (1980).

Garstang, R.H. J. Res. NBS 68A 61 (1964).

Gilbert, W.S. The Mikado (1885).

Grant, I.P. Proc. Roy. Soc. 262A 555 (1961).

Grant, I.P. Adv. Phys. 19 747 (1970).

Grant, I.P. Computer Phys. Comm. 5 263 (1973).

Grant, I.P. J. Phys. B 7 1458 (1974).

Grant, I.P. and Pyper, N.C. J. Phys. B 9 761 (1976).

Grant, I.P., Mayers, D.F. and Pyper, N.C. J. Phys. B 9 2777 (1976).

Grant, I.P. Computer Phys. Comm. 17 149 (1979).

Grant, I.P. Physica Scripta 21 443 (1980).

Grant, I.P., McKenzie, B.J., Norrington, P.H., Mayers, D.F. and Pyper, N.C. Computer Phys. Comm. 21 207 (1980).

Green, A.E.S., Sellin, S.L. and Zachor, A.S. Phys. Rev. 184 1 (1969).

Harris, M.J., Loving C.E. and Sandars, P.G.H. J. Phys. B 11 L749 (1978).

Hasert, F.J. et al. Phys. Lett. 46B 121 (1973).

Hata, J. and Grant, I.P. J. Phys. B. 16 523 (1983).

Hata, J. and Grant, I.P. J. Phys. B 16 915 (1983).

Hata, J. and Grant, I.P. J. Phys. B 16 L189 (1983).

Hata, J. and Grant, I.P. J. Phys. B 16 3725 (1983).

Hata, J. and Grant, I.P. J. Phys. B 16 3713 (1983).

Henley, E.M. and Wilets, L. Phys. Rev. 14A 1411 (1976).

Henley, E.M., Klapisch, M. and Wilets, L. Phys. Rev. Lett. 39 (1977).

Hibbert, A. Preprint.

Hollister, J.H., Apperson, G.A., Lewis, L.L., Vold, T.G., Emmons, T.P. and Fortson, E.N. Phys. Rev. Lett. 46 643 (1981).

John the Divine The Relevation of St. John the Divine (0096).

Johnson, W.R., Lin, C.D., Cheng, K.T. and Lee, C.M. Physica Scripta 21 409 (1980).

Joshua ben Sira Ecclesiasticus (-180).

Joshua the Son of Nun The book of Joshua (-1433).

Kelly, H.P. Phys. Rev. 136 B896 (1964).

Kelly, H.P. Adv. Chem. Phys. 14 129 (1969).

Kelly, H.P. and Carter, S.L. Physica Scripta 21 448 (1980).

Kepler, J. Calendar for 1604.

Khayyàm, O. The Rubaiyat of Omar Khayyàm (1100), Translated by Fitzgerald, E. 1st ed. (1859).

Khayyàm, O. The Rubaiyat of Omar Khayyàm (1100), Translated by Fitzgerald, E. 4th ed. (1879).

Khriplovich, I.B. Sov. J. Nucl. Phys. 21 538 (1975).

Landman, D. and Lurio, A. Phys. Rev. 1A 1330 (1970).

Levy, L.P. and Williams, W.L. Phys. Rev. Lett. 48 607 (1982).

Lewis, L.L., Hollister, J., Soreide, D., Lindahl, E., and Fortson, E.N. Phys. Rev. Lett. 39 795 (1977).

The LORD Private Communication to Noah (-2347). Published by Moses Genesis (-1513).

Loving, C.E. and Sandars, P.G.H. J. Phys. B 8 L336 (1975).

Loving, C.E. D.Phil. Thesis, Oxford (1978).

Mann, J.B. and Johnson, W.R. Phys. Rev. 4A 41 (1971).

Martensson, A.M., Henley, E.M. and Wilets, L. Phys. Rev. 24A 308 (1981).

McKenzie, B.J. and Grant, I.P. J. Phys. B 13 2671 (1980).

McKenzie, B.J., Grant, I.P. and Norrington, P.H. Computer Phys. Commun. 21 233 (1980).

Merzbacher, E. Quantum Mechanics, 2nd ed. (1970), Publ. Wiley, New York.

Messiah, A. Quantum Mechanics (1965), publ. North-Holland, Amsterdam.

Michel, F. Phys. Rev. 138B 408 (1965).

Mittleman, M.H. Phys. Rev. A4 893 (1971).

Mittleman, M.H. Phys. Rev. A5 2395 (1972).

Moore, C.E. Atomic Energy Levels NBS 467 (1958).

Moskalev, A.N. Sov. Phys. Usp. 19 220 (1976).

Neuffer, D.V. and Commins, E.D. Phys. Rev. 16A 844 (1977).

Neuffer, D.V. and Commins, E.D. Phys. Rev. 16A 1760 (1977).

Novikov, V.N., Sushkov, O.P. and Khriplovich, I.B. Sov. Phys. J.E.T.P. 44 872 (1976).

Phillips, G.M. and Taylor, P.J. Theory and Applications of Numerical Analysis (1973), publ. Academic Press, London.

Prescott, C.Y. et al. Phys. Lett. 77B 347 (1978).

Prescott, C.Y. et al. Phys. Lett. 84B 524 (1979).

Pyper, N.C. and Grant, I.P. J. Phys. B 10 1803 (1977).

Pyper, N.C., Grant, I.P. and Beatham, N. Computer Phys. Commun. 15 387 (1978).

Pyper, N.C. and Grant, I.P. J. Chem. Soc. Faraday II 74 1885 (1979).

Pyper, N.C. J. Phys. B. 16 L211 (1983).

Rajnak, K. Phys. Rev. 14A 1979 (1976).

Rajnak, K. and Fred, M. J. Opt. Soc. America 62 1314 (1977).

Roberts, G.J., Baird, P.E.G., Brimicombe, M.W.S.M., Sandars, P.G.H., Selby, D.R. and Stacey, D.N. J. Phys. B. 13 1389 (1980).

Roothaan, C.C.J. Rev. Mod. Phys. 23 69 (1951).

Roothaan, C.C.J. Rev. Mod. Phys. 32 179 (1960).

Roothaan, C.C.J. and Bagus, P.S. Methods. Comput. Phys. 2 47 (1963).

Rose, S.J., Grant, I.P. and Pyper, N.C. J. Phys. B 11 3499 (1978).

Rose, S.J. D.Phil. Thesis, Oxford (1979).

Salam, A. Elementary Particle Physics, Proc. 8th Nobel Symp., p.367 ed. Svartholm, N. (1968), publ. Almkvist and Wiksell, Stockholm.

Sakurai, J.J. Invariance Principles and Elementary Particles (1964), publ. Princeton Univ. Press.

Sandars, P.G.H. J. Phys. B 10 2983 (1977).

Sandars, P.G.H. Laser Spectroscopy III, ed. Hall, J.L. and Carlsten, J.L., pub. Springer-Verlag, Berlin (1977).

Sandars, P.G.H. Physica Scripta 21 284 (1980).

Shakespeare, W. Macbeth (1606).

Shun, D.H. D.Phil. Thesis, Oxford (1977).

Silver, D.M. and Bartlett, R.J. Phys. Rev. 13A 1 (1976).

Silver, D.M., Wilson, S. and Bartlett, R.J. Phys. Rev. 16 477 (1977).

Smith, K. The Calculation of Atomic Collision processes (1971) publ. Wiley, New York.

Solomon Ecclesiastes (-950).

Sternheimer, R.M. Phys. Rev. 84 244 (1951).

Sushkov, O.P., Flambaum, V.V. and Khriplovich, I.B. J.E.T.P. Letters 24 461 (1976).

Tolkein, J.J.R. The Hobbit (1937).

Tsui, D.C., Gossard, A.C., Field, B.F., Cage, M.E. and Dziuba, R.F. Phys. Rev. Lett. 48 3 (1982).

Weinberg, S. Phys. Rev. Lett. 19 126 (1967).

Zeldovich, Y.B. Sov. Phys. J.E.T.P. 9 682 (1959).

When I applied mine heart to know wisdom,
and to see the business that is done upon the
earth: (for also there is that neither day nor
night seeth sleep with his eyes:)
then I behold all the work of God, that a
man cannot find out the work that
is done under the sun: because though a
man labour to seek it out, yet he shall
not find it; yea farther; though a wise
man think to know it, yet shall he not
be able to find it.
And behold, all is vanity and a striving after wind.

Solomon (-950)

Accompanying material
stored separately.
Search OLIS for shelfmark.